

A STUDY OF LIGAND SUBSTITUTION REACTIONS IN THE FIVE COORDINATE  
COMPLEXES,  $[\text{Cu}(\text{TREN})\text{OH}_2]^{2+}$ ,  $[\text{Cu}(\text{Me}_6\text{TREN})\text{OH}_2]^{2+}$  AND  $[\text{Cu}(\text{Me}_6\text{TREN})\text{OH}]^+$ .

by



Peter Ralph Collins

B.Sc.(Hons.), University of Adelaide, 1974.

Thesis presented for the degree of  
Doctor of Philosophy

Department of Physical and Inorganic Chemistry

UNIVERSITY OF ADELAIDE

January, 1979.

*awarded January 1980*

## CONTENTS

	Page No.
CHAPTER ONE: INTRODUCTION	
I (A) Structural Aspects of Trigonal Bipyramidal Complexes, in particular, $[M(\text{Tren})\text{OH}_2]^{2+}$ and $[M(\text{Me}_6\text{Tren})\text{OH}_2]^{2+}$ .	2
<i>References</i>	7
(B) The kinetics and mechanisms of ligand substitution in labile complexes.	
(1) <i>Common mechanisms for reactions of solvated metal ions</i>	8
(2) <i>Basic kinetic terminology</i>	13
(3) <i>Anation reactions of labile metal ions</i>	
(i) <i>Alternative mechanistic pathways, Dissociative (D) or Dissociative Interchange (<math>I_d</math>)</i>	15
(ii) <i>Jahn Teller influence on solvated metal ion water exchange lability</i>	17
(4) <i>A specific anation reaction</i>	19
(5) <i>Anation reactions exhibiting five coordinate intermediates in the (D) process</i>	22
<i>References</i>	24
(C) Crystal field stabilization effect on transition metal ions (C.F.S.E.)	26
<i>References</i>	27
(D) Substitution reactions of copper chelates	28
<i>References</i>	32
(E) General review of reactions of $[M(\text{Tren})\text{OH}_2]^{2+}$ and $[M(\text{Me}_6\text{Tren})\text{OH}_2]^{2+}$ and their substituted analogues	33
<i>References</i>	40

## CHAPTER TWO: MATERIALS AND TECHNIQUES

I	Reagents and Materials (Analysis and Preparation)	42
II (A)	Kinetic Techniques and Principles	
	(i) <i>Temperature Jump Relaxation Kinetics</i>	45
	(ii) <i>The Temperature Jump Method</i>	49
	(iii) <i>Analysis of Data</i>	53
	(iv) <i>Amplitude Considerations</i>	53
	(v) <i>Calibration of the Temperature Rise</i>	55
II (B)	(i) <i>The Stopped Flow Method</i>	56
	(ii) <i>Experimental Limitations</i>	59
III	Equipment used in Spectrophotometric Analysis and pH Determination	60
	<i>References</i>	61

## CHAPTER THREE: RESULTS AND DISCUSSION

Section A: Kinetic analysis of the  $[\text{Cu}(\text{Me}_6\text{Tren})\text{OH}_2]^{2+}\text{X}^-$  system

I	(i) <i>Alternative mechanisms for the experimentally obtained kinetic data</i>	64
	(ii) <i>Evaluation of rate equations for the Eigen (<math>I_d</math>) mechanism</i>	66
	(iii) <i>The rate constant parameters in the overall Eigen curve</i>	68
II	Theoretical $K_{IP}$ determination	
	(i) <i>the theoretical Bjerrum equation</i>	69
	(ii) <i>the theoretical Fuoss equation</i>	70
	(iii) <i>modification of the Bjerrum equation to determine <math>K_{IP}</math></i>	71

III	Method of Kinetic data analysis	
	(i) <i>The Use of programme NONLIN in experimentally obtained, data analysis</i>	72
IV	Discussion of the kinetic and activation data obtained for aquation of $[\text{Cu}(\text{Me}_6\text{Tren})\text{X}]^+$ and anation of $[\text{Cu}(\text{Me}_6\text{Tren})\text{OH}_2]^{2+}$	
	(i) <i>Anation of <math>[\text{Cu}(\text{Me}_6\text{Tren})\text{OH}_2]^{2+}</math>, by <math>(\text{N}_3^-</math>, <math>\text{NCS}^-</math> and <math>\text{OCN}^-)</math></i>	77
	(ii) <i>Aquation of <math>[\text{Cu}(\text{Me}_6\text{Tren})\text{X}]^+</math>, (where <math>\text{X}^- = \text{N}_3^-</math>, <math>\text{NCS}^-</math> or <math>\text{OCN}^-)</math></i>	78
	(iii) <i>A brief discussion of the <math>K_{IP}</math> data obtained</i>	79
V	Static and kinetic equilibrium constant spectrophotometric data determination	
	(i) <i>The general method of equilibrium constant evaluation</i>	80
	(ii) <i>The method of evaluating the apparent equilibrium constant</i>	81
	(iii) <i>The <math>K_{eq}</math> (overall) data from kinetic data obtained in the analysis using programme NONLIN</i>	84
	(iv) <i>Experimental determination of <math>K_{app}</math> (spectrophotometric)</i>	84
	(v) <i>Comparative equilibrium constant data (both static and kinetic)</i>	86
 Section B: Kinetic analysis of the $[\text{Cu}(\text{Tren})\text{OH}_2]^{2+}/\text{X}^-$ system		
I	A discussion of the kinetic data obtained	88
II	A brief discussion of the limited equilibrium constant data available	91
 Section C:		
I	A comparative discussion of kinetic and activation data for the two systems, $[\text{Cu}(\text{Me}_6\text{Tren})\text{OH}_2]^{2+}/\text{X}^-$ and $[\text{Cu}(\text{Tren})\text{OH}_2]^{2+}/\text{X}^-$ (where $\text{X}^- = \text{N}_3^-$ , $\text{NCS}^-$ )	93

II	Reasons postulated for the reduced lability of the [Cu(Me <sub>6</sub> tren)OH <sub>2</sub> ] <sup>2+</sup> /X <sup>-</sup> system compared to that of [Cu(Tren)OH <sub>2</sub> ] <sup>2+</sup> /X <sup>-</sup>	
	(i) <i>Electron donating abilities of coordinated amine ligands</i>	100
	(ii) <i>Labile site environmental effects in [Cu(Tren)OH<sub>2</sub>]<sup>2+</sup> and [Cu(Me<sub>6</sub>Tren)OH<sub>2</sub>]<sup>2+</sup></i>	106
	(iii) <i>Steric hindrance considerations</i>	106
Section D: Kinetic analysis of the [Cu(Me <sub>6</sub> Tren)OH <sub>2</sub> ] <sup>2+</sup> /X <sup>-</sup> system (where X <sup>-</sup> = Br <sup>-</sup> , Cl <sup>-</sup> )		
I	Discussion and Interpretation of the kinetic data obtained	109
II	A comparative discussion of kinetic data, for aquation of complexes [Cu(Me <sub>6</sub> Tren)X] <sup>+</sup> where (X <sup>-</sup> = N <sub>3</sub> <sup>-</sup> , NCS <sup>-</sup> , OCN <sup>-</sup> , Br <sup>-</sup> and Cl <sup>-</sup> )	115
Section E: Kinetic analysis of the [Cu(Me <sub>6</sub> Tren)OH] <sup>+</sup> /X <sup>-</sup> system (where X <sup>-</sup> = N <sub>3</sub> <sup>-</sup> , NCS <sup>-</sup> and OCN <sup>-</sup> )		
I	Discussion and interpretation of the kinetic data obtained	120
II	A comparative discussion of the kinetic data obtained in the two anation systems, [Cu(Me <sub>6</sub> Tren)OH] <sup>+</sup> /X <sup>-</sup> and [Cu(Me <sub>6</sub> Tren)OH <sub>2</sub> ] <sup>2+</sup> /X <sup>-</sup> at 298 K	122
Section F: A preliminary study of the Cu(II) Me <sub>6</sub> Tren sulphito system (at 298 K)		
I	A Kinetic study (at 298 K) of the Cu(II) Me <sub>6</sub> Tren sulphito system at pH = 7.00 ± (.01)	128
II	A Kinetic study (at 298 K) at various pH values for the Cu(II) Me <sub>6</sub> Tren sulphito system	131
	<i>References</i>	132

	Page No.
GENERAL CONCLUSIONS	134
ADDENDUM: Implications of the kinetic studies in the metallo-enzyme zinc carbonic anhydrase	135
<i>References</i>	137
Appendices of the kinetic data	

## ABBREVIATIONS

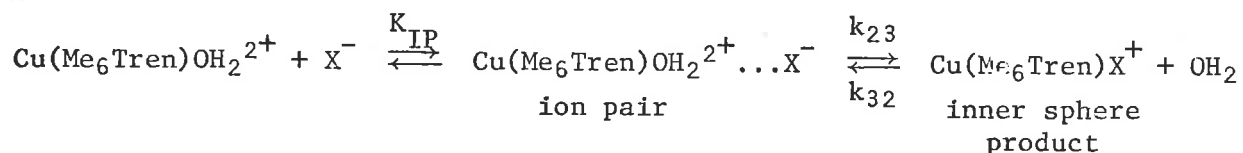
The following abbreviations appear in this thesis,

Tren	2,2',2''-triamino triethylamine
Me <sub>6</sub> Tren	2,2',2''-tri(N,N-dimethylamino)triethylamine
gly	glycine
C.F.S.E.	Crystal Field Stabilization Energy
K <sub>IP</sub>	Ion pair association constant
k <sub>-H<sub>2</sub>O</sub>	The rate constant for release of inner sphere coordinated water from the ion pair complex.
k <sub>ex</sub>	The water exchange rate in the primary hydration sphere of the metal complex.
en	1,2-diaminoethane
dien	2,2'-diaminodiethylamine
trien	N,N'-di(2-aminoethyl)-ethylenediamine
py	2-pyridyl
bipy	2,2'-dipyridyl
terpy	2,2',2''-terpyridyl
pada	pyridine-2-azo-p-dimethylaniline

## Summary

The kinetics of ligand substitution in the two five coordinate complexes,  $[\text{Cu}(\text{Tren})\text{OH}_2]^{2+}$  and  $[\text{Cu}(\text{Me}_6\text{Tren})\text{OH}_2]^{2+}$  were investigated using both the stopped flow and temperature jump techniques.

A three temperature study of  $\text{N}_3^-$ ,  $\text{NCS}^-$  and  $\text{OCN}^-$  substitution in the complex,  $[\text{Cu}(\text{Me}_6\text{Tren})\text{OH}_2]^{2+}$  was carried out. The rate constants and activation parameters for both anation and aquation reactions are reported. It is suggested that the Eigen mechanism, shown as follows,



$$K_{23} = k_{23}/k_{32} \text{ and } \text{X}^- = \text{N}_3^-, \text{NCS}^-, \text{OCN}^-$$

is operative, with the rate constants ( $k_{23}$ ) being similar for the three substituting ligands.

A three temperature study of  $\text{N}_3^-$  substitution rates in the complex,  $[\text{Cu}(\text{Tren})\text{OH}_2]^{2+}$  showed rectilinear plots with a positive slope for the narrow, (experimentally limited), range of ligand concentrations used. This work was confined to the temperature jump technique since the observed rates were too fast for stopped flow analysis. Activation parameters for the aquation of  $[\text{Cu}(\text{Tren})\text{N}_3]^+$  are reported and it is again postulated that the Eigen mechanism operates. The  $\text{NCS}^-$  substitution in  $[\text{Cu}(\text{Tren})\text{OH}_2]^{2+}$  is reported at only one temperature owing to its very high aquation rate.

The aquation rate of  $[\text{Cu}(\text{Me}_6\text{Tren})\text{X}]^+$ , compared to that of  $[\text{Cu}(\text{Tren})\text{X}]^+$ , for the same ligand ( $\text{N}_3^-$  or  $\text{NCS}^-$ ), was found to be approximately  $10^4$  times slower. The anation rate comparison should exhibit a similar difference in magnitude. Reasons for these differences are proposed in relation to electrostatic, geometrical flexibility and to a lesser extent labile site environment, considerations.

Equilibrium studies were complicated owing to the nature of the Eigen



mechanism, with its intermediate ion pair complex. Equations for this analysis are presented. The kinetic and spectrophotometric equilibrium constants are compared at only one temperature (298 K) and good agreement is obtained.

The rates of anation reactions of  $\text{Cl}^-$  and  $\text{Br}^-$  with  $[\text{Cu}(\text{Me}_6\text{Tren})\text{OH}_2]^{2+}$  were studied and straight line plots of essentially zero slope are obtained over a large ligand concentration range, at all temperatures investigated. The reasons for considering that the same Eigen mechanism is operative, are discussed.

The  $\text{SO}_3^{=}/\text{HSO}_3^-$  substitution in  $[\text{Cu}(\text{Tren})\text{OH}_2]^{2+}$  and  $[\text{Cu}(\text{Me}_6\text{Tren})\text{OH}_2]^{2+}$  again shows a reduced lability, ( $\sim 10^3$  times), for the anation of the  $[\text{Cu}(\text{Me}_6\text{Tren})\text{OH}_2]^{2+}$  complex. A kinetic investigation of the rate of substitution at various pH values was undertaken. A plot of  $k_{\text{obs}}$  over a ligand concentration range, at a particular pH, showed a straight line of positive slope even at very high ligand concentrations. An explanation of this phenomenon is given.

The substitution of the complex,  $[\text{Cu}(\text{Me}_6\text{Tren})\text{OH}]^+$  by the ligands  $\text{N}_3^-$ ,  $\text{NCS}^-$  and  $\text{OCN}^-$  at 298 K is reported. They exhibit the kinetic curve usually attributed to the Eigen mechanism.

Spectroscopic measurements were made in order to determine the equilibrium concentrations of the participating species for all the systems. Where both practicable and necessary, equilibrium constant measurements were made for detailed analysis of the kinetic data obtained.

Some implications of the present studies for the method of action of carbonic anhydrase are discussed. This relates to the hypothesis that the metal 2,2',2''-Tri(N,N-dimethylamine)triethylamine ( $\text{Me}_6\text{Tren}$ ) complex may be an analogue of this active site metallo enzyme.

This thesis contains no material previously submitted for a degree or diploma in any University, and, to the best of my knowledge and belief, contains no material previously published or written by another person, except where due reference is made in the text.

Peter R. Collins

January, 1979.

## ACKNOWLEDGEMENTS

I wish to thank my supervisor DR. J.H. COATES for his many helpful suggestions throughout my postgraduate years of research.

To DR. S.F. LINCOLN, my co-supervisor I am particularly indebted for enlightening discussions concerning the kinetic aspects of this research.

To colleagues in the Physical and Inorganic Chemistry Department go my thanks for their critical appraisal of the work reported.

I am appreciative of the assistance afforded me by the engineering, electronics and glassblowing workshops towards maintenance of apparatus.

I acknowledge the financial assistance of a Commonwealth Postgraduate Scholarship and of the Australian Research Grants Committee.

My sincerest gratitude goes to my parents for continual encouragement and support throughout my academic years.

Finally, I wish to thank Miss P. Ramos for the typing of this thesis.

## CHAPTER ONE

- I (A) Structural Aspects of Trigonal Bipyramidal Complexes, in particular,  $[M(\text{Tren})\text{OH}_2]^{2+}$  and  $[M(\text{Me}_6\text{Tren})\text{OH}_2]^{2+}$ .
- (B) The kinetics and mechanisms of ligand substitution in labile complexes.
- (1) *Common mechanisms for reactions of solvated metal ions*
  - (2) *Basic kinetic terminology*
  - (3) *Anation reactions of labile metal ions*
    - (i) *Alternative mechanistic pathways, Dissociative (D) or Dissociative Interchange (Id)*
    - (ii) *Jahn Teller influence on solvated metal ion water exchange lability*
  - (4) *A specific anation reaction*
  - (5) *Anation reactions exhibiting five coordinate intermediates in the (D) process*
- (C) Crystal field stabilization effect on transition metal ions (C.F.S.E.)
- (D) Substitution reactions of copper chelates.
- (E) General review of reactions of  $[M(\text{Tren})\text{OH}_2]^{2+}$  and  $[M(\text{Me}_6\text{Tren})\text{OH}_2]^{2+}$  and their substituted analogues.

## CHAPTER ONE

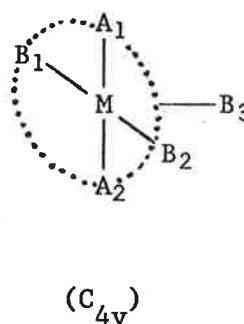
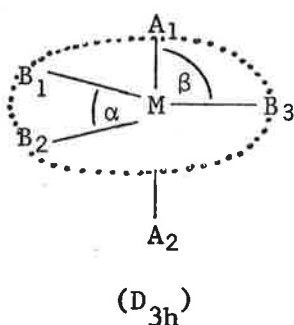
## INTRODUCTION



The research described in this thesis is mainly concerned with a study of the substitution reactions of five coordinate copper systems. In addition, the hypothesis that the metal 2,2',2''-Tri(N,N-dimethylamino)triethylamine ( $\text{Me}_6\text{Tren}$ ) complex is an analogue of the active site metallo-enzyme carbonic anhydrase, is briefly examined.

I (A) Structural Aspects of Trigonal Bipyramidal Complexes in particular,  $[\text{M}(\text{Tren})\text{OH}_2]^{2+}$  and  $[\text{M}(\text{Me}_6\text{Tren})\text{OH}_2]^{2+}$ .

Five<sup>1,5</sup> coordinate structures can be divided into two main idealized symmetrical configurations, square pyramidal ( $\text{C}_{4v}$ ) and trigonal bipyramidal ( $\text{D}_{3h}$ ), which are shown below.



These two extreme structures can be interconverted by angular distortions. The main factors<sup>1</sup> that determine the configurations in a particular complex are,

1. The nature of the metal-ligand bonds.
2. Electrostatic and non-bonding repulsion between ligands ( $\text{D}_{3h}$  is more stable).
3. Crystal field stabilization energy.
4. Shape of the ligand molecules and crystal packing forces in the solid state.

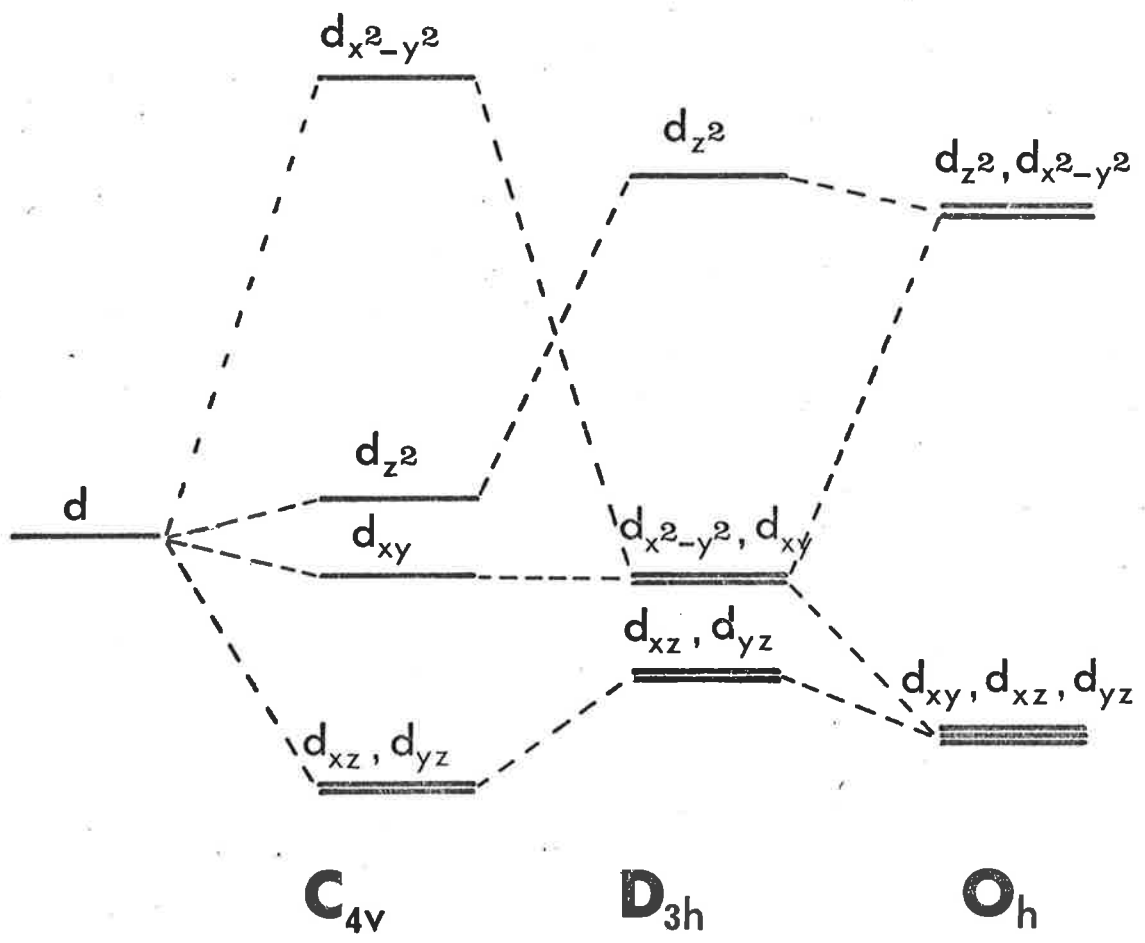
The structure<sup>2</sup> of  $[\text{Cr}(\text{NH}_3)_6][\text{CuCl}_5]$  is an example of the regular trigonal bipyramidal structure. The angle between the axial and equatorial bonds ( $\beta$ ) is assigned as the apical angle. Orbital splitting diagrams<sup>1, 5, 6</sup> for  $C_{4v}$  and  $D_{3h}$  fields appear in FIG. (1.1).

On the basis of charge repulsion, Zemann<sup>3, 6</sup> has shown that the trigonal bipyramid is the most stable configuration for five ligands  $\text{ML}_5$  at equal distances from M. Both the trigonal bipyramidal ( $D_{3h}$ ) and square pyramid ( $C_{4v}$ ) configurations occur owing to the closing and opening of various bond angles.

For  $d^1$  to  $d^9$  electronic configurations the crystal field stabilization energy (C.F.S.E.) favours the square pyramidal model. This stabilization<sup>1, 6</sup> decreases when the angle  $\text{L} \text{---} \text{M} \text{---} \text{L}$  deviates from  $90^\circ$ . For values of  $105^\circ$ , the C.F.S.E. favours trigonal bipyramidal structures. Effects<sup>4</sup> of non uniform distribution of d electrons on bond lengths in five coordinate complexes is one factor causing distortions of idealized geometries. The series<sup>6</sup> of high spin five coordinate complexes,  $[\text{M}^{\text{II}}(\text{Me}_6\text{Tren})\text{Br}]\text{Br}$  where  $\text{M} = \text{Mn}, \text{Fe}, \text{Co}, \text{Ni}, \text{Cu}, \text{Zn}$  are good examples of the stereochemical effects of d electrons in five coordinate complexes. From X-ray studies, this structure was shown to consist of trigonal bipyramidal  $[\text{M}(\text{Me}_6\text{Tren})\text{Br}]^+$  cations and  $\text{Br}^-$  ions arranged in a distorted NaCl type lattice. Plots<sup>6</sup> of M-N and M-Br distances versus atomic number in a series of the above complexes show that the equatorial M-N distances increase for Ni ( $d^8$ ) and Cu ( $d^9$ ) when  $d_{x^2-y^2}$  and  $d_{xy}$  orbitals lying in the equatorial plane are being filled. The large increase of the apical M-N distance for Zn ( $d^{10}$ ) is accounted for by filling the  $d_{z^2}$  orbital which points towards the nitrogen. See diagrams for splitting of d orbitals in FIG. (1.1). It can be seen that bond lengths and so distortions, are greatly influenced by the arrangement or distribution of d electrons within the orbitals of the complex structure.

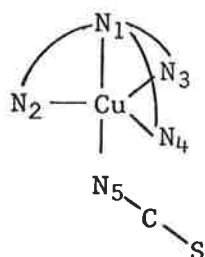
The copper complex of 2,2',2''-triaminotriethylamine (Tren) with thiocyanate,  $[\text{Cu}(\text{Tren})\text{NCS}]\text{SCN}$ , reveals a five coordinate trigonal bipyramidal structure.<sup>9</sup> The equatorial angles and bond lengths are unequal thus suggesting

**FIG 1.1**



a slight distortion. Basolo and Pearson<sup>7</sup> initially suggested that one thiocyanate ion was coordinated to the divalent copper ion through the nitrogen atom and the other through a sulphur atom in a *cis* octahedral complex. Later work by Jain<sup>8,9</sup> and Lingafelter indicated that the copper ion was surrounded by four nitrogen atoms from the Tren molecule and one from thiocyanate; in a slightly distorted trigonal bipyramid with the tertiary (N<sub>1</sub>) nitrogen atom and the thiocyanate (N<sub>5</sub>) nitrogen atom at the apices. The three primary amine nitrogen atoms (N<sub>2</sub>, N<sub>3</sub>, N<sub>4</sub>) are in the equatorial positions. It should be noted that the second thiocyanate ion is not coordinated to the copper ion.

Fig. (1.2)



Cu-NCS	=	1.95 Å°
Cu-N <sub>(av)</sub>	=	2.06 Å°
N <sub>1</sub> -Cu-N <sub>5</sub>	=	177°
N <sub>2</sub> -Cu-N <sub>3</sub>	=	N <sub>3</sub> -Cu-N <sub>4</sub> = 113° to 114°
N <sub>2</sub> -Cu-N <sub>4</sub>	=	130°

For the divalent<sup>10</sup> Nickel Tren complexes there are two thiocyanate groups forming a *cis* octahedral structure.

From X-ray work it was found that the hexamethyl derivative of Tren, Me<sub>6</sub>Tren, forms only five coordinate species with the divalent first row metal<sup>11,13</sup> ions. The complex, [Co(Me<sub>6</sub>Tren)Br]Br is a trigonal bipyramid with C<sub>3v</sub> symmetry. The greater steric hindrance provided by the equatorial methyl groups does not allow close approach of the sixth ligand that can occur in Tren.<sup>1</sup> In the spectra of complexes, [M(Me<sub>6</sub>Tren)X]X where M = Cr<sup>2+</sup>, Fe<sup>2+</sup>, Cu<sup>2+</sup> which have true C<sub>3v</sub> symmetry, two bands corresponding to d-d transitions are observed. These are due to transitions between the three energy levels (A<sub>1</sub> + 2E).

The stabilities of various coordination geometries are discussed by Sacconi.<sup>1</sup> For five coordinated complexes the order of stability is,



For octahedral complexes the order of stability is,





Maximum C.F.S.E. of hexa-aquo ions occurs with nickel, but in the five coordinate series it is expected to occur with copper. This could explain why Tren gives five coordinate species with divalent copper and cobalt ions in aqueous solution whereas divalent nickel produces an octahedral complex.

The structure of  $[\text{M}(\text{Me}_6\text{Tren})\text{X}]\text{X}$  complexes can be assigned by comparison with the spectra of typical high spin configurations. The spectra of the  $\text{Me}_6\text{Tren}$  metal ion complexes show a definite similarity to those of some high spin<sup>14</sup> cobalt and nickel divalent ion complexes of known five coordinate structure. These known structures are both trigonal bipyramidal and square pyramidal. The spectra<sup>11</sup> of complexes,  $[\text{M}(\text{Me}_6\text{Tren})\text{X}]\text{X}$ , where (M = Co, Ni) are consistent with spectra of trigonal bipyramidal compounds.<sup>12</sup> Spectroscopic<sup>11</sup> results indicate five coordination (trigonal bipyramid) for all divalent copper, nickel and cobalt  $\text{Me}_6\text{Tren}$  complexes.

The five coordinate structure of the cobalt tren complex in aqueous solution has been confirmed by its similarity in absorption spectrum with that of the solid compound,  $[\text{Co}(\text{Me}_6\text{Tren})\text{Br}]\text{Br}$ , which has been shown to have a trigonal bipyramidal structure from X-ray studies.<sup>13,17</sup> The U/V, vis spectra<sup>15</sup> of complexes  $[\text{Co}(\text{Tren})\text{X}]\text{X}$  where  $\text{X} = \text{I}^-$ ,  $\text{NCS}^-$  are very different from those of cobalt compounds with tetrahedral or octahedral stereochemistry<sup>16</sup> but are very similar to the spectrum of the five coordinated complex,  $[\text{Co}(\text{Me}_6\text{Tren})\text{Br}]\text{Br}$ . The bands in the Tren complexes are shifted to higher frequencies compared to that for  $\text{Me}_6\text{Tren}$  complexes. This is due to the greater crystal<sup>18</sup> field splitting and therefore electron donation ability of the  $\text{NH}_2$  group compared to the  $\text{N}(\text{CH}_3)_2$ . Also the frequencies exhibited by,  $[\text{Co}(\text{Tren})\text{NCS}]\text{SCN}$ , infra-red spectra are almost the same as for,  $[\text{Cu}(\text{Tren})\text{NCS}]\text{SCN}$ , whose structure<sup>9</sup> has been shown to be five coordinate trigonal bipyramidal.

To summarize, the steric<sup>11</sup> requirements of the amine tren are on the borderline of compatibility for five and six coordination. The five coor-

dinated structure is formed depending on the nature of the metal ion or the presence of other suitable ligands in solution. The Tren complexes of the divalent ions of cobalt, copper and zinc exhibit five coordination. In contrast, X-ray<sup>15,19</sup> and spectral studies have shown that all divalent nickel Tren complexes are octahedral. From results of a calorimetric study<sup>20</sup> it was found that five coordination is favoured in the order,<sup>15</sup>



The stereochemical requirements of Tren allow five coordination for three elements forming the most stable five coordinated complexes. Increasing the bulkiness of the ligands as in Me<sub>6</sub>Tren (through N-methylation), provides five coordination for all the first row transition metal ions Mn<sup>2+</sup> to Zn<sup>2+</sup>. The above discussed complexes form part of an increasingly large group of five coordinate complexes discovered and investigated throughout the last fifteen years. The general space filled models of [M(Me<sub>6</sub>Tren)OH<sub>2</sub>]<sup>2+</sup> and [M(Tren)OH<sub>2</sub>]<sup>2+</sup> appear in FIG. (1.3).

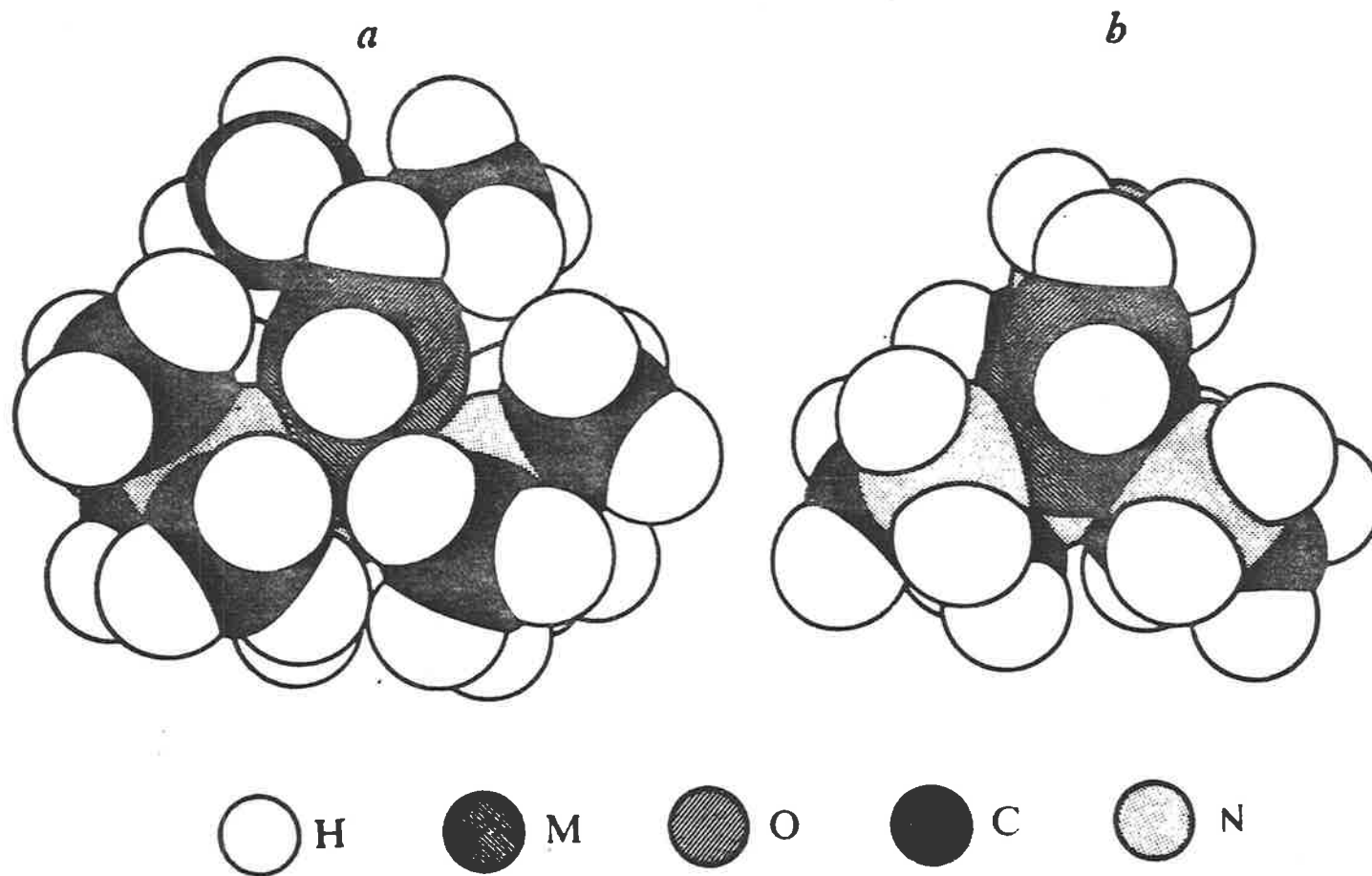


**FIG 1.3** Space filling models of  $[MMe_6trenH_2O]^{2+}$  (a) and  $[MtrenH_2O]^{2+}$  (b).

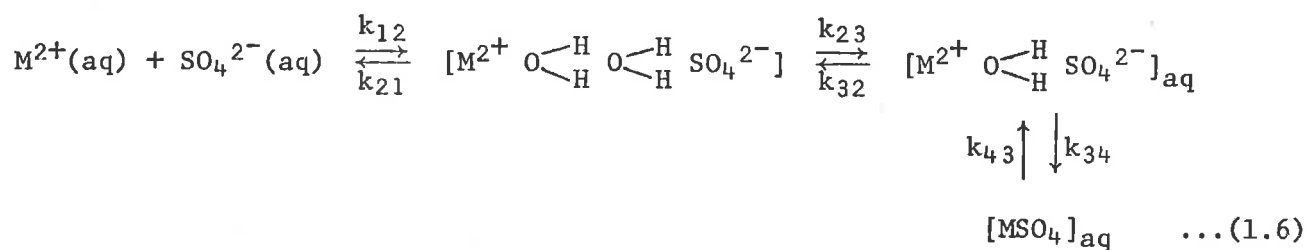
## REFERENCES

1. L. Sacconi, in "Xth International Conference on Coordination Chemistry", Plenary Lectures, Plenum Press, New York., (1967), p 95.
2. M. Mori, Y. Saito and T. Watanabe, *Bull. Chem. Soc. Japan*, 34, 295 (1961).
3. J. Zemann, *Z. Anorg. Allgem. Chem.*, 324, 241 (1963).
4. R.J. Gillespie, *J. Chem. Soc.*, 4672 (1963).
5. R. Morassi, I. Bertini and L. Sacconi, *Coord. Chem. Revs.*, 11, 343 (1973).
6. P.L. Orioli, *Coord. Chem. Revs.*, 6, 287 (1971).
7. K.N. Raymond and F. Basolo, *Inorg. Chem.*, 5, 1632 (1966).
8. P.C. Jain and E.C. Lingafelter, *J. Amer. Chem. Soc.*, 89, 724 (1967).
9. P.C. Jain and E.C. Lingafelter, *J. Amer. Chem. Soc.*, 89, 6131 (1967).
10. D.F. Koenig, *Acta Cryst.*, 18, 663 (1965).
11. M. Ciampolini and N. Nardi, *Inorg. Chem.*, 5, 41 (1966).
12. L. Sacconi, M. Ciampolini and G.P. Speroni, *J. Am. Chem. Soc.*, 87, 3102 (1965).
13. M. Ciampolini and N. Nardi, *Inorg. Chem.*, 5, 1150 (1966).
14. M. Ciampolini, *Inorg. Chem.*, 5, 35 (1966).
15. M. Ciampolini and P. Paoletti, *Inorg. Chem.*, 6, 1261 (1967).
16. R.L. Carlin in "Transition Metal Chemistry", Vol. 1, R.L. Carlin, Ed., Marcel Dekker Inc., New York, N.Y., 1965, pp.3-19.
17. M. Di Vaira and P.L. Orioli, *Inorg. Chem.*, 6, 955 (1967).
18. S.F. Pavkovic and D.W. Meek, *Inorg. Chem.*, 4, 20 (1965).
19. D. Hall and M.D. Woulfe, *Proc. Chem Soc.*, 346 (1958); S.E. Rasmussen, *Acta Chem. Scand.*, 13, 2009 (1959).
20. P. Paoletti and M. Ciampolini, *Inorg. Chem.*, 6, 64 (1967).





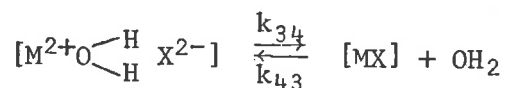
water coordinated to  $M^{2+}$ . The following reaction sequence is due to Eigen<sup>4</sup> and Tamm,



Eigen's<sup>4</sup> data for the last slower step appears in Table (1.1) and shows that  $Cu^{2+}$  and  $Zn^{2+}$  react faster than  $Ni^{2+}$  and  $Co^{2+}$ , with the  $SO_4^{2-}$  ligand. Kinetic data for the formation of  $MgSO_4$ <sup>6</sup> and  $MnSO_4$ <sup>5</sup> appears in Table (1.2) and is based on the Eigen reaction sequence shown above.

Table (1.1)

*Kinetic data for  $SO_4^{2-}$  substitution from ultrasonic sound  
absorption measurements*



Reaction	$k_{43}$ ( $s^{-1}$ )	$k_{34}$ ( $s^{-1}$ )	$r_{M^{2+}}$ ( $A^0$ )
$Be^{2+} + SO_4^{2-}$	$1.3 \times 10^3$	$1 \times 10^2$	0.35
$Mg^{2+} + SO_4^{2-}$	$8 \times 10^5$	$1 \times 10^5$	0.78
$Mg^{2+} + S_2O_3^{2-}$	$1.5 \times 10^6$	$1 \times 10^5$	0.78
$Mg^{2+} + CrO_4^{2-}$	$1.5 \times 10^6$	$1 \times 10^5$	0.78
$Ca^{2+} + CrO_4^{2-}$	$2 \times 10^8$	$2 \times 10^7$	0.99
$Mn^{2+} + SO_4^{2-}$	$2 \times 10^7$	$4 \times 10^6$	0.91
$Fe^{2+} + SO_4^{2-}$	$6 \times 10^6$	$1 \times 10^6$	0.83
$Co^{2+} + SO_3^{2-}$	$2.5 \times 10^6$	$2 \times 10^5$	0.82
$Ni^{2+} + SO_4^{2-}$	$1 \times 10^5$	$1.5 \times 10^4$	0.78
$Cu^{2+} + SO_4^{2-}$	$2 \times 10^8$	$> 10^7$	0.72
$Zn^{2+} + SO_4^{2-}$	$> 10^8$	$> 10^7$	0.83



Table (1.2)

*Kinetic data for  $SO_4^{=}$  substitution from ultrasonics sound  
absorption measurements*

	MgSO <sub>4</sub>	MnSO <sub>4</sub>
$k_{23}^a$ (s <sup>-1</sup> )	$7.2 \times 10^7$	$6.9 \times 10^7$
$k_{32}$ (s <sup>-1</sup> )	$3.7 \times 10^7$	$18.5 \times 10^7$
$K_{23}$	0.51	2.7
$k_{34}^b$ (s <sup>-1</sup> )	$1.4 \times 10^5$	$4.8 \times 10^7$
$k_{43}$ (s <sup>-1</sup> )	$8.0 \times 10^5$	$13.5 \times 10^6$
$K_{34}$	5.8	0.28

## Notes to table (1.2)

(a)  $k_{23}$  is essentially the same for the two salts. It is dependent on anion, and is considered to be "anion dehydration".

(b)  $k_{34}$  is virtually identical to the solvent exchange rate especially in the Mn<sup>2+</sup> case.

This step is considered to be "cation dehydration".

(2) *Basic kinetic terminology*

The three main mechanistic pathways stated initially, have been categorized by Langford and Gray<sup>9</sup> as follows,

Reaction (i)  $S_N1$  (*lim*), (D) process

Reaction (ii)  $S_N1$  ( $I_d$ ) or  $S_N2$  ( $I_a$ )

Reaction (iii)  $S_N2$  (*lim*), (A) process

The D (dissociative) mechanism<sup>9</sup> necessitates an intermediate of reduced coordination number, which is capable of surviving several molecular collisions before rapid association of the ligand, to form the complex. The rate of reaction will be *dependent* on the rate at which the *leaving group* dissociates and is therefore *dependent* on the *nature* of this *leaving group*. The rate will be *independent* of the *nature* of the *entering group* (neglecting effects of the entering group on the environment e.g. solvent effects). The D process will be *independent* of the ligand concentration at high ligand concentrations where a steady state situation arises.

The A (associative) process<sup>9</sup> has an intermediate of increased coordination number and the rate is *sensitive* to the *nature* of the *entering group*. The rate should show first order dependence on the entering group concentration. In this A process, both leaving and entering groups are participants in the transition state and therefore the entering group influences the activation energy determination.

When the I (interchange) mechanism has the *D like* transition state with only weak bonding to both entering and leaving groups, the rate of reaction will be *slightly dependent* on the *nature* of the *entering group* and the process is called ( $I_d$ ) dissociative interchange.<sup>10</sup> This *slight* dependence arises from the ligand/water competition ratio in the outer coordination sphere, for the vacant site on dissociation of the inner sphere coordinated water. The  $I_d$  process will be ligand concentration *independent* at high ligand concentrations where all the ligand exists in the ion pair complex as is discussed in detail later. This  $I_d$  mechanism postulated in outline as

early as 1958, is sometimes referred to as the "solvent assisted dissociative mechanism".

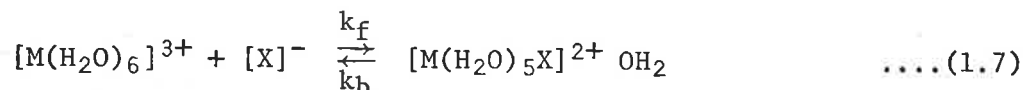
The reverse situation to that described above can occur, that is strong bonding in the transition state entering and leaving groups. This is denoted by the term  $I_a$  or  $S_N2$ .

Anation is the replacement of an aquo ligand by an anion. Aquation is the replacement of an anion with a water molecule. These two types of substitution are of wide interest. Anation is not as well documented as aquation but it is the former process which will be discussed later. In this general review, reactions will be discussed primarily to illustrate the methods employed to differentiate between D and  $I_d$  mechanisms.

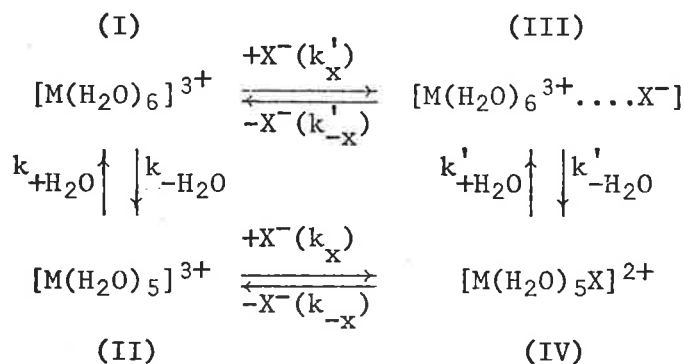
## (3) Anation Reactions of Labile Metal Ions

(i) Alternate Mechanistic Pathways, Dissociative (D) or Dissociative Interchange ( $I_d$ )

In a review by Sutin<sup>11</sup> the following reaction is discussed,



Two basic mechanistic pathways are indicated below,



(Reaction scheme as in reference 9)

If<sup>11</sup>  $k'_{-x} \gg k'_{-H_2O}$  then  $k_f$  and  $k_d$  the rate constants for formation and dissociation of  $[\text{M}(\text{H}_2\text{O})_5\text{X}]^{2+}$ , are given as follows,

$$k_f = K_{IP} k'_{-H_2O} + \frac{k_{-H_2O} k_x}{k_{+H_2O} + k_x [\text{X}^-]} \quad \dots(1.8)$$

$$k_d = k'_{+H_2O} + \frac{k_{+H_2O} k_{-x}}{k_{+H_2O} + k_x [\text{X}^-]} \quad \dots(1.9)$$

where  $K_{IP} = \frac{k'_x}{k'_{-x}}$  and is the outer sphere equilibrium association constant.

Since  $k_x \sim k'_x$  and  $k_{-H_2O} \sim k'_{-H_2O}$ , if  $k_{+H_2O} \gg k'_{-x}$  then under these conditions reaction scheme I  $\rightarrow$  III  $\rightarrow$  IV predominates with  $k_f = K_{IP} \cdot k'_{-H_2O}$  and  $k_d = k'_{+H_2O}$ .

With regard to the above ( $I_d$ ) mechanism the assumption is made that the solvent<sup>38-40</sup> exchange rate of the solvated metal ion is equal to the solvent exchange rate in the outer sphere (ion pair) complex. This is denoted

by the assumption that  $k_{-H_2O} \sim k'_{-H_2O}$ .

On the other hand if  $k'_{-x} \gg k_{+H_2O}$  then reaction sequence I  $\rightarrow$  II  $\rightarrow$  IV predominates with the rate constants for formation and dissociation of  $[M(H_2O)_5X]^{2+}$  now being as follows,

$$k_f = \frac{k_{-H_2O} k_x}{k_{+H_2O} + k_x [X^-]} \quad \text{and} \quad k_d = \frac{k_{+H_2O} k_{-x}}{k_{+H_2O} + k_x [X^-]} \quad \dots(1.10)$$

These expressions are arrived at by applying the steady state treatment in the reaction path I  $\rightarrow$  II  $\rightarrow$  IV.

The above discussion illustrates the differing rate expressions (for both formation and dissociation of  $[M(H_2O)_5X]^{2+}$ ) relative to the reaction path followed. The intermediates, of different lifetimes, formed in the two reaction paths, I  $\rightarrow$  II  $\rightarrow$  IV and I  $\rightarrow$  III  $\rightarrow$  IV are five coordinate and an outer sphere species respectively. The rate constants for many complex formation reactions have been shown to be independent of ligand concentration at high concentrations. This indicates mechanism I  $\rightarrow$  III  $\rightarrow$  IV under these conditions, but alternatively, path I  $\rightarrow$  II  $\rightarrow$  IV is followed with  $k_x [X^-] \ll 1$ . The underlying principles discussed above are the basis on which mechanistic arguments for specific anation reactions are proposed.

The study of formation of outer sphere (ion pair) complexes by rapid reaction techniques has shown two well defined steps. The first being the diffusion controlled step with the rates,

$$k_{12} \approx 10^9 - 10^{10} \text{ mol}^{-1} \text{ dm}^3 \text{ s}^{-1}$$

$$k_{21} \approx 10^8 - 10^{10} \text{ s}^{-1}$$

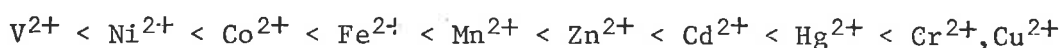
In the second step involving the formation of the outer sphere complex in which the central metal ion and the ligand are separated by a single water molecule, the rates are as follows,

$$k_{23} \approx 10^8 - 10^9 \text{ s}^{-1}$$

$$k_{32} \approx 10^7 - 10^{10} \text{ s}^{-1}$$

The subscripts refer to Equation (1.6), Eigen's<sup>4</sup> modified reaction sequence stated earlier.

Reactions<sup>11</sup> of  $[\text{Ni}(\text{H}_2\text{O})_6]^{2+}$  with various ligands have been studied and the second order formation rate constants were found to be in the range  $10^3$  to  $10^4 \text{ mol}^{-1} \text{ dm}^3 \text{ s}^{-1}$ . It is interesting to note that the second order rate constant for water exchange in the divalent hexa-aquo nickel complex is  $3 \times 10^3 \text{ mol}^{-1} \text{ dm}^3 \text{ s}^{-1}$  at 298K. This would support a D or  $I_d$  mechanism. Since the water exchange rate and the forward rate for inner sphere complex formation are similar then a table of water<sup>12</sup> exchange rates would be a measure of the lability of various divalent metal ion species. This order of water exchange is well documented<sup>13,13(a)</sup> and is as follows,



The slow rates of  $[\text{V}(\text{H}_2\text{O})_6]^{2+}$  ( $d^3$ ) and  $[\text{Ni}(\text{H}_2\text{O})_6]^{2+}$  ( $d^8$ ) are predicted on the basis of crystal field stabilization theory.

(ii) *Jahn Teller influence on solvated metal ion water exchange lability*

The rapid rates of  $[\text{Cr}(\text{H}_2\text{O})_6]^{2+}$  ( $d^4$ ) and  $[\text{Cu}(\text{H}_2\text{O})_6]^{2+}$  ( $d^9$ ) water exchange are attributed to the Jahn<sup>14</sup> Teller distortion of the octahedral structures.

The divalent copper hexaaquo complex exists in solution as a distorted octahedron consisting of four equatorial and two axial positions of very different bond character. The two ligands in the axial configuration are weakly held and therefore are readily replaceable. Different lifetimes in this coordination structure would be expected for water molecules in different spatial configurations. In the copper hexaaquo complex a rapid intramolecular transformation of the tetragonal structure makes all the positions equivalent and accounts for the rapid ligand exchange. The rate<sup>14</sup> of inversion (in which two equatorial positions become axial) will determine the rate of substitution of the much more strongly bound equatorial positions. Work carried out by Swift and Connick suggests water exchange at the axial positions. The water exchange rate for the divalent copper hexaaquo complex is

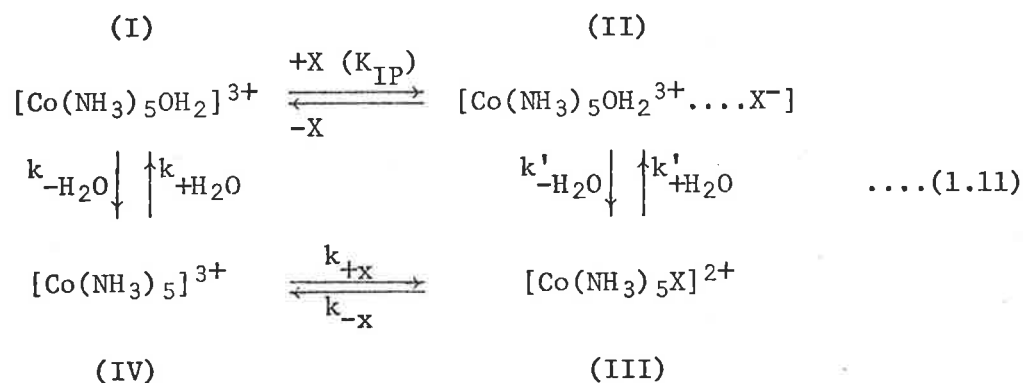
usually quoted as  $8 \times 10^9 \text{ s}^{-1}$ .<sup>15</sup> For the hexaaquo complexes of the divalent ions of  $\text{Cr}^{2+}$ ,  $\text{Ni}^{2+}$ ,  $\text{Co}^{2+}$  the values are,  $7 \times 10^9 \text{ s}^{-1}$ ,  $3 \times 10^4 \text{ s}^{-1}$  and  $1 \times 10^6 \text{ s}^{-1}$  respectively. Basolo<sup>13</sup> and Pearson have suggested that the axial elongation of the divalent copper hexaaquo complex results in reactions of this complex resembling those of square planar systems more closely than those of octahedral structure.

The very high lability<sup>16</sup> of the divalent copper ion species has significantly precluded investigation of this ion and this is the reason that the well documented reactions comprise  $\text{Co}^{2+}$ ,  $\text{Co}^{3+}$ ,  $\text{Ni}^{2+}$  and  $\text{Cr}^{3+}$  ions.

Chelation<sup>17,18</sup> of the divalent copper ion has been shown to dramatically reduce the water exchange rate, this is attributed to the removal of the intramolecular inversion process produced by the Jahn Teller effect. This reduced solvent exchange rate on chelation is fundamental to the work described in this thesis.

(4) *A Specific Anation Reaction*

Two possible mechanisms for the reaction are shown in the following reaction scheme,<sup>19</sup>



where  $K_{\text{IP}}$  is the outer sphere (ion pair) equilibrium association constant

Langford<sup>20</sup> and Muir proposed a mechanistic scheme in which the transition state is reached dissociatively but assumes no intermediate along the reaction pathway of sufficient stability to be selective in its reactions with the species in the outer coordination sphere. Reaction sequence  $\text{I} \rightarrow \text{II} \rightarrow \text{III}$  denotes this. For the latter reaction scheme, Langford and Stengle<sup>19</sup> proposed a dissociative interchange  $I_d$  mechanism. The intermediate species is weakened by partial bond weakening of the inner sphere coordinated water molecule. This unstable intermediate reacts with any available ligand in the outer coordination sphere. For a 1:1 outer-sphere (ion pair) complex, (S-1) of the outer sphere sites will be occupied by water molecules if S is the solvation number of the complex. If the anion occupies outer sphere sites randomly, dissociation of the coordinated water will not necessarily occur adjacent to the anion. Therefore (S-1)/S dissociative events will lead to anation. The  $I_d$  mechanism predicts anation to be approximately 1/S times the inner sphere water exchange rate ( $k_{\text{ex}}$ ).

For the  $I_d$ <sup>9,20</sup> mechanism a limiting rate should be reached at high anion concentration when the metal cations are completely ion paired and every subsequent dissociation within the ion pair leads to a substituted product. This limiting rate is graphically illustrated by Langford<sup>20</sup> and Muir. The



rates of  $[\text{Co}(\text{NH}_3)_5\text{X}]^{2+}$  formation from  $[\text{Co}(\text{NH}_3)_5\text{OH}_2]^{3+} \dots \text{X}^-$  have been reported relative to the water exchange rate, for  $\text{X} = \text{SO}_4^{=}$ ,<sup>20,21</sup>  $\text{Cl}^-$ ,  $\text{NCS}^-$  and  $\text{H}_2\text{PO}_4^-$ .<sup>22</sup> These values are 0.24, 0.21, 0.16, 0.13 respectively. These values vary by a factor of two for ligands differing in stability constants by about two powers of ten. Also the spread of values fits within the differences in their probability of occupancy of the outer sphere site adjacent to the leaving water molecule. This probability of occupancy depends on such factors as the size, shape and charge of the ligand in the outer sphere complex. All the above ratios suggest that the statistical factor ranges between  $1/8$  and  $1/5$ .

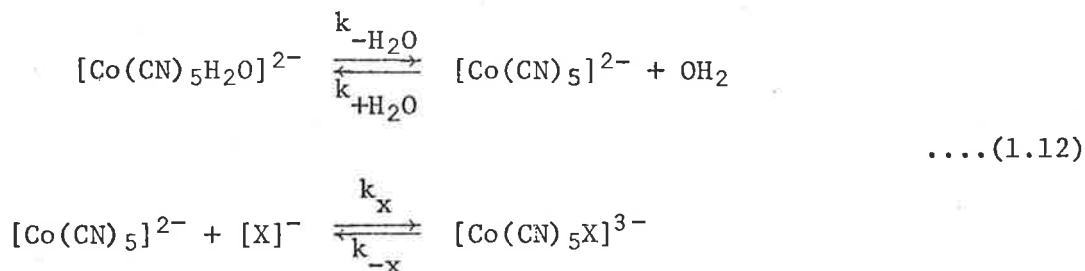
The statistical relation between  $k'_{-\text{H}_2\text{O}}$  and  $k_{\text{ex}}$  indicates that a  $[\text{Co}(\text{NH}_3)_5]^{3+}$  intermediate species is not formed. The inference that the probability of entry is determined by the initial population of the encounter complex shows that the entering group enters before re-arrangement of the encounter complex. Work by Pearson<sup>41</sup> and Moore confirms this idea. The labile nature of the intermediate, resulting in  $k_{\text{anation}}$  being less than  $k_{\text{water exchange}}$  is reflected in work by Duffy<sup>23</sup> and Earley who compared the rate of entry of  $\text{Cl}^-$  and  $\text{SCN}^-$  into  $[\text{Cr}(\text{NH}_3)_5\text{OH}_2]^{3+}$  to that of water exchange. From independent determination of ion association constants they estimated the anation rates in the ion pairs to be about 5% of the water exchange rate. Murray<sup>24</sup> and Barraclough found the rate of sulphate anation in the ion pair *cis*- $[\text{Co en}_2 (\text{OH}_2)_2]^{3+} \dots \text{SO}_4^{=}$  to be 0.25 times the water exchange of the free solvated metal cation. It is this statistical factor which distinguishes the  $\text{I}_d$  and D mechanisms. The D mechanism producing a longer lifetime, more selective, intermediate would show  $k_{\text{anation}}$  equal to  $k_{\text{water exchange}}$ .<sup>25</sup> The D mechanism (as does the  $\text{I}_d$  mechanism) would show a limiting rate when the concentration of the anion is such that it reacts with the intermediate as soon as it is formed. This leads to the steady state situation where the rate of formation of the intermediate is equal to the rate of its removal. This would result in the rate being independent of anion concentration at high anion concentrations.

For the reverse aquation reaction Langford calculated the linear free energy relationship by plotting the rates of aquation versus the negative logarithm of the equilibrium constants for a series of anions. The slope of this line is  $1.0^{26-28}$  which indicates that the environment of the leaving group in the transition state is the same as in the product. A dissociative process is envisaged for aquation.

In the various anation reactions of the complex  $[\text{Co}(\text{NH}_3)_5\text{OH}_2]^{3+}$  for a variety of anions, one anomaly<sup>29</sup> arises. In the case of  $\text{N}_3^-$  the  $k_{\text{anation}}$  ( $k'_{-\text{H}_2\text{O}}$ ) value equals the water exchange rate. This is explained by postulating that the azide anion is hydrogen bonded to the inner sphere coordinated water molecule. Thus as soon as the water molecule dissociates in the rate determining step, the azide ion immediately occupies the vacant site. Therefore the aligning nature of hydrogen bonding removes the statistical probability factor.

(5) Anation reactions exhibiting five coordinate intermediates in the (D) process

Reactions<sup>11,30-33</sup> of  $[\text{Co}(\text{CN})_5\text{H}_2\text{O}]^{2-}$  with  $\text{X}^-$  are described by the following reaction sequence,



Both water and  $\text{X}^-$  compete for the five coordinate intermediate  $[\text{Co}(\text{CN})_5]^{2-}$ . Outer sphere complexes are unlikely due to the like charges of the initial metal complex and the ligand. Applying the steady state treatment, the rate equation for formation of  $[\text{Co}(\text{CN})_5\text{X}]^{3-}$  is as follows,<sup>13,34</sup>

$$k_{\text{obs}} = \frac{k_{-\text{H}_2\text{O}}[\text{X}^-] + k_{+\text{H}_2\text{O}}k_{-\text{X}}/k_{\text{X}}}{\frac{k_{+\text{H}_2\text{O}}}{k_{\text{X}}} + [\text{X}^-]} \quad \dots(1.13)$$

and the various ratios of  $k_{+\text{H}_2\text{O}}/k_{\text{X}}$  have been calculated for  $\text{N}_3^-$ ,  $\text{SCN}^-$ ,  $\text{I}^-$  and  $\text{Br}^-$ . These ratios<sup>31,32</sup> are 1.9, 2.95, 5.15, 10.0 respectively. These numbers represent the relative efficiencies with which water competes with the various ligands for the  $[\text{Co}(\text{CN})_5]^{2-}$  intermediate.<sup>34,35</sup> The water exchange rate of  $[\text{Co}(\text{CN})_5\text{H}_2\text{O}]^{2-}$  has been measured using  $^{59}\text{Co}$  N.M.R. and is quoted as between  $1.0$  to  $1.3 \times 10^{-3} \text{ s}^{-1}$ . The value of  $k_{-\text{H}_2\text{O}}$  deduced from the anation studies of  $[\text{Co}(\text{CN})_5\text{H}_2\text{O}]^{2-}$  is given as  $1.6 \times 10^{-3} \text{ s}^{-1}$ . There is very good agreement between these two values which is required for a D mechanism. The aquation of  $[\text{Co}(\text{CN})_5\text{X}]^{3-}$  where  $\text{X} = \text{N}_3^-$ ,  $\text{NCS}^-$ ,  $\text{I}^-$ ,  $\text{Br}^-$ , as well as the reaction of  $[\text{Co}(\text{CN})_5\text{N}_3]^{3-}$  with  $\text{NCS}^-$ , show the same D mechanism.

There are a number of factors that support the five coordinate intermediate in the anation reaction of  $[\text{Co}(\text{CN})_5\text{H}_2\text{O}]^{2-}$ . One being the fact that negatively charged  $\text{CN}^-$  groups produce a high charge density at the cobalt atom which leads to weakening of the cobalt to oxygen bond. The rapid exchange

of water on the  $[\text{Co}(\text{CN})_5\text{H}_2\text{O}]^{2-}$  complex lends support to this argument. The weakening of the cobalt to oxygen bond lowers the activation energy for the  $\text{S}_{\text{N}}1$  (*lim*) reaction. The electron withdrawing facility of the  $\text{CN}^-$  groups stabilize the five coordinate intermediate by metal<sup>34</sup> to ligand  $\pi$  bonding.

Plots of the pseudo first order rates of anation versus anion concentration indicate definite curvature. This is to be expected based on earlier discussions for a D process. The rate equation for  $k_{\text{obs}}$  can be manipulated into a usable form by making reasonable assumptions. The results of this manipulation are well documented.

The generally accepted mechanisms discussed so far are also found for the nickel divalent<sup>3</sup> cation complex formation reactions. The basic premise remains, that the loss of water from the inner hydration sphere of the metal cation is rate determining. In nickel complexes it has been found that there is a labilizing<sup>37</sup> of the remaining water molecules upon successive substitution in the aquo ion.

## REFERENCES

1. D.J. Hewkin and R.H. Prince, *Coord. Chem. Revs.*, 5, 45 (1970).
2. C.H. Langford and V.S. Sastri, in "International Review of Science: Inorganic Chemistry, Series One Volume 9", M.L. Tobe, Ed., Butterworths, London., (1972), p 203.
3. C.H. Langford, *J. Chem. Educ.*, 46, 557 (1969).
4. M. Eigen and K. Tamm, *Z. Elektrochem.*, 66, 107 (1962).
5. G. Atkinson and S.K. Kor, *J Phys. Chem.*, 69, 128 (1965).
6. G. Atkinson and S. Petruccio, *J. Phys. Chem.*, 70, 3122 (1966).
7. M. Eigen, *Discuss Faraday Soc.*, 24, 25 (1957).
8. H.S. Frank and W.Y. Wen, *Discuss Faraday Soc.*, 24, 133 (1957-9)
9. "Ligand Substitution Processes", C.H. Langford and H.B. Gray, W.A. Benjamin, Inc., New York, (1965), p 14.
10. T.W. Swaddle, *Coord. Chem. Revs.*, 14, 217 (1974)
11. N. Sutin, *Ann. Rev. Phys. Chem.*, 17, 119 (1966).
12. T.J. Swift and R.E. Connick, *J. Chem. Phys.*, 37, 307 (1962).
13. "Mechanisms of Inorganic Reactions", F. Basolo and R.G. Pearson, Wiley, 2nd Edn, New York., (1967), p 152.
- 13(a) K. Kustin and J. Swinehart, in "Progress in Inorganic Chemistry", J.O. Edwards, Ed., Interscience, New York., (1970), p 107.
14. R. Poupko and Z. Luz, *J. Chem. Phys.*, 57, 3311 (1972).
15. R.E. Connick and R.S. Marianelli, *Abst. Amer. Chem. Soc. Div. Phys. Chem. Summer Symposium.*, Buffalo, June, (1965).
16. M. Eigen, *Pure and Applied Chemistry.*, 6, 105 (1963).
17. D.B. Rorabacher and D.W. Margerum, *Inorg. Chem.*, 3, 382 (1964).
18. D.W. Margerum and R.K. Steinhaus, *J. Amer. Chem. Soc.*, 87, 4643 (1965).
19. C.H. Langford and T.R. Stengle, *Ann. Rev. Phys. Chem.*, 19, 193 (1968).

20. C.H. Langford and W.R. Muir, *J. Amer. Chem. Soc.*, 89, 3141 (1967).
21. H. Taube and F.A. Posey, *J. Amer. Chem. Soc.*, 75, 1463 (1953).
22. W. Schmidt and H. Taube, *Inorg. Chem.*, 2, 698 (1963).
23. N.V. Duffy and J.E. Earley, *J. Amer. Chem. Soc.*, 89, 816 (1967).
24. R. Murray and C. Barraclough, *J. Chem. Soc.*, 7047 (1965).
25. A.M. Chmelnick and D. Fiat, *J. Chem. Phys.*, 47, 3986 (1967).
26. F. Basolo, in "Xth International Conference on Coordination Chemistry," Plenary Lectures, Plenum Press, New York., (1967), p 37.
27. C.H. Langford, *Inorg. Chem.*, 4, 265 (1965).
28. N.A. Maes, M.S. Nozari and J.A. McLean, *Inorg. Chem.*, 12, 750 (1973).
29. T.W. Swaddle and G. Guastella, *Inorg. Chem.*, 8, 1604 (1969).
30. A. McAuley and J. Hill, *Quart Revs.*, 23, 33 (1969).
31. A. Haim and W.K. Wilmarth, *Inorg. Chem.*, 1, 573, 583 (1962).
32. A. Haim, R.J. Grassi and W.K. Wilmarth, *Adv. Chem. Ser.*, 49, 31 (1965).
33. "Inorganic Reaction Mechanisms", M.L. Tobe, Nelson, London., (1972), p 92.
34. A. Haim, R.J. Grassi and W.K. Wilmarth, *Inorg. Chem.*, 6, 237, 243 (1967).
35. A. Haim and H. Taube, *Inorg. Chem.*, 2, 1199 (1963).
36. J.P. Hunt and R.H. Plane, *J. Amer. Chem. Soc.*, 76, 5960 (1954).
37. A.C. Desai, H.W. Dodgen and J.P. Hunt, *J. Amer. Chem. Soc.*, 92, 798 (1970).
38. F. Monacelli, *Inorg. Chim. Acta.*, 2, 263 (1968).
39. E. Borghi, F. Monacelli and T. Prospero, *Inorg. Nucl. Chem. Lett.*, 6, 667 (1970).
40. E. Borghi and F. Monacelli, *Inorg. Chim. Acta.*, 5, 211 (1971).
41. R.G. Pearson and J.W. Moore, *Inorg. Chem.*, 3, 1334 (1964).

I (C) Crystal field stabilization effect on transition metal ions (C.F.S.E.)<sup>23</sup>

Transition metal complexes are stabilized<sup>1</sup> (C.F.S.E.) by placing non-bonding electrons in d orbitals spatially distributed away from the ligands. The five d orbitals are not spatially<sup>2</sup> equivalent. In an octahedron, three of the d orbitals ( $d_{xy}$ ,  $d_{yz}$ ,  $d_{xz}$ ) are directed between the ligands and therefore certain electrons are of lower energy than those in the two orbitals ( $d_{x^2-y^2}$ ,  $d_{z^2}$ ), directed towards the ligands. FIG.(1.1) shows the energy level diagrams for both trigonal bipyramidal and octahedral systems. The C.F.S.E.<sup>3</sup> is only a small part of the bonding energies in any system. There will be large contributions towards the activation energy from ligand to ligand repulsions, metal to ligand attractions etc. The C.F.S.E.<sup>4</sup> is calculated for various structures corresponding to the initial configuration and the final complex arrangement. The loss or gain of C.F.S.E. for a reaction in a particular direction can be estimated in units of  $D_q$ .

Looking at the stabilization<sup>3</sup> energies, systems can be grouped,

$d^3, d^6, d^8$	these systems have an unfavourable C.F.S.E. shown by a reduced lability for a particular reaction.
$d^0, d^1, d^2, d^5, d^{10}$	never lose any C.F.S.E.
$d^4, d^9$	these systems have a favourable C.F.S.E. reflected in high water exchange rates (increased lability).

The Jahn Teller effect discussed briefly for the divalent copper hexaquo complex is referred to in more detail by Kettle.<sup>5</sup>

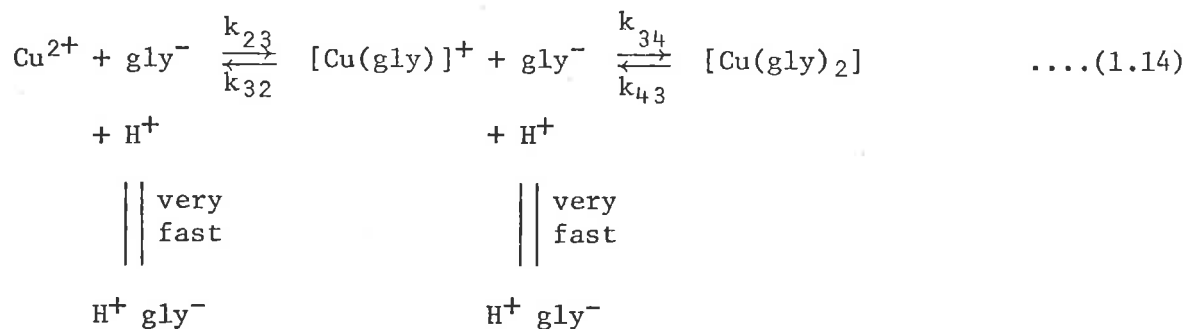
## REFERENCES

1. "Inorganic Reaction Mechanisms", J.O. Edwards, W.A. Benjamin, Inc., New York, (1965), p 92.
2. "Electronic Spectra of Transition Metal Complexes", D. Sutton, McGraw-Hill, London., (1968), p 104.
3. "Mechanisms of Inorganic Reactions", F. Basolo and R.G. Pearson, Wiley, 2nd Edn, New York., (1967), p 65.
4. "Coordination Chemistry", F. Basolo and R. Johnson, W.A. Benjamin, Inc., New York, (1964), p 38.
5. "Coordination Compounds", S.F.A. Kettle, Nelson, London., (1969), p 110.

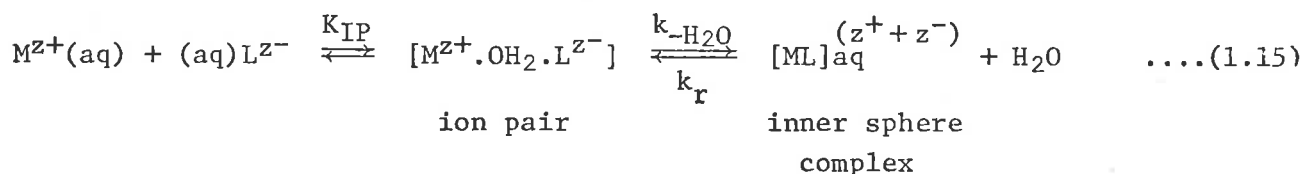


## I (D) Substitution reactions of copper chelates

Pearlmutter<sup>1</sup> and Stuehr reported the copper glycine reactions and the postulated mechanism is as follows,



As described previously the general method of complex formation is based on the Eigen postulate with the release of inner sphere coordinated water as the rate determining step. This is shown schematically in the following mechanism,



The  $k_{\text{formation}}$  for the first and second glycine substitutions ( $k_{23}$  and  $k_{34}$  respectively) is given by the general equation,

$$k_f = K_{\text{IP}} \frac{\gamma_+ \gamma_-}{\gamma^\ddagger} k_{-\text{H}_2\text{O}} \dots(1.16)$$

where  $K_{\text{IP}}$ , the ion pair association constant, was calculated independently using the Fuoss equation.

The activity coefficients for the reacting species and the transition state were calculated using the Davies<sup>2</sup> equation.

The uni-molecular rate constant, ( $k_{-\text{H}_2\text{O}}$ ) is the rate of removal of inner sphere coordinated water from the ion pair. The results for the successive glycine substitutions indicated in equation (1.14) are shown in the following table abstracted from the reference by Pearlmutter<sup>1</sup> and Stuehr,

Table (1.3)

$$\text{Cu}(\text{gly})_{n-1} + \text{gly} \rightleftharpoons \text{Cu}(\text{gly})_n$$

n	$k_{\text{forward}}$ mol <sup>-1</sup> dm <sup>3</sup> s <sup>-1</sup>	$k_{-\text{H}_2\text{O}}$ s <sup>-1</sup>	$k_{\text{reverse}}$ s <sup>-1</sup>
1	$4.0 \times 10^9$	$2 \times 10^9$	34
2	$4.9 \times 10^8$	$5 \times 10^8$	50

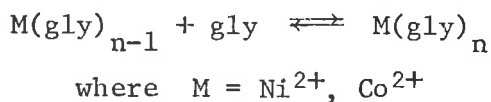
The value of water exchange ( $k_{\text{ex}}$ ) in the primary hydration sphere for the divalent copper hexaquo complex is usually quoted as  $\geq 3 \times 10^9 \text{ s}^{-1}$  from O<sup>17</sup> studies.<sup>3,4</sup> There is good agreement between the  $k_{-\text{H}_2\text{O}}$  for the first glycine attack and the  $k_{\text{ex}}$  value. Work on the divalent copper acetate system gave a value of  $k_{-\text{H}_2\text{O}} \approx 1 \times 10^9 \text{ s}^{-1}$ .

If the positions on the divalent copper ion were strongly bound by the entering ligand, then the axial - equatorial inversion process would be impeded. This would be evident in that a slower rate of water exchange for the second glycine addition would be expected. In fact this does occur and is reflected in the  $k_{-\text{H}_2\text{O}}$  value being  $5 \times 10^8 \text{ s}^{-1}$ .

The rate constants for the formation of divalent copper complexes with  $\alpha$  alanate<sup>5</sup> were measured. The forward rate constants for  $\alpha$  alanate ( $1.3 \times 10^9$  and  $1.5 \times 10^8 \text{ mol}^{-1} \text{ dm}^3 \text{ s}^{-1}$ ) for the first and second addition illustrate "normal" kinetics of divalent copper. Comparison of  $k_{\text{forward}}$  for the  $\alpha$  alanate reaction with the corresponding glycine data show very good agreement. Also the  $k_{-\text{H}_2\text{O}}$  values can be compared for the systems studied. These values for mono substitution are  $\geq 3 \times 10^9$ ,  $\approx 1 \times 10^9$ ,  $2 \times 10^9$ ,  $1 \times 10^9 \text{ s}^{-1}$  for the copper aquo, acetate, glycinate and  $\alpha$  alanate respectively.

Hammes<sup>6</sup> and Steinfeld reported work on the divalent nickel and cobalt glycine systems. The results are as follows,

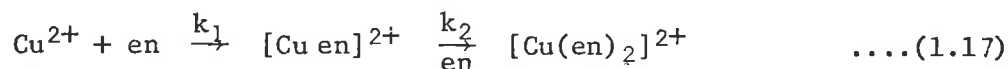
Table (1.4)



	n	$k_{-\text{H}_2\text{O}} (\text{s}^{-1})$
Ni <sup>++</sup>	1	$0.9 \times 10^4$
	2	$1.2 \times 10^5$
	3	$4.0 \times 10^5$
Co <sup>++</sup>	1	$2.6 \times 10^5$
	2	$4.4 \times 10^6$
	3	$8.6 \times 10^6$

These values agree reasonably well with the respective water exchange rates ( $k_{\text{ex}}$ ). The data shows a difference from the copper glycine system in that the rate constants increase with successive association of the ligand with the metal. This is interpreted as loosening of the water molecules in the primary hydration sphere. This weakening being due to drainage of positive charge from the metal ion, between it and the negatively charged carboxyl groups of the glycine ion. Reactions of divalent nickel and cobalt with diglycine do not show this increase in rate and the reason postulated by Rosenberg<sup>7</sup> is that bonding takes place through the amino nitrogen and the oxygen of the peptide carbonyl group.

Roche<sup>8,9</sup> and Wilkins reported work on divalent copper substitutions which obeyed the normal divalent copper reaction scheme. Also Kirschenbaum<sup>10</sup> and Kustin reported work on the reaction,



en = ethylenediamine

where  $k_1 = (3.8 \pm 1.6) \times 10^9 \text{ s}^{-1}$

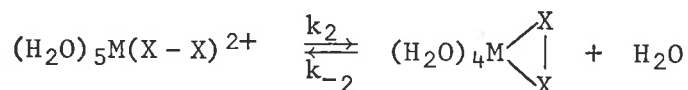
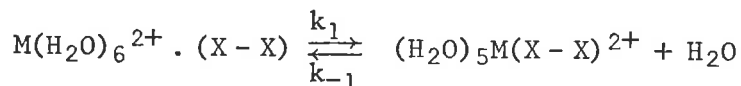
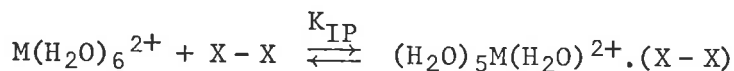
$k_2 = (1.9 \pm 0.3) \times 10^9 \text{ s}^{-1}$

$$k_{-1} = 1 \times 10^{-1} \text{ s}^{-1}$$

$$k_{-2} = 1.5 \text{ s}^{-1}$$

The values for en substitution agree very well with water exchange rates of the hexaaquo divalent copper ion complex.

Finally the general reaction scheme for chelation is,<sup>11</sup>



where X-X is a bidentate ligand

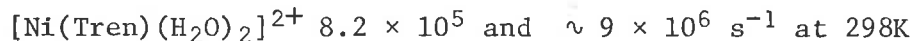
Providing  $k_2 \gg k_{-1}$  then complex formation has as its rate determining step the replacement of the inner sphere coordinated water of the metal ion. The rate of dissociation depends on the rupture of the second metal ion, donor atom ligand bond. The rate<sup>12</sup> constants for the formation of  $[\text{Ni}(\text{py})(\text{H}_2\text{O})_5]^{2+}$ ,  $[\text{Ni}(\text{bipy})(\text{H}_2\text{O})_4]^{2+}$  and  $[\text{Ni}(\text{terpy})(\text{H}_2\text{O})_3]^{2+}$  are all about  $2 \times 10^3 \text{ mol}^{-1} \text{ dm}^3 \text{ s}^{-1}$  at 298K which suggests a common rate determining step. The same similarity of rate for polyamine complexes of nickel occurs. This suggests a similar rate determining step. For reactions of  $[\text{Ni}(\text{H}_2\text{O})_6]^{2+}$  with en, dien and trien, the loss of coordinated water from the inner sphere coordination shell of the metal cation is rate determining. This observation only occurs when the two donor atoms are the same.

## REFERENCES

1. A.F. Pearlmutter and J.E. Stuehr, *J. Amer. Chem. Soc.*, 90, 858 (1968).
2. "Ion Association", C.W. Davies, Butterworth, Inc., Washington D.C., (1962), p 41.
3. C.W. Meredith, Ph.D. Thesis, University of California, Berkeley (1965).
4. J. Swift and R.E. Connick, *J. Chem. Phys.*, 37, 307 (1962).
5. W.B. Makinen, A.F. Pearlmutter and J.E. Stuehr, *J. Amer. Chem. Soc.*, 91, 4083 (1969).
6. G.G. Hammes and J.I. Steinfeld, *J. Amer. Chem. Soc.*, 84, 4639 (1962).
7. A. Rosenberg, *Acta Chem. Scand.*, 11, 1390 (1957).
8. T.S. Roche and R.G. Wilkins, *J. Amer. Chem. Soc.*, 96, 5082 (1974).
9. T.S. Roche and R.G. Wilkins, *Chem. Comm, D.*, 1681 (1970).
10. L.J. Kirschenbaum and K. Kustin, *J. Chem. Soc, A.*, 684 (1970).
11. N. Sutin, *Ann. Rev. Phys. Chem.*, 17, 119 (1966).
12. R.G. Wilkins, *Accounts Chem. Res.*, 3, 411 (1970).

I (E) General review of reactions of  $[M(\text{Tren})\text{OH}_2]^{2+}$  and  $[M(\text{Me}_6\text{Tren})\text{OH}_2]^{2+}$  and their substituted analogues

The water exchange kinetics of Tren complexes of divalent nickel and copper are reported as follows,<sup>1</sup>



The  $\Delta H^\ddagger$  values are all positive and in the range 33.4 to 41.8 kJ mol<sup>-1</sup> the two values for water exchange in the nickel complex result from the two bound water molecules in a *cis* octahedral arrangement reacting at different rates.

Cayley *et al.*<sup>2</sup> provide evidence for reactions of divalent copper complexes occurring at slower rates when the Jahn Teller distortion is removed. The substitutions of the divalent copper hexaquo complexes are as described earlier,<sup>3-5</sup> with the rate determining step being substitution into the axial coordination position, followed by Jahn Teller<sup>6</sup> inversion. Providing there are two water molecules in a *cis* configuration in the reacting complex, the substitution of divalent copper follows the usual pattern. The presence of Tren<sup>2</sup> in the inner coordination sphere of divalent copper reduces the formation constant by a factor of 3000 compared to reactions with the divalent copper hexaquo complex. The reverse aquation reaction for the  $[\text{Cu}(\text{Tren})\text{-imidazole}]^{2+}$  complex is also approximately 3000 times slower than the corresponding aquation of the complex,  $[\text{Cu}(\text{H}_2\text{O})_5\text{imidazole}]^{2+}$ . Therefore the stability constants for the formation of final complexes for both  $[\text{Cu}(\text{H}_2\text{O})_6]^{2+}$  and  $[\text{Cu}(\text{Tren})\text{H}_2\text{O}]^{2+}$  with imidazole, are the same. Table (1.5) has been abstracted from the reference by Cayley *et al.*<sup>2</sup> and shows the formation rate constants for substitution reactions of Cu<sup>II</sup> complexes at 298K.

The lack of dependence of the formation rate constants on the nature of the incoming ligand once again substantiates the usual mechanism of substitution at the labile metal ion centre, that is I<sub>d</sub>.

In the case of divalent<sup>7-9</sup> nickel and cobalt the increased number of

nitrogen atoms in the inner sphere leads to a faster rate of complex formation and water exchange. The slower formation constants for divalent copper tren could be explained by slow solvent exchange at the "equatorial<sup>2</sup> like" water without the assistance of the Jahn Teller effect. This water exchange is now comparable to metal ions of similar radius e.g.<sup>11</sup>  $[\text{Co}(\text{H}_2\text{O})_6]^{2+} + \text{NH}_3$ ;  $k_f = 1.1 \times 10^5 \text{ mol}^{-1} \text{ dm}^3 \text{ s}^{-1}$ .

Lincoln<sup>12</sup> and West examined the solvent exchange rate for  $[\text{Cu}(\text{MeCN})_6]^{2+}$  and  $[\text{Cu}(\text{Tren})(\text{MeCN})]^{2+}$  in acetonitrile. Acetonitrile is at least 3000 times more labile in  $[\text{Cu}(\text{MeCN})_6]^{2+}$  than in  $[\text{Cu}(\text{Tren})(\text{MeCN})]^{2+}$ . The opposite effect occurs in the nickel and cobalt<sup>15</sup> analogous systems.

In the case of  $[\text{Cu}(\text{MeCN})_6]^{2+}$  there is a Jahn Teller effect present, with an associated inversion process. The interconversion time being approximately  $10^{-11}$  seconds.<sup>13,14</sup> The long axial copper nitrogen bonds result in lower  $\Delta H^\ddagger$  values for exchange than in the cobalt and nickel systems. The six acetonitrile positions are labilized as in the hexaquo complex by intramolecular inversion. The divalent nickel and cobalt hexa acetonitrile complexes do not exhibit Jahn Teller effects.

The formation of  $[\text{Cu}(\text{Tren})(\text{MeCN})]^{2+}$  removes the Jahn Teller process for acetonitrile exchange and this loss in lability is not overcome by the  $\text{NH}_2$  group, electron donation.

The different water exchange rates of  $[\text{Cu}(\text{H}_2\text{O})_6]^{2+}$  and  $[\text{Cu}(\text{Tren})\text{H}_2\text{O}]^{2+}$  complexes will be examined in the light of the suppression of the Jahn Teller effect.

Table (1.5)

*Formation rate constants for substitution reactions  
of Cu<sup>II</sup> complexes (298K)*

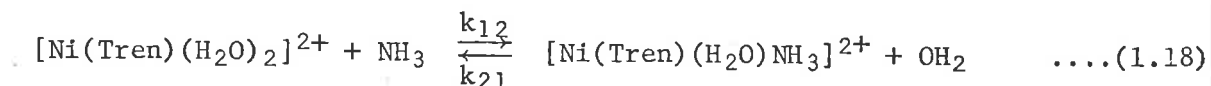
	$k_f/\text{mol}^{-1} \cdot \text{dm}^3 \text{s}^{-1}$	$k_d/\text{s}^{-1}$	Ref.
$[\text{Cu}(\text{H}_2\text{O})_6]^{2+}$ imidazole	$5.7 \times 10^8$	$2.6 \times 10^4$	10
$[\text{Cu}(\text{Tren})(\text{H}_2\text{O})]^{2+}$ + pyridine	$1.6 \times 10^5$	$1.7 \times 10^3$	2
$[\text{Cu}(\text{Tren})(\text{H}_2\text{O})]^{2+}$ + 3-methyl pyridine	$1.8 \times 10^5$	$9.4 \times 10^2$	2
$[\text{Cu}(\text{Tren})(\text{H}_2\text{O})]^{2+}$ + 4-methyl pyridine	$2.4 \times 10^5$	$8.0 \times 10^2$	2
$[\text{Cu}(\text{Tren})(\text{H}_2\text{O})]^{2+}$ + imidazole	$\approx 2.0 \times 10^5$	$\approx 150$	2
$[\text{Cu}(\text{Tren})(\text{H}_2\text{O})]^{2+}$ + $\text{H}_2\text{O}$	$2.5 \times 10^{5b}$	-	1
$[\text{Cu}(\text{en})(\text{H}_2\text{O})_4]^{2+}$ + pada <sup>c</sup>	$\approx 3.5 \times 10^8$	$\approx 1.0 \times 10^4$	6
$[\text{Cu}(\text{dien})(\text{H}_2\text{O})_3]^{2+}$ + pada <sup>c</sup>	$1.0 \times 10^8$	$5.0 \times 10^4$	6

<sup>b</sup> First order rate constant, units  $\text{s}^{-1}$ .

<sup>c</sup> Rate constants from ref. 6 have been converted to overall rate constants rather than statistically adjusted constants as reported.



Substitution reactions have been carried out on the replacement of bound water with ammonia<sup>16</sup> in  $[\text{Ni}(\text{Tren})(\text{H}_2\text{O})_2]^{2+}$ , as well as other nickel polyamine complexes, using stopped flow methods.



$$\begin{aligned} k_{12} &= 2.6 \times 10^5 \text{ mol}^{-1} \text{ dm}^3 \text{ s}^{-1} \\ k_{21} &= 4.9 \times 10^3 \text{ s}^{-1} \end{aligned} \quad \text{at 279K}$$

For the trien<sup>19</sup> nickel complex reaction with ammonia, the rate data is as follows,

$$\begin{aligned} k_{12} &= 1.2 \times 10^5 \text{ mol}^{-1} \text{ dm}^3 \text{ s}^{-1} \\ k_{21} &= 7.6 \times 10^2 \text{ s}^{-1} \end{aligned} \quad \text{at 279K}$$

The  $k_{12}$  values compare favourably with the  $[\text{Ni}(\text{Tren})(\text{H}_2\text{O})_2]^{2+}$  water exchange value of  $8.2 \times 10^5 \text{ s}^{-1}$ .

The acetonitrile exchange data in various nickel complexes is tabulated below,<sup>15</sup>

1.  $[\text{Ni}(\text{Tren})(\text{CH}_3\text{CN})_2]^{2+}$ 

$$k_{1\alpha} = 165 \times 10^3 \text{ s}^{-1} \text{ at 298K}$$

$$k_{1\beta} = > 2000 \times 10^3 \text{ s}^{-1} \text{ at 313K}$$

where  $k_{1\alpha}$  and  $k_{1\beta}$  are the rate constants for acetonitrile exchange on the two acetonitrile coordinated sites.
2.  $[\text{Ni}(\text{CH}_3\text{CN})_6]^{2+}$ 

$$k_1 = 2 \times 10^3 \text{ s}^{-1} \text{ at 298K}$$
3.  $[\text{Ni}(\text{Me}_6\text{Tren})(\text{CH}_3\text{CN})]^{2+}$ 

$$k_1 \text{ is less than } 0.1 \times 10^3 \text{ s}^{-1} \text{ at 353K}$$

The two acetonitrile exchange values in the first complex indicate two different environments<sup>18</sup> as seen in  $[\text{Ni}(\text{Tren})(\text{H}_2\text{O})_2]^{2+}$ . The single exchange value for  $[\text{Ni}(\text{Me}_6\text{Tren})(\text{CH}_3\text{CN})]^{2+}$  is due to the single site in the sterically crowded five coordinated complex.

Similar studies at 298K on cobalt complexes are reported,<sup>15</sup>

1.  $[\text{Co}(\text{Tren})\text{CH}_3\text{CN}]^{2+}$ 

$$k_1 > 2000 \times 10^3 \text{ s}^{-1}$$
2.  $[\text{Co}(\text{CH}_3\text{CN})_6]^{2+}$ 

$$k_1 \approx 320 \times 10^3 \text{ s}^{-1}$$
3.  $[\text{Co}(\text{Me}_6\text{Tren})\text{CH}_3\text{CN}]^{2+}$ 

$$k_1 \text{ is less than } 0.1 \times 10^3 \text{ s}^{-1} \text{ at 353K}$$

The above data shows solvent labilisation<sup>19</sup> on polydentate ammine complexation but not in the case of  $[M(\text{Me}_6\text{Tren})\text{CH}_3\text{CN}]^{2+}$  complexes of cobalt and nickel.

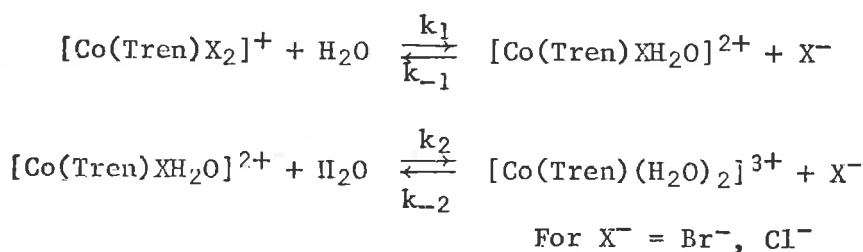
The acetonitrile exchange reactions of  $[\text{Co}(\text{Tren})\text{CH}_3\text{CN}]^{2+}$  and  $[\text{Co}(\text{Me}_6\text{Tren})\text{CH}_3\text{CN}]^{2+}$  were compared by West.<sup>17</sup> It was found that the loosely coordinate Tren complex exhibited a similar lability (for acetonitrile exchange) to other solvated divalent cobalt species. The more rigidly five coordinate  $\text{Me}_6\text{Tren}$  complex underwent solvent exchange at a rate which was too slow to be measured by N.M.R. techniques ( $< 0.1 \times 10^3 \text{ s}^{-1}$ ). The same thing occurred for the  $[\text{Ni}(\text{Me}_6\text{Tren})\text{CH}_3\text{CN}]^{2+}$  complex. It is suggested that the bulky  $\text{Me}_6\text{Tren}$  complex prevents close approach of the solvent to the metal ion and hinders rapid solvent exchange. The reduced flexibility of the more sterically crowded complexes may preclude geometrical re-arrangement in the transition state.

The kinetics of water replacement by  $\text{NH}_3$  and chelating nitrogen ligands in  $[\text{Ni}(\text{Tren})(\text{H}_2\text{O})_2]^{2+}$  have been reported,<sup>20</sup>

	$k_f$ ( $\text{mol}^{-1} \text{ dm}^3 \text{ s}^{-1}$ )	
$\text{NH}_3$	$260 \times 10^3$	
phen	$13 \times 10^3$	
orn $\text{H}^+$	$12 \times 10^3$	orn = $(\text{NH}_3(\text{CH}_2)_3\text{CH}(\text{NH}_2)\text{COO}^-)$
bipy	$10 \times 10^3$	
gly	$90 \times 10^3$	

The formation rate constants are similar for the range of ligands shown above. The  $\text{NH}_3$  ligand is both small and unidentate and this may account for the higher  $k_f$  value.

Reactions of trivalent cobalt polyamine complexes in the aquation path are shown in the following scheme,<sup>19</sup>



These reactions have been outlined by Zipp, Zipp and Madan.<sup>19</sup>

The bromide anation reaction of  $[\text{Co}(\text{Tren})(\text{OH}_2)_2]^{3+}$  has been studied,  $k_{\text{an}} \sim 10^{-4} \text{ mol}^{-1} \text{ dm}^3 \text{ s}^{-1}$  at ionic strength equal to  $2.0 \text{ mol dm}^{-3}$ . The  $\Delta H^\ddagger$  and  $\Delta S^\ddagger$  values are  $105 \text{ kJ mol}^{-1}$  and  $0.79 \text{ J deg}^{-1} \text{ mol}^{-1}$  respectively. The mechanism for the anation is believed to be an outer sphere to inner sphere interchange process ( $I_d$ ).

The rate of primary acid hydrolysis of the dichloro, dibromo and difluoro Tren species has been compared with the rates of the corresponding *cis*-bis(ethylenediamine)cobalt III complexes.

The rate ratio  $[\text{Co}(\text{Tren})\text{X}_2]^+ / [\text{Co}(\text{en})_2\text{X}_2]^+$  is found to be 30, 12, 3 for dibromo, dichloro and difluoro respectively. This acceleration<sup>22</sup> of the first aquation for the cobalt III Tren species has been attributed to the combined effects of strain caused by the coordinated Tren molecule and the geometric arrangement of Tren, which causes steric crowding at the halide position *cis* to the tertiary nitrogen of Tren.

Miller<sup>23,24</sup> and Madan studied the aquation of both  $[\text{Co}(\text{Tren})\text{ClH}_2\text{O}]^{2+}$  and  $[\text{Co}(\text{Tren})\text{BrH}_2\text{O}]^{2+}$ . The chloro aquo complex is found to react 1.5 times faster than the corresponding ethylenediamine complex. Similar comparison is made for the bromo aquo complex. This shows that the second halide ion is considerably less labile than the first, due to the loss of some of the strain in the complex.

The aquation of  $[\text{Co}(\text{Tren})\text{ClBr}]^+$  was reported<sup>22</sup> to proceed via two parallel pseudo first order reactions. One releases chloride, the other bromide. For aquation of  $[\text{Co}(\text{Tren})\text{ClBr}]^+$ ,

$$k_\alpha = 3.21 \times 10^{-3} \text{ s}^{-1}$$

$$k_\beta = 3.38 \times 10^{-2} \text{ s}^{-1}$$

where  $\alpha$  and  $\beta$  refer to release of chloride and bromide respectively from the  $\alpha$  and  $\beta$  isomers

These agree reasonably well with values for the aquation<sup>22</sup> of

$$[\text{Co}(\text{Tren})\text{Cl}_2]^+ \quad k_{1\text{Cl}} \quad 2.96 \times 10^{-3} \text{ s}^{-1}$$



$$k_{1\text{Br}} \quad 2.84 \times 10^{-2} \text{ s}^{-1}$$

It can be concluded<sup>22</sup> that, during the primary aquation of the chlorobromo species, the halide ligand which is *trans* to the tertiary nitrogen of the tren has very little effect on the leaving group, which is *cis* to the tertiary nitrogen of the tren ligand.

The work outlined in this section is intended as a guide to the present state of research in Tren and Me<sub>6</sub>Tren ligand and water exchange substitution reactions. The little work reported is confined to the slower reacting divalent and trivalent, cobalt and nickel systems. My research interest was confined the ligand substitution on the two complexes, [Cu(Tren)H<sub>2</sub>O]<sup>2+</sup> and [Cu(Me<sub>6</sub>Tren)H<sub>2</sub>O]<sup>2+</sup> and the results are reported in this thesis.

## REFERENCES

1. P. Rablen, W. Dodgen and J.P. Hunt, *J. Amer. Chem. Soc.*, 94, 1771 (1972).
2. G. Cayley, D. Cross and P. Knowles, *Chem. Comm.*, 13, 837 (1976).
3. D.J. Hewkin and R.H. Prince, *Coord. Chem. Revs.*, 5, 45 (1970).
4. M. Eigen and R.G. Wilkins, *Adv. Chem. Ser.*, 49, 55 (1965).
5. T.S. Roche and R.G. Wilkins, *J. Amer. Chem. Soc.*, 96, 5082 (1974).
6. M. Eigen, *Ber. Bunsenges Phys. Chem.*, 67, 753 (1963).
7. D.W. Margerum and H.M. Rosen, *J. Amer. Chem. Soc.*, 89, 1088 (1967).
8. J.P. Hunt, *Coord. Chem. Revs.*, 1, 1 (1971).
9. D.F. Rablen, H.W. Dodgen and J.P. Hunt, *Inorg. Chem.*, 15, 931 (1976).
10. H. Diebler and Ph. Rosen, *Ber. Bunsenges Phys. Chem.*, 76, 1031 (1972).
11. D.B. Rorabacher, *Inorg. Chem.*, 5, 1891 (1966).
12. R. J. West and S.F. Lincoln, *J. Chem. Soc, Dalton.*, 281 (1974).
13. A.L. Companion, *J. Phys. Chem.*, 73, 739 (1969).
14. A. McAuley and J. Hill, *Quart. Revs.*, 23 27 (1969).
15. R.J. West and S.F. Lincoln, *Inorg. Chem.*, 12, 494 (1973).
16. J.P. Jones, E.J. Billo and D.W. Margerum, *J. Amer. Chem. Soc.*, 92, 1875 (1970).
17. R.J. West, Ph.D. Thesis, University of Adelaide (1973).
18. S.E. Rasmussen, *Acta Chem. Scand.*, 13, 2009 (1959).
19. S.G. Zipp, A.G. Zipp and S.K. Madan, *Coord. Chem. Revs.*, 14, 29 (1974).
20. R.G. Wilkins, *Accounts Chem. Res.*, 3, 411 (1970).
21. K. Kuo and S.K. Madan, *Inorg. Chim. Acta.*, 7, 110 (1973).
22. S.T. Yuan, W.V. Miller and S.K. Madan, *Inorg. Chim. Acta.*, 7, 134 (1973).
23. W.V. Miller and S.K. Madan, *Inorg. Chem.*, 10, 1250 (1971).
24. W.V. Miller and S.K. Madan, *Inorg. Chem.*, 9, 2362 (1970).

## CHAPTER TWO

## I Reagents and Materials (Analysis and Preparation)

## II (A) Kinetic Techniques and Principles

- (i) *Temperature Jump Relaxation Kinetics*
- (ii) *The Temperature Jump Method*
- (iii) *Analysis of Data*
- (iv) *Amplitude Considerations*
- (v) *Calibration of the Temperature Rise*

(B) (i) *The Stopped Flow Method*

- (ii) *Experimental Limitations*

## III Equipment used in Spectrophotometric Analysis and pH Determination

## CHAPTER TWO

## EXPERIMENTAL

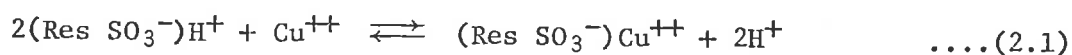
## I Reagents and Materials (Analysis and Preparation)

All reagents used were of analytical grade and volumetric glassware was A-grade. The ionic strength of all reaction solutions was adjusted to 1.0 by using varying volumes of a previously prepared stock  $2.50 \text{ mol dm}^{-3}$  sodium perchlorate solution. Water, deionised and then glass distilled, was used in the preparation of the solutions. Concentrated perchloric acid and sodium hydroxide solutions were prepared for use in pH adjustments of reaction solutions.

A carbonate free sodium hydroxide solution was obtained by allowing a saturated solution to stand for a few days. The clear supernatant solution was used in subsequent dilutions. Sodium hydroxide solutions were standardised with reference to solid potassium hydrogen phthalate.

Two methods were used in the preparation of  $\text{Cu}[\text{Me}_6\text{Tren ClO}_4]\text{ClO}_4$ .<sup>1</sup> Firstly the light yellow liquid,  $\text{Me}_6\text{Tren}$ , previously prepared,<sup>1</sup> was re-distilled under nitrogen and reduced pressure to obtain colourless pure  $\text{Me}_6\text{Tren}$ . Aqueous solutions of pure  $\text{Me}_6\text{Tren}$  were prepared and their concentration determined by volumetric titration using a Radiometer PHM 4 pH meter. On titrating a known volume of  $\text{Me}_6\text{Tren}$  versus a  $0.117 \text{ mol dm}^{-3}$  HCl solution, the titration curve was obtained as shown in Fig. (2.1). Protonation of the three  $\text{N}(\text{CH}_3)_2$  groups occurs resulting in a single equivalence point owing to the closeness of the dissociation constants.

An aqueous divalent copper ion solution was prepared from its perchlorate salt. A cationic<sup>2</sup> exchange column was used to determine the percentage of copper ion in copper perchlorate.



The liberated acid was titrated against a standardised sodium hydroxide solution. The resin employed was Amberlite (Zeo-Karb 225). The pure  $\text{Me}_6\text{Tren}$

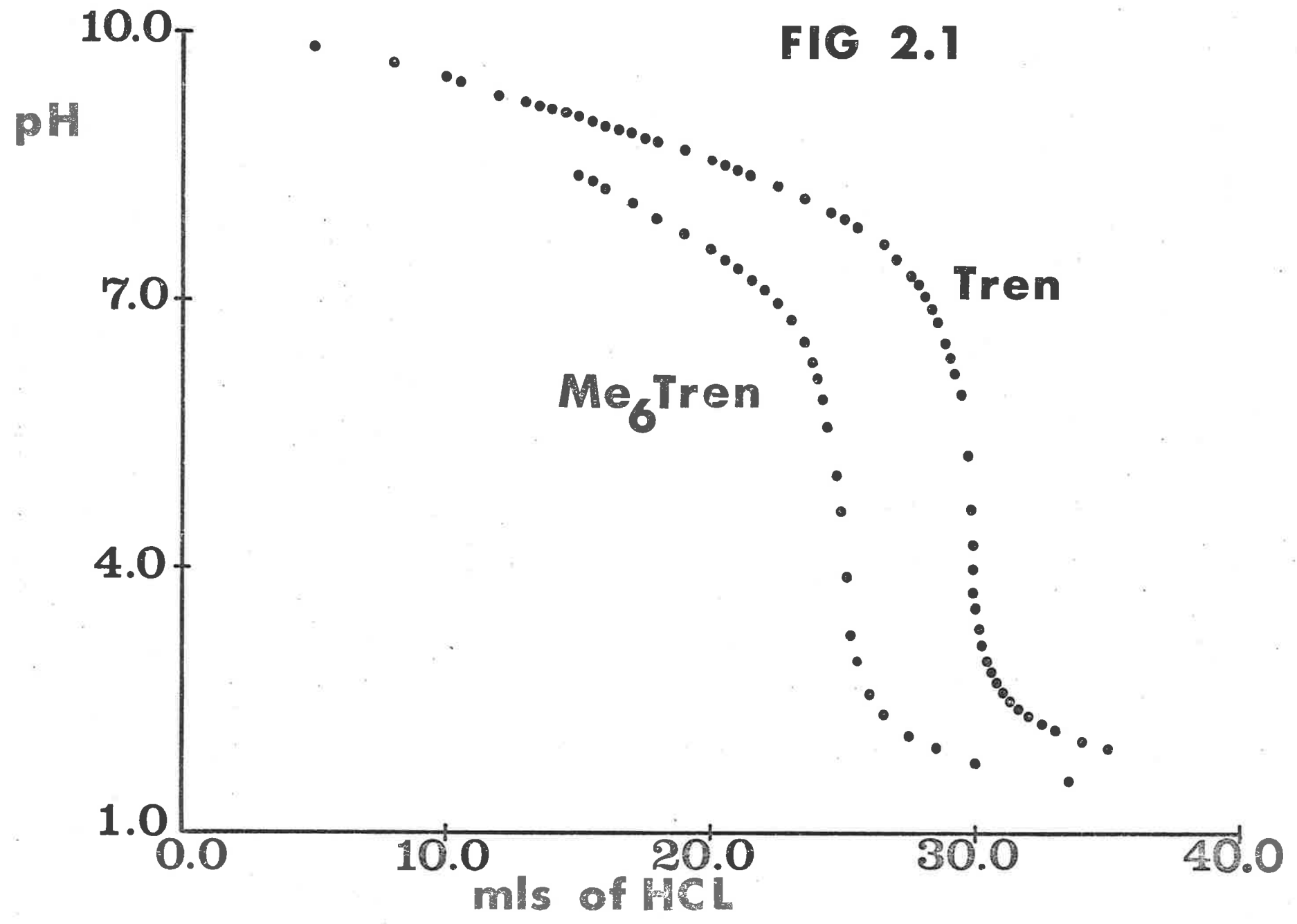
FIG. (2.1)

VOLUMETRIC TITRATION CURVES USED IN THE DETERMINATION OF THE CONCENTRATIONS OF AQUEOUS SOLUTIONS OF THE LIGANDS TREN AND Me<sub>6</sub>TREN.

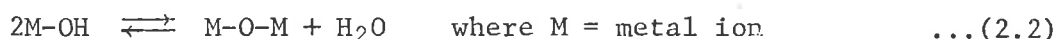
The titration curves do not superimpose owing to the different concentrations of these aqueous solutions.



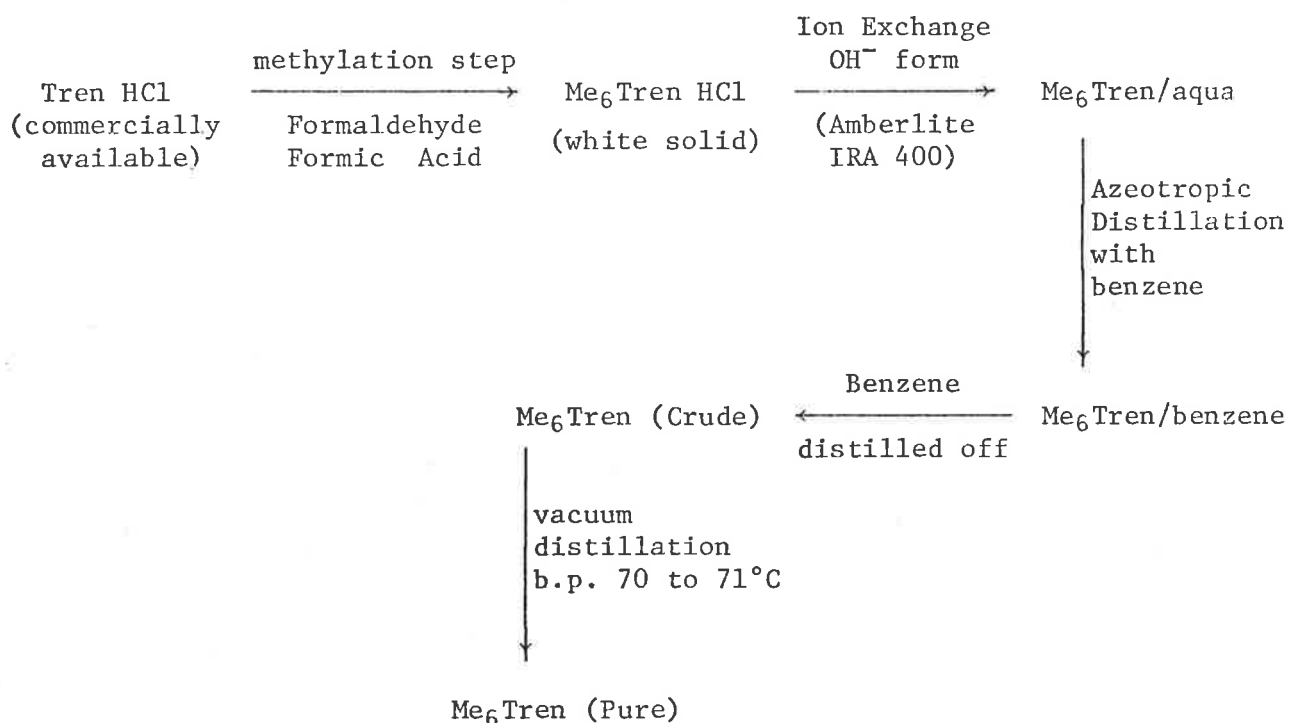
**FIG 2.1**



solution was added in slight excess (1%) to the copper perchlorate solution to prevent the possibility of olation occurring. Olation being the result of water removal between hydroxo species of the metal complex which would result in the following polymerization reaction.



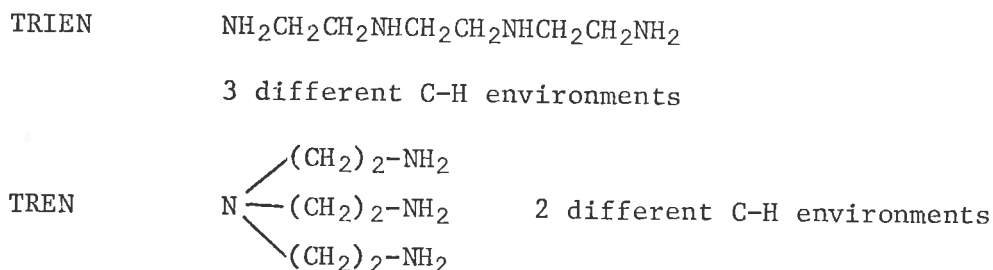
The second method used to prepare  $[Cu(Me_6Tren)ClO_4]ClO_4$  was to prepare the  $Me_6Tren$  ligand freshly, by a modification of the process outlined by Ciampolini<sup>1</sup> and Nardi. The process<sup>3</sup> is shown in the following schematic diagram.



The Amberlite IRA-400 resin was obtained in the  $Cl^-$  form and was converted to the  $OH^-$  form by passing approximately three bed volumes of one molar sodium hydroxide down it. In the azeotropic distillation the water is distilled until only  $Me_6Tren/benzene$  remains. The remaining steps are the same as in the above reference. The resultant pure clear liquid,  $Me_6Tren$ , was mixed directly with copper perchlorate as outlined by Ciampolini<sup>1</sup> and Nardi, to produce  $[Cu(Me_6Tren)ClO_4]ClO_4$ , which was then recrystallized.

The tren liquid which is commercially available was analyzed by the N.M.R. technique. The resulting spectra showed a 5% trien impurity. The

formulae for Trien and Tren are,



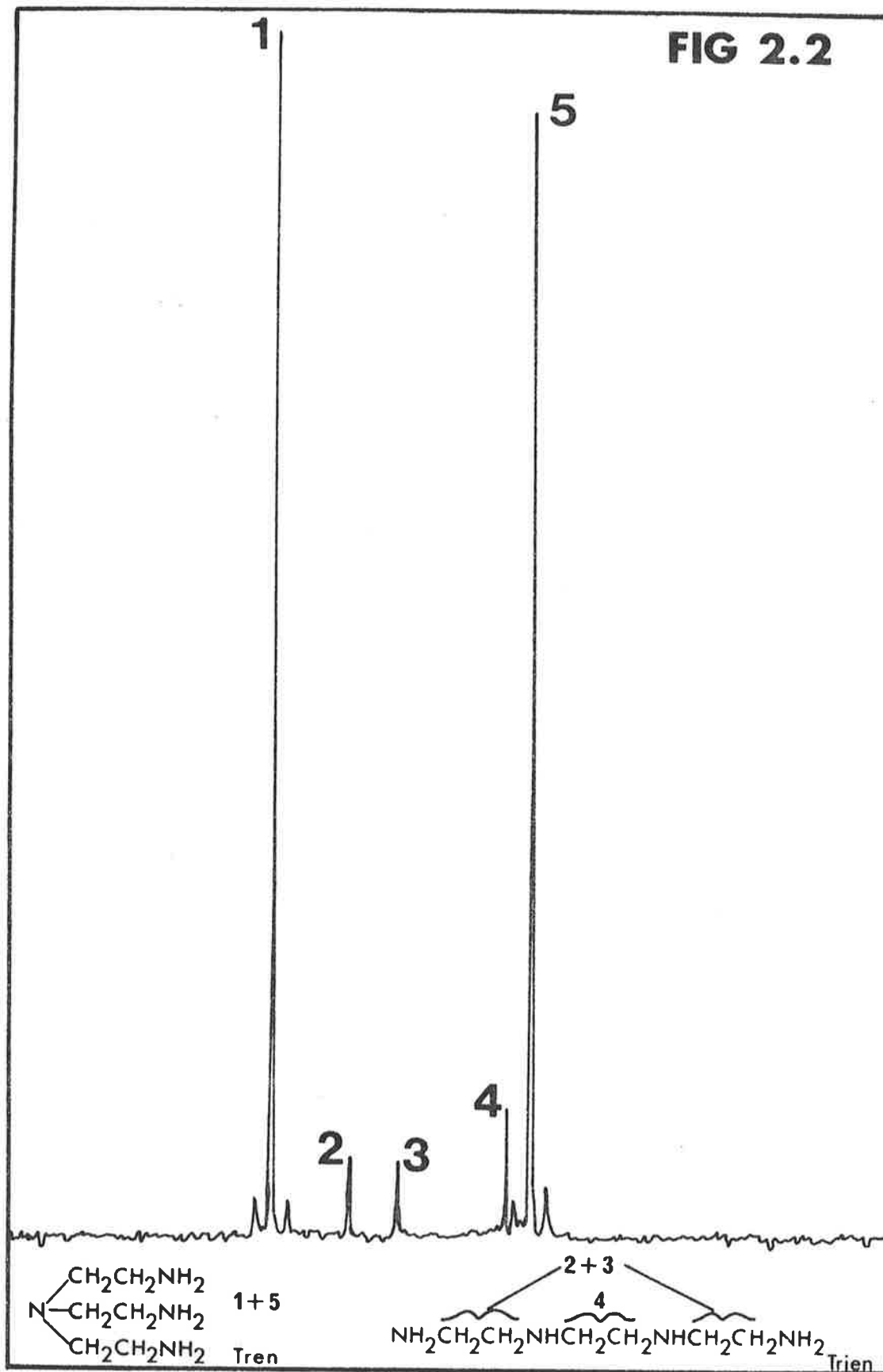
The commercially available Tren gave 5 peaks in the N.M.R. spectra indicating the Trien impurity. This is shown in Fig. (2.2). Commercially available Tren HCl was obtained and its  $\text{C}^{13}$  N.M.R. spectrum was measured. No Trien impurity was found to be present. The Tren HCl was passed down an anionic exchange column (De-Acidite F.F. Resin in the  $\text{Cl}^-$  form). The column was converted to the  $\text{OH}^-$  form before passing Tren HCl through it, on the basis of a 50% capacity of the column. The resulting pure Tren was titrated against HCl and the titration curve obtained appears in Fig. (2.1). An indicator, bromothymol blue, and the PHM 4 pH meter were used in the volumetric titration.

The hydrogen ion instability constants for Tren are stated in the literature as follows,<sup>4a</sup>

	$\text{pK}_1$	$\text{pK}_2$	$\text{pK}_3$
283K	10.45	9.55	8.28
293K	10.15	9.26	7.98
303K	9.91	9.00	7.71
313K	9.63	8.65	7.48

Finally the Tren solution was added to a copper perchlorate solution, with Tren being 1% in excess, to give  $[\text{Cu}(\text{Tren})\text{ClO}_4]\text{ClO}_4$ .

FIG 2.2

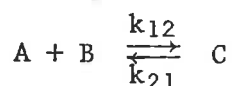


## II (A) Kinetic Techniques and Principles

### (i) Temperature Jump Relaxation Kinetics

Consider a reaction that is in chemical equilibrium. The concentrations of the reactants and products will remain constant at a particular temperature. The Temperature<sup>5</sup> Jump method involves such a system at equilibrium being perturbed by a sudden temperature rise. If the equilibrium is temperature<sup>11,12</sup> dependent and the species involved are coloured, the subsequent re-equilibration at the higher temperature can be followed by means of spectrophotometry. The re-equilibration is displayed as an exponential oscilloscope trace of varying complexity. For small deviations from equilibrium a linearization of the rate equation is possible and the rate of disappearance of a small difference between the actual and equilibrium concentration is proportional to the difference itself. The linear relaxation process is characterized by a time constant "relaxation time" which can be related to a rate constant. A multistep process is represented by a whole spectrum of relaxation times.

For clarification of the above statements the single<sup>13</sup> step mechanism is discussed.



$$\Delta C_A = \Delta C_A^0 e^{-t/\tau}$$

$$\Delta C_A = \bar{C}_A - C_A$$

$$\Delta C_B = \bar{C}_B - C_B \quad \text{where } \bar{C}_n \text{ is the equilibrium concentration of species } n.$$

The kinetic equation is as follows,

$$-\frac{dC_A}{dt} = -\frac{dC_B}{dt} = \frac{dC_C}{dt} = k_{12}C_A C_B - k_{21}C_C \quad \dots(2.3)$$

If the equilibrium is perturbed by a small amount then the above equation can be written as

$$-\frac{d(\bar{C}_A + C_A)}{dt} = -\frac{d\Delta C_A}{dt} = k_{12}(\bar{C}_A + \Delta C_A)(\bar{C}_B + \Delta C_B) - k_{21}(\bar{C}_C + \Delta C_C) \quad \dots(2.4)$$

Now  $\Delta C_A = \Delta C_B = -\Delta C_C$

Since  $\Delta C_A, \Delta C_B, \Delta C_C$  are all small quantities the assumption is made that  $(\Delta C_A)^2, (\Delta C_B)^2$  and  $(\Delta C_C)^2$  can be neglected. It is the deletion of the squared term which gives rise to linearization of the rate equation.

$$\therefore -\frac{d\Delta C_A}{dt} = [k_{12}(\bar{C}_A + \bar{C}_B) + k_{21}]\Delta C_A \quad \dots (2.5)$$

$$\int_{\Delta C_A^\circ}^{\Delta C_A} \frac{d\Delta C_A}{\Delta C_A} = \int_{t=0}^{t=t} -\left(\frac{1}{\tau}\right) dt$$

$$\ln \frac{\Delta C_A}{\Delta C_A^\circ} = -\frac{t}{\tau} \quad \text{OR} \quad \Delta C_A = \Delta C_A^\circ e^{-t/\tau}$$

which is the equation initially stated

$$\frac{1}{\tau} = k_{12}(\bar{C}_A + \bar{C}_B) + k_{21} \quad \dots (2.6)$$

where  $\bar{C}_A + \bar{C}_B$  are the equilibrium concentrations of reactants A and B

A plot of  $\ln \frac{\Delta C}{\Delta C_0}$  versus time gives a slope =  $-\frac{1}{\tau}$

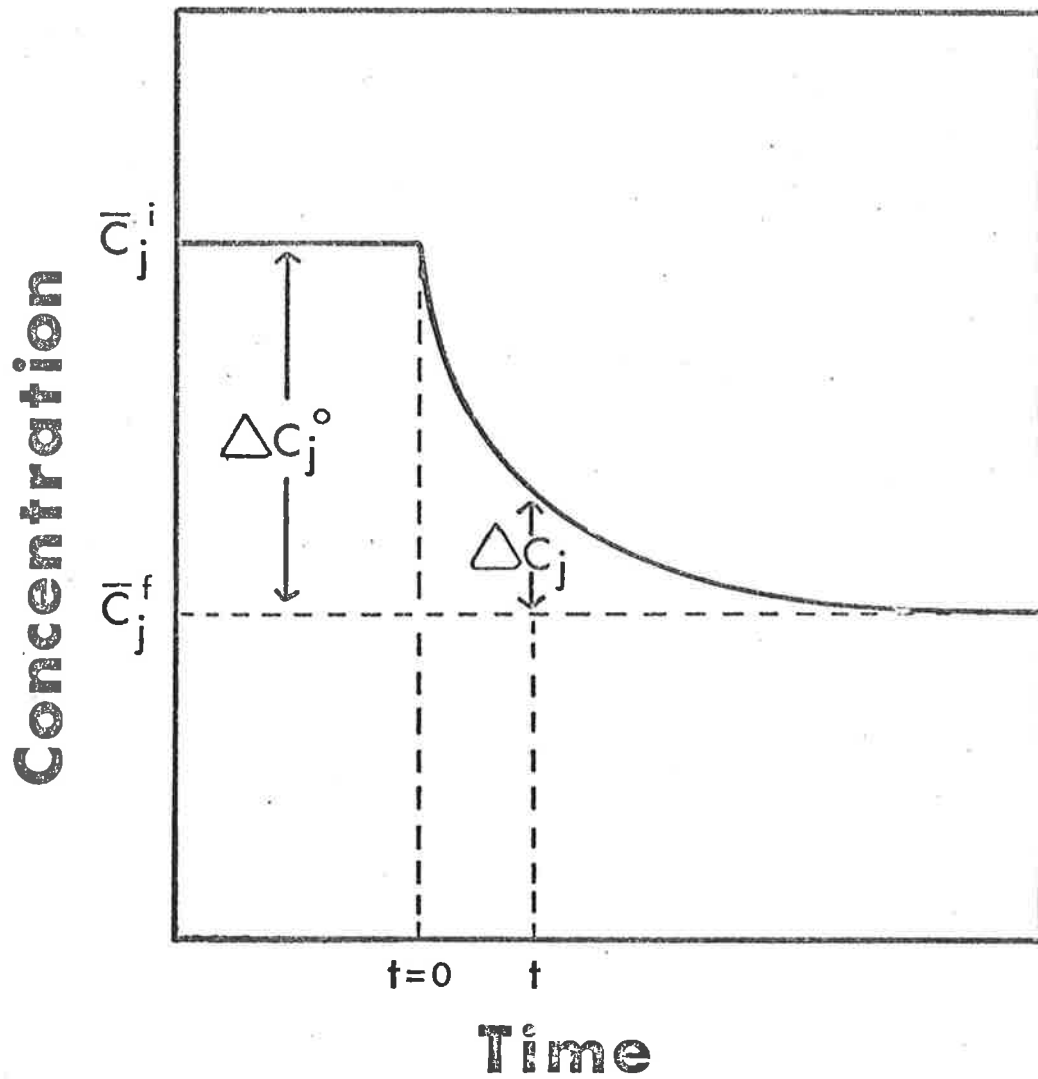
To summarize a general linearized rate equation can be expressed as

$$\frac{dx_i}{dt} + \left(\frac{1}{\tau}\right)x_i = \left(\frac{1}{\tau}\right)x_i^- \quad \text{for small perturbations.} \quad \dots (2.7)$$

A generalization of Relaxation Time Expressions for Single Step equilibria is found in the text "Relaxation Kinetics" by Bernasconi.<sup>5</sup> A diagram from this text appears as Fig. (2.3) and describes the concept of relaxation time concisely.

FIG 2.3

after ref 5



$$\begin{aligned}\Delta C_j &= \Delta C_j^0 \exp(-t/\tau) \\ \bar{c}_j &= \bar{c}_j^f + \Delta C_j^0 \exp(-t/\tau) \\ \Delta C_j^0 &= \bar{c}_j^i - \bar{c}_j^f\end{aligned}$$

Relaxation Time corresponds to the time needed for  $\Delta C_j$  to decrease by a factor of  $e$  ( $e = 2.718$ ).

The subscripts  $i$  and  $f$  refer to initial and final conditions respectively.

The above discussion is centered around the single-step mechanism but in practice multi-step mechanisms are often encountered. From a practical point of view the treatment of such results depends on the time separation of the individual processes which may or may not enable individual infinity exponential curve base lines to be interpolated. These multi-step processes with their associated complex computer calculations are documented by Amdur and Hammes.<sup>13</sup> It is often essential to vary the concentrations of reactants in such a way as to emphasize a particular process so a particular relaxation time predominates and can be measured.

In the multi-step systems, solutions of various transformation<sup>10</sup> matrices are required. To summarize, in a multi-step mechanism  $n$  independent concentration variables will give  $n$  independent rate equations.



(ii) *The Temperature Jump Method*

As discussed, the Temperature<sup>5-8</sup> Jump method involves the perturbation of a solution at equilibrium by means of a sudden temperature rise. This temperature rise can be accomplished by discharging an electrical current from a capacitor through the reaction solution between two stainless steel electrodes. The solution must be conducting to allow the passage of an electrical current and therefore all solutions were made up in one molar sodium perchlorate.

Resistances were measured on the various solutions in the cell assembly resulting in values of approximately 30 ohms. Therefore the time constant for the apparatus is of the order of 1.5 microseconds. The time constant for the temperature rise is given by  $RC/2$  where  $C$  = capacitance of condenser (0.1 microfarad) and  $R$  = resistance of solution. It is possible to compute the temperature rise of the solution on discharging in the following way,<sup>9,14</sup>

$$V_t = V_o e^{-t/RC} \quad \dots(2.8) \quad \text{where } V_t = \text{voltage at time } t$$

$V_o$  = an initial voltage

Energy  $E$  dissipated in time  $dt$

$R$  = circuit resistance

$C$  = capacitance

$$dE = \frac{V_t^2}{R} dt \quad \dots(2.9)$$

$t$  = time at constant pressure

Temperature rise  $\Delta T$  after time  $t$  is

$$\Delta T(t) = \int_0^t \frac{V_o^2}{C_p R} e^{-2t/RC} dt \quad \dots(2.10)$$

$C_p$  = heat capacity of solution at constant pressure

Volume of Reaction Solution is  $V$

Density of Reaction Solution is  $\rho$

$$\Delta T(t) = \int_0^t \frac{V_o^2}{V \rho C_p R} e^{-2t/RC} dt \quad \dots(2.11)$$

where  $RC/2$  is the time constant for the temperature rise.

This is important for very fast reactions since a chemical relaxation process must be slower than the heating pulse for this method to be applicable.

TOTAL TEMPERATURE RISE

$$\Delta T(\infty) = \frac{1}{2} \frac{CV_0^2}{V\rho C_p} \quad \dots(2.12)$$

Since the Temperature Jump technique uses a rapid electrical discharge through a small volume of solution there arises the danger of "cavitation effects". These occur when the temperature rise occurs so rapidly that inertial effects prevent the consequent volume change following the temperature rise. The result is a shock wave which interferes with the passage of light through the solution. One method to avoid "cavitation" is to reduce the temperature rise. The parameters involved in this were discussed previously. The experimental work was carried out from initial temperatures of 5.1, 14.8 and 25.0°C with a temperature rise of 10.33°C. This temperature rise resulted from a  $V_0 = 25$  kV. Under these conditions no "cavitation" problems were encountered in this one molar medium.

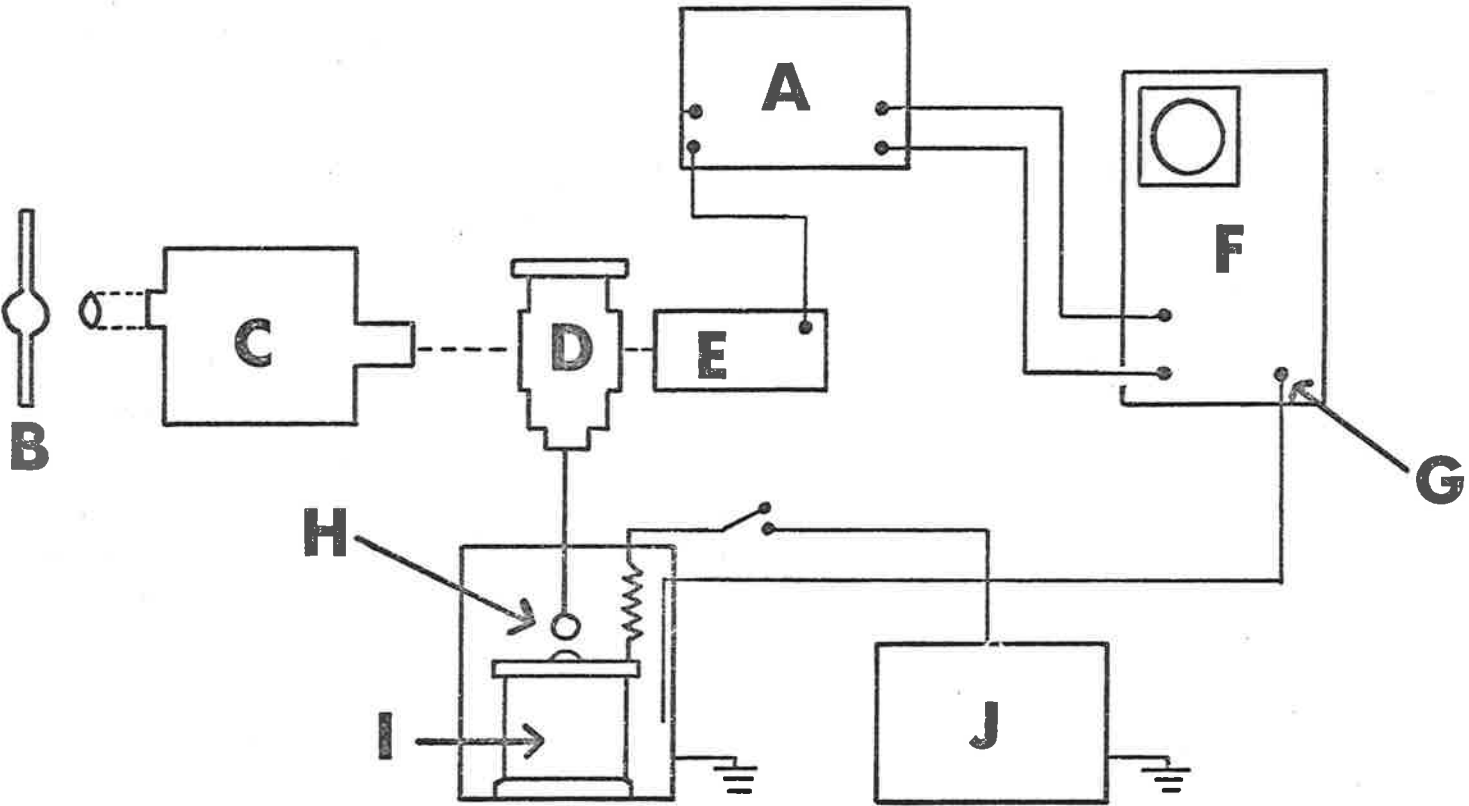
A Brandenburg E.H.T. Generator (Type MR 50/R) was used to charge the 0.1 micro farad condenser. The discharge of electrical energy was carried out manually by closing a spark gap and a 500 mΩ charging resistor is incorporated in series with the capacitor. Both the condenser and charging resistor were shielded from the remaining circuitry by means of aluminium and iron boxes, to reduce electrical and magnetic disturbances. The oscilloscope was triggered by an unshielded wire antenna inside of the capacitor discharge box connected to the oscilloscope external trigger. For the overall schematic of the principle components of the apparatus See Fig. (2.4). Co-axial cables were used to carry signals. The signals generated from the photomultiplier passed through a cathode follower and into the high gain differential pre-amplifier plug in unit of the Tektronix type 549 storage oscilloscope. These signals were backed off against a constant voltage

FIG. (2.4)

SCHEMATIC DIAGRAM OF THE TEMPERATURE JUMP APPARATUS

- A = cathode follower
- B = Xe-Hg arc lamp
- C = Bausch and Lomb high intensity grating monochromator
- D = cell assembly
- E = photomultiplier, type E.M.I. 6256/S
- F = Tektronix type 549 storage oscilloscope
- G = external trigger
- H = moveable spark gap
- I = 35 kV-0.1  $\mu$ F capacitor
- J = 0-50 kV power supply

**FIG 2.4**



supply in the form of two 1.35 volt mercury batteries in series. This voltage was checked internally and by using an external monitoring meter. The photomultipliers themselves were type E.M.I. 6256/S using either five or seven dynodes which were powered from a Nuclear Enterprises Ltd. type N.E. 5307 E.H.T. supply.

The spectrophotometric light source of the apparatus is a Philips type 7023 (100 watt, 12 volt) quartz iodide lamp mounted in a housing which has both vertical and horizontal movement for alignment. The light passes through the entrance and exit slits of a Bausch and Lomb high intensity grating monochromator (1350 grooves/mm) which is designed as a source of monochromatic light of high intensity throughout UV and visible regions. A manual shutter was incorporated before the entrance slit of the monochromator. The amount of monochromator stray light was minimised by maintaining the correct ratio of entrance to exit slit width. A diaphragm was used to regulate the width of the beam of light entering the solution in the cell assembly.

The cell assembly itself depicted in Fig. (2.5), has a volume of approximately 1.50 mls and is filled through two narrow capillary inlets. Syringes with teflon plungers are mounted above the cell assembly and the solution is forced down one inlet into the cell chamber and out of the other. The cell chamber is washed by this method and then filled without the presence of bubbles. Any excess solution remaining in the capillary after the cell chamber is filled is removed by the vacuum pump. This was done because on discharge of the capacitor the temperature of this solution is cooler than that in the cell chamber itself. If this cooler solution was drawn back into the cell, optical distortions may have resulted. All solutions were introduced into the mounted syringes by way of a millipore filter to ensure no foreign matter entered the cell compartment. This would result in distortions of the light beam being manifest as irregular oscilloscope traces. Since bubbles would have the same effect, all solutions were degassed using the

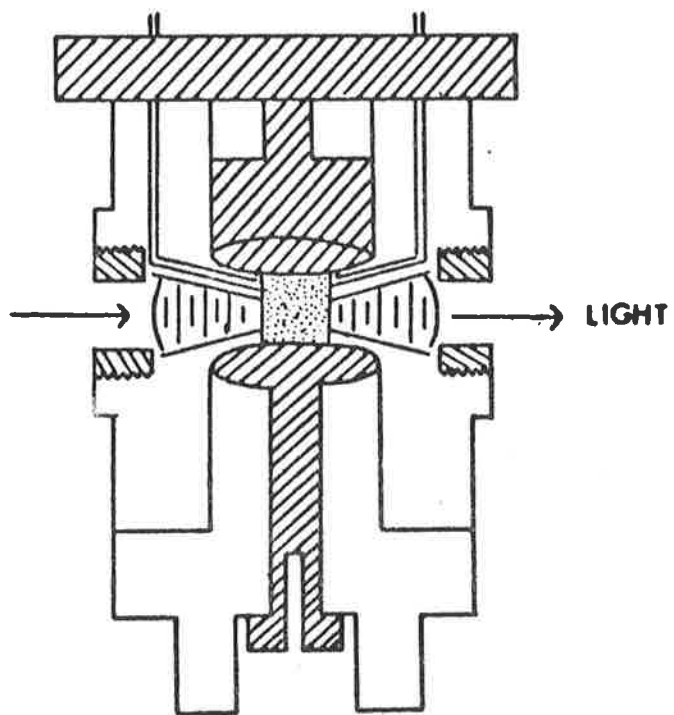
"freeze pump thaw" method.






Two quartz conical windows were used to focus the beam of light at the centre of the cell chamber to minimize optical distortions. The cell body is made of perspex and the high grade stainless steel electrodes are rounded off to prevent spark over. The electrodes were periodically buffed up to maintain a smooth highly polished finish.

When the cell is assembled, thin ring polythene gaskets are placed on the electrodes which are compressed together by rubber O rings. These rubber rings are tightened before filling the cell to prevent leakage. The cell when filled is placed in a cell jacket and is thermostatted by passing water from a regulated water bath around the top and bottom of this jacket. The intensity of light passing through the solution is maximised before thermostating by manually rotating the cell while in the jacket.

# FIG 2.5

## TEMPERATURE JUMP CELL - SCHEMATIC



- |         |   |   |
|---------|---|---|
| PERSPEX |  |  SILICA   |
| STEEL   |  |  TEFLON   |
|         |   |  SOLUTION |

(iii) *Analysis of Data*

When a smooth exponential curve was obtained on the Tektronix 549 storage oscilloscope, it was photographed and then measured using a sliding vernier scale which gives a digital readout of the distance in millimetres that the vernier moves. This apparatus was built by Dr. G.S. Laurence in this department. The vertical scale of the oscilloscope trace relates to the electrical signal measured in millivolts which is generated by the photomultiplier. The horizontal scale is a measure of time. Vertical change in the oscilloscope trace is proportional to a change in light intensity, for small perturbations this change in light intensity is proportional to  $\Delta OD$ .

For the evaluation of  $\tau$  a time infinity base line is drawn on the trace and the distance  $|\Delta d|$  in millimetres between the relaxation curve and the infinity line at various times is measured. Since  $\Delta d$  is proportional to  $\Delta OD$ , a plot of  $\log |\Delta d|$  versus time provides a straight line with the slope equal to  $-1/2.303 \tau$  for first order kinetic effects. Approximately six photographs were taken for each reaction mixture and an average of the reciprocal relaxation times obtained was used, resulting in a single point on the kinetic curve obtained. The standard deviation on each individual point on the kinetic curve of  $1/\tau$  versus concentration is always in the range of  $\pm 1\%$  to  $\pm 8\%$  with the majority of S.D. values being better than  $\pm 5\%$ . The formula used for S.D. is as follows,

$$\text{S.D.} = \sqrt{\frac{\sum (x_i - \bar{x})^2}{N-1}}$$

$\bar{x}$  is the average value  
 $x_i$  are individual values  
 $N$  number of values

(iv) *Amplitude Considerations* ....(2.13)

In discussing the magnitude of the amplitude change when equilibrium is perturbed by a temperature jump, it is necessary to use the Van't Hoff<sup>5</sup> equation.



$$\left(\frac{d \ln K}{dT}\right)_p = \frac{\Delta H}{RT^2} \quad \dots(2.14)$$

thus, 
$$\frac{\Delta K}{K} = \frac{\Delta H}{RT^2} \Delta T \quad \text{for small changes} \quad \dots(2.15)$$

Unless  $\Delta H$  is extremely small or equal to zero, a temperature jump of a few degrees would produce an equilibrium shift which would result in a measurable concentration change. It is important that the equilibrium constant should be near unity for the maximum effect. The two parameters important in determining amplitudes are  $\Delta H$  and  $K_{eq}$ .

For a given reaction ( $A + B \rightarrow C$ ), with a particular  $\Delta H$  and  $K_{eq}$ , the magnitude of the amplitude change is dependent on the initial concentrations of the reactant species. These initial concentrations were varied for theoretical amplitude calculations. The parameter  $\Gamma$ , defined in detail by Hammes and Schimmel and shown below, is proportional to the amplitude.

$$\Gamma = \text{const.} \frac{1}{\frac{1}{(a_0-c)} + \frac{1}{(b_0-c)} + \frac{1}{c}} \quad \dots(2.16)$$

where  $a_0$  and  $b_0$  are the initial reactant concentrations and  $c$  is the final complex concentration.

Since the equilibrium constants for the particular reactions studied, were determined, the optimum conditions for the temperature jump experiments were evaluated using the equation shown above.

(v) *Calibration of the Temperature Rise*

It is necessary to know what temperature rise will result from a particular capacitor voltage setting and therefore each temperature jump cell must be calibrated. A phenol red-tris buffer solution at pH 7.4 was prepared and the change in absorbance with temperature was measured spectrophotometrically at 555 nm. A subsequent plot of optical density versus temperature was obtained.

The capacitor was charged at various voltages for five RC times of the charging circuit and was then discharged through the dye-buffer solution at these various capacitor voltage settings. The change in optical density ( $\Delta OD$ ) at 555 nm was measured from the oscilloscope traces obtained, using the following equation,  $\Delta OD = \log \left( 1 + \frac{\Delta V}{V} \right)$  where  $\Delta V$  is the vertical amplitude change from the oscilloscope trace and  $V$  is the back off voltage. The  $\Delta OD$  values obtained are related to the plot of OD versus Temperature obtained spectrophotometrically. Therefore a final plot of  $V_o^2$  versus Temperature Rise ( $^{\circ}C$ ) was obtained and used to calibrate the cell. For the small volume cell holding 1.50 mls at a capacitor voltage setting of 25 KV ( $V_o$ ), the resultant temperature rise was  $10.33^{\circ}C$ .

## II (B) Kinetic Techniques and Principles

### (i) *The Stopped Flow Method*

The stopped flow technique<sup>5,8</sup> is another method utilised in determining kinetic parameters and the typical time range is  $10^2$  to  $10^{-3}$  seconds. The methods employed to follow the reaction are usually spectrophotometric or fluorimetric. This can be compared to the previously described Temperature Jump method which is in the range 1 to  $10^{-5}$  seconds. All stopped flow experiments involve mixing of solutions. Therefore the mixing time will determine the relaxation times that can be measured.

The stopped flow apparatus employs two basic components, a fast mixing device and a fast monitoring system. There are many varieties of stopped flow systems in existence, each with their own experimental limitations. The apparatus shown in Fig. (2.6) is based on the concept outlined by E. Faeder.<sup>15</sup> This instrument is a modification of the Durrum-Gibson apparatus, in that the method of driving the solutions into the mixing chamber is by means of a piston which propels two drive syringes. The piston is connected to a rod on which is a threaded cylindrical mechanical stop. The mechanical stop is wound back seven revolutions and then pressure is introduced behind the piston from a nitrogen gas cylinder at 8 p.s.i. pressure. On application of this pressure by means of a valve switch on the pressure line, the piston moves forward introducing a small equal amount of solution from both syringes into the mixing chamber. The piston is moved forward until the mechanical stop actuates a micro-switch thus triggering the tektronix 549 storage oscilloscope. The syringes can be filled by means of two 3 position luer lock valves.

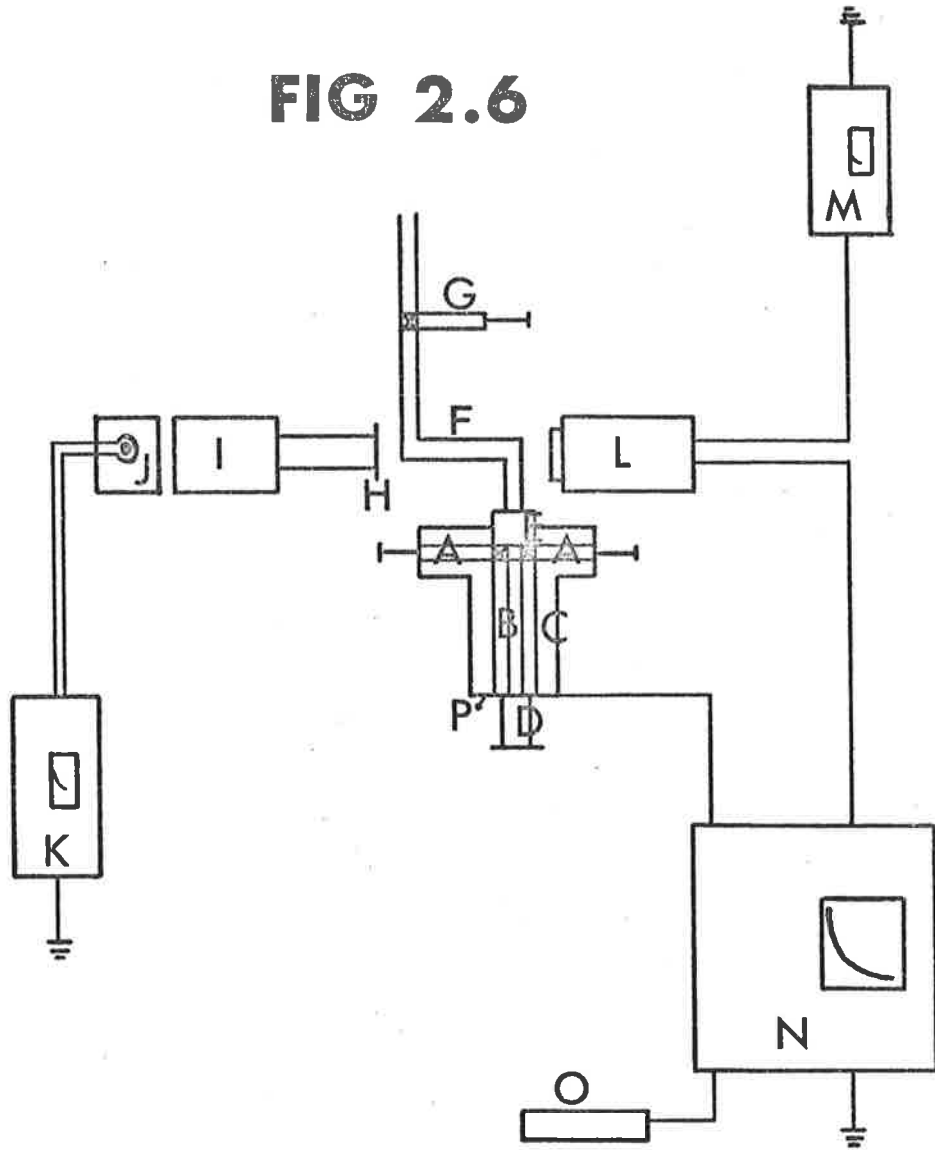
The mixing system in this instrument consists of an eight jet<sup>6</sup> tangential mixer. This is described in Fig. (2.7). The mixing chamber must be both efficient and fast. The observation point must be positioned as near to the mixer as practicable since the time between mixing and observation should be minimised. A fast flow is required for efficient mixing and the

FIG. (2.6)

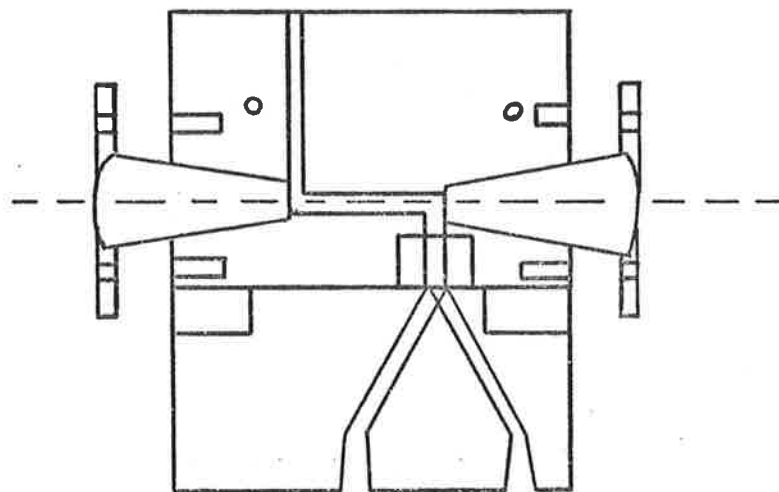
SCHEMATIC DIAGRAM OF THE STOPPED FLOW APPARATUS

- A: the thermostatted reservoir syringes
- B: the drive syringes
- C: the thermostatted brass block
- D: the piston rod, on which is wound the cylindrical mechanical stop
- E: the mixing chamber
- F: the observation tube
- G: the drainage syringe
- H: the diaphragm
- I: the Bausch and Lomb high intensity grating monochromator
- J: the Philips 7023 (100 watt, 12 volt) lamp and housing
- K: the lamp voltage supply
- L: the photomultiplier, type E.M.I. 6256/S
- M: the photomultiplier E.H.T. supply  
(Nuclear Enterprises Ltd. type N.E. 5307)
- N: the tektronix type 549 storage oscilloscope
- O: the constant (2.70 volts) back off voltage
- P: the micro switch

**FIG 2.6**

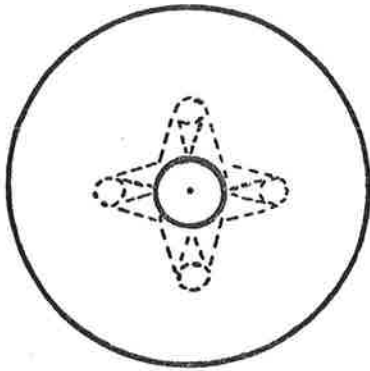


**FIG 2.8**

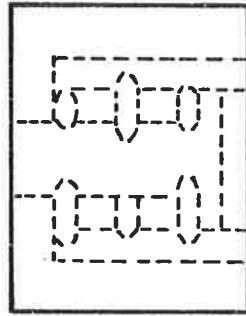


**THE OBSERVATION CHAMBER**

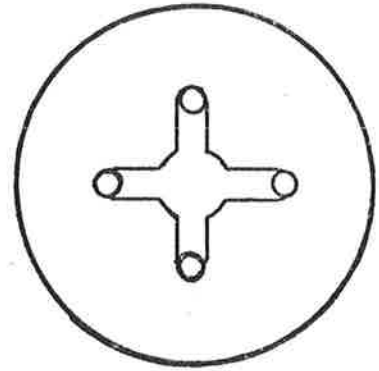
**FIG 2.7**



**FRONT VIEW**

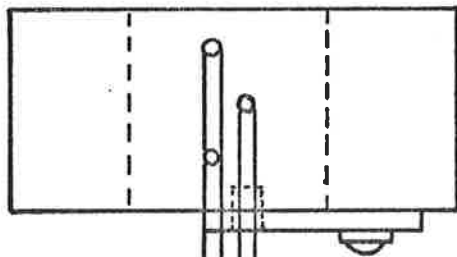


**SIDE VIEW**

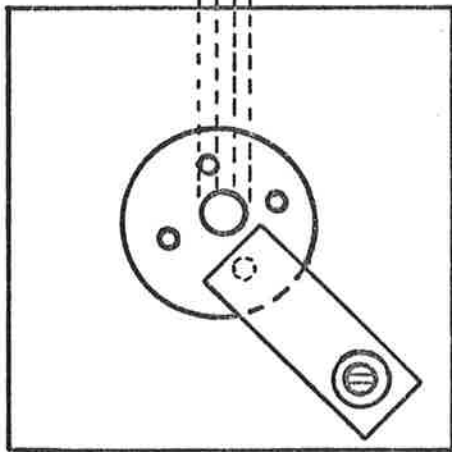


**REAR VIEW**

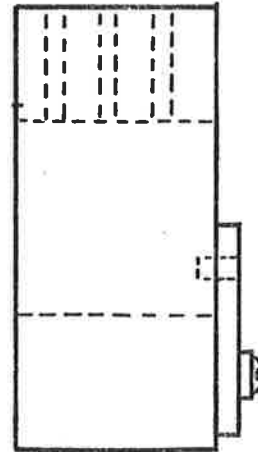
**MIXING CHAMBER**



**TOP VIEW**



**FRONT VIEW**



**SIDE VIEW**

**JIG FOR MIXING CHAMBER**

flow must be rapidly stopped to enable meaningful observation as soon as possible after mixing. The faster the stop the faster the reaction that can be measured. The mixing chamber is made of Kel F and has two sets of four tangentially arranged jets.

The mixing chamber leads to the observation chamber described in Fig. (2.8), by way of a 2 millimetre diameter tube. The diagram shows the shape of the observation tube. The path length in this instrument is two centimetres but in some instruments this can be two millimetres. It has been suggested<sup>8</sup> that for first order reactions no error is encountered if the light beam passes along the tube instead of across it. Two conical quartz windows, one at each end of the two centimetre long observation tube are contained in window holders held tight by screws.

The reaction solution in the observation tube is analyzed photometrically. The light source is a quartz iodide lamp, type Philips 7023 (100 watt, 12 volt), mounted on a stable bracket. The entire lamp is enclosed in a light proof housing and is connected to a constant voltage supply as in the temperature jump technique. The light passes through a Bausch and Lomb high intensity grating monochromator by way of entrance and exit slits. Further along, a diaphragm can be adjusted to alter the width of the light beam. The photomultiplier is a type E.M.I.6256/S powered from a Nuclear Enterprises Ltd. type N.E. 5307 E.H.T. supply. As for the temperature jump technique, the output of the photomultiplier is fed into the input of the Tektronix type 549 storage oscilloscope with a type 1A7A time base, by way of a high gain differential pre-amplifier plug-in unit. The same back off voltage principle is applied. Triggering is by way of a co-axial cable from the stop microswitch to the trigger input of the storage oscilloscope. The decay of the initial complex on the formation of the product is characterised as an exponential trace on the oscilloscope screen. These traces are analysed by the method previously described.

Solutions in the drive syringes are thermostatted by circulating water through enclosing brass blocks. These blocks have been machined to provide the necessary channels and input, exit ports for this circulation. The reservoir syringes were also thermostatted by means of an aluminium block screw-on assembly connected in series with the water circulating system of the drive syringes.

The reason that both temperature jump and stopped flow techniques were employed was the large variation of relaxation times encountered for the complex substitution reactions studied. The temperature jump relaxation method does not produce a radical change in the environment but only alters the equilibrium position by means of temperature perturbation. This contrasts with the stopped flow method which is initiated by a mixing process. This complicates the mathematical treatment and puts a limitation on the relaxation times that can be measured. To simplify the mathematical treatment all experiments in the stopped flow study were carried out under pseudo first order conditions. The ligand concentration was always at least ten times that of the metal ion.



(ii) *Experimental Limitations*

The stopped flow instrument is limited by the mixing and observation times discussed earlier. Also the "dead time" of the instrument must be measured. The "dead time" is defined to be the time the liquid takes to move from the mixing chamber to the middle of the observation chamber. This time depends on two main physical dimensions. The first being the path length which is two centimetres in this case and secondly, on the complexity of the observation tube leading from the mixing chamber. Taking this into account a "dead time" of approximately 15 milliseconds was expected. The observed<sup>16</sup> "dead time" was 13 milliseconds.

It was found after trials that degassing of the solutions was unnecessary. The other main limitation on kinetic measurement resulted from small amplitude signals. The smaller signals required maximum E.H.T. voltage for the photomultiplier used and were consequently accompanied by substantial increases in noise level on the exponential trace. This increased noise level paralleled an increase in the standard deviations of the experimental points on the reciprocal relaxation time versus concentration plots. To conclude, there are both physical and electronic limitations in the application of the stopped flow apparatus as a kinetic tool.

### III Equipment used in Spectrophotometric Analysis and pH Determination

The commercially available Perkin Elmer 402 and Zeiss DMR 10 recording spectrophotometers were used to obtain the ultraviolet and visible spectra shown in this thesis. The Zeiss PMQ II spectrophotometer was used to measure individual absorbances for equilibrium constant calculations.

Instruments employed to adjust the pH of the reaction solutions were either the Radiometer PHM 4 pH meter or the digital readout Radiometer pH meter.

## REFERENCES

1. M. Ciampolini and N. Nardi, *Inorg. Chem.*, 5, 41 (1966).
2. "Ion Exchangers: Properties and Applications", K. Dorfner, Ann Arbor Science, Inc., Michigan, (1972), p 4.
3. D.M.M.A. Hadi, Private Communication.
4. S.F. Lincoln, Private Communication.
- 4a. "Stability Constants of Metal Ion Complexes", L.G. Sillen and A.E. Martell., Chem. Soc, Special Publ. No 17, London., (1964), p 493.
5. "Relaxation Kinetics", C.F. Bernasconi, Academic Press, New York., (1976), p 7.
6. "Technique of Organic Chemistry: Rates and Mechanisms of Reactions, Part II", A. Weissberger, S. Friess and E.S. Lewis, Eds., Interscience, New York., (1963), p 969.
7. R.J. Blagrove, Ph.D. Thesis, University of Adelaide (1976).
8. "Fast Reactions in Solution", E.F. Caldin, Blackwell Scientific, Oxford., (1964), p 64.
9. D.R. Turner, Ph.D. Thesis, University of Adelaide (1976).
10. "Chemical Relaxation", G.H. Czerlinski, M. Dekker, Inc., New York, (1966), p 53.
11. "Comprehensive Chemical Kinetics", C.H. Bamford and C.F.H. Tipper, Elsevier, Amsterdam., (1969), p 134.
12. E.M. Eyring and D.L. Cole, in "Fast Reactions and Primary Processes in Chemical Kinetics", S. Claesson, Ed., Almqvist and Wiksell, Stockholm., (1967), p 255.
13. "Chemical Kinetics: Principles and Selected Topics", I. Amdur and G.G. Hammes, McGraw-Hill, New York., (1966), p 140.
14. G. Czerlinski and M. Eigen, *Zeit. Elektrochem.*, 63, 652 (1959).
15. E.J. Faeder, Ph.D. Thesis, Cornell University, Ithaca, New York (1970).
16. B. Doddridge, Private Communication.

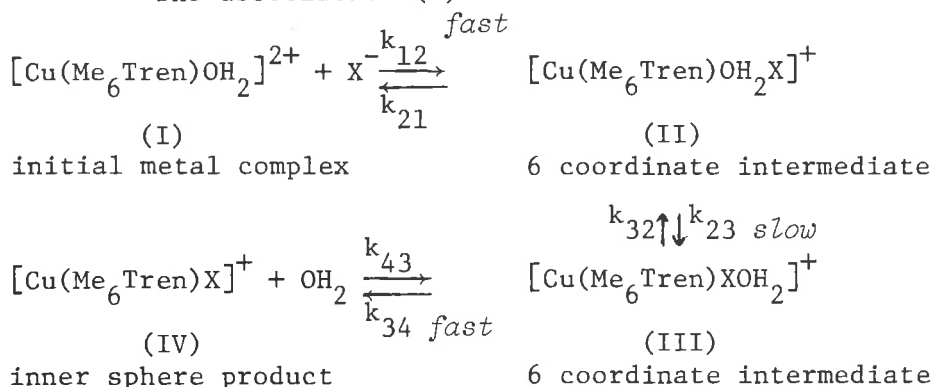
CHAPTER THREE: RESULTS AND DISCUSSION

Section A: Kinetic analysis of the  $[\text{Cu}(\text{Me}_6\text{Tren})\text{OH}_2]^{2+}\text{X}^-$  system

- I (i) *Alternative mechanisms for the experimentally obtained kinetic data*
- (ii) *Evaluation of rate equations for the Eigen ( $I_d$ ) mechanism*
- (iii) *The rate constant parameters in the overall Eigen curve*
- II Theoretical  $K_{IP}$  determination
- (i) *the theoretical Bjerrum equation*
- (ii) *the theoretical Fuoss equation*
- (iii) *modification of the Bjerrum equation to determine  $K_{IP}$*
- III Method of Kinetic data analysis
- (i) *The Use of programme NONLIN in experimentally obtained, data analysis*
- IV Discussion of the kinetic and activation data obtained for aquation of  $[\text{Cu}(\text{Me}_6\text{Tren})\text{X}]^+$  and aquation of  $[\text{Cu}(\text{Me}_6\text{Tren})\text{OH}_2]^{2+}$
- (i) *Aquation of  $[\text{Cu}(\text{Me}_6\text{Tren})\text{OH}_2]^{2+}$ , by ( $\text{N}_3^-$ ,  $\text{NCS}^-$  and  $\text{OCN}^-$ )*
- (ii) *Aquation of  $[\text{Cu}(\text{Me}_6\text{Tren})\text{X}]^+$ , (where  $\text{X}^- = \text{N}_3^-$ ,  $\text{NCS}^-$  or  $\text{OCN}^-$ )*
- (iii) *A brief discussion of the  $K_{IP}$  data obtained*
- V Static and kinetic equilibrium constant spectrophotometric data determination
- (i) *The general method of equilibrium constant evaluation*
- (ii) *The method of evaluating the apparent equilibrium constant*

- (iii) The  $K_{eq}$  (overall) data from kinetic data obtained in analysis using programme NONLIN
- (iv) Experimental determination of  $K_{app}$  (spectrophotometric)
- (v) Comparative equilibrium constant data (both static and kinetic)

The associative (A) mechanism is shown as follows,



The form of the equation for the associative mechanism is similar to that of the Id mechanism, (see page 66), but the rate constants have different meanings. These are as follows,

- (i)  $k_{12}$ : rate constant for the formation of a 6 coordinate intermediate, (species (II)), with the entering ligand ( $\text{X}^-$ ) in a labile axial position.
- (ii)  $k_{21}$ : rate constant for the release of  $\text{X}^-$  from the labile axial position to form the initial metal complex, (species (I)).
- (iii)  $k_{23}$ : *limiting* rate constant for intra-molecular rearrangement of the 6 coordinate intermediate, (species (II)), to place the aqua ligand in a labile axial position.
- (iv)  $k_{32}$ : *limiting* rate constant for intra-molecular rearrangement of species (III) to form species (II), where  $\text{X}^-$  is in the labile axial position.
- (v)  $k_{34}$ : rate constant for the rapid release of the aqua ligand in the labile axial position of species (III).
- (vi)  $k_{43}$ : rate constant for the formation of species (III) from the five coordinate inner sphere product, species (IV).

In the associative mechanism the,  $k_{23}$ , rate constant would be slightly dependent on the nature of  $\text{X}^-$  because the latter is part of the rearrangement species in (II). In contrast, in the Id mechanism this slight dependence of  $k_{23}$  on the nature of  $\text{X}^-$  is due to competition between aqua and  $\text{X}^-$  in the outer coordination sphere for the inner sphere vacated site.

Reasons for considering an associative mechanism unlikely are as follows,

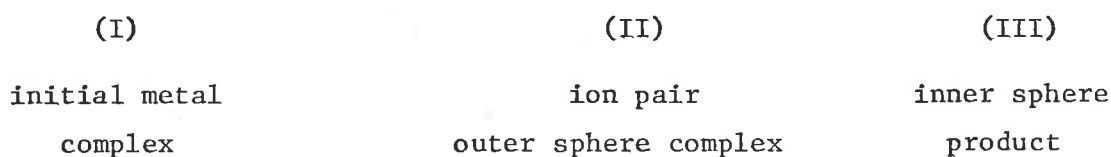
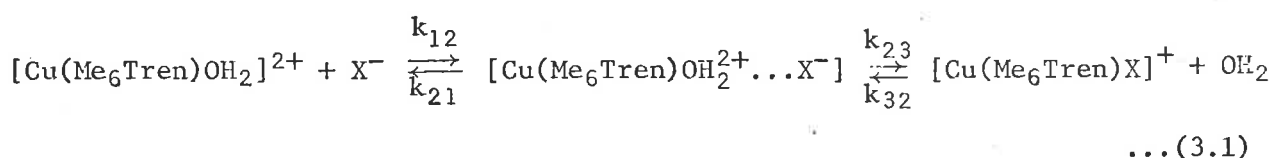
- (i) The associative mechanism necessitates the formation of a 6 coordinate intermediate which is *highly improbable* owing to the *already* considerable steric constraints placed on the labile site in the five coordinate complex,  $[\text{Cu}(\text{Me}_6\text{Tren})\text{OH}_2]^{2+}$ , (see FIG. 1.3). Geometrical rearrangement in the associative mechanism would require considerable flexibility in the transition state which is *unlikely* because of the bulky  $\text{CH}_3$  groups attached to the secondary nitrogens.
- (ii) It is noteworthy that anation reactions substantially reflect the primary water exchange values for the following sequence of complexes,  $[\text{Cu}(\text{OH}_2)_6]^{2+}$ ,  $[\text{Cu}(\text{Tren})\text{OH}_2]^{2+}$  and  $[\text{Cu}(\text{Me}_6\text{Tren})\text{OH}_2]^{2+}$ , (see page 96). Therefore, this would also indicate that ligand substitution by an associative mechanism is *improbable*.
- (iii) The associative mechanism is more complex than the Id mechanism owing to the addition of an extra step which is intrinsically undesirable.

## CHAPTER THREE: RESULTS AND DISCUSSION

Section A: Kinetic analysis of the  $[\text{Cu}(\text{Me}_6\text{Tren})\text{OH}_2]^{2+}/\text{X}^-$  systemI (i) *Alternative mechanisms for the experimentally obtained kinetic data*

A three temperature study of  $\text{N}_3^-$ ,  $\text{NCS}^-$  and  $\text{OCN}^-$  substitutions in the complex,  $[\text{Cu}(\text{Me}_6\text{Tren})\text{OH}_2]^{2+}$  was carried out using both temperature jump and stopped flow spectrophotometric kinetic techniques (discussed in Chapter Two).

The composite kinetic plots of  $1/\tau$  versus  $[\bar{a} + \bar{b}]$  and  $k_{\text{obs}}$  versus  $[\text{X}^-]$  data, are consistent with the Eigen ( $\text{I}_d$ ) mechanism;<sup>7</sup>



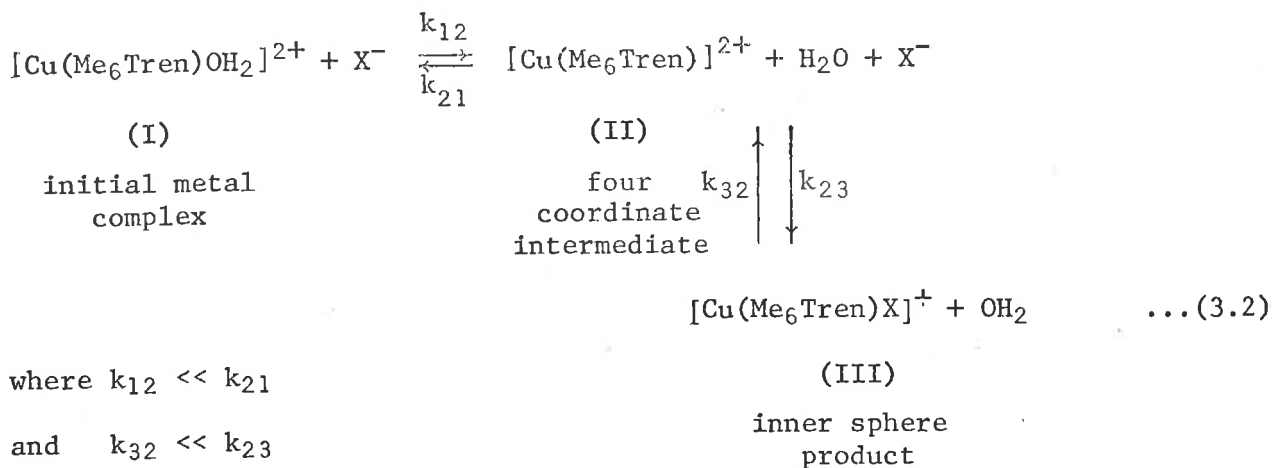
where  $\text{X}^- = \text{N}_3^-$ ,  $\text{NCS}^-$  or  $\text{OCN}^-$  and  $K_{\text{IP}} = k_{12}/k_{21}$

The Eigen ( $\text{I}_d$ ) mechanism<sup>7</sup> requires a rapid equilibration process to form the ion pair complex (species II), characterised by the parameter  $K_{\text{IP}}$ . This precedes the rate determining loss of inner sphere  $\text{H}_2\text{O}$  to form the inner sphere product (species III), characterised by the parameter  $k_{23}$ .

It is noteworthy that the alternative dissociative (D) mechanism would produce similar shaped  $1/\tau$  versus  $[\bar{a} + \bar{b}]$  and  $k_{\text{obs}}$  versus  $[\text{X}^-]$  composite kinetic curves, to that for the Eigen ( $\text{I}_d$ ) mechanism.<sup>7</sup>

The dissociative (D) mechanism is shown as follows,

(There is also the formal possibility of an associative mechanism involving a six coordinate intermediate, this is discussed on the opposite page.)



where  $k_{12} \ll k_{21}$

and  $k_{32} \ll k_{23}$

The rate of appearance of species (III) is :

$$\frac{d[\text{III}]}{dt} = k_{23}[\text{II}][\text{X}^-] - k_{32}[\text{III}] \quad \dots(3.3)$$

and under steady state conditions,

$$\frac{d[\text{II}]}{dt} = k_{12}[\text{I}] - k_{21}[\text{II}] + k_{32}[\text{III}] - k_{23}[\text{II}][\text{X}^-] = 0 \quad \dots(3.4)$$

by substitution,

$$\frac{d[\text{III}]}{dt} = k_{23}[\text{X}^-] \left\{ \frac{(k_{12}[\text{I}] + k_{32}[\text{III}])}{(k_{21} + k_{23}[\text{X}^-])} \right\} - k_{32}[\text{III}] \quad \dots(3.5)$$

When  $k_{23}[\text{X}^-] \gg k_{21}$  at high  $[\text{X}^-]$ ,  $\frac{d[\text{III}]}{dt} = k_{12}[\text{I}]$

and when  $[\text{X}^-] = 0$ ,  $\frac{d[\text{III}]}{dt} = -k_{32}[\text{III}]$

From the dissociative (D) mechanism,  $k_{12}(=k_{-\text{H}_2\text{O}})$  and  $k_{32}$  are the dissociation rate constants for the aqua and  $\text{X}^-$  species respectively. It is feasible that the reactive four coordinate intermediate  $[\text{Cu}(\text{Me}_6\text{Tren})]^{2+}$  would be capable of surviving several molecular collisions as required by the D mechanism, in view of the strained molecular geometry of the  $[\text{Cu}(\text{Me}_6\text{Tren})\text{OH}_2]^{2+}$  complex.

The oppositely charged metal ion complex and ligand reactant species would suggest a high probability of an encounter complex being formed. In view of this and lacking a diagnostic test to differentiate between the  $\text{I}_d$  and D mechanisms, the kinetic data is discussed in terms of the Eigen ( $\text{I}_d$ )

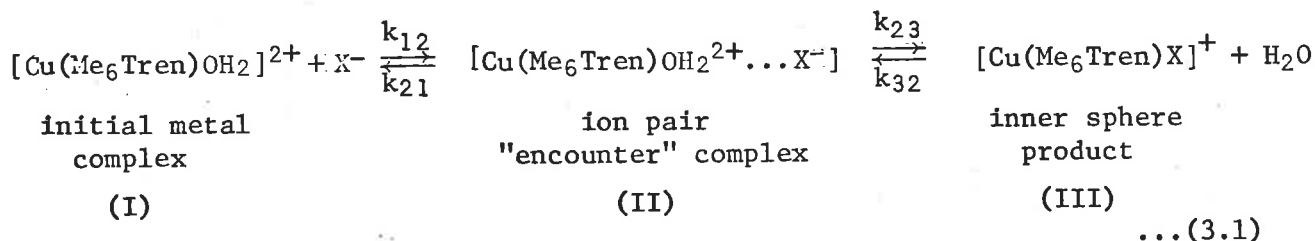


mechanism.<sup>7</sup>

The reactions of  $[\text{Co}(\text{NH}_3)_5\text{OH}_2]^{3+}$  and  $[\text{Co}(\text{CN})_5\text{OH}_2]^{2-}$  with  $\text{X}^-$ , (which were previously discussed in equations (1.7) to (1.10) illustrate the alternative mechanisms  $\text{I}_d$  and D respectively.

### I (ii) Evaluation of Rate Equations for the Eigen ( $\text{I}_d$ ) mechanism

The method of evaluation of the rate equations for the Eigen ( $\text{I}_d$ ) mechanism is as follows. Consider eqn. (3.1):



at equilibrium

$$\frac{[\text{II}]_{\text{eq}}}{[\text{I}]_{\text{eq}} \cdot [\text{X}^-]_{\text{eq}}} = K_{\text{IP}}$$

also,

$$[\text{II}]_{\text{eq}} = K_{\text{IP}} \cdot [\text{I}]_{\text{eq}} \cdot [\text{X}^-]_{\text{eq}}$$

$$[\text{III}]_{\text{eq}} \cdot k_{32} = [\text{II}]_{\text{eq}} \cdot k_{23}$$

If the first step is always in equilibrium then effectively,

$$[\text{II}] = K_{\text{IP}} [\text{I}] [\text{X}^-]$$

$$[\text{Cu}^{2+}]_{\text{total}} = [\text{II}] + [\text{I}] + [\text{III}] = [\text{III}] + (K_{\text{IP}} [\text{X}^-] + 1) [\text{I}]$$

where

$$[\text{Cu}^{2+}]_{\text{total}} \equiv [\text{Cu}(\text{Me}_6\text{Tren})\text{OH}_2^{2+}]_{\text{total}}$$

$$[\text{Cu}^{2+}]_{\text{total}} = [\text{II}]_{\text{eq}} + [\text{I}]_{\text{eq}} + [\text{III}]_{\text{eq}}$$

$$\frac{d[\text{III}]}{dt} = k_{23} [\text{II}] - k_{32} [\text{III}]$$

$$\frac{d[\text{III}]}{dt} = \frac{k_{23} K_{\text{IP}} [\text{X}^-] ([\text{Cu}^{2+}]_{\text{total}} - [\text{III}])}{(K_{\text{IP}} [\text{X}^-] + 1)} - k_{32} [\text{III}]$$

where

$$[I] = \frac{[Cu^{2+}]_{total} - [III]}{(K_{IP}[X^-] + 1)}$$

$$\frac{-d[III]}{dt} = \left( \frac{k_{23}K_{IP}[X^-]}{(K_{IP}[X^-] + 1)} + k_{32} \right) [III] - \frac{k_{23}K_{IP}[X^-][Cu^{2+}]_{total}}{(K_{IP}[X^-] + 1)} = 0$$

at final equilibrium

$$\left( \frac{k_{23} \cdot K_{IP} \cdot [X^-]}{K_{IP} \cdot [X^-] + 1} + k_{32} \right) [III]_{\infty} - \frac{k_{23} \cdot K_{IP} \cdot [X^-][Cu^{2+}]_{total}}{K_{IP} \cdot [X^-] + 1} = 0$$

$$\frac{-d[III]}{dt} = \frac{-d([III] - [III]_{\infty})}{dt} = \left( \frac{k_{23} \cdot K_{IP} \cdot [X^-]}{K_{IP}[X^-] + 1} + k_{32} \right) ([III] - [III]_{\infty})$$

$$\therefore \frac{d([III] - [III]_{\infty})}{([III] - [III]_{\infty})} = \left( \frac{k_{23} \cdot K_{IP} \cdot [X^-]}{(K_{IP} \cdot [X^-] + 1)} + k_{32} \right) dt$$

$$\therefore k_{obs} = k_{32} + \frac{k_{23}K_{IP}[X^-]}{1 + K_{IP}[X^-]} \quad \dots(3.6)$$

(pseudo 1st  
order)

Rate equation for stopped flow analysis.

where  $[X^-]$  is the initial ligand concentration

$[X^-]_{initial} = [X^-]_{free}$  under pseudo 1st order conditions

$k_{obs}$  is the overall rate constant for the approach to equilibrium

Similarly,

$$k_{obs} = \frac{1}{\tau} = k_{32} + \frac{k_{23}K_{IP}[\bar{a} + \bar{b}]}{1 + K_{IP}[\bar{a} + \bar{b}]} \quad \dots(3.7)$$

In the rate equation for temperature jump analysis

$[\bar{a} + \bar{b}]$  is the sum of the equilibrium concentrations of the metal ion and ligand respectively

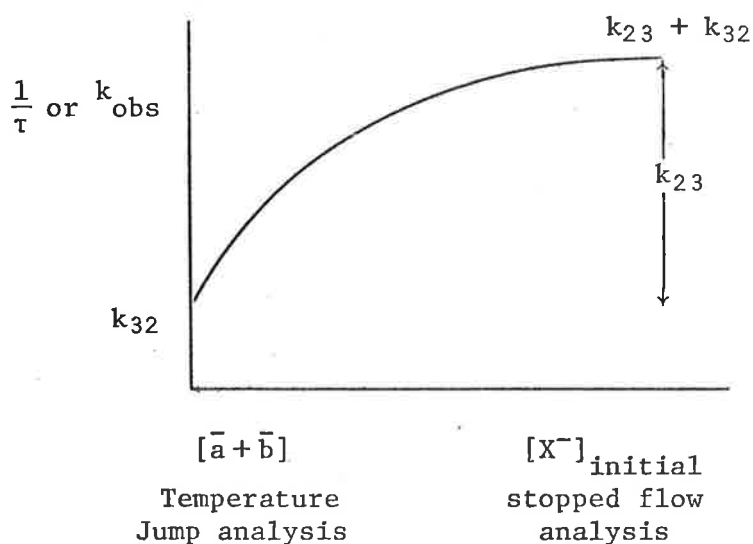
$\frac{1}{\tau}$  is the reciprocal relaxation time

I (iii) *The rate constant parameters in the overall Eigen curve*

Referring to the derived rate equation ((3.6)), the individual parameters are defined below,

- (i)  $k_{23}$ : rate constant for the release of  $H_2O$  from the ion pair encounter complex (species II in equation (3.1))
- (ii)  $k_{32}$ : rate constant for dissociation out of the inner sphere product,  $[Cu(Me_6Tren)X]^+$
- (iii)  $K_{IP}$ : the ion pair association equilibrium constant

The theoretical composite plot of  $\frac{1}{\tau}$  versus  $[\bar{a} + \bar{b}]$  and  $k_{obs}$  versus  $[X^-]$  data is shown below,



The plateau region is obtained when all of the metal is in the ion pair complex. Therefore the subsequent rate of dissociation into and out of the ion pair will be independent of ligand  $[X^-]$ . Referring to equation (3.6), this means that  $K_{IP}[X^-] \gg 1$ .

From a theoretical treatment of the Eigen ( $I_d$ ) mechanism,<sup>7</sup> three different relaxation times should be observed. This is expected from the Eigen and Tamm examination of the outer sphere association between ion and ligand as discussed in chapter one (see equation (1.6)).

Using equation (3.1), two expressions for reciprocal relaxation times are as follows,

$$\frac{1}{\tau_I} = k_{12}[\bar{a} + \bar{b}] + k_{21} \quad \dots(3.8)$$

$$\frac{1}{\tau_{II}} = k_{32} + \frac{k_{23} \cdot K_{IP} [\bar{a} + \bar{b}]}{1 + K_{IP} [\bar{a} + \bar{b}]} \quad \dots(3.7)$$

where  $\frac{1}{\tau_{II}}$  is the slower measurable reciprocal relaxation time.

The complete Eigen mechanism includes a third reciprocal relaxation time which is similar to  $\frac{1}{\tau_I}$  and again cannot be observed using the temperature jump apparatus.

Experimentally, the  $k_{32}$  and  $k_{23}$  parameters are calculated from the stopped flow and temperature jump spectrophotometric data, by NONLIN analysis. The  $K_{IP}$  parameter can be determined from either NONLIN data analysis or calculated from theoretical equations.

## II Theoretical $K_{IP}$ determination<sup>1,2</sup>

Association constants of ion pairs may be obtained from chemical relaxation measurements. Theoretically,<sup>3</sup> models have been used to obtain an estimate of these constants. The definition of what constitutes an ion pair has proven to be difficult. Both Bjerrum and Fuoss have proposed equations to evaluate the association constant for ion pair formation.

### II (i) *The Theoretical Bjerrum equation*

Bjerrum<sup>3</sup> calculated the association equilibrium constant ( $K_{IP}$ ) using the assumption that all ions interacting with coulombic energy  $\mu \geq 2KT$ , are associated. The derived equation is as follows,

$$K_{IP} = \frac{4\pi N}{1000} a^3 b^3 Q(b) \quad \dots(3.9)$$

where  $a$ : is the distance of closest approach

$N$ : is Avogadro's number

$$Q(b) = \int_2^b y^{-4} e^y dy$$

$$\text{and } b = \frac{z_+ |z_-| e_0^2}{\epsilon k T a} = 1.671 \times 10^{-3} \frac{z_+ |z_-|}{\epsilon \cdot T \cdot a}$$

$b$  represents the ratio between P.E. and K.E. and is large for small highly charged ions.

The individual terms are defined as follows,

$\epsilon$ : is the dielectric constant

$z_+, z_-$ : are the valencies of the associating ions

$e_0$ : is the electronic charge

$k$ : is the Boltzmann's constant

$T$ : is the absolute temperature

when  $b$  is large then,

$$K_{IP} = \frac{4\pi N a^3}{1000} \frac{e^b}{b} \quad \dots(3.10)$$

## II (ii) *The Theoretical Fuoss equation*

Fuoss<sup>4,5</sup> derived another expression for the association constant in which the cations of an electrolyte are represented by charged spheres of radius  $a$  and the anions by charged point masses. Only those anions which are within the sphere of volume  $V = \frac{4}{3} \pi a^3$  of a cation are counted as ion pairs. The above hypothesis applies to the reaction  $M + X \rightleftharpoons MX$  and contrasts with the Bjerrum idea that the average effects of ion pair formation may be calculated on the basis that oppositely charged ions within a certain critical distance of one another are "associated" into ion pairs.

The Fuoss equation appears below,

$$K_{IP} = \frac{4\pi N a^3 e^b}{3000} \quad \dots(3.11)$$

where  $b$ : is the Bjerrum ratio between P.E. and K.E.

$a$ : is the minimum approach distance between the charged particles.

$N$ : is Avogadro's number.

II (iii) *Modification of the Bjerrum equation to determine  $K_{IP}$* 

$K_{IP}$  values can be evaluated using a modification of the Bjerrum theory as follows,

$$K_{IP} = \frac{4\pi N_A^3}{3000} e \left( \frac{-z_1 z_2 e^2}{D k T a} + \frac{E_s}{kT} \right) \dots (3.12)$$

where  $e$ : is the charge on the electron

$k$ : is the Boltzmann's constant

$D$ : is the dielectric constant

$E_s$ : is the term for ion-dipole interactions and coulombic terms

Basolo and Pearson<sup>6</sup> have documented  $K_{IP}$  values for various  $z_1$  and  $z_2$  charged species.

*Experimentally determined association constants for outer sphere complex ions at 298K in water at zero ionic strength*

Ion pair	$K_{IP}$ (mol <sup>-1</sup> dm <sup>3</sup> )
$[\text{Co}(\text{NH}_3)_6]^{3+}, \text{Cl}^-$	74
$[\text{Co}(\text{NH}_3)_6]^{3+}, \text{Br}^-$	46
$[\text{Co}(\text{NH}_3)_6]^{3+}, \text{I}^-$	17
$[\text{Co}(\text{NH}_3)_6]^{3+}, \text{N}_3^-$	20
$[\text{Co}(\text{NH}_3)_6]^{3+}, \text{OH}^-$	71
$[\text{Co}(\text{en})_3]^{3+}, \text{Br}^-$	21
$[\text{Co}(\text{en})_3]^{3+}, \text{I}^-$	9
$[\text{Co}(\text{en})_3]^{3+}, \text{N}_3^-$	11
$[\text{Co}(\text{en})_3]^{3+}, \text{Cl}^-$	52
$[\text{Co}(\text{NH}_3)_5\text{Cl}]^{2+}, \text{Cl}^-$	10
$[\text{Co}(\text{NH}_3)_5\text{Cl}]^{2+}, \text{N}_3^-$	13

Abstract of Table (1.11) in ref. 6.

The table shows the  $K_{IP}$  dependence on the charges of the associating ions.

### III Method of Kinetic Data Analysis

#### (i) Use of programme NONLIN in experimentally obtained, data analysis

The experimentally obtained temperature jump and stopped flow spectrophotometric kinetic data was analysed using programme NONLIN. The method employed is as follows,

Using the rate equation shown below,

$$k_{\text{obs}} = \frac{1}{\tau} = k_{32} + \frac{k_{23} \cdot K_{\text{IP}} [\bar{a} + \bar{b}]}{1 + K_{\text{IP}} [\bar{a} + \bar{b}]} \quad \dots(3.7)$$

a limiting form occurs when  $K_{\text{IP}} [\bar{a} + \bar{b}] \ll 1$  resulting in the following equation,

$$k_{\text{obs}} = \frac{1}{\tau} = k_{32} + k_{23} K_{\text{IP}} [\bar{a} + \bar{b}] \quad \dots(3.13)$$

This limiting form is applicable for an  $[a_0 + b_0]$  value up to approximately  $2.5 \times 10^{-3} \text{ mol dm}^{-3}$ , where  $[a_0 + b_0]$  is the sum of the initial concentrations of  $[\text{Cu}(\text{Me}_6\text{Tren})\text{OH}_2]^{2+}$  and  $\text{X}^-$  respectively.

The  $k_{32}$  parameter is evaluated using the temperature jump work which comprises the low ligand concentration region in the overall composite kinetic curve of  $k_{\text{obs}}$  versus  $[\text{X}^-]$  and  $\frac{1}{\tau}$  versus  $[\bar{a} + \bar{b}]$ .

The sequence of NONLIN data analysis is as follows,

1. An initial plot of  $\frac{1}{\tau}$  versus  $[a_0 + b_0]$  was analysed using a rectilinear least squares programme to obtain the value of the  $k_{32}$  parameter.
  2. The  $k_{32}$  value obtained is introduced into programme NONLIN as a fixed term, together with estimates of  $k_{23}$  and  $K_{\text{IP}}$ . The NONLIN programme utilises an iterative process based on the rate equation shown in (3.7). It progressively varies  $k_{23}$  and  $K_{\text{IP}}$  until the mean of the squares of the residuals between the best fit curve and the  $k_{\text{obs}}$ , equally weighted input data, over the entire ligand concentration range, is minimised.
- The programme NONLIN output data was obtained for the kinetic parameters,  $k_{23}$  and  $K_{\text{IP}}$  together with the fixed value of  $k_{32}$ .

3. Using the Eigen mechanism shown in equation (3.1), the overall equilibrium constant is calculated as follows,

$$K_{eq}(\text{overall}) = \frac{K_{IP} \cdot k_{23}}{k_{32}}$$

The initial programme NONLIN output data is used to calculate  $K_{eq}(\text{overall})$  and the  $[\bar{a} + \bar{b}]$  data for the temperature jump work was determined. The  $[\bar{a} + \bar{b}]$  is the sum of the equilibrium concentrations of metal ion and ligand respectively.

Using the initial fixed  $k_{32}$  value and the original estimates of  $k_{23}$  and  $K_{IP}$ , new temperature jump  $\frac{1}{\tau}$  versus  $[\bar{a} + \bar{b}]$  input data together with the stopped flow data is introduced into programme NONLIN.

The resulting output gives a refinement of the  $k_{23}$  and  $K_{IP}$  values.

4. A new  $K_{eq}(\text{overall})$  value is calculated and the new temperature jump input data is introduced. Again a refinement of the  $k_{23}$  and  $K_{IP}$  values is obtained. The procedure was repeated and the output data from the third and fourth iterative procedures agreed to within 1%.

The kinetic data presented in Tables (3.1), (3.3) and (3.5) is the result of the final iterative procedure. The fit between experimentally obtained and NONLIN evaluated data points is very good. This is shown in the kinetic curves for the plot of  $k_{obs}$  over the entire ligand concentration range for  $N_3^-$ ,  $NCS^-$  or  $OCN^-$  substitution in  $[Cu(Me_6Tren)OH_2]^{2+}$ . These plots are presented in FIGS. (3.1), (3.3) and (3.6) respectively.

- (i) The points were equally weighted because of the small range of observed rates at a particular temperature in the overall Eigen curve.
- (ii) The parameter  $k_{32}$  was fixed because the low  $[\bar{a} + \bar{b}]$  values investigated in the temperature jump analysis, together with the linearity of this  $\frac{1}{\tau}$  versus  $[\bar{a} + \bar{b}]$  plot enabled the  $k_{32}$  value to be determined accurately from a rectilinear analysis.

It is acknowledged that an alternative method of NONLIN analysis is



is to introduce estimates of all three unknown parameters  $k_{32}$ ,  $k_{23}$  and  $K_{IP}$  into programme NONLIN utilising the iterative procedure. However, owing to the necessity of employing two techniques to obtain the experimental data, a different  $k_{32}$  value compared with that from the rectilinear analysis was obtained at a particular temperature.

Owing to the large number of data points in the low  $[\bar{a} + \bar{b}]$  region, the former rectilinear method of data analysis was decided upon in determining  $k_{32}$ .

It is important to appreciate that any small differences between the  $k_{32}$  values obtained from the two procedures described above will not materially affect the discussion of the substitution systems studied. This is because the (anation or aquation) reactions of  $[\text{Cu}(\text{Me}_6\text{Tren})\text{OH}_2]^{2+}/\text{X}^-$  and  $[\text{Cu}(\text{Tren})\text{OH}_2]^{2+}/\text{X}^-$  systems show an approximately  $10^4$  times difference in the observed rates.

FIG. (3.1)

The variation of the observed first order rate constant  $k_{\text{obs}}$  for the approach to equilibrium of the  $[\text{Cu}(\text{Me}_6\text{Tren})\text{OH}_2]^{2+}/\text{N}_3^-$  system, plotted against  $[\text{N}_3^-]$ . The open and closed symbols are temperature jump and stopped flow spectrophotometric data points respectively. The inset diagram shows the low concentration data on an enlarged scale. The smooth curves represent the best fits of the data to equations (3.6) and (3.7), from analysis using programme NONLIN.

*Temperature jump spectrophotometric measurements:*

( $\lambda = 386 \text{ nm}$  and  $\text{pH} = 6.75 \pm 0.05$ )

This was investigated at a constant  $[\text{Cu}(\text{Me}_6\text{Tren})\text{OH}_2^{2+}]$  of  $3.92 \times 10^{-4} \text{ mol dm}^{-3}$ . The ligand ( $\text{N}_3^-$ ) concentration was varied from

$4.0 \times 10^{-4} \text{ mol dm}^{-3}$  to  $7.0 \times 10^{-3} \text{ mol dm}^{-3}$  at 288 K

and from

$1.2 \times 10^{-4} \text{ mol dm}^{-3}$  to  $8.0 \times 10^{-3} \text{ mol dm}^{-3}$  at 298 K, 308 K.

*Stopped flow spectrophotometric measurements:*

( $\lambda = 386 \text{ nm}$  and  $\text{pH} = 6.75 \pm 0.05$ )

This was investigated at a constant  $[\text{Cu}(\text{Me}_6\text{Tren})\text{OH}_2^{2+}]$  of  $6.0 \times 10^{-4} \text{ mol dm}^{-3}$ . The ligand concentration range was varied from

$7.0 \times 10^{-3} \text{ mol dm}^{-3}$  to  $3.0 \times 10^{-1} \text{ mol dm}^{-3}$  at 288 K, 298 K, 308 K.

The spectral variation accompanying the formation of  $[\text{Cu}(\text{Me}_6\text{Tren})\text{N}_3]^+$  appears in FIG. (3.2).

The individual spectrophotometric data points in the plot of  $k_{\text{obs}}$  over the entire azide concentration range, appear in Appendix (3.1).

**FIG 3.1**

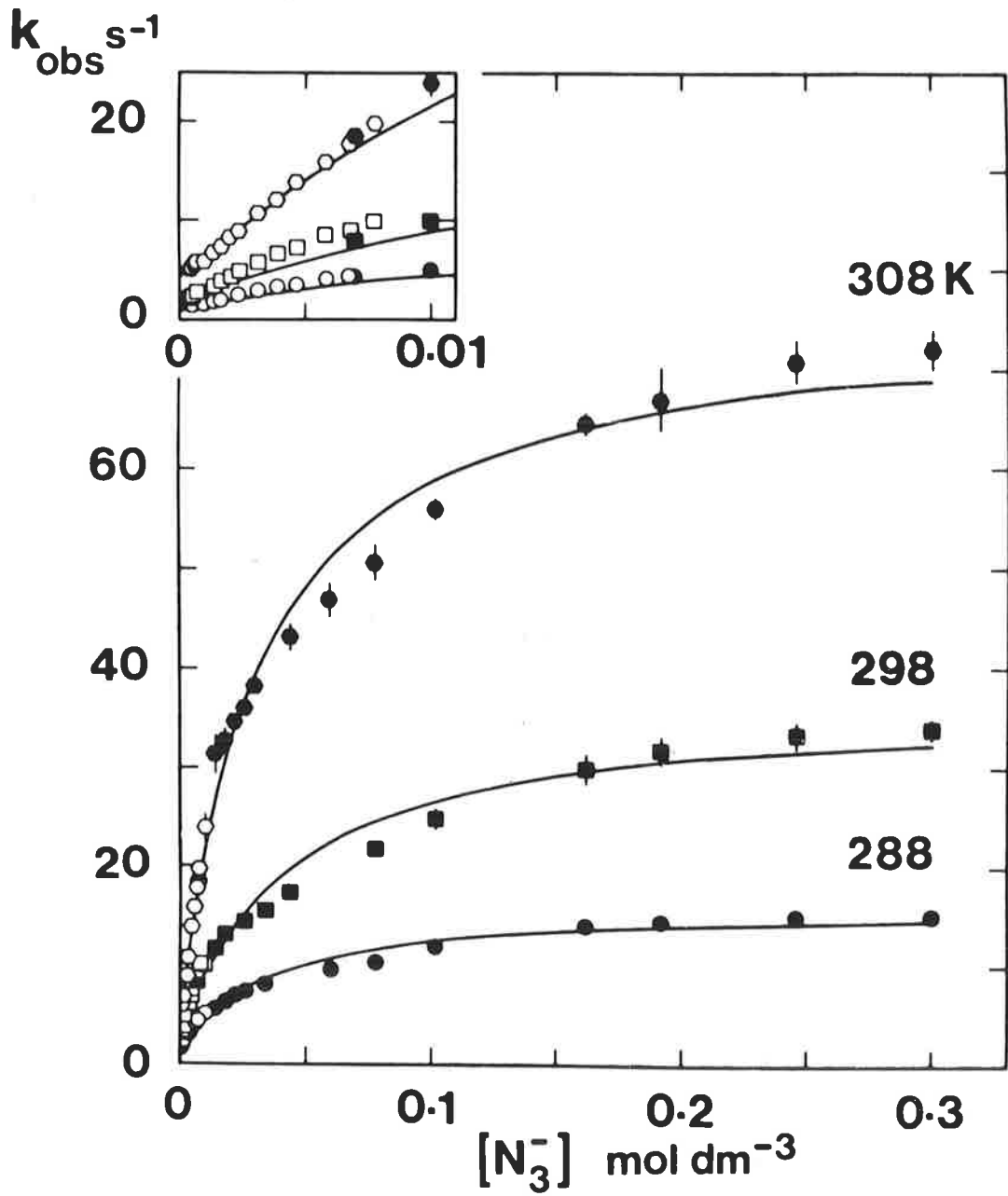


FIG. (3.2)

THE SPECTRAL VARIATION ACCOMPANYING THE FORMATION OF  $[\text{Cu}(\text{Me}_6\text{Tren})\text{N}_3]^+$ .

(pH =  $6.80 \pm (.05)$  and the ionic strength =  $1.0 \text{ mol dm}^{-3}$  (sodium perchlorate))

The initial individual metal ion and ligand concentrations in the reaction solutions are:

	$[\text{Cu}(\text{Me}_6\text{Tren})\text{OH}_2^{2+}]$ $\text{mol dm}^{-3} (\times 10^4)$	$[\text{N}_3^-]$ $\text{mol dm}^{-3} (\times 10^4)$
A	2.61	3.0
B	2.61	6.0
C	2.61	8.0
D	2.61	10.0
E	2.61	14.0
F	2.61	20.0
G	2.61	24.0

The  $\lambda_{\text{max}} = 386 \text{ nm}$  for  $[\text{Cu}(\text{Me}_6\text{Tren})\text{N}_3]^+$

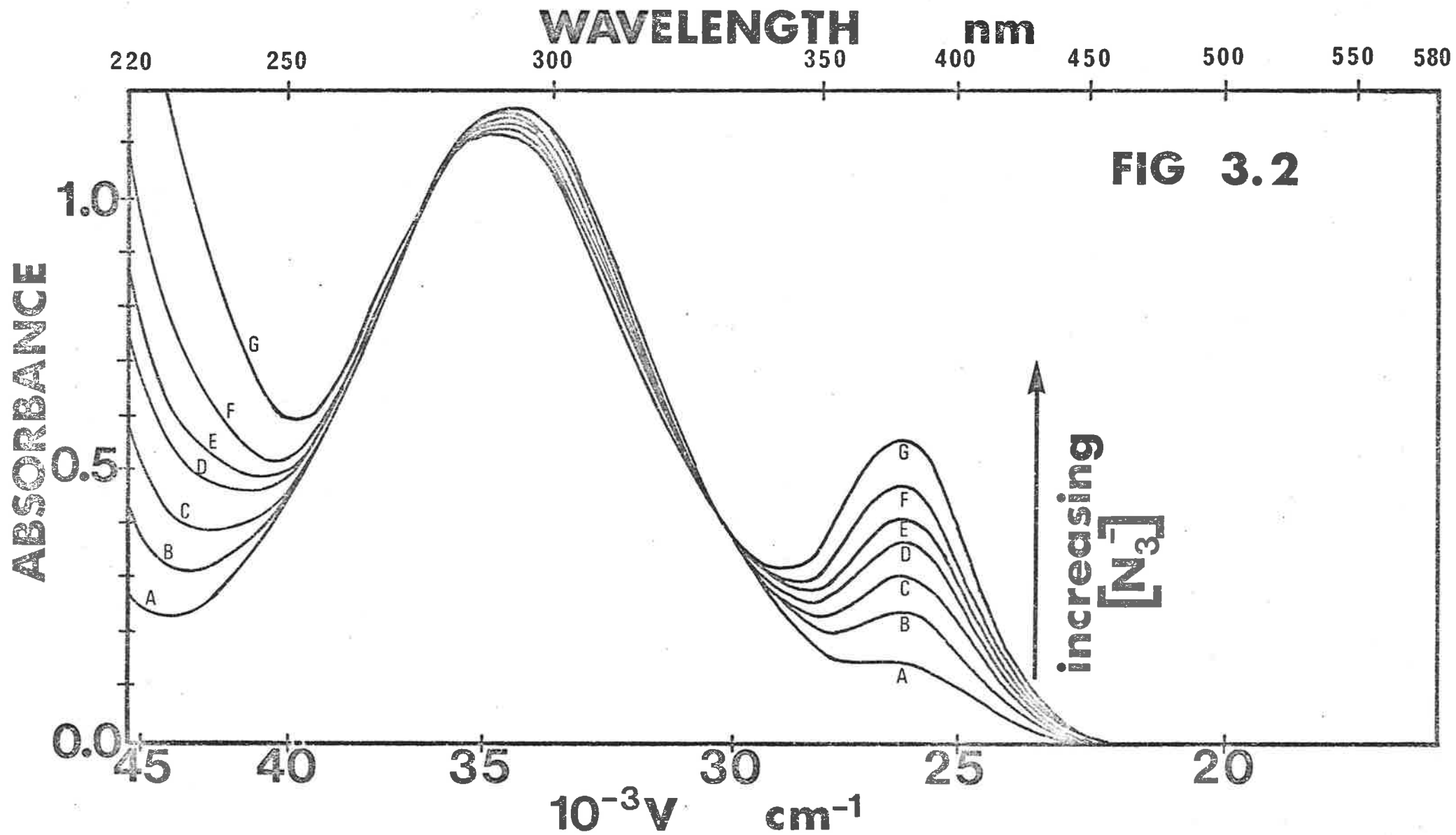


FIG. (3.3)

The variation of the observed first order rate constant  $k_{\text{obs}}$  for the approach to equilibrium of the  $[\text{Cu}(\text{Me}_6\text{Tren})\text{OH}_2]^{2+}/\text{NCS}^-$  system, plotted against  $[\text{NCS}^-]$ . The open and closed symbols are temperature jump and stopped flow spectrophotometric data points respectively. The inset diagram shows the low concentration data on an enlarged scale. The smooth curves represent the best fits of the data to equations (3.6) and (3.7), from analysis using programme NONLIN.

*Temperature jump spectrophotometric measurements:*

$$(\lambda = 370 \text{ nm and pH} = 6.75 \pm 0.05)$$

This was examined at a constant  $[\text{Cu}(\text{Me}_6\text{Tren})\text{OH}_2^{2+}]$  of  $6.0 \times 10^{-4} \text{ mol dm}^{-3}$ . The ligand ( $\text{NCS}^-$ ) concentration range was varied from

$$4.0 \times 10^{-4} \text{ mol dm}^{-3} \text{ to } 4.8 \times 10^{-3} \text{ mol dm}^{-3} \text{ at } 288 \text{ K, } 298 \text{ K, } 308 \text{ K.}$$

*Stopped flow spectrophotometric measurements:*

$$(\lambda = 370 \text{ nm and pH} = 6.75 \pm 0.05)$$

This was investigated at a constant  $[\text{Cu}(\text{Me}_6\text{Tren})\text{OH}_2^{2+}]$  of  $6.0 \times 10^{-4} \text{ mol dm}^{-3}$ . The ligand concentration was varied from

$$6.0 \times 10^{-3} \text{ mol dm}^{-3} \text{ to } 5.0 \times 10^{-1} \text{ mol dm}^{-3} \text{ at } 288 \text{ K, } 298 \text{ K}$$

and from

$$6.0 \times 10^{-3} \text{ mol dm}^{-3} \text{ to } 6.0 \times 10^{-1} \text{ mol dm}^{-3} \text{ at } 308 \text{ K.}$$

The spectral variation accompanying the formation of  $[\text{Cu}(\text{Me}_6\text{Tren})\text{NCS}]^+$  appear in FIGS. (3.4) and (3.5).

The individual spectrophotometric data points in the plot of  $k_{\text{obs}}$  over the entire thiocyanate concentration range, appear in Appendix (3.2).

**FIG 3.3**

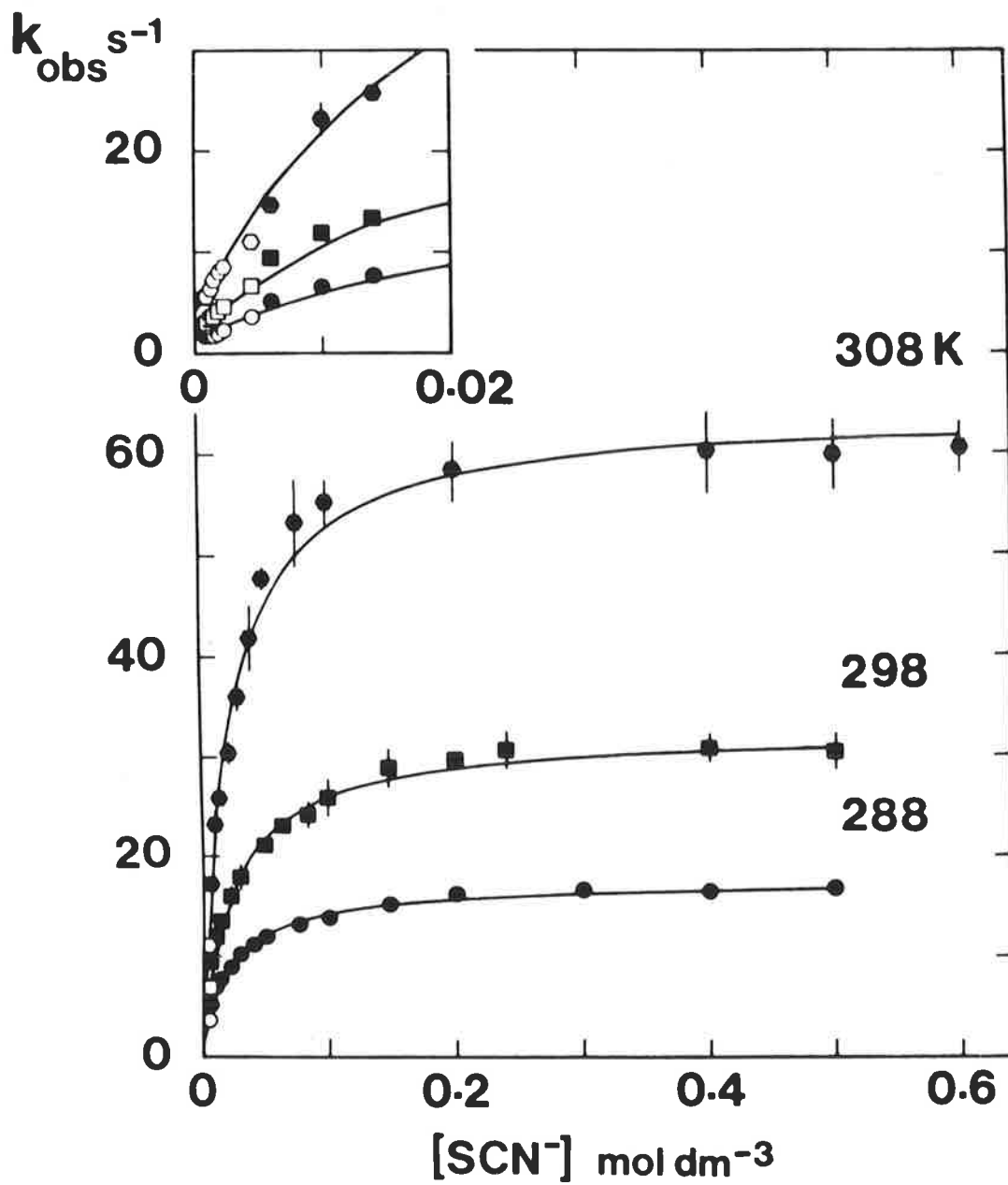


FIG. (3.4)

THE SPECTRAL VARIATION ACCOMPANYING THE FORMATION OF  $[\text{Cu}(\text{Me}_6\text{Tren})\text{NCS}]^+$   
in the WAVELENGTH REGION 320 to 430 nm.

(pH =  $6.80 \pm (.05)$  and the ionic strength =  $1.0 \text{ mol dm}^{-3}$  (sodium perchlorate))

The initial individual metal ion and ligand concentrations in the reaction solutions are:

	$[\text{Cu}(\text{Me}_6\text{Tren})\text{OH}_2^{2+}]$ $\text{mol dm}^{-3} (\times 10^3)$	$[\text{NCS}^-]$ $\text{mol dm}^{-3} (\times 10^3)$
A	1.14	0.0
B	1.14	0.4
C	1.14	0.8
D	1.14	1.4
E	1.14	3.0
F	1.14	4.0
G	1.14	1000

The wavelength at which the kinetic data was obtained was 370 nm.



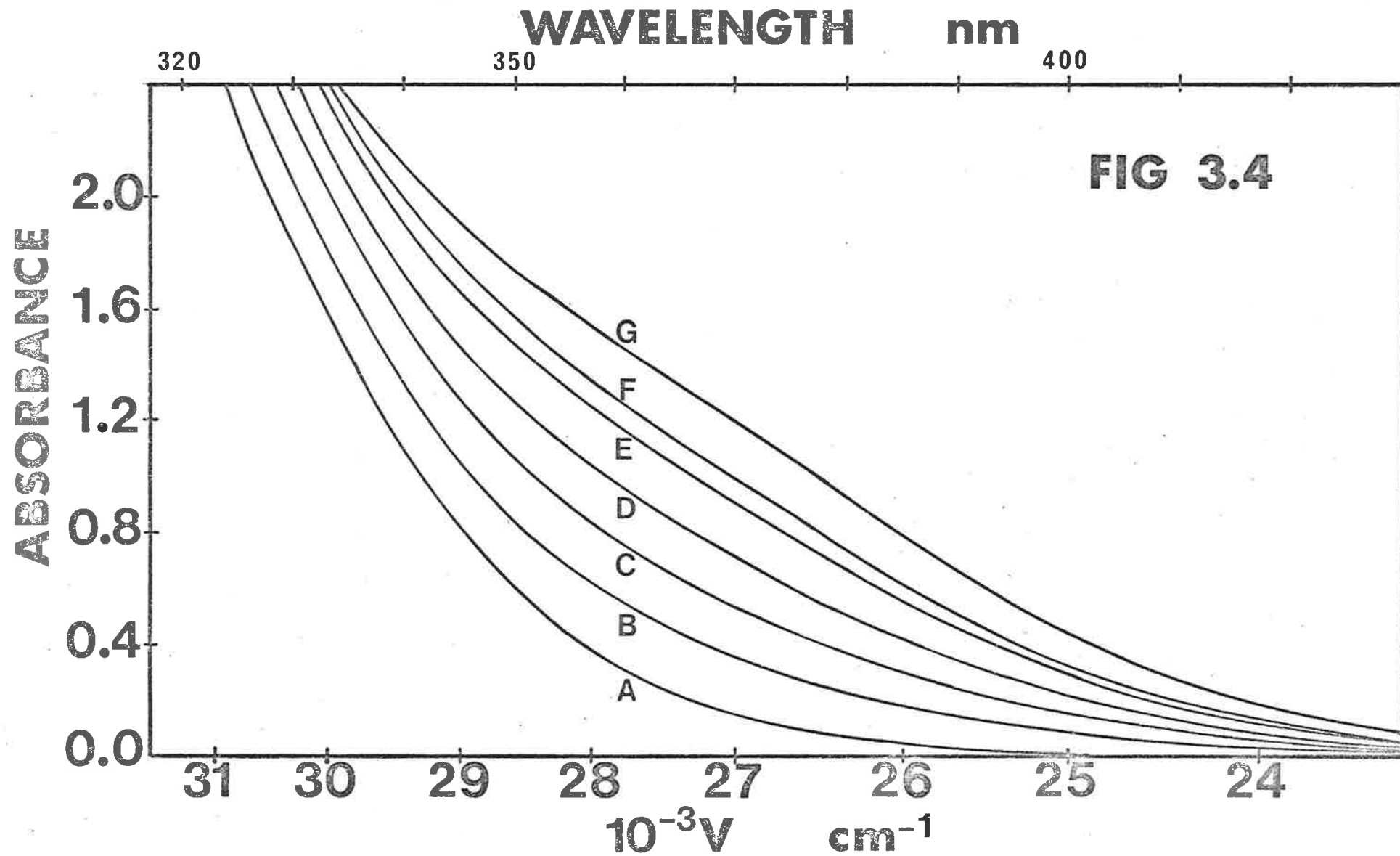


FIG 3.4

FIG. (3.5)

THE SPECTRAL VARIATION ACCOMPANYING THE FORMATION OF  $[\text{Cu}(\text{Me}_6\text{Tren})\text{NCS}]^+$

(pH =  $6.80 \pm (.05)$  and the ionic strength =  $1.0 \text{ mol dm}^{-3}$  (sodium perchlorate))

The initial individual metal ion and ligand concentrations in the reaction solutions are:

	$[\text{Cu}(\text{Me}_6\text{Tren})\text{OH}_2^{2+}]$ $\text{mol dm}^{-3} (\times 10^3)$	$[\text{NCS}^-]$ $\text{mol dm}^{-3}$
A	1.61	0.0
B	1.61	1.0

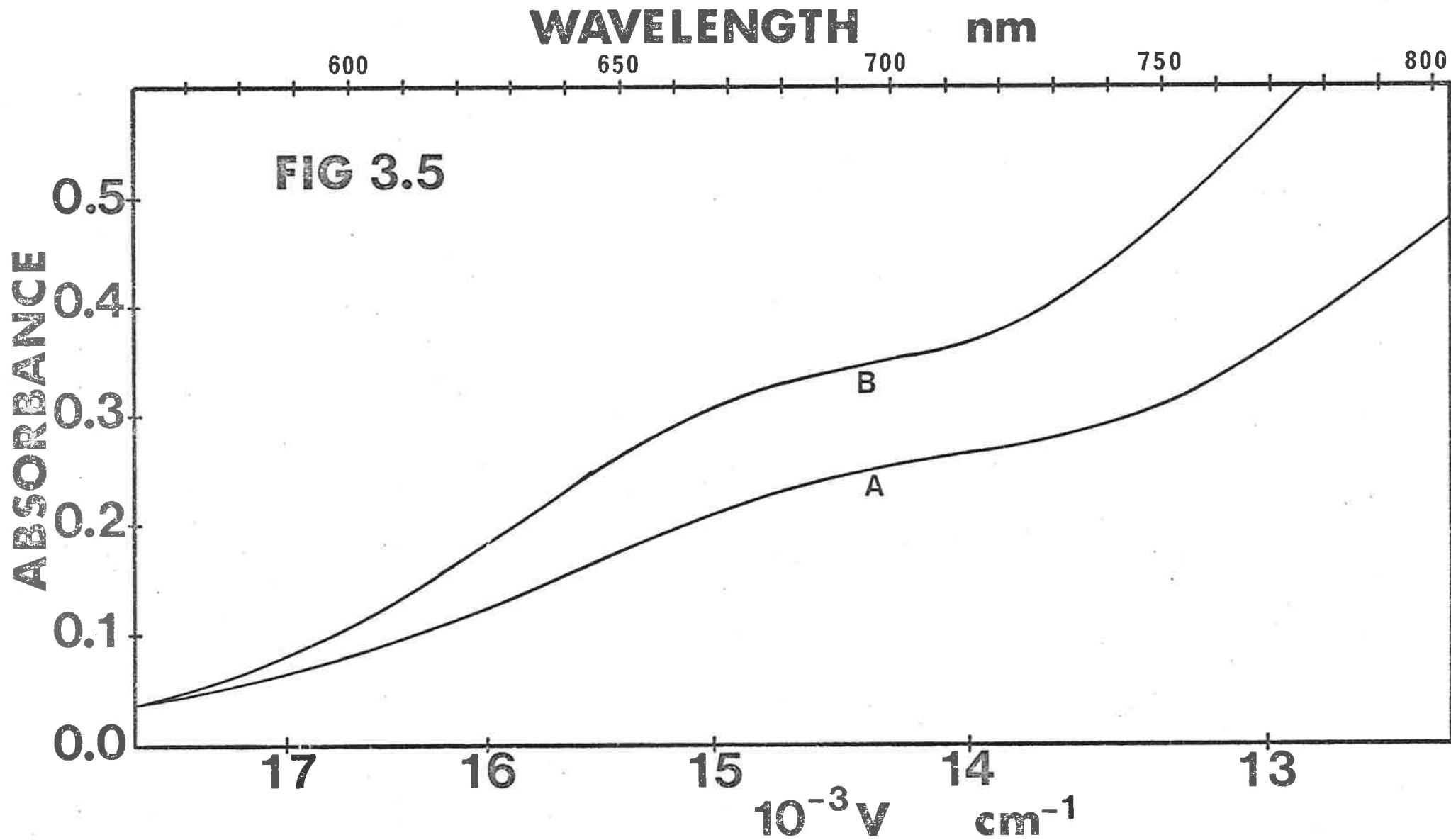


FIG. (3.6)

The variation of the observed first order rate constant for the approach to equilibrium of the  $[\text{Cu}(\text{Me}_6\text{Tren})\text{OH}_2]^{2+}/\text{OCN}^-$  system, plotted against  $[\text{OCN}^-]$ . The open and closed symbols represent only stopped flow data points, at various temperatures. The smooth curves represent the best fits of the data to equation (3.6), from analysis using programme NONLIN.

*Stopped flow spectrophotometric measurements:*

( $\lambda = 710 \text{ nm}$  and  $\text{pH} = 6.70 \pm 0.05$ )

This was examined at a constant  $[\text{Cu}(\text{Me}_6\text{Tren})\text{OH}_2^{2+}]$  of  $5.0 \times 10^{-5} \text{ mol dm}^{-3}$ . The ligand ( $\text{OCN}^-$ ) concentration range was varied from

$5.0 \times 10^{-4} \text{ mol dm}^{-3}$  to  $5.0 \times 10^{-1} \text{ mol dm}^{-3}$  at 288 K, 303 K

and from

$5.0 \times 10^{-4} \text{ mol dm}^{-3}$  to  $6.0 \times 10^{-1} \text{ mol dm}^{-3}$  at 298 K.

*Note:* In an attempted temperature jump study, very small electrical signals generated from the photomultiplier produced oscilloscope traces of insufficient amplitude for evaluation of  $\tau$ .

The spectral variation accompanying the formation of  $[\text{Cu}(\text{Me}_6\text{Tren})\text{OCN}]^+$  as shown in FIG. (3.7) demonstrates the small absorbance change (approx. 0.1) at 710 nm.

The individual spectrophotometric data points in the plot of  $k_{\text{obs}}$  over the entire cyanate concentration range, appear in Appendix (3.3).

**FIG 3.6**

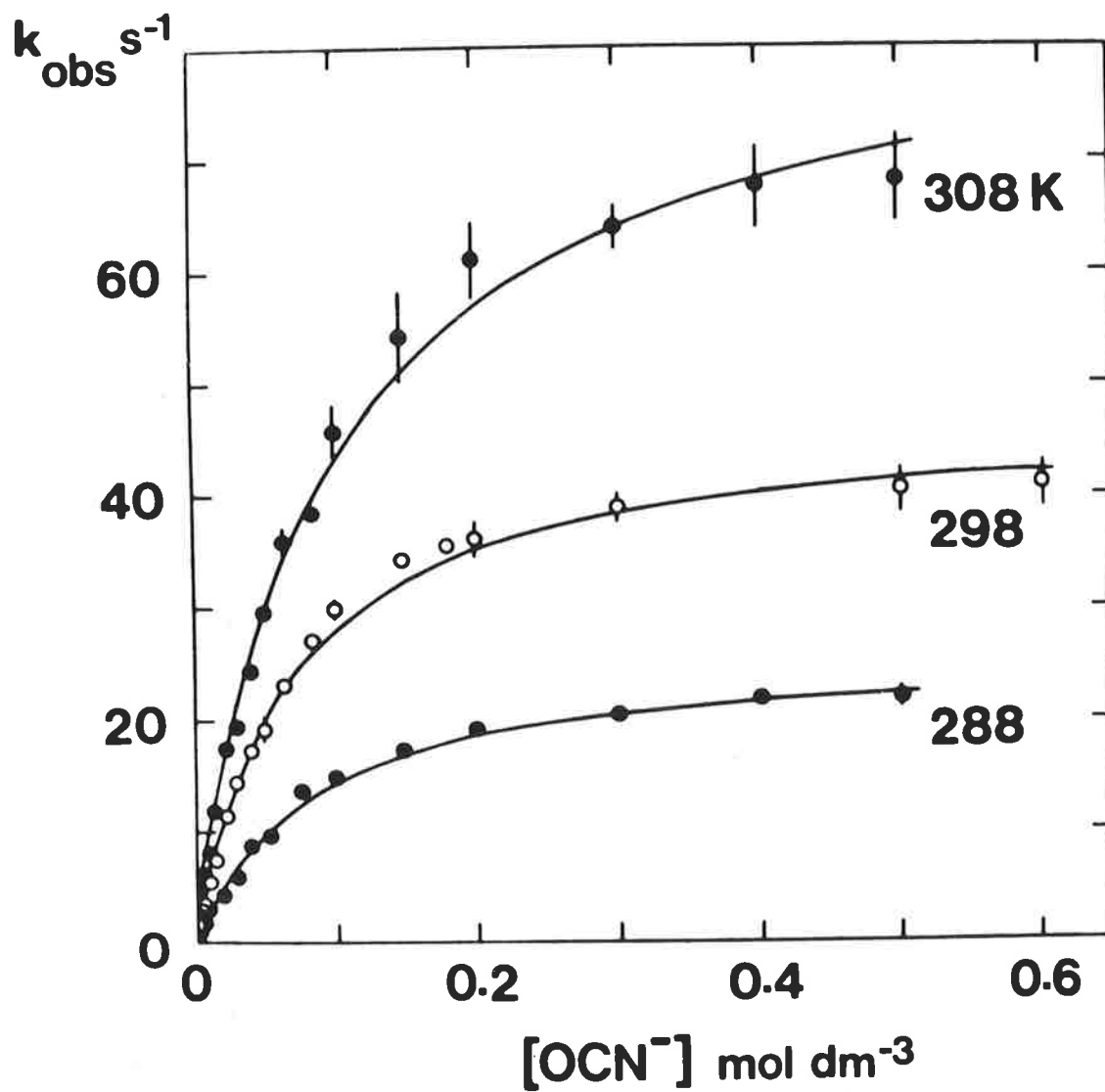


FIG. (3.7)

THE SPECTRAL VARIATION ACCOMPANYING THE FORMATION OF  $[\text{Cu}(\text{Me}_6\text{Tren})\text{OCN}]^+$

(pH =  $6.80 \pm (.05)$  and the ionic strength =  $1.0 \text{ mol dm}^{-3}$  (sodium perchlorate))

The initial individual metal ion and ligand concentrations in the reaction solutions are:

	$[\text{Cu}(\text{Me}_6\text{Tren})\text{OH}_2^{2+}]$ $\text{mol dm}^{-3} (\times 10^3)$	$[\text{OCN}^-]$ $\text{mol dm}^{-3} (\times 10^3)$
A	2.04	0.0
B	2.04	8.0
C	2.04	800.0

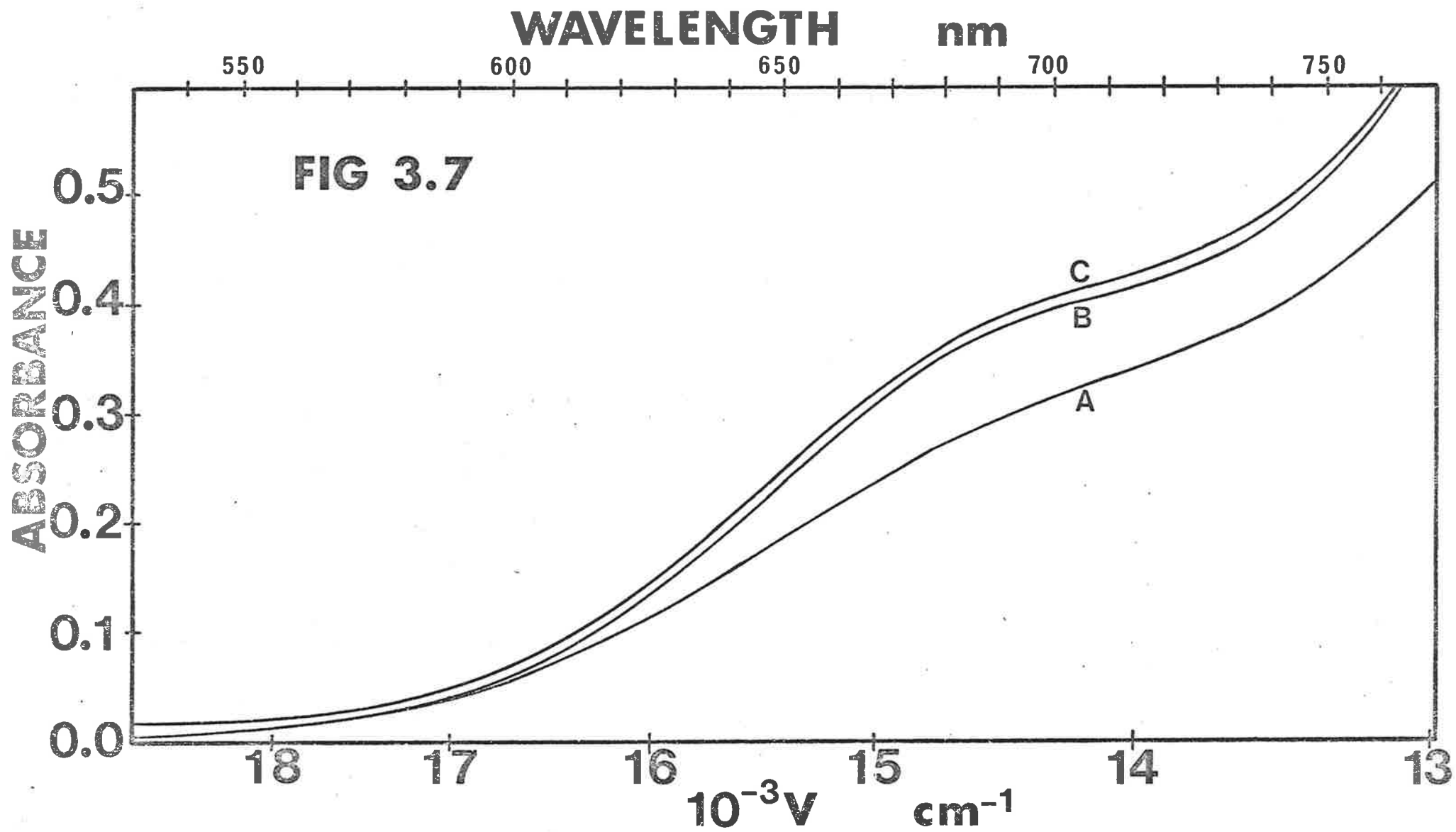


TABLE (3.1)

*Kinetic data for the anation of [Cu(Me<sub>6</sub>Tren)OH<sub>2</sub>]<sup>2+</sup>*

T(K)	N <sub>3</sub> <sup>-</sup>	NCS <sup>-</sup>	OCN <sup>-</sup>
	k <sub>23</sub> (s <sup>-1</sup> )	k <sub>23</sub> (s <sup>-1</sup> )	k <sub>23</sub> (s <sup>-1</sup> )
288	15.2 ± (0.5)	16.2 ± (0.2)	26.0 ± (0.5)
298	34.6 ± (1.3)	30.4 ± (0.4)	46.1 ± (0.8)
308	71.6 ± (1.5)	60.3 ± (0.9)	81.8 ± (2.0)

TABLE (3.2)

*Activation data for the anation of [Cu(Me<sub>6</sub>Tren)OH<sub>2</sub>]<sup>2+</sup>*

	ΔH <sup>‡</sup> (kJ mol <sup>-1</sup> )	ΔS <sup>‡</sup> (J K <sup>-1</sup> mol <sup>-1</sup> )	k <sub>23</sub> (298 K) (s <sup>-1</sup> )
X <sup>-</sup> = N <sub>3</sub> <sup>-</sup>	+ 54.8 ± (1.0)	- 31.7 ± (3.5)	34.6 ± (1.3)
X <sup>-</sup> = NCS <sup>-</sup>	+ 46.2 ± (1.9)	- 61.4 ± (6.7)	30.4 ± (0.4)
X <sup>-</sup> = OCN <sup>-</sup>	+ 39.8 ± (0.8)	- 79.3 ± (0.3)	46.1 ± (0.8)

TABLE (3.3)

*Kinetic data for the aquation of [Cu(Me<sub>6</sub>Tren)X]<sup>+</sup>*

T(K)	X <sup>-</sup> = N <sub>3</sub> <sup>-</sup>	X <sup>-</sup> = NCS <sup>-</sup>	X <sup>-</sup> = OCN <sup>-</sup>
	k <sub>32</sub> (s <sup>-1</sup> )	k <sub>32</sub> (s <sup>-1</sup> )	k <sub>32</sub> (s <sup>-1</sup> )
288	0.95 ± (0.08)	1.36 ± (0.08)	0.39 ± (0.07)
298	1.98 ± (0.03)	2.03 ± (0.11)	1.18 ± (0.10)
308	4.21 ± (0.10)	3.91 ± (0.30)	3.34 ± (0.08)

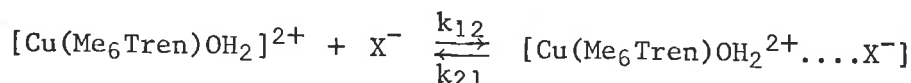


TABLE (3.4)

Activation data for the aquation of  $[\text{Cu}(\text{Me}_6\text{Tren})\text{X}]^+$

	$\Delta H^\ddagger$ (kJ mol <sup>-1</sup> )	$\Delta S^\ddagger$ (J K <sup>-1</sup> mol <sup>-1</sup> )	$k_{32}$ (298 K) (s <sup>-1</sup> )
$\text{X}^- = \text{N}_3^-$	$+52.5 \pm (1.4)$	$-62.8 \pm (4.7)$	$1.98 \pm (0.03)$
$\text{X}^- = \text{NCS}^-$	$+36.5 \pm (6.1)$	$-115.8 \pm (20.6)$	$2.03 \pm (0.11)$
$\text{X}^- = \text{OCN}^-$	$+76.9 \pm (7.4)$	$+14.5 \pm (24.9)$	$1.18 \pm (0.10)$

TABLE (3.5)



$$\text{where } K_{\text{IP}} = k_{12}/k_{21}$$

and the ionic strength is unity

	$\text{X}^- = \text{N}_3^-$	$\text{X}^- = \text{NCS}^-$	$\text{X}^- = \text{OCN}^-$
T(K)	$K_{\text{IP}}$ (mol <sup>-1</sup> dm <sup>3</sup> )	$K_{\text{IP}}$ (mol <sup>-1</sup> dm <sup>3</sup> )	$K_{\text{IP}}$ (mol <sup>-1</sup> dm <sup>3</sup> )
288	$30.3 \pm (3.2)$	$39.8 \pm (1.2)$	$11.4 \pm (0.6)$
298	$24.4 \pm (2.8)$	$38.3 \pm (1.9)$	$14.2 \pm (0.7)$
308	$31.9 \pm (2.0)$	$42.7 \pm (2.6)$	$9.6 \pm (0.6)$

The transition state equation was used to evaluate the activation data, shown above. The equation used is as follows,

$$k_{\text{obs}} = \frac{k_{\text{b}} T}{h} e^{-\Delta H^\ddagger/RT} e^{\Delta S^\ddagger/R} \quad \dots(3.14)$$

$$\ln \left( \frac{k_{\text{obs}}}{T} \right) = \ln \left( \frac{k_{\text{b}}}{h} \right) - \frac{\Delta H^\ddagger}{RT} + \frac{\Delta S^\ddagger}{R} \quad \dots(3.15)$$

∴ a plot of  $\ln \left( \frac{k_{\text{obs}}}{T} \right)$  versus  $\frac{1}{T}$  gives,

$$\text{slope} = -\frac{\Delta H^\ddagger}{R}$$

$$\text{intercept} = \ln \left( \frac{k_{\text{b}}}{h} \right) + \frac{\Delta S^\ddagger}{R}$$

where  $k_{\text{b}}$  is Boltzmann's constant

$h$  is Planck's constant

$T$  is the absolute temperature

A rectilinear least squares programme was used to analyse the data.

IV Discussion of the kinetic and activation data obtained for aquation of  $[\text{Cu}(\text{Me}_6\text{Tren})\text{X}]^+$  and anation of  $[\text{Cu}(\text{Me}_6\text{Tren})\text{OH}_2]^{2+}$

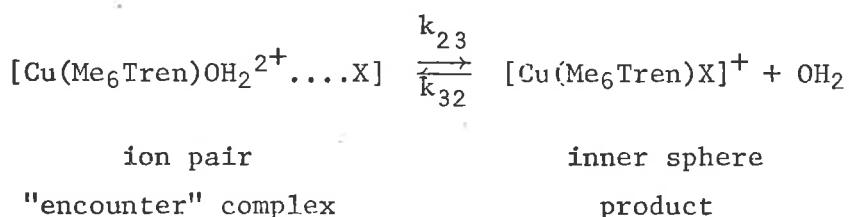
(i) Anation of  $[\text{Cu}(\text{Me}_6\text{Tren})\text{OH}_2]^{2+}$  by  $(\text{N}_3^-$ ,  $\text{NCS}^-$  and  $\text{OCN}^-)$

The Eigen-Wilkins ( $\text{I}_d$ ) mechanism<sup>7</sup> has as its rate determining step the release of an inner sphere aqua ligand from the ion pair. The vacant site on release of  $\text{H}_2\text{O}$  is occupied by either  $\text{H}_2\text{O}$  or  $\text{X}^-$  from the outer coordination sphere. If this mechanism is operative, then the  $\Delta\text{H}^\ddagger$  values for the anation of  $[\text{Cu}(\text{Me}_6\text{Tren})\text{OH}_2]^{2+}$  should be similar for  $\text{X}^- = \text{N}_3^-$ ,  $\text{NCS}^-$  or  $\text{OCN}^-$ . The  $\Delta\text{H}^\ddagger$  values should also be similar to the  $\Delta\text{H}^\ddagger$  value for primary water exchange in  $[\text{Cu}(\text{Me}_6\text{Tren})\text{OH}_2]^{2+}$ . The last postulate cannot be tested since the water exchange value of  $[\text{Cu}(\text{Me}_6\text{Tren})\text{OH}_2]^{2+}$  has not been measured quantitatively.

In Table (3.2), the  $\Delta\text{H}^\ddagger$  values for  $\text{X}^- = \text{N}_3^-$ ,  $\text{NCS}^-$  and  $\text{OCN}^-$  show a reasonable similarity as required by the  $\text{I}_d$  mechanism.

The  $\Delta\text{S}^\ddagger$  values for the anation reactions of  $(\text{N}_3^-$ ,  $\text{NCS}^-$  and  $\text{OCN}^-)$  in  $[\text{Cu}(\text{Me}_6\text{Tren})\text{OH}_2]^{2+}$ , are expected in part to reflect the ability of  $\text{X}^-$  in the outer coordination sphere to compete with outer sphere  $\text{H}_2\text{O}$  for the vacated site. The  $\Delta\text{S}^\ddagger$  values are all negative indicating an increase of order in going from the ion pair to the transition state.

The activation data in Tables (3.2) and (3.4) refer to the following part of the overall Eigen mechanism,



The  $\text{X}^-$  or outer coordination sphere water in the ion pair complex is poised in a configuration that has a high probability of substitution for the vacated site on dissociation of an inner sphere aqua ligand.

In Table (3.2), the spread of -ve  $\Delta\text{S}^\ddagger$  values indicates differing

$X^-/H_2O$  outer sphere competition ratios. The  $\Delta S^\ddagger$  term for the  $[Cu(Me_6Tren)OH_2]^{2+}/N_3^-$  system is approximately half that for the  $NCS^-$  and  $OCN^-$  systems, for the temperature range investigated. This may reflect the higher symmetry of the  $N_3^-$  ligand allowing it a statistical advantage over the other substituting ligands.

The  $\Delta S^\ddagger$  term is difficult to interpret precisely. For example, when the metal ion to aqua ligand bond breaks in the ion pair, the resulting  $\Delta S^\ddagger$  will be positive or negative depending on the allowed vibrational modes of the methyl groups on the secondary nitrogens of the divalent copper  $Me_6Tren$  complex.

To conclude,  $\Delta S^\ddagger$  considerations are by no means definitive, although the transfer of  $X^-$  or  $H_2O$  from the outer coordination sphere to the inner sphere of the divalent copper ion must be a major consideration, (see discussion of the Frank and Wen model on page 8).

The individual  $k_{23}$  values obtained for the system,  $[Cu(Me_6Tren)OH_2]^{2+}/X^-$ , (where  $X^- = N_3^-$ ,  $NCS^-$  or  $OCN^-$ ) are shown in Table (3.1). There is a reasonable spread of  $k_{23}$  values for the various ligands at a particular temperature. These different aquation rate constants are attributed to differing competition ratios in the outer coordination sphere.

#### IV (ii) Aquation of $[Cu(Me_6Tren)X]^+$ , (where $X^- = N_3^-$ , $NCS^-$ or $OCN^-$ )

Table (3.3) contains the kinetic data ( $k_{32}$ ) for aquation of  $[Cu(Me_6Tren)X]^+$ . The similarity of  $k_{32}$  values for  $N_3^-$  and  $NCS^-$  aquation systems at a particular temperature, suggests that the bond broken is Cu-N in both cases. Obviously for the  $[Cu(Me_6Tren)N_3]^+/H_2O$  system, the Cu-N bond is broken preceding the formation of the ion pair encounter complex. The lower  $k_{32}$  values for the system,  $[Cu(Me_6Tren)OCN]^+/H_2O$  (at a comparable temperature to that for the other two systems) suggest that the bond ruptured is Cu-O because oxygen is more electronegative than nitrogen resulting in

the Cu-O bond being stronger than the Cu-N bond.

The activation data for aquation of  $[\text{Cu}(\text{Me}_6\text{Tren})\text{X}]^+$  is presented in Table (3.4). The differing  $\Delta H^\ddagger$  values for  $\text{X}^- = \text{N}_3^-$ ,  $\text{NCS}^-$  and  $\text{OCN}^-$  reflect the different natures of the leaving groups as mentioned above. The  $\Delta S^\ddagger$  values were calculated using equation (3.15). The  $\Delta S^\ddagger$  for  $\text{X}^- = \text{N}_3^-$  is again approximately half of that for the  $\text{NCS}^-$  ligand. Statistical competition factors as well as the symmetry of  $\text{N}_3^-$  may explain this difference.

The errors quoted for the activation data in the  $[\text{Cu}(\text{Me}_6\text{Tren})\text{OCN}]^+/\text{H}_2\text{O}$  aquation system are based on an estimate of the experimental error for the rate constant,  $k_{32}$ .

#### IV (iii) A brief discussion of the $K_{\text{IP}}$ data obtained

The  $K_{\text{IP}}$  values are shown in Table (3.5), on page 76. For  $\text{X}^- = \text{OCN}^-$  the values are in the range  $9.6$  to  $11.4 \text{ mol}^{-1}\text{dm}^3$  (308K to 288K). These experimentally obtained values are for a 2+,1- system in a one molar ionic strength (sodium perchlorate) medium. The literature<sup>6</sup>  $K_{\text{IP}}$  data shown on page 71, for similar 2+,1- systems was determined at 298K in water at zero ionic strength. Using this data a  $K_{\text{IP}}$  value of  $>1 \text{ mol}^{-1}\text{dm}^3$  may be predicted for these 2+,1- systems in a one molar ionic strength (sodium perchlorate) medium. The agreement between the predicted and experimentally obtained  $K_{\text{IP}}$  data for  $\text{X}^- = \text{OCN}^-$  was reasonable, considering the  $K_{\text{IP}}$  sensitivity to the  $k_{23}$  and  $k_{32}$  input data of programme NONLIN. This is reflected in the random fluctuation of the  $K_{\text{IP}}$  values with temperature for  $\text{X}^- = \text{OCN}^-$  which is shown in Table (3.5).

From Table (3.5), for  $\text{X}^- = \text{N}_3^-$  and  $\text{NCS}^-$ , the  $K_{\text{IP}}$  values are somewhat higher than for  $\text{X}^- = \text{OCN}^-$ . I *acknowledge* that the experimentally obtained  $K_{\text{IP}}$  data for both the  $\text{N}_3^-$  and the  $\text{NCS}^-$  anation reactions with  $[\text{Cu}(\text{Me}_6\text{Tren})\text{OH}_2]^{2+}$  were *higher* by almost an order of magnitude than would be expected for a 2+,1- system at one molar ionic strength. The reasons for not considering an associative mechanism applicable for these two anation systems, in which  $K_{\text{IP}}$  would be the formation rate constant for a 6 coordinate intermediate, were presented opposite page 64. Therefore, differences between the predicted and experimentally obtained  $K_{\text{IP}}$  data were attributed to labile site environmental considerations. The environment of the labile site (aqua) is *hydrophobic* in  $[\text{Cu}(\text{Me}_6\text{Tren})\text{OH}_2]^{2+}$  because of the alkyl  $\text{CH}_3$  groups attached to the secondary nitrogens. Ordered water in an *hydrophobic* environment may assist in ion pair formation since ion pairs are formed as a result of electrostatic effects transmitted through solvent molecules between the central metal ion and the anion.

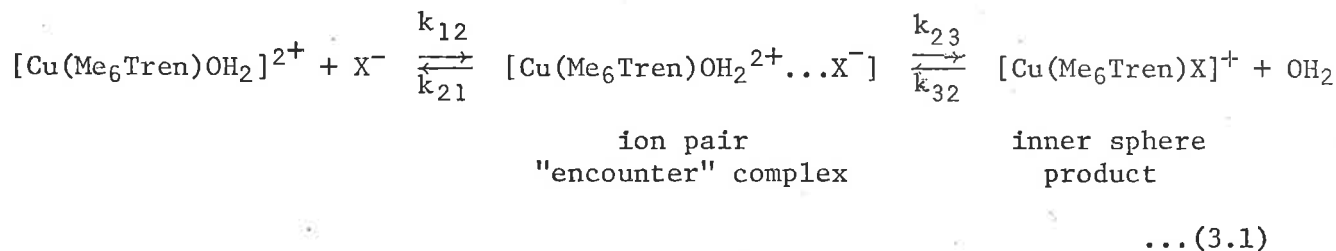
To summarise, the factors affecting the magnitude of  $K_{\text{IP}}$  are,

- (i) the charges of the associating ions.
- (ii) the symmetry, size and charge densities of the associating ions.
- (iii) The environments of both the associating ions,  $[\text{Cu}(\text{Me}_6\text{Tren})\text{OH}_2]^{2+}$  and  $\text{X}^-$ .

V Static and Kinetic Equilibrium Constant Spectrophotometric Data  
Determination

(i) *The general method of equilibrium constant evaluation*

The equilibrium constant data obtained refers to the reaction sequence shown below,



$$\text{where } K_{\text{IP}} = k_{12}/k_{21}$$

The method of calculating Kapp (spectrophotometric) is as follows,

$$\text{absorbance} = \epsilon_{\text{I}} [\text{Cu}(\text{Me}_6\text{Tren})\text{OH}_2^{2+}]_{\text{eq}} + \epsilon_{\text{III}} [\text{Cu}(\text{Me}_6\text{Tren})\text{X}^+]_{\text{eq}} \quad \dots (1)$$

$$[\text{Cu}(\text{Me}_6\text{Tren})\text{OH}_2^{2+}]_{\text{eq}} + [\text{Cu}(\text{Me}_6\text{Tren})\text{X}^+]_{\text{eq}} = [\text{Cu}(\text{Me}_6\text{Tren})\text{OH}_2^{2+}]_{\text{total}} \quad \dots (2)$$

Substitute (2) into (1),

$$\text{absorbance} = \left( \left( [\text{Cu}(\text{Me}_6\text{Tren})\text{OH}_2^{2+}]_{\text{total}} - [\text{Cu}(\text{Me}_6\text{Tren})\text{X}^+]_{\text{eq}} \right) \cdot \epsilon_{\text{I}} + [\text{Cu}(\text{Me}_6\text{Tren})\text{X}^+]_{\text{eq}} \cdot \epsilon_{\text{III}} \right)$$

$$\text{absorbance} = \left( [\text{Cu}(\text{Me}_6\text{Tren})\text{OH}_2^{2+}]_{\text{total}} \cdot \epsilon_{\text{I}} \right) + \Delta\epsilon \cdot [\text{Cu}(\text{Me}_6\text{Tren})\text{X}^+]_{\text{eq}} \quad \dots (3.16)$$

$$\text{where } \Delta\epsilon \text{ (mol}^{-1} \text{ dm}^3 \text{ cm}^{-1}) = \epsilon_{\text{III}} - \epsilon_{\text{I}}$$

and  $\epsilon_n$  is the extinction coefficient of species n

The  $\epsilon_{\text{I}}$  value is measured using pure  $[\text{Cu}(\text{Me}_6\text{Tren})\text{OH}_2]^{2+}$  solutions, at the required wavelengths using a Zeiss PMQ II spectrophotometer.

The  $\epsilon_{\text{III}}$  value is calculated by increasing the ligand ( $\text{X}^-$ ) concentration until an absorbance plateau is reached. At this point is assumed that all of the available  $[\text{Cu}(\text{Me}_6\text{Tren})\text{OH}_2^{2+}]_{\text{total}}$  has reacted with  $\text{X}^-$ . Therefore,

$$\epsilon_{\text{III}} = \frac{\text{Absorbance}}{[\text{Cu}(\text{Me}_6\text{Tren})\text{OH}_2^{2+}]_{\text{total}}} \text{ (plateau region)} \quad \dots (3.17)$$

From equation (3.16), it is seen that,

$$\text{absorbance} = \frac{[\text{Cu}(\text{Me}_6\text{Tren})\text{OH}_2^{2+}]}{\text{total}} \cdot \epsilon_I + [\text{Cu}(\text{Me}_6\text{Tren})\text{X}^+]_{\text{eq}} \cdot (\epsilon_{\text{III}} - \epsilon_I)$$

$$\therefore \frac{\text{absorbance}}{\frac{[\text{Cu}(\text{Me}_6\text{Tren})\text{OH}_2^{2+}]}{\text{total}}} = \epsilon_I + \frac{[\text{Cu}(\text{Me}_6\text{Tren})\text{X}^+]_{\text{eq}}}{\frac{[\text{Cu}(\text{Me}_6\text{Tren})\text{OH}_2^{2+}]}{\text{total}}} \cdot (\epsilon_{\text{III}} - \epsilon_I)$$

$$\text{if } \frac{[\text{Cu}(\text{Me}_6\text{Tren})\text{OH}_2^{2+}]}{\text{total}} \approx [\text{Cu}(\text{Me}_6\text{Tren})\text{X}^+]_{\text{eq}}$$

$$\text{then } \frac{\text{absorbance}}{\frac{[\text{Cu}(\text{Me}_6\text{Tren})\text{OH}_2^{2+}]}{\text{total}}} = \epsilon_{\text{III}} \quad (\text{as in eqn. (3.17)})$$

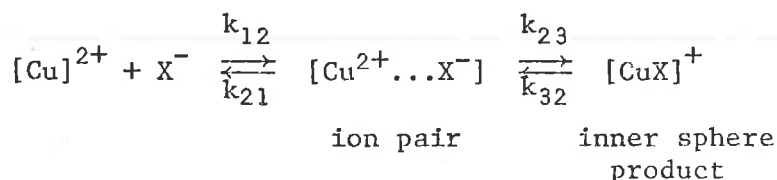
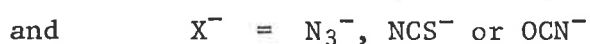
Owing to the coupled equilibria shown in the Eigen mechanism above, the *ratio* of the concentration of the ion pair species and inner sphere complex is a constant.

Therefore at excess  $[\text{X}^-]$  values, (as in stopped flow work), the  $[\text{Cu}(\text{Me}_6\text{Tren})\text{X}]^+$  spectrum cannot be directly determined (*unless*  $k_{32} \ll k_{23}$ ). Also,  $[\text{Cu}(\text{Me}_6\text{Tren})\text{OH}_2^{2+} \dots \text{X}^-]$  cannot be directly determined owing to the rapidity with which the equilibria for the formation/dissociation of the ion pair is established.

Static equilibrium measurements were carried out at 298 K, to test the treatment of the kinetic data. Reasonable agreement between static and kinetic equilibrium constants would establish internal consistency within the postulated Eigen mechanism.

(ii) *The Method of evaluating the apparent equilibrium constant*

A set of equations for the apparent equilibrium constant calculation relating to equation (3.1), appears below,



For equilibrium conditions,

$$[\text{CuX}^+] = [\text{Cu}^{2+}\dots\text{X}^-] \cdot \frac{k_{23}}{k_{32}} \quad \text{and} \quad [\text{Cu}^{2+}\dots\text{X}^-] = K_{\text{IP}}[\text{Cu}^{2+}][\text{X}^-]$$

$$\therefore [\text{CuX}^+][\text{Cu}^{2+}]^{-1}[\text{X}^-]^{-1} = \frac{K_{\text{IP}} \cdot k_{23}}{k_{32}} = K_{\text{eq}} \text{ (overall)} \quad \dots(3.18)$$

However, when an apparent equilibrium constant ( $K_{\text{app}}$ ) is determined spectrophotometrically the absorbance of the solution is given in general as follows,

$$\text{absorbance} = \epsilon_{\text{I}}[\text{Cu}^{2+}] + \epsilon_{\text{II}}[\text{Cu}^{2+}\dots\text{X}^-] + \epsilon_{\text{III}}[\text{CuX}^+] \quad \dots(3.19)$$

where  $\epsilon_n$  is the extinction coefficient of species n

In the limiting case, at high ligand concentrations, the  $[\text{Cu}^{2+}\dots\text{X}^-]$  and  $[\text{CuX}^+]$  species predominate. This corresponds to the plateau region in the  $k_{\text{obs}}$  plot.

Referring to equations (3.6) and (3.7) it is seen that for FIGS. (3.1), (3.3) and (3.6) when  $[\text{X}^-]$  is  $> 0.2 \text{ mol dm}^{-3}$ ,  $> 0.2 \text{ mol dm}^{-3}$  and  $> 0.3 \text{ mol dm}^{-3}$  respectively,  $K_{\text{IP}}[\text{X}^-] \gg 1$  in all cases. Consequently the first term in equation (3.19) becomes negligible and the absorbance is given as follows,

$$\text{absorbance} = \epsilon_{\text{II}}[\text{Cu}^{2+}\dots\text{X}^-] + \epsilon_{\text{III}}[\text{CuX}^+]$$

with  $[\text{Cu}^{2+}\dots\text{X}^-]$  and  $[\text{CuX}^+]$  always occurring in a fixed ratio at equilibrium.

$$\text{Since } [\text{Cu}^{2+}\dots\text{X}^-] = [\text{CuX}^+] \cdot \frac{k_{32}}{k_{23}} \text{ for equilibrium conditions}$$

then,

$$\text{absorbance} = \epsilon_{\text{II}}[\text{CuX}^+] \cdot \frac{k_{32}}{k_{23}} + \epsilon_{\text{III}}[\text{CuX}^+] \quad \dots(3.20)$$

$$\text{absorbance} = \epsilon_{\text{app}} \left( [\text{CuX}^+] + \frac{k_{32}}{k_{23}} [\text{CuX}^+] \right) \quad \dots(3.21)$$

Equating equations (3.20) and (3.21) results in,

$$\frac{\epsilon_{\text{II}} \cdot \frac{k_{32}}{k_{23}} + \epsilon_{\text{III}}}{\frac{k_{32}}{k_{23}} + 1} = \epsilon_{\text{app}}$$

where  $\epsilon_{\text{app}}$  is the apparent extinction coefficient

it can be seen that for  $k_{23} \gg k_{32}$ ,  $\epsilon_{app} = \epsilon_{III}$

$$\text{and } \frac{\text{absorbance}}{\epsilon_{app}} = [\text{Cu}^{2+} \dots \text{X}^-] + [\text{CuX}^+]$$

On the basis of the above,  $K_{app}$  may be defined as follows since both species contribute to the absorbance,

$$\therefore K_{app} = \frac{[\text{CuX}^+] + [\text{Cu}^{2+} \dots \text{X}^-]}{[\text{Cu}^{2+}][\text{X}^-]}$$

$$\therefore K_{app} = K_{eq}(\text{overall}) + K_{IP} = \left( K_{IP} \cdot \frac{k_{23}}{k_{32}} \right) + K_{IP}$$

$$\therefore K_{app} = K_{IP} \left( 1 + \frac{k_{23}}{k_{32}} \right) \quad \dots (3.22)$$

Referring to equation (3.22) it is seen that  $K_{app}$  (spectrophotometric) should be independent of ligand ( $\text{X}^-$ ) concentration.

This was found experimentally where the plots of  $\frac{1}{K_{app}}$  versus  $[\text{X}^-]$  indicated slopes of 0.061, 0.058 and 0.030 for  $\text{X}^- = \text{N}_3^-$ ,  $\text{NCS}^-$  and  $\text{OCN}^-$  respectively. Allowing for experimental error these slopes are essentially zero.

At 298 K, the  $K_{app}$  (spectrophotometric) equilibrium constants for  $\text{X}^- = \text{N}_3^-$ ,  $\text{NCS}^-$  and  $\text{OCN}^-$  were obtained as the mean of the reciprocals of the individual  $\frac{1}{K_{app}}$  values in the plot of  $\frac{1}{K_{app}}$  versus  $[\text{X}^-]$ , using the standard derivation formula shown on page 53.



V (iii) *The  $K_{eq}$  (overall) data from the kinetic data obtained in the analysis using programme NONLIN*

Using equation (3.18), the  $K_{eq}$  (overall) values from the NONLIN kinetic data analysis appear below,

TABLE (3.6)

*Equilibrium data for the formation of  $[\text{Cu}(\text{Me}_6\text{Tren})\text{X}]^+$*

T(K)	$\text{X}^- = \text{N}_3^-$	$\text{X}^- = \text{NCS}^-$	$\text{X}^- = \text{OCN}^-$
	$K_{eq}$ (overall) $\text{mol}^{-1} \text{ dm}^3$	$K_{eq}$ (overall) $\text{mol}^{-1} \text{ dm}^3$	$K_{eq}$ (overall) $\text{mol}^{-1} \text{ dm}^3$
288	485 ± (120)	474 ± (51)	760 ± (234)
298	426 ± (75)	574 ± (71)	555 ± (92)
308	542 ± (61)	659 ± (109)	235 ± (27)

The above  $K_{eq}$  (overall) values refer to the Eigen ( $I_d$ ) mechanism<sup>7</sup> as shown in equation (3.1). The kinetic data used to calculate the equilibrium constant values in Table (3.6) appear in Tables (3.1), (3.3) and (3.5). The error bars quoted in Table (3.6) mainly reflect those of the  $K_{IP}$  parameter which is sensitive to the  $k_{23}$  and  $k_{32}$  values in the NONLIN analysis. This sensitivity of  $K_{eq}$  (overall) to the parameter  $K_{IP}$  is reflected in the somewhat random temperature dependence of  $K_{eq}$  (overall).

V (iv) *Experimental determination of  $K_{app}$  (spectrophotometric)*

The spectrophotometric apparent equilibrium constant was determined at 298 K using the ZEISS PMQ II spectrophotometer. Reaction solutions of constant metal ion concentration and variable ligand concentration were prepared and the absorbance measured. The temperature was maintained by means of a calibrated thermistor probe.

A summary of the main experimental conditions in the spectrophotometric

apparent equilibrium constant determination is as follows,

(i) *The Formation of [Cu(Me<sub>6</sub>Tren)N<sub>3</sub>]<sup>+</sup> at 298 K:*

$$\lambda = 386 \text{ nm}$$

$$\text{pH} = 6.85 \pm (.05)$$

$$\begin{aligned} [\text{Cu}(\text{Me}_6\text{Tren})\text{OH}_2]^{2+} \quad \epsilon_{386 \text{ nm}} &= 45.1 \text{ mol}^{-1} \text{ dm}^3 \text{ cm}^{-1} \\ [\text{Cu}(\text{Me}_6\text{Tren})\text{N}_3]^+ \quad \epsilon_{386 \text{ nm}} &= 3.43 \times 10^3 \text{ mol}^{-1} \text{ dm}^3 \text{ cm}^{-1} \\ [\text{Cu}(\text{Me}_6\text{Tren})\text{OH}_2^{2+}]_{\text{total}} &= 3.40 \times 10^{-4} \text{ mol dm}^{-3} \end{aligned}$$

(ii) *The Formation of [Cu(Me<sub>6</sub>Tren)NCS]<sup>+</sup> at 298 K:*

$$\lambda = 680 \text{ nm}$$

$$\text{pH} = 6.85 \pm (.05)$$

$$\begin{aligned} [\text{Cu}(\text{Me}_6\text{Tren})\text{OH}_2]^{2+} \quad \epsilon_{680 \text{ nm}} &= 150.5 \text{ mol}^{-1} \text{ dm}^3 \text{ cm}^{-1} \\ [\text{Cu}(\text{Me}_6\text{Tren})\text{NCS}]^+ \quad \epsilon_{680 \text{ nm}} &= 207.1 \text{ mol}^{-1} \text{ dm}^3 \text{ cm}^{-1} \\ [\text{Cu}(\text{Me}_6\text{Tren})\text{OH}_2^{2+}]_{\text{total}} &= 1.61 \times 10^{-3} \text{ mol dm}^{-3} \end{aligned}$$

(iii) *The formation of [Cu(Me<sub>6</sub>Tren)OCN]<sup>+</sup> at 298 K:*

$$\lambda = 710 \text{ nm}$$

$$\text{pH} = 6.70 \pm (.05)$$

$$\begin{aligned} [\text{Cu}(\text{Me}_6\text{Tren})\text{OH}_2]^{2+} \quad \epsilon_{710 \text{ nm}} &= 154.4 \text{ mol}^{-1} \text{ dm}^3 \text{ cm}^{-1} \\ [\text{Cu}(\text{Me}_6\text{Tren})\text{OCN}]^+ \quad \epsilon_{710 \text{ nm}} &= 236.5 \text{ mol}^{-1} \text{ dm}^3 \text{ cm}^{-1} \\ [\text{Cu}(\text{Me}_6\text{Tren})\text{OH}_2^{2+}]_{\text{total}} &= 1.60 \times 10^{-3} \text{ mol dm}^{-3} \end{aligned}$$

*Note:* The spectrophotometric and kinetic work was carried out at the same wavelength except in the case of the formation of [Cu(Me<sub>6</sub>Tren)NCS]<sup>+</sup> where these wavelengths were 680 and 370 nm respectively. This was necessary owing to charge transfer band interference at 370 nm. In this region the spectra for [Cu(Me<sub>6</sub>Tren)NCS]<sup>+</sup> formation exhibited a *shoulder*, rather than a definite peak as shown in the spectra for [Cu(Me<sub>6</sub>Tren)N<sub>3</sub>]<sup>+</sup> formation at 386 nm.

V (v) *Comparative equilibrium constant data (both static and kinetic)*

The static and kinetic equilibrium constant data appear in the following table,

TABLE (3.7)

*Comparative equilibrium constant data for the formation of  $[\text{Cu}(\text{Me}_6\text{Tren})\text{X}]^+$  at 298 K*

	$\text{X}^- = \text{N}_3^-$ ( $\lambda = 386 \text{ nm}$ )	$\text{X}^- = \text{NCS}^-$ ( $\lambda = 370^*, 680 \text{ nm}$ )	$\text{X}^- = \text{OCN}^-$ ( $\lambda = 710 \text{ nm}$ )
$K_{\text{eq}}$ (overall) ( $\text{mol}^{-1} \text{ dm}^3$ )	$426 \pm (75)$	$574 \pm (71)$	$555 \pm (92)$
$K_{\text{app}}$ (kinetic) ( $\text{mol}^{-1} \text{ dm}^3$ )	$451 \pm (77)$	$612 \pm (73)$	$569 \pm (103)$
$K_{\text{app}}$ (spectrophotometric) ( $\text{mol}^{-1} \text{ dm}^3$ )	$539 \pm (25)$	$647 \pm (53)$	$629 \pm (8)$

The  $K_{\text{app}}$  (kinetic) and  $K_{\text{app}}$  (spectrophotometric) values show a reasonable agreement and therefore provide an acceptable demonstration of the consistency of the interpretation of the kinetic and static data.

CHAPTER THREE: RESULTS AND DISCUSSION

Section B; Kinetic analysis of the  $[\text{Cu}(\text{Tren})\text{OH}_2]^{2+}/\text{X}^-$  system

- I A discussion of the kinetic data obtained
- II A brief discussion of the limited equilibrium constant data available

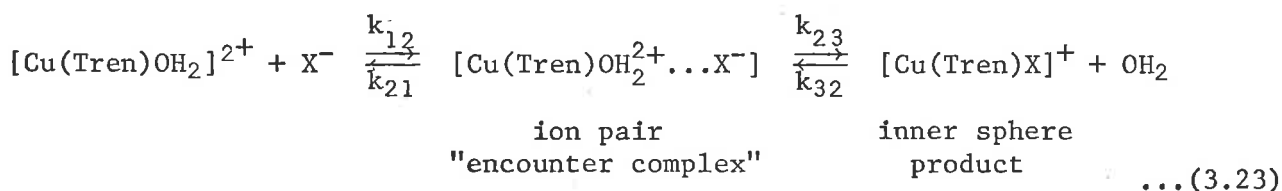
Section B: Kinetic analysis of the  $[\text{Cu}(\text{Tren})\text{OH}_2]^{2+}/\text{X}^-$  system

## I A discussion of the kinetic data obtained

A three temperature investigation, (278, 288, 298 K), for the formation of  $[\text{Cu}(\text{Tren})\text{N}_3]^+$ , together with an experimentally limited one temperature (288 K) study of the formation of  $[\text{Cu}(\text{Tren})\text{NCS}]^+$  is presented. The appropriate kinetic plots of  $\frac{1}{\tau}$  versus  $[a_0 + b_0]$  appear in FIG. (3.8). The kinetic data obtained from a rectilinear analysis of the data points in FIG. (3.8) together with the activation data, appear in Tables (3.8), (3.9) and (3.10).

It is seen from FIG. (3.8) that for both the  $[\text{Cu}(\text{Tren})\text{OH}_2]^{2+}/\text{N}_3^-$  and  $[\text{Cu}(\text{Tren})\text{OH}_2]^{2+}/\text{NCS}^-$  substitution systems, the plots of  $\frac{1}{\tau}$  versus  $[a_0 + b_0]$  are straight lines of positive slope.

It is again postulated that these systems follow the Eigen ( $I_d$ )<sup>7</sup> mechanism, (eqn. 3.23).



$$\text{where } K_{\text{IP}} = k_{12}/k_{21} \quad \text{and} \quad \text{X}^- = \text{N}_3^-, \text{NCS}^-$$

The  $[\text{Cu}(\text{Tren})\text{OH}_2]^{2+}/\text{OCN}^-$  system could not be investigated using the temperature jump technique owing to the unmeasureably small signals from the photomultiplier.

It is suggested that if work were able to be carried out in the  $[\text{Cu}(\text{Tren})\text{OH}_2]^{2+}/\text{X}^-$  systems, (where  $\text{X}^- = \text{N}_3^-, \text{NCS}^-$ ) over a much larger ligand ( $\text{X}^-$ ) concentration range, then curvature of the plot  $\frac{1}{\tau}$  versus  $[a_0 + b_0]$  would be obtained as in the  $[\text{Cu}(\text{Me}_6\text{Tren})\text{OH}_2]^{2+}/\text{X}^-$  system.

It was impracticable, owing to the rapidity of the observed rates (approaching the heating time of the temperature jump apparatus), together with the reduction in the electrical signal from the photomultiplier at the higher ligand ( $\text{X}^-$ ) concentrations, (see page 54).

FIG. (3.8)

The variation of  $\frac{1}{\tau}$  with  $[a_0 + b_0]$  for the  $[\text{Cu}(\text{Tren})\text{OH}_2]^{2+}/\text{N}_3^-$  system is shown as  $\bigcirc$ ,  $\square$ , and  $\triangle$  at 288, 298 and 308 K respectively, and for the  $[\text{Cu}(\text{Tren})\text{OH}_2]^{2+}/\text{NCS}^-$  system as  $\diamond$  at 288 K. Only the temperature jump technique was used to obtain kinetic data, for the two systems shown above.

*The formation of  $[\text{Cu}(\text{Tren})\text{N}_3]^+$ : ( $\lambda = 362$  nm and  $\text{pH } 6.80 \pm .05$ )*

This was investigated at a constant  $[\text{Cu}(\text{Tren})\text{OH}_2^{2+}]_{\text{total}}$  of  $1.52 \times 10^{-3}$  mol  $\text{dm}^{-3}$ . The ligand ( $\text{N}_3^-$ ) concentration range is from

$8.0 \times 10^{-4}$  mol  $\text{dm}^{-3}$  to  $2.4 \times 10^{-2}$  mol  $\text{dm}^{-3}$  at 278 K, 288 K

and from

$4.0 \times 10^{-4}$  mol  $\text{dm}^{-3}$  to  $2.4 \times 10^{-2}$  mol  $\text{dm}^{-3}$  at 298 K

The spectral variation accompanying the formation of  $[\text{Cu}(\text{Tren})\text{N}_3]^+$  appears in FIG. (3.9).

*The formation of  $[\text{Cu}(\text{Tren})\text{NCS}]^+$ : ( $\lambda = 360$  nm and  $\text{pH } 6.80 \pm .05$ )*

This was investigated at a constant  $[\text{Cu}(\text{Tren})\text{OH}_2^{2+}]_{\text{total}}$  of  $5.03 \times 10^{-3}$  mol  $\text{dm}^{-3}$ . The ligand ( $\text{NCS}^-$ ) concentration range is from

$4.0 \times 10^{-3}$  mol  $\text{dm}^{-3}$  to  $2.6 \times 10^{-2}$  mol  $\text{dm}^{-3}$  at 288 K

$[a_0 + b_0]$  is the sum of the initial metal ion and ligand concentrations respectively.

The individual data points in the plot of  $\frac{1}{\tau}$  versus  $[A_0 + B_0]$  for the systems described above, appear in Appendix (3.4).

FIG 3.8

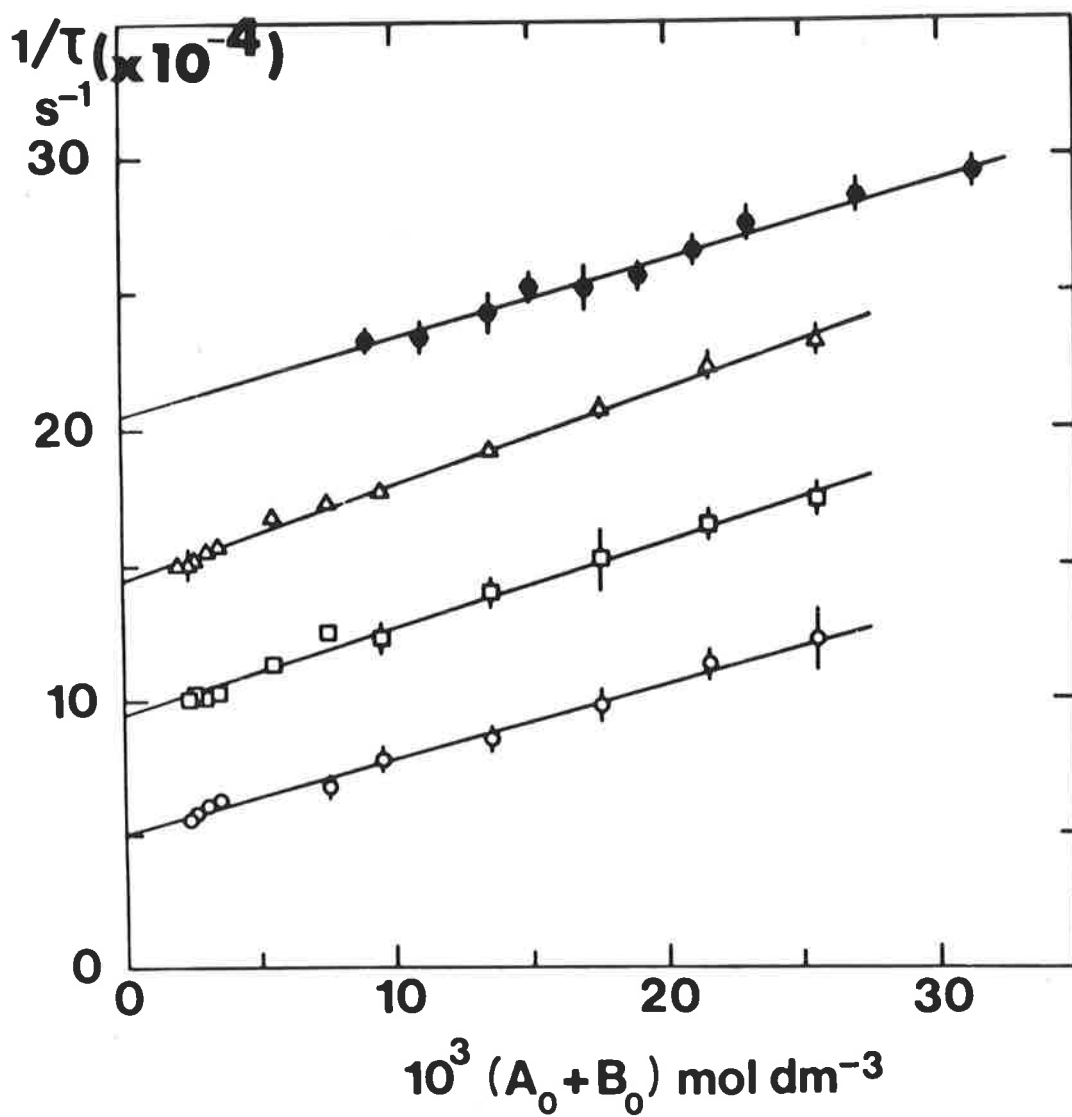


FIG. (3.9)

THE SPECTRAL VARIATION ACCOMPANYING THE FORMATION OF  $[\text{Cu}(\text{Tren})\text{N}_3]^+$

(pH =  $6.75 \pm (.05)$  and the ionic strength =  $1.0 \text{ mol dm}^{-3}$  (sodium perchlorate))

The initial individual metal ion and ligand concentrations in the reaction solutions are:

	$[\text{Cu}(\text{Me}_6\text{Tren})\text{OH}_2^{2+}]$ mol $\text{dm}^{-3}$ ( $\times 10^4$ )	$[\text{N}_3^-]$ mol $\text{dm}^{-3}$ ( $\times 10^3$ )
A	3.38	0.0
B	3.38	8.0
C	3.38	12.0
D	3.38	16.0
E	3.38	20.0
F	3.38	24.0
G	3.38	28.0
H	3.38	32.0
I	3.38	40.0
J	3.38	400.0
K	3.38	1080

The  $\lambda_{\text{max}} = 362 \text{ nm}$  for  $[\text{Cu}(\text{Tren})\text{N}_3]^+$



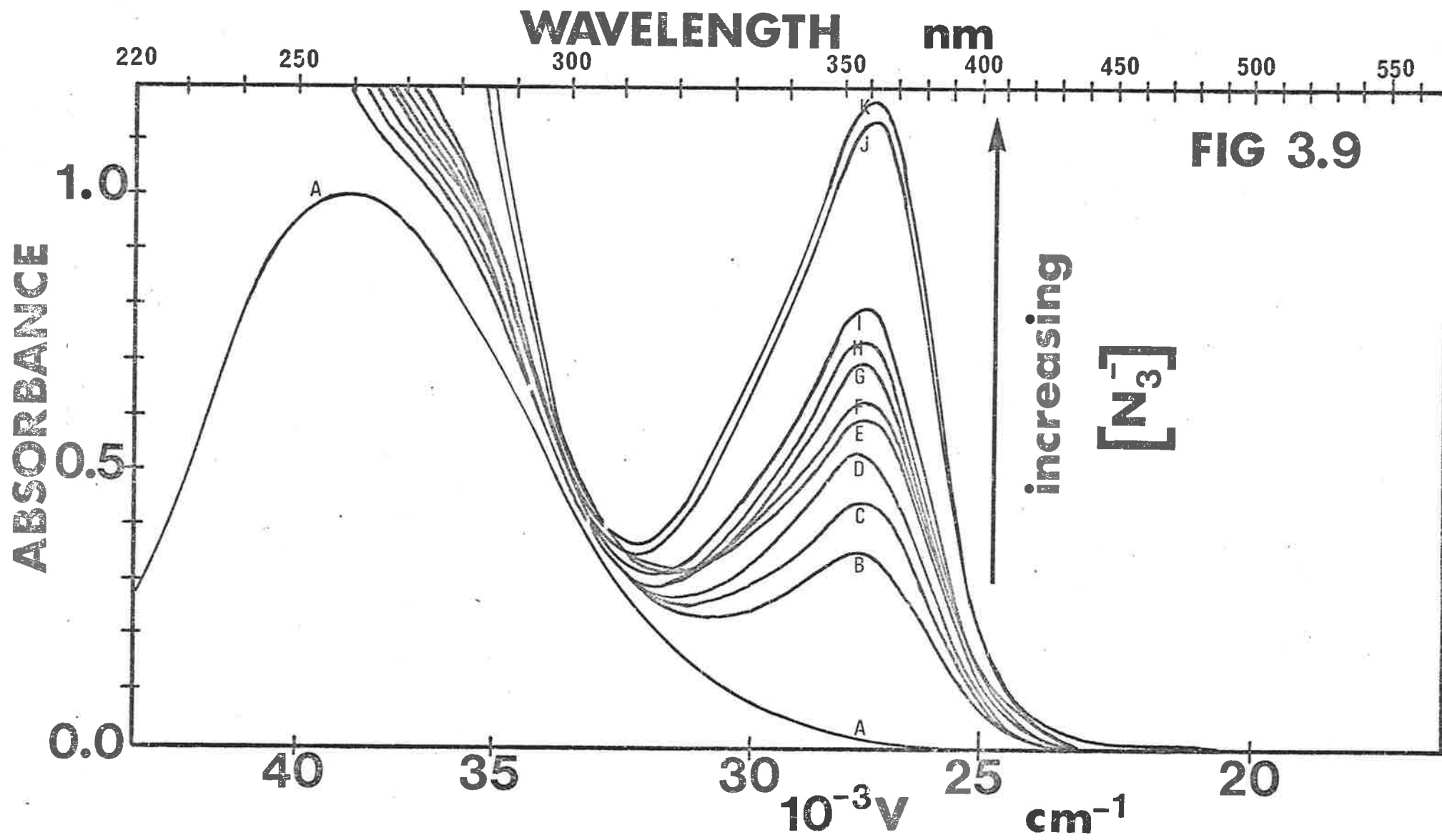


TABLE (3.8)

Kinetic data for the aquation of  $[\text{Cu}(\text{Tren})\text{N}_3]^+$ 

T(K)	(i)	(ii)	(iii)
	$k_{32}$	$k_{32}$	$k_{32}$
	$(\text{s}^{-1}) \times 10^{-4}$	$(\text{s}^{-1}) \times 10^{-4}$	$(\text{s}^{-1}) \times 10^{-4}$
278	$4.97 \pm (0.12)$	$5.26 \pm (0.10)$	$5.37 \pm (0.11)$
288	$9.43 \pm (0.15)$	$9.80 \pm (0.19)$	$9.93 \pm (0.19)$
298	$14.4 \pm (0.1)$	$14.8 \pm (0.1)$	$14.9 \pm (0.1)$

TABLE (3.9)

Kinetic data for the aquation of  $[\text{Cu}(\text{Tren})\text{NCS}]^+$ 

T(K)	(i)	(ii)	(iii)
	$k_{32}$	$k_{32}$	$k_{32}$
	$(\text{s}^{-1}) \times 10^{-4}$	$(\text{s}^{-1}) \times 10^{-4}$	$(\text{s}^{-1}) \times 10^{-4}$
288	$20.6 \pm (0.3)$	$22.1 \pm (0.2)$	$22.5 \pm (0.2)$

TABLE (3.10)

Activation data for the aquation of  $[\text{Cu}(\text{Tren})\text{N}_3]^+$ 

$\Delta H^\ddagger$ ( $\text{kJ mol}^{-1}$ )	$\Delta S^\ddagger$ ( $\text{J K}^{-1} \text{mol}^{-1}$ )	$k_{32}(298 \text{ K})$ ( $\text{s}^{-1} \times 10^{-4}$ )	
$+34.5 \pm (4.2)$	$-30.0 \pm (14.4)$	$14.4 \pm (0.1)$	(i)
$+33.4 \pm (4.1)$	$-33.7 \pm (14.3)$	$14.8 \pm (0.1)$	(ii)
$+33.0 \pm (4.0)$	$-34.9 \pm (14.1)$	$14.9 \pm (0.1)$	(iii)

(i) Derived from a plot of  $\frac{1}{\tau}$  versus  $[a_0 + b_0]$ (ii) Derived from plot of  $\frac{1}{\tau}$  versus  $[\bar{a} + \bar{b}]$  assuming  $K_{\text{eq}}(\text{overall}) = 500$  ( $\text{mol}^{-1} \text{dm}^3$ )(iii) Derived from a plot of  $\frac{1}{\tau}$  versus  $[\bar{a} + \bar{b}]$  assuming  $K_{\text{eq}}(\text{overall}) = 1000$  ( $\text{mol}^{-1} \text{dm}^3$ )

In the very low  $[a_0 + b_0]$  concentration region of the temperature jump work, the rate equation for the Eigen mechanism, (as in eqn. (3.7)), is modified to the following,

$$\frac{1}{\tau} = k_{\text{obs}} = k_{32} + k_{23} K_{\text{IP}} [\bar{a} + \bar{b}] \quad \dots(3.24)$$

$$\text{when } K_{\text{IP}} [\bar{a} + \bar{b}] \ll 1$$

The plateau region ( $k_{23} + k_{32}$ ) of the overall Eigen ( $I_d$ ) curve shown in FIGS. (3.1), (3.3) and (3.6), is not obtained for the  $[\text{Cu}(\text{Tren})\text{OH}_2]^{2+}/\text{X}^-$  substituting systems, owing to the experimentally limited range of ligand concentrations investigated. This means that programme NONLTN could not be utilized for experimentally obtained data analysis. The result is that the individual values of  $K_{\text{IP}}$  and  $k_{23}$  cannot be determined.

The  $k_{32}$  parameter represents the aquation of the  $[\text{Cu}(\text{Tren})\text{X}]^+$  complex, (where  $\text{X}^- = \text{N}_3^-, \text{NCS}^-$ ), and is reported in Tables (3.8) and (3.9).

The  $k_{32}$  values were determined from a rectilinear least squares fit of the plots of  $k_{\text{obs}}$  versus  $[a_0 + b_0]$  where  $[a_0 + b_0]$  is the sum of the initial metal ion and ligand ( $\text{X}^-$ ) concentrations respectively.

The kinetic data in Tables (3.8) and (3.9) is obtained from the plot of  $\frac{1}{\tau}$  versus  $[a_0 + b_0]$  and for  $\frac{1}{\tau}$  versus  $[\bar{a} + \bar{b}]$ , where the hypothetical  $K_{\text{eq}}$  (overall) values used to calculate  $[\bar{a} + \bar{b}]$  were probably unrealistically high. The object was to see what possible effect the  $K_{\text{eq}}$  (overall) value has on the  $k_{32}$  parameter determination. The kinetic data shows this effect to be negligible even for the extremely large hypothetical  $K_{\text{eq}}$  (overall) values assigned.

It was decided to plot the data in FIG. (3.8) as  $\frac{1}{\tau}$  versus  $[a_0 + b_0]$  owing to the fact that the spectrophotometric data indicated an apparent equilibrium constant of approximately 50 (see Table 3.11).

## II A Brief discussion of the limited equilibrium constant data available

Owing to the limited kinetic data available, a detailed equilibrium constant analysis was not possible. The  $K_{\text{app}}$  (spectrophotometric) values were determined for the formation of  $[\text{Cu}(\text{Tren})\text{N}_3]^+$ , by the method discussed previously.

The formation of  $[\text{Cu}(\text{Tren})\text{N}_3]^+$  at 278 K, 288 K, 298 K:

$$\lambda = 362 \text{ nm}$$

$$\text{pH} = 6.80 \pm (0.05)$$

$$\begin{aligned} [\text{Cu}(\text{Tren})\text{OH}_2]^{2+} \quad \epsilon_{362 \text{ nm}} &= 33.6 \text{ mol}^{-1} \text{ dm}^3 \text{ cm}^{-1} \\ [\text{Cu}(\text{Tren})\text{N}_3]^+ \quad \epsilon_{362 \text{ nm}} &= 3.67 \times 10^3 \text{ mol}^{-1} \text{ dm}^3 \text{ cm}^{-1} \\ [\text{Cu}(\text{Tren})\text{OH}_2^{2+}]_{\text{total}} &= 3.38 \times 10^{-4} \text{ mol dm}^{-3} \end{aligned}$$

The equilibrium constant data is shown below,

TABLE (3.11)

*Equilibrium constant data for the formation of*  
 $[\text{Cu}(\text{Tren})\text{N}_3]^+$ , (at  $\lambda = 362 \text{ nm}$ )

T(K)	$K_{\text{app}}$ (spectrophotometric)
278	57.6 $\pm$ (11.5)
288	49.2 $\pm$ (9.8)
298	43.2 $\pm$ (8.6)

The errors were obtained from a standard deviation calculation as discussed previously.

## CHAPTER THREE: RESULTS AND DISCUSSION

## Section C:

- I A comparative discussion of kinetic and activation data for the two systems,  $[\text{Cu}(\text{Me}_6\text{Tren})\text{OH}_2]^{2+}/\text{X}^-$  and  $[\text{Cu}(\text{Tren})\text{OH}_2]^{2+}/\text{X}^-$  (where  $\text{X}^- = \text{N}_3^-, \text{NCS}^-$ )
- II Reasons postulated for the reduced lability of the  $[\text{Cu}(\text{Me}_6\text{Tren})\text{OH}_2]^{2+}/\text{X}^-$  system compared to that of  $[\text{Cu}(\text{Tren})\text{OH}_2]^{2+}/\text{X}^-$
- (i) *Electron donating abilities of coordinated amine ligands*
  - (ii) *Labile site environmental effects in  $[\text{Cu}(\text{Tren})\text{OH}_2]^{2+}$   $[\text{Cu}(\text{Me}_6\text{Tren})\text{OH}_2]^{2+}$*
  - (iii) *Steric hindrance considerations*

## Section C:

I A comparative discussion of kinetic and activation data for the two systems,  $[\text{Cu}(\text{Me}_6\text{Tren})\text{OH}_2]^{2+}/\text{X}^-$  and  $[\text{Cu}(\text{Tren})\text{OH}_2]^{2+}/\text{X}^-$ , (where  $\text{X}^- = \text{N}_3^-$ ,  $\text{NCS}^-$ )

Ligand substitution in the systems,  $[\text{Cu}(\text{Me}_6\text{Tren})\text{OH}_2]^{2+}/\text{X}^-$  and  $[\text{Cu}(\text{Tren})\text{OH}_2]^{2+}/\text{X}^-$ , (where  $\text{X}^- = \text{N}_3^-$ ,  $\text{NCS}^-$ ), is consistent with the Eigen-Wilkins ( $I_d$ ) mechanism, in which the rate determining step for the formation of  $[\text{Cu}(\text{Me}_6\text{Tren})\text{X}]^+$  or  $[\text{Cu}(\text{Tren})\text{X}]^+$  is denoted by the parameter  $k_{23}$ . The rate constant,  $k_{23}$ , is a measure of the rapidity of the dissociation of the inner sphere coordinated aqua ligand, from the ion pair to form the inner sphere product. Theoretically, the  $k_{23}$  value should be equal to the primary water exchange rate of the divalent copper ion, ( $k_{\text{ex}}$ ), in  $[\text{Cu}(\text{Me}_6\text{Tren})\text{OH}_2]^{2+}$  or  $[\text{Cu}(\text{Tren})\text{OH}_2]^{2+}$  depending on the system under investigation. In fact, from the kinetic data obtained, the  $k_{23}$  value is less than the  $k_{\text{ex}}$  value. This is due to the competition between  $\text{X}^-$  and the outer coordination sphere water for the vacant site on dissociation of an inner sphere coordinated  $\text{H}_2\text{O}$  in the ion pair complex. The statistical probability factor  $\alpha$  for substitution of the vacant site was introduced on pages 19 and 20.

$$\text{Thus,} \quad k_{23} = \alpha \cdot k_{\text{ex}} \quad \dots(3.25)$$

experimentally obtained (this study)      experimentally obtained (NMR studies)<sup>8,9</sup>

where  $\alpha$  is the statistical factor and is  $\leq 1$

The value of primary water exchange ( $k_{\text{ex}}$ ) was determined<sup>8</sup> for  $[\text{Cu}(\text{Tren})\text{OH}_2]^{2+}$  at 298 K and found to be  $2.5 \times 10^5 \text{ (s}^{-1}\text{)}$ .

Using N.M.R. techniques for acetonitrile exchange<sup>9</sup> ( $k_{\text{CH}_3\text{CN}}$ ) in the complex,  $[\text{Cu}(\text{Me}_6\text{Tren})\text{CH}_3\text{CN}]^{2+}$ , a value of  $< 100$  at 350 K was indicated. This value is several orders of magnitude slower than that for acetonitrile

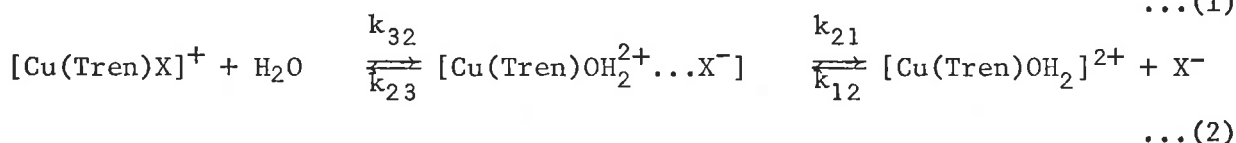
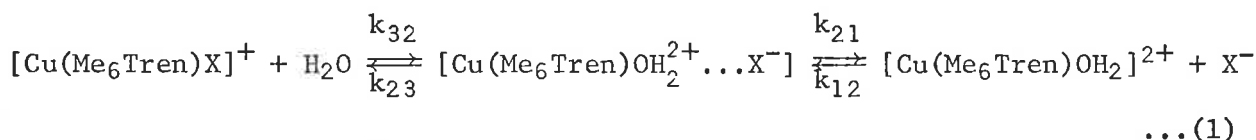
exchange<sup>9</sup> in the complex  $[\text{Cu}(\text{Tren})\text{CH}_3\text{CN}]^{2+}$ .

If a similar expectation is reasonable for the aqua systems then from the acetonitrile exchange data<sup>9</sup> and the experimentally obtained  $k_{23}$  values, the  $k_{\text{ex}}$  for  $[\text{Cu}(\text{Me}_6\text{Tren})\text{OH}_2]^{2+}$  would be in the range 46.1 to 100 (where 46.1 is the largest  $k_{23}$  value from Table (3.1) at 298 K).

The acetonitrile exchange data are shown in Table (3.14) and on page 36.

The comparative kinetic data for aquation in the two systems  $[\text{Cu}(\text{Me}_6\text{Tren})\text{X}]^+/\text{H}_2\text{O}$  and  $[\text{Cu}(\text{Tren})\text{X}]^+/\text{H}_2\text{O}$  appear in the following table,

TABLE (3.12)



T(K)	Complex	$k_{32}$ ( $\text{s}^{-1}$ )	Ratio $k_{32}^{(2)}/k_{32}^{(1)}$
288	$[\text{Cu}(\text{Me}_6\text{Tren})\text{N}_3]^+$	$0.95 \pm (0.08)$	$9.93 \times 10^4$
288	$[\text{Cu}(\text{Tren})\text{N}_3]^+$	$9.43 \pm (0.15) \times 10^4$	
.....			
298	$[\text{Cu}(\text{Me}_6\text{Tren})\text{N}_3]^+$	$1.98 \pm (0.03)$	$7.27 \times 10^4$
298	$[\text{Cu}(\text{Tren})\text{N}_3]^+$	$14.4 \pm (0.1) \times 10^4$	
.....			
288	$[\text{Cu}(\text{Me}_6\text{Tren})\text{NCS}]^+$	$1.36 \pm (0.08)$	$15.2 \times 10^4$
288	$[\text{Cu}(\text{Tren})\text{NCS}]^+$	$20.6 \pm (0.3) \times 10^4$	

The  $[\text{Cu}(\text{Tren})\text{X}]^+$  kinetic data from Tables (3.8) and (3.9) on page (79) is from the plot  $\frac{1}{\tau}$  versus  $[a_0 + b_0]$ .

The comparative kinetic data for anation in the two systems  $[\text{Cu}(\text{Me}_6\text{Tren})\text{OH}_2]^{2+}/\text{X}^-$  and  $[\text{Cu}(\text{Tren})\text{OH}_2]^{2+}/\text{X}^-$  appears in the following table,

TABLE (3.13)

$$[\text{Cu}(\text{Me}_6\text{Tren})\text{OH}_2]^{2+} + \text{X}^- \xrightleftharpoons[k_{21}]{k_{12}} [\text{Cu}(\text{Me}_6\text{Tren})\text{OH}_2^{2+} \dots \text{X}^-] \xrightleftharpoons[k_{32}]{k_{23}} [\text{Cu}(\text{Me}_6\text{Tren})\text{X}]^+ + \text{OH}_2 \dots (3)$$

$$[\text{Cu}(\text{Tren})\text{OH}_2]^{2+} + \text{X}^- \xrightleftharpoons[k_{21}]{k_{12}} [\text{Cu}(\text{Tren})\text{OH}_2^{2+} \dots \text{X}^-] \xrightleftharpoons[k_{32}]{k_{23}} [\text{Cu}(\text{Tren})\text{X}]^+ + \text{OH}_2 \dots (4)$$

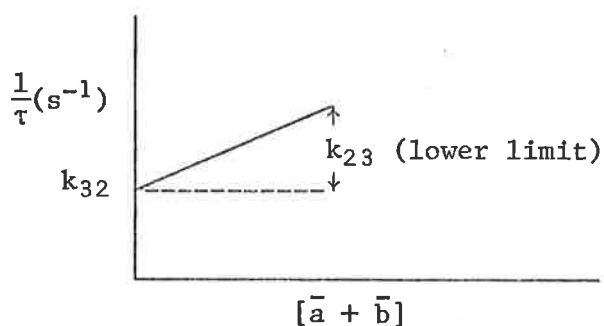
T(K)	Complex	X <sup>-</sup>	k <sub>23</sub> (s <sup>-1</sup> )	Ratio k <sub>23</sub> <sup>(4)</sup> /k <sub>23</sub> <sup>(3)</sup>
288	[Cu(Me <sub>6</sub> Tren)OH <sub>2</sub> ] <sup>2+</sup>	N <sub>3</sub> <sup>-</sup>	15.2 ± (0.5)	> 0.5 × 10 <sup>4</sup>
288	[Cu(Tren)OH <sub>2</sub> ] <sup>2+</sup>	N <sub>3</sub> <sup>-</sup>	> 7.94 × 10 <sup>4</sup>	
.....				
298	[Cu(Me <sub>6</sub> Tren)OH <sub>2</sub> ] <sup>2+</sup>	N <sub>3</sub> <sup>-</sup>	34.6 ± (1.3)	> 0.25 × 10 <sup>4</sup>
298	[Cu(Tren)OH <sub>2</sub> ] <sup>2+</sup>	N <sub>3</sub> <sup>-</sup>	> 8.76 × 10 <sup>4</sup>	
.....				
288	[Cu(Me <sub>6</sub> Tren)OH <sub>2</sub> ] <sup>2+</sup>	NCS <sup>-</sup>	16.2 ± (0.2)	> 0.47 × 10 <sup>4</sup>
288	[Cu(Tren)OH <sub>2</sub> ] <sup>2+</sup>	NCS <sup>-</sup>	> 7.63 × 10 <sup>4</sup>	

The k<sub>23</sub> values in Table (3.13) for anation of [Cu(Tren)OH<sub>2</sub>]<sup>2+</sup> cannot be determined exactly although a lower limit of k<sub>23</sub> can be determined, as follows.

A number of  $\frac{1}{\tau}$  values at varying  $[\bar{a} + \bar{b}]$  were calculated from experimentally obtained data using the temperature jump technique. The rate constant, k<sub>32</sub>, was found from a rectilinear analysis of this data as discussed previously. The lower limit for the rate constant, k<sub>23</sub>, was assigned as the difference between the k<sub>32</sub> value and the  $\frac{1}{\tau}$  value at the highest  $[\bar{a} + \bar{b}]$  investigated (at a particular temperature). Therefore, although the plateau region (k<sub>23</sub> + k<sub>32</sub>) is not reached for the [Cu(Tren)OH<sub>2</sub>]<sup>2+</sup>/X<sup>-</sup> anation system, a lower limit for k<sub>23</sub> can be evaluated. This enables the two anation systems to be compared,



as shown in Table (3.13).



The ratio

$$\frac{k_{\text{ex}} \text{ for } [\text{Cu}(\text{Tren})\text{OH}_2]^{2+}}{k_{\text{ex}} \text{ for } [\text{Cu}(\text{Me}_6\text{Tren})\text{OH}_2]^{2+}} = \frac{2.5 \times 10^5 \text{ (s}^{-1}\text{)}}{< 100 \text{ (s}^{-1}\text{)}}$$

which is  $> 0.25 \times 10^4$  at 298 K

This assumes that the ratio of acetonitrile exchange in the two systems,  $[\text{Cu}(\text{Tren})\text{CH}_3\text{CN}]^{2+}$  and  $[\text{Cu}(\text{Me}_6\text{Tren})\text{CH}_3\text{CN}]^{2+}$  is comparable to the ratio of water exchange in the two systems,  $[\text{Cu}(\text{Tren})\text{OH}_2]^{2+}$  and  $[\text{Cu}(\text{Me}_6\text{Tren})\text{OH}_2]^{2+}$ .

The  $k_{\text{ex}}$  ratio obtained is very similar to the  $k_{23}$  ratios in Table (3.13), which is to be expected for the  $I_d$  mechanism.

The following table summarises work on acetonitrile exchange,

TABLE (3.14)

*Rate parameters for the exchange of acetonitrile  
on bivalent metal complexes*

Complex	$k_{\text{ex}}$ (298 K) ( $\text{s}^{-1}$ )	$\Delta H^\ddagger$ $\text{kJ mol}^{-1}$	$\Delta S^\ddagger$ $\text{J K}^{-1} \text{mol}^{-1}$	Ref.
$[\text{Cu}(\text{MeCN})_6]^{2+}$	$\geq 1.6 \times 10^7$ (228 K)	-	-	9
$[\text{Cu}(\text{Tren})(\text{MeCN})]^{2+}$	$(1.7 \pm 0.2) \times 10^6$ $(5.1 \pm 0.7) \times 10^3$ (228 K)	$45 \pm 4$	$26 \pm 16$	9
$[\text{Cu}(\text{Trenol})(\text{MeCN})_2]^{2+}$	$(2.6 \pm 0.5) \times 10^6$ $(8.0 \pm 2.0) \times 10^4$ (228 K)	$26 \pm 8$	$-34 \pm 32$	9
$[\text{Cu}(\text{Me}_6\text{Tren})(\text{MeCN})]^{2+}$	$< 100^c$	-	-	9
$[\text{Co}(\text{MeCN})_6]^{2+}$	$(3.2 \pm 0.3) \times 10^5$	$48 \pm 2$	$22 \pm 8$	10
$[\text{Co}(\text{Tren})(\text{MeCN})]^{2+}$	$\geq 2 \times 10^6$	-	-	10
$[\text{Ni}(\text{MeCN})_6]^{2+}$	$(2.0 \pm 0.3) \times 10^3$	$69 \pm 2$	$50 \pm 8$	10
<sup>a</sup> $[\text{Ni}(\text{Tren})(\text{MeCN})_2]^{2+}$	$(16.5 \pm 3.5) \times 10^4$	$45 \pm 6$	$6 \pm 21$	10
<sup>b</sup> $[\text{Ni}(\text{Tren})\text{MeCN}]_2]^{2+}$	$\geq 2 \times 10^6$	-	-	10

*a* MeCN trans to the tertiary amine group

*b* MeCN cis to the tertiary amine group

*c* At 350 K

Table abstracted from reference 9.

Referring to Table (3.12), the dissociation of  $\text{N}_3^-$  from  $[\text{Cu}(\text{Tren})\text{N}_3]^+$  occurs at  $9.93 \times 10^4$  (288 K) and  $7.27 \times 10^4$  (298 K), times more rapidly than for the corresponding dissociation from the  $[\text{Cu}(\text{Me}_6\text{Tren})\text{N}_3]^+$  complex. In the case of  $\text{NCS}^-$ , the dissociation from  $[\text{Cu}(\text{Tren})\text{NCS}]^+$  is  $15.2 \times 10^4$  times more rapid than from  $[\text{Cu}(\text{Me}_6\text{Tren})\text{NCS}]^+$ , at 288 K.

The comparative activation data for aquation in the systems,  $[\text{Cu}(\text{Tren})\text{X}]^+/\text{H}_2\text{O}$  and  $[\text{Cu}(\text{Me}_6\text{Tren})\text{X}]^+/\text{H}_2\text{O}$ , appear in Table (3.15).

TABLE (3.15)

*Activation data for the aquation of  $[\text{Cu}(\text{Me}_6\text{Tren})\text{N}_3]^+$  ... (1)*

*Activation data for the aquation of  $[\text{Cu}(\text{Tren})\text{N}_3]^+$  ... (2)*

	$\Delta H^\ddagger$ (kJ mol <sup>-1</sup> )	$\Delta S^\ddagger$ (J K <sup>-1</sup> mol <sup>-1</sup> )
(1)	+52.5 ± (1.4)	-62.8 ± (4.7)
(2)	+34.5 ± (4.2)	-30.0 ± (14.4)

The data in (2) are obtained from plots of  $\frac{1}{\tau}$  versus  $[a_0 + b_0]$  measured at three different temperatures.

From the activation data in Table (3.15), it can be seen that the much faster dissociation of  $\text{X}^-$  from  $[\text{Cu}(\text{Tren})\text{X}]^+$  compared to that from  $[\text{Cu}(\text{Me}_6\text{Tren})\text{X}]^+$ , results from both the enthalpy and entropy factors.

Solid state X-ray crystallographic studies have shown that the labile site ( $\text{X}^-$ ) in  $[\text{Cu}(\text{Me}_6\text{Tren})\text{X}]^+$  occupies a small hydrophobic<sup>11</sup> pocket whereas in  $[\text{Cu}(\text{Tren})\text{X}]^+$ , the  $\text{X}^-$  occupies a much more exposed hydrophilic<sup>12</sup> environment. If solvation effects are important in the determination of transition state energetics (inner sphere product  $\ddagger$  ion pair), then dissociation of  $\text{X}^-$  from  $[\text{Cu}(\text{Tren})\text{X}]^+$  would be more labile than from  $[\text{Cu}(\text{Me}_6\text{Tren})\text{X}]^+$ . The bulky methyl groups on the secondary nitrogens in  $[\text{Cu}(\text{Me}_6\text{Tren})\text{X}]^+$  produce considerable steric constraint on the labile site ( $\text{X}^-$ ) and therefore it is less accessible to the solvent.

This same idea is used in part to account for the slower water exchange rates in the primary hydration sphere of divalent copper in  $[\text{Cu}(\text{Me}_6\text{Tren})\text{OH}_2]^{2+}$  compared with that for  $[\text{Cu}(\text{Tren})\text{OH}_2]^{2+}$ . Both the steric constraints imparted by methyl groups and the ordered  $\text{H}_2\text{O}$  surrounding the leaving group in a hydrophobic environment are probably important in determining the apparent slow water exchange<sup>9</sup> in  $[\text{Cu}(\text{Me}_6\text{Tren})\text{OH}_2]^{2+}$  compared with  $[\text{Cu}(\text{Tren})\text{OH}_2]^{2+}$ . The

reduced lability of  $[\text{Cu}(\text{Tren})\text{OH}_2]^{2+}$  compared with  $[\text{Cu}(\text{OH}_2)_6]^{2+}$  was found from water exchange measurements using the N.M.R.<sup>8,9,14</sup> technique. This results from the removal of the Jahn Teller<sup>13</sup> effect (as discussed on page 17).

This phenomenon also occurs in the systems,  $[\text{Cu}(\text{CH}_3\text{CN})_6]^{2+}$ ,  $[\text{Cu}(\text{Tren})\text{CH}_3\text{CN}]^{2+}$  and  $[\text{Cu}(\text{Me}_6\text{Tren})\text{CH}_3\text{CN}]^{2+}$ , with the relevant acetonitrile exchange data<sup>9</sup> shown in Table (3.14).

Studies reported in this thesis for anation and aquation in the systems,  $[\text{Cu}(\text{Tren})\text{OH}_2]^{2+}/\text{X}^-$  and  $[\text{Cu}(\text{Me}_6\text{Tren})\text{OH}_2]^{2+}/\text{X}^-$ , again show this reduction in lability upon chelation of  $[\text{Cu}(\text{OH}_2)_6]^{2+}$ . This is shown in the following data,

(1) anation: (at 298 K)	$[\text{Cu}(\text{OH}_2)_6]^{2+}$	$k_{\text{ex}} = 8 \times 10^9 \text{ s}^{-1}$ (ref. 14)
	$[\text{Cu}(\text{Tren})\text{OH}_2]^{2+}$	$k_{23} \sim 10^5 \text{ s}^{-1}$
	$[\text{Cu}(\text{Me}_6\text{Tren})\text{OH}_2]^{2+}$	$k_{23} = 34.6 \text{ s}^{-1}$
(2) aquation: (at 298 K)	$[\text{Cu}(\text{OH}_2)_6]^{2+}$	$k_{\text{ex}} = 8 \times 10^9 \text{ s}^{-1}$ (ref. 14)
	$[\text{Cu}(\text{Tren})\text{N}_3]^+$	$k_{32} = 1.44 \times 10^5 \text{ s}^{-1}$
	$[\text{Cu}(\text{Me}_6\text{Tren})\text{N}_3]^+$	$k_{32} = 1.98 \text{ s}^{-1}$

## II Reasons postulated for the reduced lability of the $[\text{Cu}(\text{Me}_6\text{Tren})\text{OH}_2]^{2+}/\text{X}^-$ system compared to that for $[\text{Cu}(\text{Tren})\text{OH}_2]^{2+}/\text{X}^-$

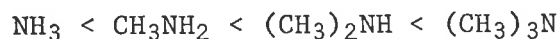
The possible reasons will be discussed in the following sequence:

- (i) *electron donating abilities of coordinated amine ligands*
- (ii) *labile site environment*: hydrophobic and hydrophilic for the labile site in the systems  $[\text{Cu}(\text{Me}_6\text{Tren})\text{OH}_2]^{2+}/\text{X}^-$  and  $[\text{Cu}(\text{Tren})\text{OH}_2]^{2+}/\text{X}^-$  respectively.
- (iii) *steric hindrance considerations*: (see the 3 dimensional model in FIG. (1.3)).

II (i) *Electron donating abilities of coordinated amine ligands*

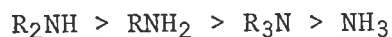
It is necessary to consider the relative donating abilities of the groups  $-\text{NH}_2$  and  $-\text{N}(\text{CH}_3)_2$  in  $[\text{Cu}(\text{Tren})\text{OH}_2]^{2+}$  and  $[\text{Cu}(\text{Me}_6\text{Tren})\text{OH}_2]^{2+}$ , respectively.

In a bonding configuration; lone pair polarization follows the inductive order for a series of amines as follows,



For these secondary nitrogens, from purely inductive considerations increasing the number of alkyl substituents on nitrogen increases electron donating ability (and so basicity). Therefore, in the above sequence  $\text{N}(\text{CH}_3)_3$  should be the strongest Lewis<sup>15</sup> base.

For a series of alkylamines, the following sequence of basicity in water is observed, which is in conformity with the Lewis base sequence.



decreasing  
basicity

The above sequence suggests that increasing alkyl substitution on the nitrogen would produce better ligands than ammonia. However, it has been found<sup>17</sup> that primary aliphatic amines coordinate less readily than ammonia, secondary amines coordinate less readily than do primary, and tertiary amines show almost no ability to coordinate to metal ions, (however in  $[\text{Cu}(\text{Me}_6\text{Tren})\text{OH}_2]^{2+}$  and  $[\text{Cu}(\text{Tren})\text{OH}_2]^{2+}$  the tertiary nitrogen does coordinate to divalent copper).

The above inconsistency with the basicity sequence as determined from purely inductive effects, leads to the necessity of considering steric effects on increasing alkylation.

The contributions to Ni(II) - ligand interactions from inductive and steric effects in octahedral complexes have been investigated.<sup>16</sup>



The N-monoalkyl-substituted<sup>16</sup> amine complexes become slightly more basic with increasing the length of the alkyl chain.<sup>18</sup> However, the spectra of nickel complexes of these same ligands show a systematic decrease in  $D_q$  values as the alkyl group becomes more complex. The same trend was found in the  $D_q$  values of the N,N'-dialkylethylenediamine complexes.

Although the ethyl group is more electron releasing than the methyl group, this effect is often offset by its larger steric requirements. In the case of simple amines, trimethylamine is a stronger base toward trimethylborane than ethyldimethylamine<sup>19</sup> or triethylamine.<sup>20</sup> The steric effects outweigh the inductive effects.

Since both N,N'-dimethylethylenediamine and N-methyl-N'-ethylethylenediamine are stronger bases than ethylenediamine, the smaller  $D_q$  values (in the Ni(II) complexes) of these two ligands indicate that the magnitude of the steric effects again outweighs the inductive considerations.<sup>16</sup>

TABLE (3.16)

Data Derived from Aqueous Solution Spectra of the Ni(II) Complexes

ligand	(at $\lambda_{\text{max}}$ ) $\text{cm}^{-1}$ $\nu$	
en	11,230	$\nu_1$ ${}^3A_{2g} \rightarrow {}^3T_{2g}$
	12,600	$\nu_2$ ${}^3A_{2g} \rightarrow {}^1E_g$
	18,320	$\nu_3$ ${}^3A_{2g} \rightarrow {}^3T_{1g}(F)$
	28,990	$\nu_4$ ${}^3A_{2g} \rightarrow {}^3T_{1g}(P)$
N-methylen	10,870	
	12,350	
	17,860	
	28,410	
N-ethylen	10,730	
	12,790	
	17,390	
	28,010	
N-propylen	10,570	
	12,850	
	17,320	
	27,930	

Abstracted from Table IV in reference 16.

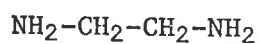
Table (3.16) shows that the  $\lambda_{\text{max}}$  values are shifted to lower frequencies on increasing the alkylation of en (that is, Ni(II) complexes with en have larger  $D_q$  values than for N-propylen).

TABLE (3.17)  
*Data derived from Solution Spectra Using the  
 Respective Ligands as Solvents*

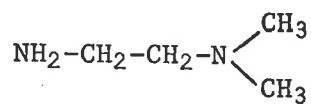
Ligand	(at $\lambda_{\text{max}}$ ) $\text{cm}^{-1}$ $\nu$	$D_q \cdot \text{cm}^{-1}$ ( $\pm 4 \text{ cm}^{-1}$ )
en	11,360	1136
	12,500	
	18,350	
	29,070	
N-methylen	10,940	1094
	12,500	
	17,950	
	28,490	
N-ethylen	10,760	1076
	12,500	
	17,860	
	28,260	
N-propylen	10,660	1066
	12,500	
	17,790	
	28,170	
N,N-dimethylen	10,000	1000
	12,500	
	16,860	
	27,170	

The above table is abstracted from Table III in ref. 16.

Table (3.17) shows a systematic decrease in  $D_q$  values on alkylation of the en ligand in the Ni(II) complexes. Compare the following structures,



(en)



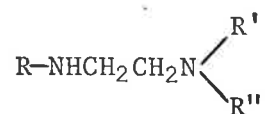
N,N-dimethylen

→  
 decreasing  $D$  from spectral measurements



The  $D_q$  value is a measure of the interaction between the metal ion and ligand, with the greatest interaction having the larger  $D_q$  values. In Table (3.17) it is shown that en has the largest  $D_q$  value in the Ni(II) complex.

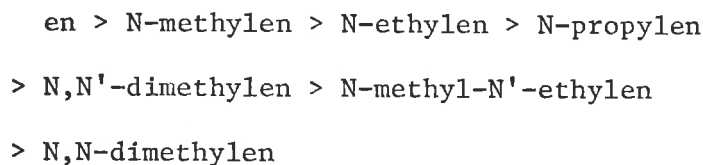
For a metal ion and ligand interaction, Pavkovic and Meek<sup>16</sup> studied the systematic variance of the  $D_q$  values for the ligand,



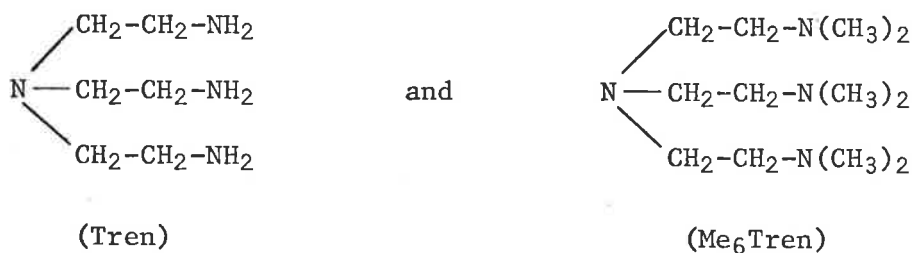
in the complex  $[\text{Ni}(\text{ligand})_3](\text{ClO}_4)_2$ , in the solid, in ligand solution, and in aqueous solution.

In the aqueous environment,  $\text{R}'$  and  $\text{R}'' = \text{H}$  and  $\text{R}$  is varied from H, Me, Et, Pr (Et = ethyl and Pr = propyl). The resulting Ni(II) complexes showed a reduction in  $D_q$  values with increased alkylation of the ligand. This is in accord with the less alkylated species having a greater electron donation ability.

The  $D_q$  values, which reflect the net result of steric and inductive factors, produce the following spectrochemical series:<sup>16</sup>



The two ligands of interest here are:



*Note:* The electron donating ability of either  $-\text{NH}_2$  or  $-\text{N}(\text{CH}_3)_2$  will depend on the spatial distribution of both metal ion and ligand orbitals. If the ligand is capable of donating electrons, the metal ion must

have a d orbital in position to accept these electrons. Distortions of the spatial distribution of the d orbitals resulting from changes in structural configurations (e.g. octahedral and trigonal bipyramidal) may affect ligand electron donation abilities. It is for this reason that the previously discussed Ni(II) octahedral complexes are used only as a guide to the effect of alkylation on electron donation in  $[\text{Cu}(\text{Me}_6\text{Tren})\text{OH}_2]^{2+}$  and  $[\text{Cu}(\text{Tren})\text{OH}_2]^{2+}$ .

Acid dissociation constants of coordinated water molecules in the general complexes,  $[\text{M}(\text{Tren})\text{OH}_2]^{2+}$  and  $[\text{M}(\text{Me}_6\text{Tren})\text{OH}_2]^{2+}$  were investigated.<sup>21</sup> It was suggested that the  $\text{pK}_a$  variation may arise in part from differences in electron donation to the central metal ion between the  $-\text{NH}_2$  and  $-\text{N}(\text{CH}_3)_2$  groups of Tren and  $\text{Me}_6\text{Tren}$  respectively.

The crystal field splitting<sup>22</sup> of  $[\text{Co}(\text{Tren})\text{OH}_2]^{2+}$  has been shown to be greater than for the methylated analogue (all bands of Tren complexes  $[\text{Co}(\text{Tren})\text{X}]_2$  are shifted to higher frequencies with respect to the  $\text{Me}_6\text{Tren}$  complexes). This is in agreement with the greater crystal field strength of the  $\text{NH}_2$  group in comparison to that of  $-\text{N}(\text{CH}_3)_2$ .<sup>16</sup>

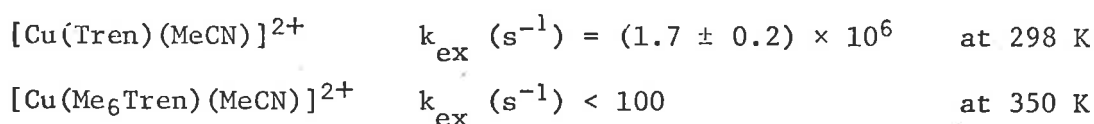
On the basis of the above discussion, the postulated greater electron donation to the central metal ion in  $[\text{M}(\text{Tren})\text{OH}_2]^{2+}$  may result in higher  $\text{pK}_a$  values for these complexes than for the  $[\text{M}(\text{Me}_6\text{Tren})\text{OH}_2]^{2+}$  series. This was a trend found experimentally.<sup>21</sup>

From the above discussion, it is concluded that the  $-\text{NH}_2$  group is more electron donating than  $-\text{N}(\text{CH}_3)_2$  in the  $[\text{Cu}(\text{Tren})\text{OH}_2]^{2+}$  and  $[\text{Cu}(\text{Me}_6\text{Tren})\text{OH}_2]^{2+}$  complexes, respectively. The result is a reduction in positive charge of the central metal ion in  $[\text{Cu}(\text{Tren})\text{OH}_2]^{2+}$  consequently weakening the copper(II) to leaving group bond. This bond weakening in part contributes to the greater lability of the  $[\text{Cu}(\text{Tren})\text{OH}_2]^{2+}/\text{X}^-$  system in comparison with the  $[\text{Cu}(\text{Me}_6\text{Tren})\text{OH}_2]^{2+}/\text{X}^-$  system.

II (ii) *Labile site environmental effects in*  $[\text{Cu}(\text{Tren})\text{OH}_2]^{2+}$  *and*  
 $[\text{Cu}(\text{Me}_6\text{Tren})\text{OH}_2]^{2+}$

The labile site environments in  $[\text{Cu}(\text{Tren})\text{OH}_2]^{2+}$  and  $[\text{Cu}(\text{Me}_6\text{Tren})\text{OH}_2]^{2+}$  are hydrophilic and hydrophobic respectively. This phenomenon was discussed previously in the light of solvation effects being important in transition state energy determinations ( $\Delta H^\ddagger$  and  $\Delta S^\ddagger$ ). From work<sup>9</sup> outlined in Table (3.14), it is concluded that the hydrophobic environment factor, although significant, is not the major factor determining the relative labilities of the  $[\text{Cu}(\text{Tren})\text{OH}_2]^{2+}$  and  $[\text{Cu}(\text{Me}_6\text{Tren})\text{OH}_2]^{2+}$  complexes.

The acetonitrile exchange data for the divalent copper Tren and  $\text{Me}_6\text{Tren}$  systems are as follows,<sup>9</sup>



The large differences in labilities for the two acetonitrile exchange systems shown above parallel work on substitution in the systems,  $[\text{Cu}(\text{Tren})\text{OH}_2]^{2+}/\text{X}^-$  and  $[\text{Cu}(\text{Me}_6\text{Tren})\text{OH}_2]^{2+}/\text{X}^-$ .

In the acetonitrile exchange systems the "ice-like" structure of the solvent is not present although there is a large difference in labilities for the two complexes,  $[\text{Cu}(\text{Tren})(\text{MeCN})]^{2+}$  and  $[\text{Cu}(\text{Me}_6\text{Tren})(\text{MeCN})]^{2+}$ . This would suggest that solvent ordering considerations concerning the labile site are not the major factors in determining the different observed rates for substitution in the divalent copper Tren and  $\text{Me}_6\text{Tren}$  complexes.

II (iii) *Steric hindrance considerations:* (see FIG. (1.3))

The clustered methyl groups in  $[\text{Cu}(\text{Me}_6\text{Tren})\text{OH}_2]^{2+}$  and  $[\text{Cu}(\text{Me}_6\text{Tren})\text{X}]^+$ , would substantially hinder the removal of the respective leaving groups. The leaving group will have to vacate a confined space for the entering group whereas in the  $[\text{Cu}(\text{Tren})\text{OH}_2]^{2+}$  complex the labile site is relatively

open to substitution. The models shown in FIG. (1.3) clearly show the constraint placed on the labile site in  $[\text{Cu}(\text{Me}_6\text{Tren})\text{OH}_2]^{2+}$ . It is postulated that the bulky methyl groups may also preclude geometrical re-arrangement in the transition state - reflected by the slower observed substitution rates in the  $[\text{Cu}(\text{Me}_6\text{Tren})\text{OH}_2]^{2+}/\text{X}^-$  system.

## CHAPTER THREE: RESULTS AND DISCUSSION

Section D: Kinetic analysis of the  $[\text{Cu}(\text{Me}_6\text{Tren})\text{OH}_2]^{2+}/\text{X}^-$  system

(where  $\text{X}^- = \text{Br}^-, \text{Cl}^-$ )

- I Discussion and Interpretation of the kinetic data obtained
- II A comparative discussion of kinetic data, for aquation of the complexes  $[\text{Cu}(\text{Me}_6\text{Tren})\text{X}]^+$  where ( $\text{X}^- = \text{N}_3^-, \text{NCS}^-, \text{OCN}^-, \text{Br}^-$  and  $\text{Cl}^-$ )

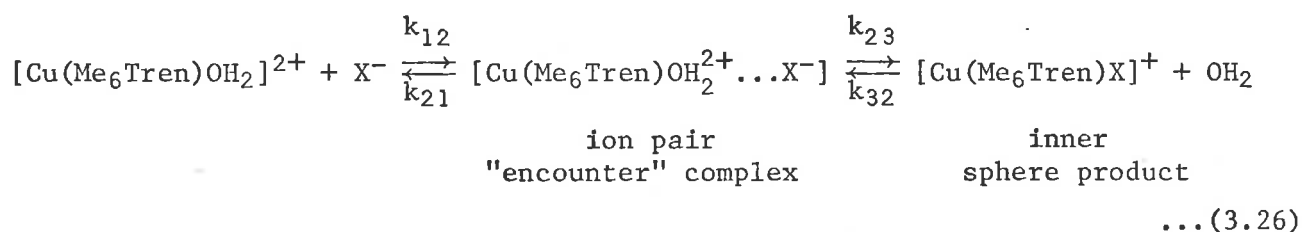
Section D: Kinetic analysis of the  $[\text{Cu}(\text{Me}_6\text{Tren})\text{OH}_2]^{2+}/\text{X}^-$  system,

(where  $\text{X}^- = \text{Br}^-, \text{Cl}^-$ )

### I Discussion and Interpretation of the Kinetic Data Obtained

The plots of  $k_{\text{obs}}$  over the entire ligand ( $\text{Br}^-, \text{Cl}^-$ ) concentration range for the two systems,  $[\text{Cu}(\text{Me}_6\text{Tren})\text{OH}_2]^{2+}/\text{Br}^-$  and  $[\text{Cu}(\text{Me}_6\text{Tren})\text{OH}_2]^{2+}/\text{Cl}^-$  appear in FIG. (3.10). The kinetic data was obtained under pseudo first order conditions. The wavelength for investigation was determined from photomultiplier electrical signal amplitude measurements at various wavelengths using the stopped flow apparatus, together with spectral analyses on the Zeiss DMR 10 recording spectrophotometer, (see FIGS. (3.11) to (3.14) inclusive).

The plots of  $k_{\text{obs}}$  against  $[\text{X}^-]$  shown in FIG. (3.10) are straight lines of essentially zero slope, at all temperatures investigated. The Eigen-Wilkins ( $\text{I}_d$ )<sup>7</sup> mechanism is again considered operative as shown below,



where  $K_{\text{IP}} = k_{12}/k_{21}$  and  $\text{X}^- = \text{Br}^-, \text{Cl}^-$

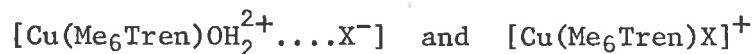
It is suggested that the curvature of the plots  $k_{\text{obs}}$  versus  $[\text{X}^-]$  shown in FIGS. (3.1), (3.3) and (3.6) is not apparent in the  $\text{Cl}^-$ ,  $\text{Br}^-$  substitutions in  $[\text{Cu}(\text{Me}_6\text{Tren})\text{OH}_2]^{2+}$  because,

$$k_{32} \gg k_{23} \quad \dots(3.27)$$

That is, the equilibrium between the ion pair "encounter" complex and the inner sphere product greatly favours the ion pair. Therefore, the straight line plots of essentially zero slope are in fact the usual Eigen curves but that this curvature lies within the standard deviations of the individual  $k_{\text{obs}}$  values (at all temperatures studied). The  $k_{32}$  values obtained from a rectilinear least squares analysis of the plots  $k_{\text{obs}}$  versus  $[\text{X}^-]$ , ( $\text{X}^- = \text{Br}^-$ ,

$\text{Cl}^-$ ) will be accurate to within the standard deviations of  $k_{\text{obs}}$ .

The satisfactory amplitudes of the signals obtained from the photomultiplier on mixing the reactants in the stopped flow apparatus indicate a large extinction coefficient difference between the two complexes,



where  $\text{X}^- = \text{Br}^-, \text{Cl}^-$

*Note:* Temperature jump analysis of the  $[\text{Cu}(\text{Me}_6\text{Tren})\text{OH}_2]^{2+}/\text{Br}^-$  and  $[\text{Cu}(\text{Me}_6\text{Tren})\text{OH}_2]^{2+}/\text{Cl}^-$  ligand substitution systems was unsuccessful owing to the very small, photomultiplier signals.

FIG. (3.10)

The variation of the observed first order rate constant  $k_{\text{obs}}$  for the approach to equilibrium of the  $[\text{Cu}(\text{Me}_6\text{Tren})\text{OH}_2]^{2+}/\text{Br}^-$  and  $[\text{Cu}(\text{Me}_6\text{Tren})\text{OH}_2]^{2+}/\text{Cl}^-$  systems, plotted against  $[\text{Br}^-]$  and  $[\text{Cl}^-]$  respectively.

The closed symbols represent stopped flow spectrophotometric data points in the  $[\text{Cu}(\text{Me}_6\text{Tren})\text{OH}_2]^{2+}/\text{Br}^-$  system at 278, 283 and 288 K.

The open symbols represent stopped flow spectrophotometric data points in the  $[\text{Cu}(\text{Me}_6\text{Tren})\text{OH}_2]^{2+}/\text{Cl}^-$  system at 278, 288 and 298 K.

The lines of best fit were obtained by rectilinear least squares analysis of the spectrophotometric data points.

*The formation of  $[\text{Cu}(\text{Me}_6\text{Tren})\text{Cl}]^+$ : ( $\lambda = 725 \text{ nm}$  and  $\text{pH} = 6.85 \pm .05$ )*

This system was investigated at a constant  $[\text{Cu}(\text{Me}_6\text{Tren})\text{OH}_2]_{\text{total}}^{2+}$  of  $2.0 \times 10^{-3} \text{ mol dm}^{-3}$ .

The ligand ( $\text{Cl}^-$ ) concentration range was from  $2.4 \times 10^{-2} \text{ mol dm}^{-3}$  to  $4.96 \times 10^{-1} \text{ mol dm}^{-3}$  at 278, 288 and 298 K.

The spectral variation accompanying the formation of  $[\text{Cu}(\text{Me}_6\text{Tren})\text{Cl}]^+$  appear in FIGS. (3.11) and (3.12).

*The formation of  $[\text{Cu}(\text{Me}_6\text{Tren})\text{Br}]^+$ : ( $\lambda = 725 \text{ nm}$  and  $\text{pH} = 6.85 \pm .05$ )*

This stopped flow system was investigated at a constant  $[\text{Cu}(\text{Me}_6\text{Tren})\text{OH}_2]_{\text{total}}^{2+}$  of  $2.0 \times 10^{-3} \text{ mol dm}^{-3}$ .

The ligand ( $\text{Br}^-$ ) concentration was varied from  $2.4 \times 10^{-2} \text{ mol dm}^{-3}$  to  $4.96 \times 10^{-1} \text{ mol dm}^{-3}$  at 278, 283 K and from  $3.2 \times 10^{-2} \text{ mol dm}^{-3}$  to  $4.96 \times 10^{-1} \text{ mol dm}^{-3}$  at 288 K.

The spectral variation accompanying the formation of  $[\text{Cu}(\text{Me}_6\text{Tren})\text{Br}]^+$  appear in FIGS. (3.13) and (3.14).

The individual spectrophotometric data points in the plot of  $k_{\text{obs}}$  over the entire  $\text{Br}^-$ ,  $\text{Cl}^-$  concentration range, appear in Appendix (3.5). The ionic strength was maintained at  $1.0 \text{ mol dm}^{-3}$  (sodium perchlorate) for the two ligand substitution systems described above.



FIG 3.10

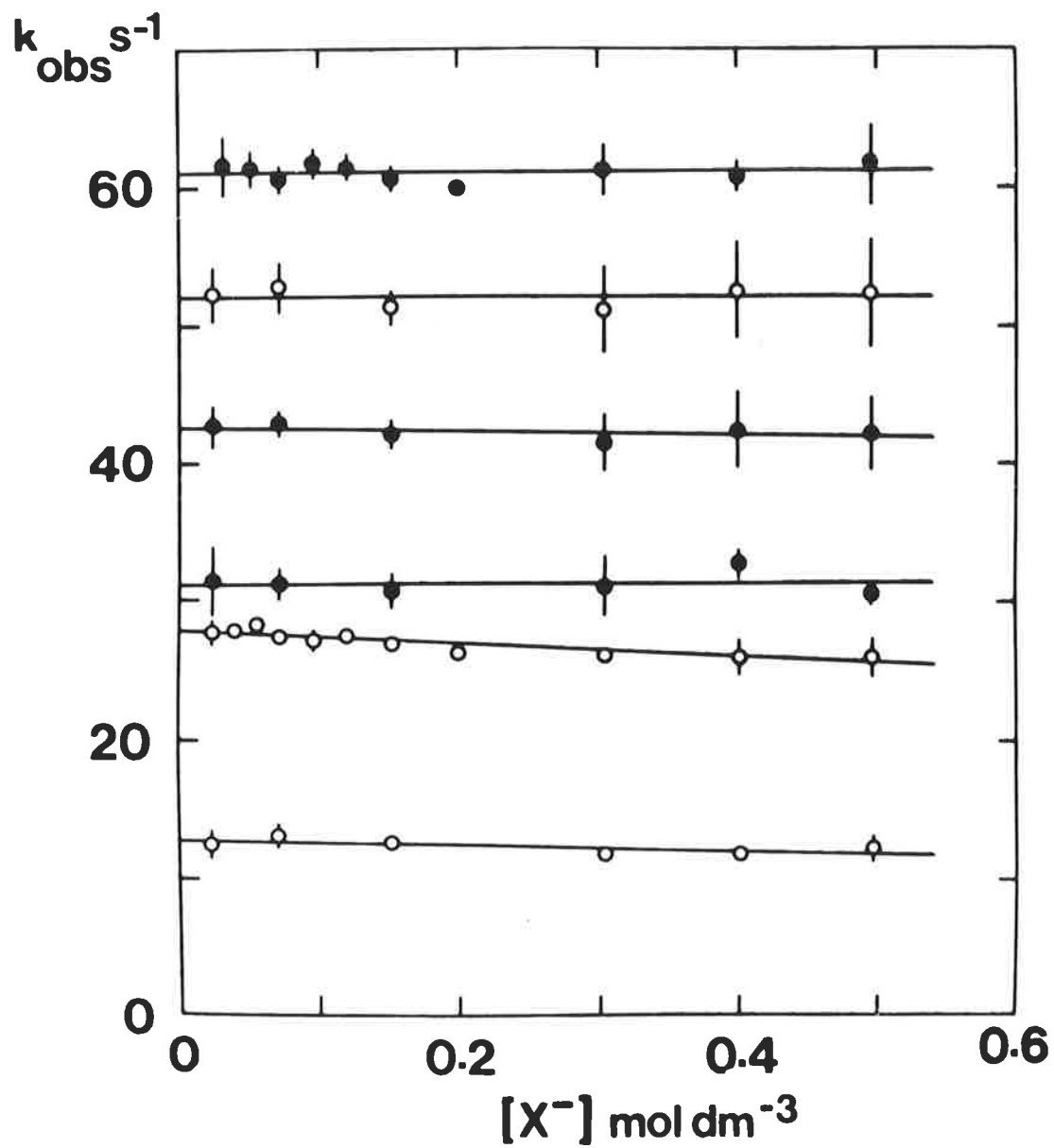


FIG. (3.11)

THE SPECTRAL VARIATION ACCOMPANYING THE FORMATION OF  $[\text{Cu}(\text{Me}_6\text{Tren})\text{Cl}]^+$

(pH =  $6.85 \pm (.05)$  and the ionic strength =  $1.0 \text{ mol dm}^{-3}$  (sodium perchlorate))

The initial individual metal ion and ligand concentrations in the reaction solutions are:

	$[\text{Cu}(\text{Me}_6\text{Tren})\text{OH}_2^{2+}]$ $\text{mol dm}^{-3} (\times 10^3)$	$[\text{Cl}^-]$ $\text{mol dm}^{-3} (\times 10^3)$
A	1.82	0.0
B	1.82	8.0
C	1.82	20.0
D	1.82	48.0
E	1.82	100
F	1.82	200
G	1.82	960

The  $\lambda_{\text{max}} = 291 \text{ nm}$  for  $[\text{Cu}(\text{Me}_6\text{Tren})\text{OH}_2]^{2+}$

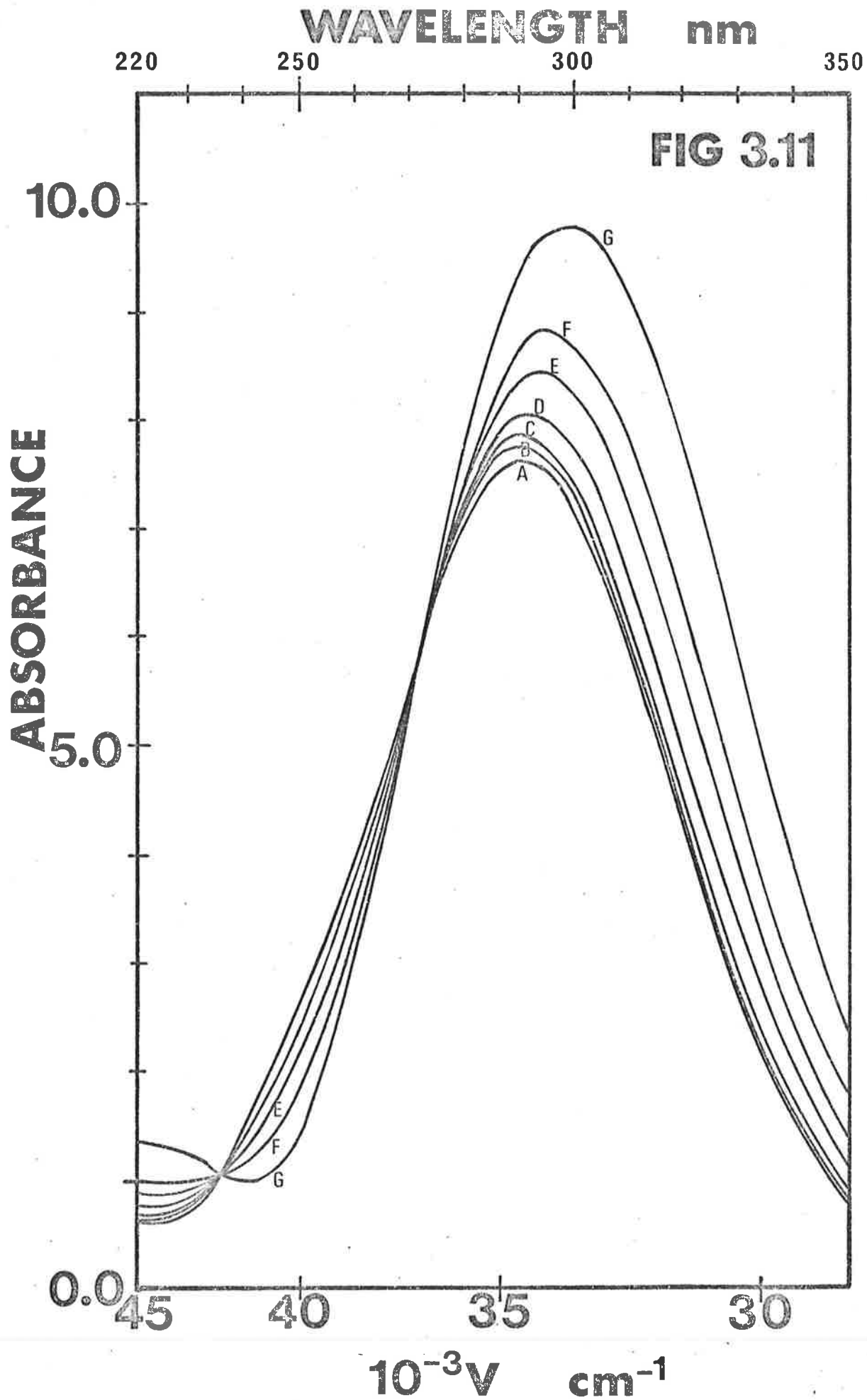


FIG. (3.12)

THE SPECTRAL VARIATION ACCOMPANYING THE FORMATION OF  $[\text{Cu}(\text{Me}_6\text{Tren})\text{Cl}]^+$

(pH =  $6.85 \pm (.05)$  and the ionic strength =  $1.0 \text{ mol dm}^{-3}$  (sodium perchlorate))

The initial individual metal ion and ligand concentrations in the reaction solutions are:

	$[\text{Cu}(\text{Me}_6\text{Tren})\text{OH}_2^{2+}]$ mol $\text{dm}^{-3}$ ( $\times 10^3$ )	$[\text{Cl}^-]$ mol $\text{dm}^{-3}$ ( $\times 10^3$ )
A	1.82	0.0
B	1.82	8.0
C	1.82	20.0
D	1.82	48.0
E	1.82	100
F	1.82	200
G	1.82	960

Changes in absorbance as the  $[\text{Cl}^-]$  is increased is indicated in this high wavelength spectral region of investigation.

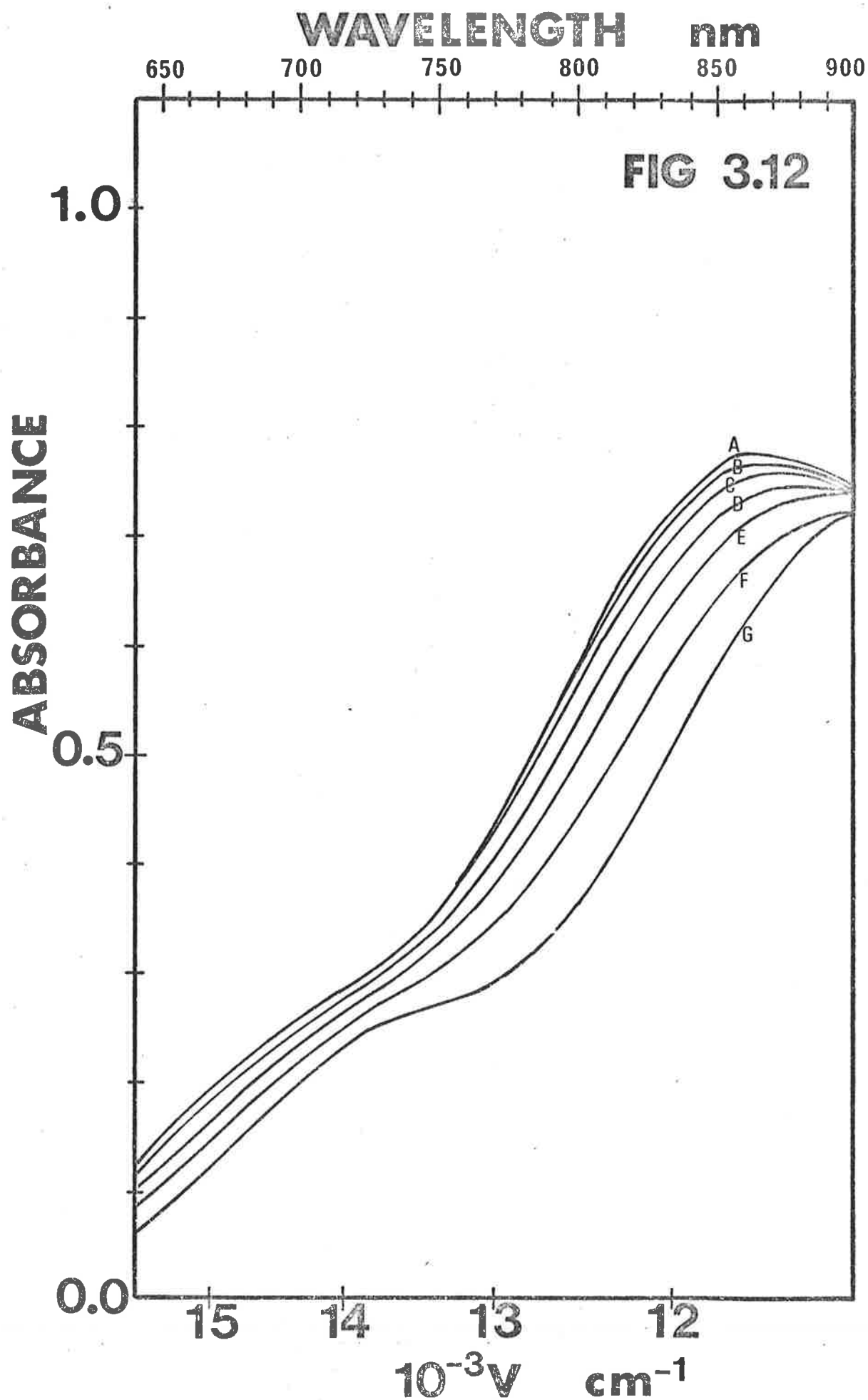


FIG. (3.13)

THE SPECTRAL VARIATION ACCOMPANYING THE FORMATION OF  $[\text{Cu}(\text{Me}_6\text{Tren})\text{Br}]^+$

(pH =  $6.85 \pm (.05)$  and the ionic strength =  $1.0 \text{ mol dm}^{-3}$  (sodium perchlorate))

The initial individual metal ion and ligand concentrations in the reaction solutions are:

	$[\text{Cu}(\text{Me}_6\text{Tren})\text{OH}_2^{2+}]$ $\text{mol dm}^{-3} (\times 10^3)$	$[\text{Br}^-]$ $\text{mol dm}^{-3} (\times 10^3)$
A	1.45	0.0
B	1.45	8.0
C	1.45	20.0
D	1.45	48.0
E	1.45	100
F	1.45	200
G	1.45	520
H	1.45	960

The  $\lambda_{\text{max}} = 291 \text{ nm}$  for  $[\text{Cu}(\text{Me}_6\text{Tren})\text{OH}_2]^{2+}$

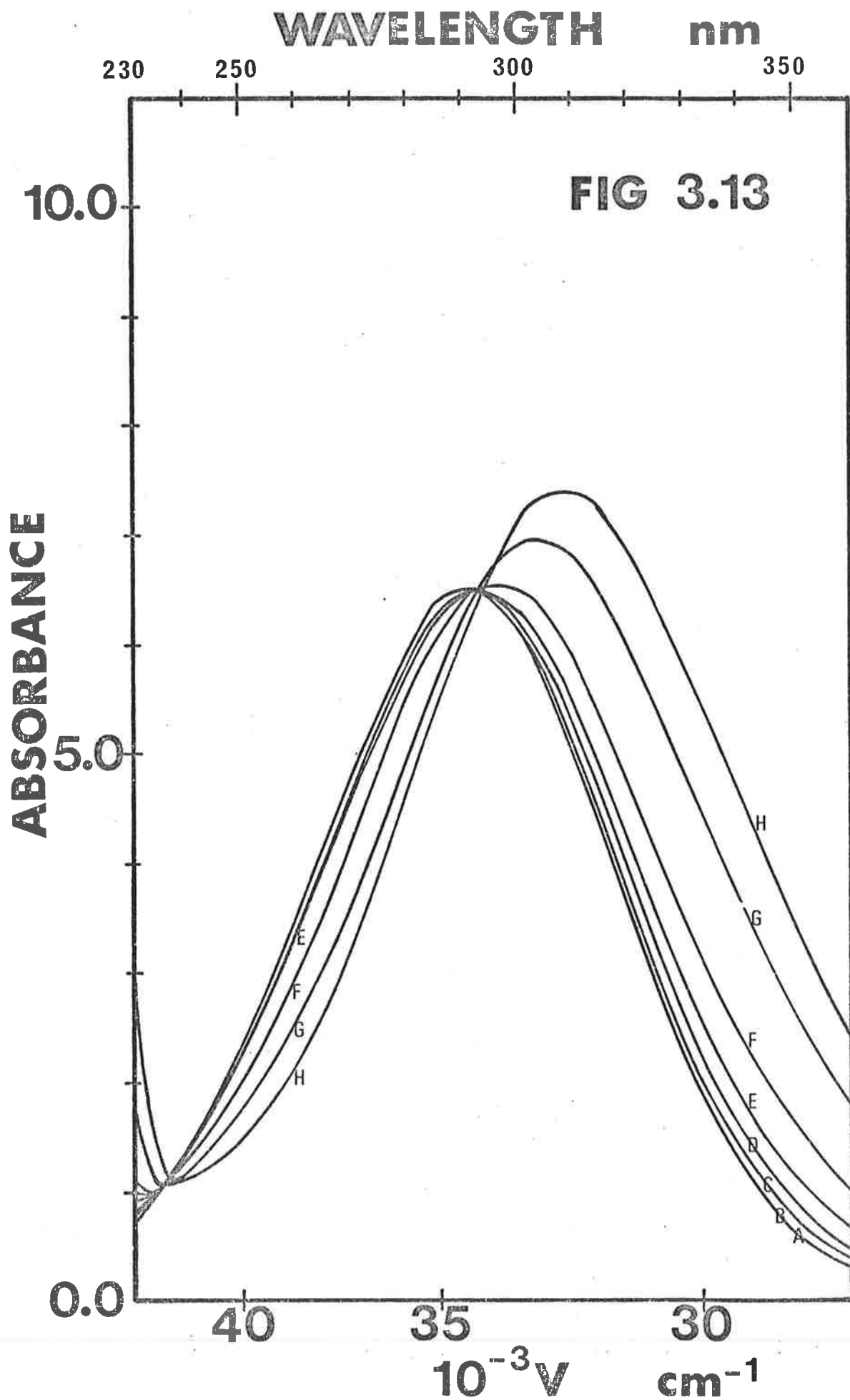


FIG. (3.14)

THE SPECTRAL VARIATION ACCOMPANYING THE FORMATION OF  $[\text{Cu}(\text{Me}_6\text{Tren})\text{Br}]^+$

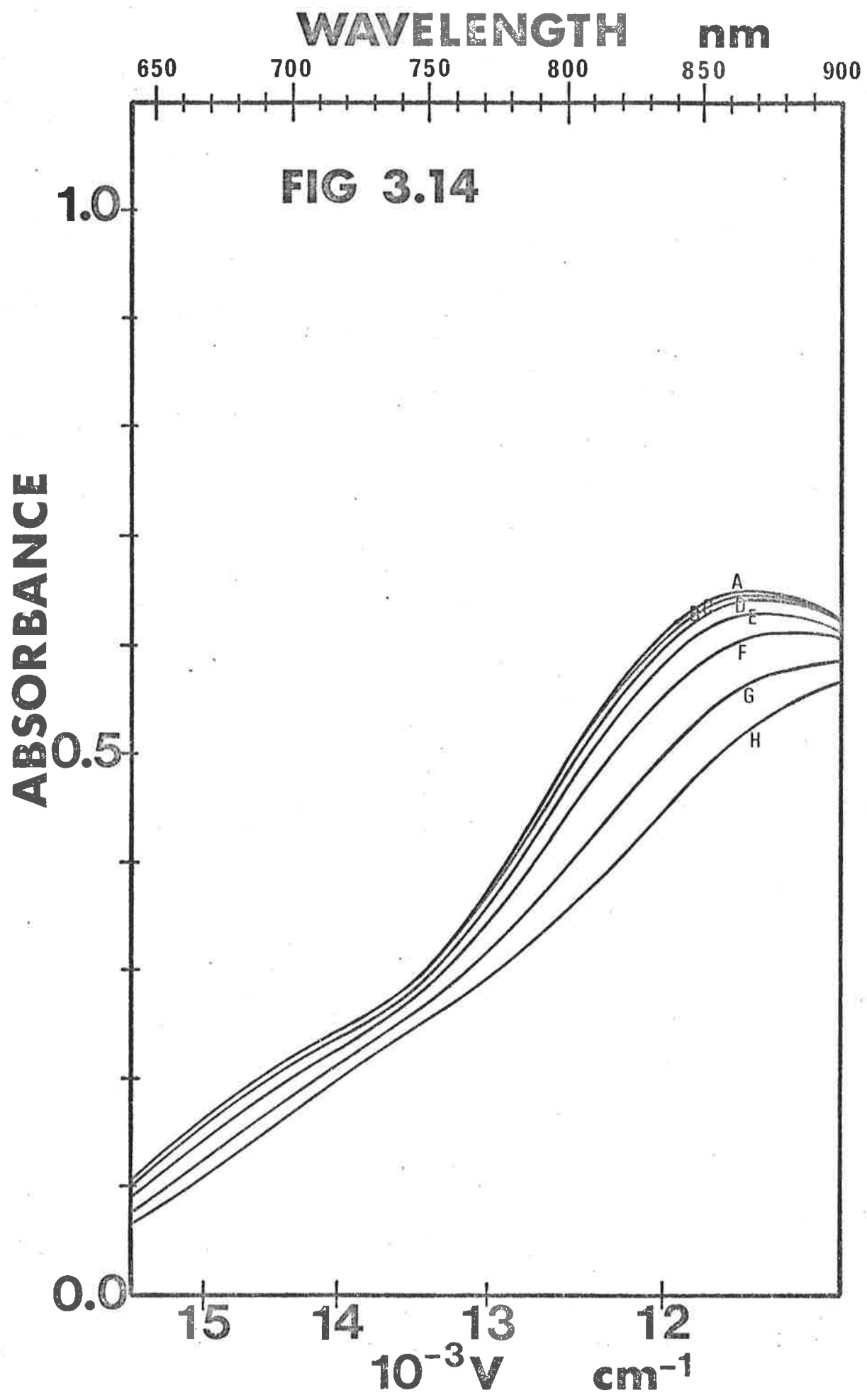
(pH =  $6.85 \pm (.05)$  and the ionic strength =  $1.0 \text{ mol dm}^{-3}$  (sodium perchlorate))

The initial individual metal ion and ligand concentrations in the reaction solutions are:

	$[\text{Cu}(\text{Me}_6\text{Tren})\text{OH}_2^{2+}]$ mol $\text{dm}^{-3}$ ( $\times 10^3$ )	$[\text{Br}^-]$ mol $\text{dm}^{-3}$ ( $\times 10^3$ )
A	1.45	0.0
B	1.45	8.0
C	1.45	20.0
D	1.45	48.0
E	1.45	100
F	1.45	200
G	1.45	520
H	1.45	960

Changes in absorbance as the  $[\text{Br}^-]$  is increased is indicated in this high wavelength spectral region of investigation.





To substantiate the assumption that  $k_{32} \gg k_{23}$ , spectral variation relating to the formation of  $[\text{Cu}(\text{Me}_6\text{Tren})\text{Cl}]^+$  and  $[\text{Cu}(\text{Me}_6\text{Tren})\text{Br}]^+$  were obtained. Both systems show absorbance changes on increasing the respective ligand concentrations, as shown in FIGS. (3.11) to (3.14) inclusive.

The method of  $K_{\text{app}}$  evaluation is as outlined in Section A part (V). For the  $[\text{Cu}(\text{Me}_6\text{Tren})\text{OH}_2]^{2+}/\text{Br}^-, \text{Cl}^-$  ligand substitution systems,  $K_{\text{app}}$  was determined from absorbance data obtained from the Zeiss DMR 10 spectra (FIGS. (3.11) to (3.14) inclusive).

A summary of the main experimental conditions in the spectrophotometric equilibrium constant determination is as follows,

(i) *The formation of  $[\text{Cu}(\text{Me}_6\text{Tren})\text{Cl}]^+$  at 288 K (FIG. (3.12))*

$$\lambda = 725 \text{ nm}$$

$$\text{pH} = 6.85 \pm (.05)$$

$$[\text{Cu}(\text{Me}_6\text{Tren})\text{OH}_2]^{2+} \quad \epsilon_{725 \text{ nm}} = 169.1 \text{ mol}^{-1} \text{ dm}^3 \text{ cm}^{-1}$$

$$[\text{Cu}(\text{Me}_6\text{Tren})\text{Cl}]^+ \quad \epsilon_{725 \text{ nm}} = 140.4 \text{ mol}^{-1} \text{ dm}^3 \text{ cm}^{-1}$$

$$[\text{Cu}(\text{Me}_6\text{Tren})\text{OH}_2^{2+}]_{\text{total}} = 1.82 \times 10^{-3} \text{ mol dm}^{-3}$$

(ii) *The formation of  $[\text{Cu}(\text{Me}_6\text{Tren})\text{Br}]^+$  at 288 K (FIG. (3.14))*

$$\lambda = 725 \text{ nm}$$

$$\text{pH} = 6.85 \pm (.05)$$

$$[\text{Cu}(\text{Me}_6\text{Tren})\text{OH}_2]^{2+} \quad \epsilon_{725 \text{ nm}} = 169.1 \text{ mol}^{-1} \text{ dm}^3 \text{ cm}^{-1}$$

$$[\text{Cu}(\text{Me}_6\text{Tren})\text{Br}]^+ \quad \epsilon_{725 \text{ nm}} = 144.8 \text{ mol}^{-1} \text{ dm}^3 \text{ cm}^{-1}$$

$$[\text{Cu}(\text{Me}_6\text{Tren})\text{OH}_2^{2+}]_{\text{total}} = 1.45 \times 10^{-3} \text{ mol dm}^{-3}$$

*Note:* In the  $[\text{Cu}(\text{Me}_6\text{Tren})\text{OH}_2]^{2+}/\text{Cl}^-$  system, a plot of absorbance versus  $[\text{Cl}^-]$  obtained from the spectrum shown in FIG. (3.12) indicated that the limiting absorbance had been reached at the highest  $[\text{Cl}^-]$  investigated. This enabled  $\epsilon_{\text{III}}$  for  $[\text{Cu}(\text{Me}_6\text{Tren})\text{Cl}]^+$  to be determined accurately (see eqn. (3.17) on page (80)).

In contrast, a similar plot for the  $[\text{Cu}(\text{Me}_6\text{Tren})\text{OH}_2]^{2+}/\text{Br}^-$  system

did not show a well defined plateau region although curvature was apparent. Therefore, the limiting absorbance was obtained by extrapolation. The  $\epsilon_{\text{III}}$  value for  $[\text{Cu}(\text{Me}_6\text{Tren})\text{Br}]^+$  was calculated from absorbance data in FIG. (3.14).

The  $K_{\text{app}}$  (spectrophotometric) data at 288 K appear below,

TABLE (3.18)

	$\text{X}^- = \text{Cl}^-$ ( $\lambda = 725 \text{ nm}$ )	$\text{X}^- = \text{Br}^-$ ( $\lambda = 725 \text{ nm}$ )
$K_{\text{app}}$ (spectrophotometric) ( $\text{mol}^{-1} \text{ dm}^3$ )	$5.9 \pm (1.2)$	$1.9 \pm (0.3)$

The errors quoted above were obtained using the standard deviation formula on the individual  $K_{\text{app}}$  values at various  $[\text{Cl}^-]$  or  $[\text{Br}^-]$ , (see chapter one).

$K_{\text{app}}$  values were evaluated at various wavelengths to ensure that  $K_{\text{app}}$  was independent of wavelength. The resulting data at 288 K appear below,

TABLE (3.19)

$\lambda$ (nm)	$K_{\text{app}}$ (spectrophotometric) ( $\text{mol}^{-1} \text{ dm}^3$ )	$K_{\text{app}}$ (spectrophotometric) ( $\text{mol}^{-1} \text{ dm}^3$ )
	$\text{X}^- = \text{Cl}^-$	$\text{X}^- = \text{Br}^-$
800	$5.9 \pm (0.9)$	$1.6 \pm (0.3)$
775	$5.9 \pm (0.8)$	$1.5 \pm (0.5)$
360	$5.1 \pm (0.9)$	$1.6 \pm (0.1)$

Referring to equation (3.22) on page 83, the expression for  $K_{\text{app}}$  is,

$$K_{\text{app}} = K_{\text{IP}} \left( 1 + \frac{k_{23}}{k_{32}} \right)$$

Since  $k_{32} \gg k_{23}$ ,  $\left(1 + \frac{k_{23}}{k_{32}}\right) \approx 1$

and  $K_{app} \approx K_{IP}$

The  $K_{app}$  data shown in Table (3.18) is then a measure of the  $K_{IP}$  values for the two systems  $[\text{Cu}(\text{Me}_6\text{Tren})\text{OH}_2]^{2+}/\text{Cl}^-$  and  $[\text{Cu}(\text{Me}_6\text{Tren})\text{OH}_2]^{2+}/\text{Br}^-$ . The  $K_{IP}$  values are consistent with other 2+, - systems although they are lower than for the systems described in Section A.

The ligand substitution systems,  $[\text{Cu}(\text{Me}_6\text{Tren})\text{OH}_2]^{2+}/(\text{N}_3^-, \text{NCS}^- \text{ or } \text{OCN}^-)$  have much larger  $K_{app}$  values than for their corresponding chloro and bromo complexes, (see Table (3.7) on page (86)).

It has been shown previously for the  $[\text{Cu}(\text{Me}_6\text{Tren})\text{OH}_2]^{2+}/(\text{N}_3^-, \text{NCS}^- \text{ or } \text{OCN}^-)$  systems that a lower  $K_{IP}$  value results in a shallower slope in the plot of  $k_{obs}$  against  $[\text{X}^-]$ . This phenomenon is consistent with the assumption that curvature in the plot of  $k_{obs}$  against  $[\text{X}^-]$  for the  $[\text{Cu}(\text{Me}_6\text{Tren})\text{OH}_2]^{2+}/\text{Cl}^-$  and  $[\text{Cu}(\text{Me}_6\text{Tren})\text{OH}_2]^{2+}/\text{Br}^-$  systems lies within the standard deviations of the  $k_{obs}$  values.

The low  $K_{IP}$  and  $k_{23}$  values for the bromo and chloro systems suggested that the outer coordination sphere is very important in determining the magnitude of the rate constant,  $k_{23}$ .

The following kinetic and activation data for the systems  $[\text{Cu}(\text{Me}_6\text{Tren})\text{OH}_2]^{2+}/\text{Br}^-$  and  $[\text{Cu}(\text{Me}_6\text{Tren})\text{OH}_2]^{2+}/\text{Cl}^-$  were obtained using a rectilinear least squares procedure on the plots of  $k_{obs}$  versus  $[\text{X}^-]$ .

TABLE (3.20)

*Kinetic data for the aquation of  $[\text{Cu}(\text{Me}_6\text{Tren})\text{X}]^+$*

T(K)	$\text{X}^- = \text{Br}^-$ $k_{32} \text{ (s}^{-1}\text{)}$	$\text{X}^- = \text{Cl}^-$ $k_{32} \text{ (s}^{-1}\text{)}$
278	$31.2 \pm (0.6)$	$12.8 \pm (0.3)$
283	$42.6 \pm (0.3)$	-
288	$61.1 \pm (0.4)$	$27.8 \pm (0.2)$
298	-	$52.1 \pm (0.5)$

TABLE (3.21)

Activation data for the aquation of  $[\text{Cu}(\text{Me}_6\text{Tren})\text{X}]^+$

	$\text{X}^- = \text{Br}^-$	$\text{X}^- = \text{Cl}^-$
$\Delta\text{H}^\ddagger$ (kJ mol <sup>-1</sup> )	+42.5 ± (2.0)	+46.1 ± (1.9)
$\Delta\text{S}^\ddagger$ (J K <sup>-1</sup> mol <sup>-1</sup> )	-63.0 ± (7.1)	-57.3 ± (6.5)

obtained using equation (3.15) on page (76)

The kinetic data shown in Table (3.20) indicates the greater lability of the  $[\text{Cu}(\text{Me}_6\text{Tren})\text{Br}]^+/\text{H}_2\text{O}$  system compared to that in  $[\text{Cu}(\text{Me}_6\text{Tren})\text{Cl}]^+/\text{H}_2\text{O}$ .

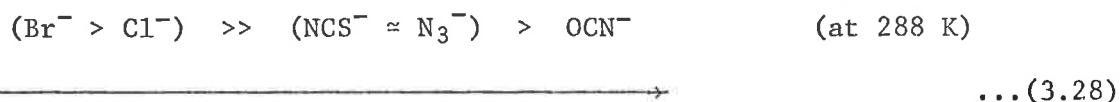
From the activation data in Table (3.21) it is seen that the greater lability of the  $[\text{Cu}(\text{Me}_6\text{Tren})\text{Br}]^+/\text{H}_2\text{O}$  system compared to that of  $[\text{Cu}(\text{Me}_6\text{Tren})\text{Cl}]^+/\text{H}_2\text{O}$  is essentially enthalpic in nature. These  $\Delta\text{H}^\ddagger$  values are +42.5 and +46.1 respectively for the bromo and chloro systems.

The chloride ion has a smaller ionic radius, higher electronegativity and greater surface charge density than does the bromide ion. These differences should result in the Cu-Cl being a stronger bond than Cu-Br on the basis of the electrostatic argument. The larger, more positive  $\Delta\text{H}^\ddagger$  values for dissociation of  $\text{Cl}^-$  from  $[\text{Cu}(\text{Me}_6\text{Tren})\text{Cl}]^+$  apparently reflects the greater strength of the Cu-Cl bond.

The almost identical  $\Delta\text{S}^\ddagger$  values suggest similar solvation effects for both  $\text{Cl}^-$  and  $\text{Br}^-$  on dissociation from the respective inner sphere complexes to the ion pair.

II A Comparative Discussion of Kinetic Data, for aquation of the  
Complexes  $[\text{Cu}(\text{Me}_6\text{Tren})\text{X}]^+$ , where ( $\text{X}^- = \text{N}_3^-, \text{NCS}^-, \text{OCN}^-, \text{Br}^-$  and  $\text{Cl}^-$ )

At a particular temperature, the dissociation rate constant of  $\text{X}^-$  from the complex  $[\text{Cu}(\text{Me}_6\text{Tren})\text{X}]^+$  follows the sequence,



decreasing lability of  $\text{X}^-$  for dissociation  
from  $[\text{Cu}(\text{Me}_6\text{Tren})\text{X}]^+$

...(3.28)

The comparative kinetic and activation data appears in the following tables,

TABLE (3.22)

*Kinetic data for aquation of  $[\text{Cu}(\text{Me}_6\text{Tren})\text{X}]^+$*

T(K)	$\text{X}^- = \text{N}_3^-$ $k_{32} \text{ (s}^{-1}\text{)}$	$\text{X}^- = \text{NCS}^-$ $k_{32} \text{ (s}^{-1}\text{)}$	$\text{X}^- = \text{OCN}^-$ $k_{32} \text{ (s}^{-1}\text{)}$	$\text{X}^- = \text{Br}^-$ $k_{32} \text{ (s}^{-1}\text{)}$	$\text{X}^- = \text{Cl}^-$ $k_{32} \text{ (s}^{-1}\text{)}$
278	-	-	-	$31.2 \pm (0.6)$	$12.8 \pm (0.3)$
283	-	-	-	$42.6 \pm (0.3)$	-
288	$0.95 \pm (0.08)$	$1.36 \pm (0.08)$	$0.39 \pm (0.07)$	$61.1 \pm (0.4)$	$27.8 \pm (0.2)$
298	$1.98 \pm (0.03)$	$2.03 \pm (0.11)$	$1.18 \pm (0.10)$	-	$52.1 \pm (0.5)$
308	$4.21 \pm (0.10)$	$3.91 \pm (0.30)$	$3.34 \pm (0.08)$	-	-

TABLE (3.23)

*Activation data for aquation of  $[\text{Cu}(\text{Me}_6\text{Tren})\text{X}]^+$*

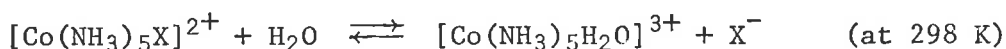
$\text{X}^-$	$\Delta H^\ddagger$ (kJ mol <sup>-1</sup> )	$\Delta S^\ddagger$ (J K <sup>-1</sup> mol <sup>-1</sup> )
$\text{N}_3^-$	$+52.5 \pm (1.4)$	$-62.8 \pm (4.7)$
$\text{NCS}^-$	$+36.5 \pm (6.1)$	$-115.8 \pm (20.6)$
$\text{Br}^-$	$+42.5 \pm (2.0)$	$-63.0 \pm (7.1)$
$\text{Cl}^-$	$+46.1 \pm (1.9)$	$-57.3 \pm (6.5)$
$\text{OCN}^-$	$+76.9 \pm (7.4)$	$+14.5 \pm (24.9)$

From the kinetic data shown in Table (3.22) the ratios for dissociation from  $[\text{Cu}(\text{Me}_6\text{Tren})\text{X}]^+$  for various  $\text{X}^-$  at 288 and 298 K can be determined. These ratios are indicated below,

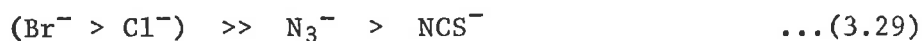
288 K	288 K	298 K
$\text{Br}^-/\text{N}_3^- = 64.4$	$\text{Cl}^-/\text{N}_3^- = 29.3$	$\text{Cl}^-/\text{N}_3^- = 26.3$
$\text{Br}^-/\text{NCS}^- = 45.0$	$\text{Cl}^-/\text{NCS}^- = 20.4$	$\text{Cl}^-/\text{NCS}^- = 25.7$
$\text{Br}^-/\text{OCN}^- = 157$	$\text{Cl}^-/\text{OCN}^- = 71.3$	$\text{Cl}^-/\text{OCN}^- = 44.2$

These large observed rate differences are not unique to the  $[\text{Cu}(\text{Me}_6\text{Tren})\text{OH}_2]^{2+}/\text{X}^-$  substitution systems.

The following reaction which is considered to proceed through an  $\text{I}_d$  mechanism is discussed by A. Haim,<sup>23</sup>



The result from a plot of  $\log k$  ( $\text{min}^{-1}$ ) for aquation against  $-\log K_{\text{eq}}$  shows a linear plot with slope of unity. The sequence of labilities for aquation is as follows,



$\xrightarrow{\hspace{10em}}$   
 decreasing lability of  $\text{X}^-$  for  
 dissociation from  $[\text{Cu}(\text{Me}_6\text{Tren})\text{X}]^+$

The similar sequences observed in ... (3.28) and ... (3.29) is consistent with the mechanism postulated for the  $[\text{Cu}(\text{Me}_6\text{Tren})\text{X}]^+$  system.

The activation data in Table (3.23) for the aquation system,  $[\text{Cu}(\text{Me}_6\text{Tren})\text{X}]^+/\text{H}_2\text{O}$  shows +ve  $\Delta H^\ddagger$  values for all the ligands ( $\text{X}^-$ ) studied. The spread of  $\Delta H^\ddagger$  values substantially reflects the different nature of the leaving groups (that is copper(II) - leaving group bond strength). Similarly the  $\Delta S^\ddagger$  values reflect the different ligand ( $\text{X}^-$ ) characters. The spread of these  $\Delta S^\ddagger$  values is *in part* a measure of different solvation effects of these ( $\text{X}^-$ ) ions on dissociating from  $[\text{Cu}(\text{Me}_6\text{Tren})\text{X}]^+$ . Previous discussions of the activation data obtained for aquation of  $[\text{Cu}(\text{Me}_6\text{Tren})\text{X}]^+$  in Section A

are applicable to aquation in the  $[\text{Cu}(\text{Me}_6\text{Tren})\text{X}]^+/\text{H}_2\text{O}$  systems, (where  $\text{X}^- = \text{Br}^-$ ,  $\text{Cl}^-$ ).

The low  $K_{\text{IP}}$  values for the anation system,  $[\text{Cu}(\text{Me}_6\text{Tren})\text{OH}_2]^{2+}/\text{X}^-$  (where  $\text{X}^- = \text{Br}^-$ ,  $\text{Cl}^-$ ) and also the low  $k_{23}$  values shown in Table (3.24) suggests that the outer coordination sphere of Cu(II) is important in determining the magnitude of both  $K_{\text{IP}}$  and  $k_{23}$ . If in fact the primary hydration sphere of Cu(II) were of sole importance then the  $k_{23}$  value should be constant.

A. Haim<sup>23</sup> has discussed the ligand substitution reactions of  $[\text{Co}(\text{NH}_3)_5\text{OH}_2]^{3+}$  in terms of the  $I_{\text{d}}$  mechanism. For a range of substituting ligands the  $k_{23}$  value was found to be effectively constant. In the present studies, it is suggested that the hydrophobic environment of the labile site in  $[\text{Cu}(\text{Me}_6\text{Tren})\text{OH}_2]^{2+}$  may explain the difference in  $k_{23}$  values observed for ligand substitution of this complex.

The very low  $k_{23}$  values in the system,  $[\text{Cu}(\text{Me}_6\text{Tren})\text{OH}_2]^{2+}/\text{X}^-$  (where  $\text{X}^- = \text{Br}^-$ ,  $\text{Cl}^-$ ) suggests a much lower competition ratio between  $\text{X}^-$  and  $\text{H}_2\text{O}$  in the outer coordination sphere for  $\text{X}^- = \text{Br}^-$ ,  $\text{Cl}^-$  compared with ( $\text{N}_3^-$ ,  $\text{NCS}^-$  and  $\text{OCN}^-$ ).

The alternative possibility is that the Cu(II)-X bond formation in the anation step is more pronounced. This leads to the possibility of anation occurring via an associative mechanism. However, it is noteworthy that anation reactions substantially reflect the primary water exchange values for the following sequence of complexes,  $[\text{Cu}(\text{H}_2\text{O})_6]^{2+}$ ,  $[\text{Cu}(\text{Tren})\text{OH}_2]^{2+}$  and  $[\text{Cu}(\text{Me}_6\text{Tren})\text{OH}_2]^{2+}$ . Therefore this would indicate that ligand substitution by an associative mechanism is improbable.

The following Table contains *estimates* of the rate constant,  $k_{23}$ , based on the original assumption that the Eigen curve lies within the standard deviations (SD) of the individual  $k_{\text{obs}}$  values in the plot of  $k_{\text{obs}}$  versus  $[\text{X}^-]$ ,



for the system  $[\text{Cu}(\text{Me}_6\text{Tren})\text{OH}_2]^{2+}/\text{X}^-$  (where  $\text{X}^- = \text{Br}^-, \text{Cl}^-$ ).

TABLE (3.24)

T(K)	$\text{X}^- = \text{Cl}^-$ $k_{23} (\text{s}^{-1})$	$\text{X}^- = \text{Br}^-$ $k_{23} (\text{s}^{-1})$
278	$\sim 1.7$	$\sim 2.6$
283	-	$\sim 3.2$
288	$\sim 0.6$	$\sim 5.2$
298	$\sim 6.2$	-

## CHAPTER THREE: RESULTS AND DISCUSSION

Section E: Kinetic analysis of the  $[\text{Cu}(\text{Me}_6\text{Tren})\text{OH}]^+/\text{X}^-$  system

(where  $\text{X}^- = \text{N}_3^-$ ,  $\text{NCS}^-$  and  $\text{OCN}^-$ )

- I Discussion and interpretation of the kinetic data obtained
- II A comparative discussion of the kinetic data obtained in the two anation systems,  $[\text{Cu}(\text{Me}_6\text{Tren})\text{OH}]^+/\text{X}^-$  and  $[\text{Cu}(\text{Me}_6\text{Tren})\text{OH}_2]^{2+}/\text{X}^-$  at 298 K

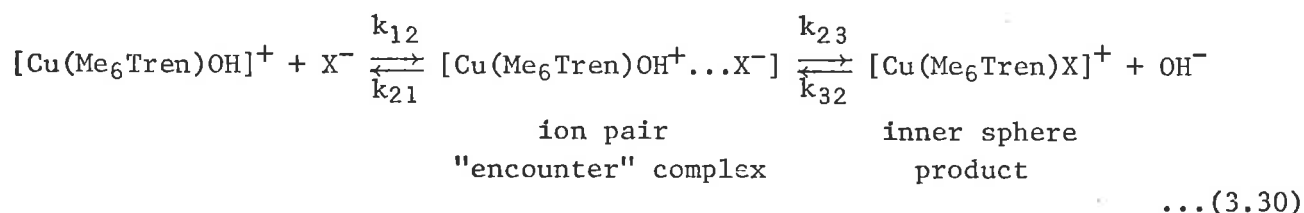
Section E: Kinetic analysis of the  $[\text{Cu}(\text{Me}_6\text{Tren})\text{OH}]^+/\text{X}^-$  system,

(where  $\text{X}^- = \text{N}_3^-$ ,  $\text{NCS}^-$  and  $\text{OCN}^-$ )

### I Discussion and interpretation of the kinetic data obtained

The ligand substitution, under pseudo 1st order conditions, in the complex  $[\text{Cu}(\text{Me}_6\text{Tren})\text{OH}]^+$ , (with  $\text{N}_3^-$ ,  $\text{NCS}^-$  or  $\text{OCN}^-$ ), is reported at 298 K. The appropriate kinetic plots of  $k_{\text{obs}}$  versus  $[\text{X}^-]$  appear in FIGS. (3.15) and (3.16).

The Eigen-Wilkins ( $I_d$ ) mechanism<sup>7</sup> is considered operative and is shown as follows,



where  $K_{\text{IP}} = k_{12}/k_{21}$  and  $\text{X}^- = \text{N}_3^-$ ,  $\text{NCS}^-$  or  $\text{OCN}^-$

This system was investigated at only one temperature since the effect of changing the leaving group from  $\text{H}_2\text{O}$  to  $\text{OH}^-$  on the observed anation rates, was of primary interest.

For kinetic data analysis, it was assumed that the  $k_{32}$  values for the  $[\text{Cu}(\text{Me}_6\text{Tren})\text{X}]^+/\text{H}_2\text{O}$  system, (shown in Table (3.3)) are applicable to the  $[\text{Cu}(\text{Me}_6\text{Tren})\text{X}]^+/\text{OH}^-$  system since the dissociation of  $\text{X}^-$  from  $[\text{Cu}(\text{Me}_6\text{Tren})\text{X}]^+$  is common to both systems.

In conjunction with the mechanism shown in equation (3.30) there is an equilibrium situation as follows,



This very fast proton transfer reaction cannot be measured directly using the stopped flow apparatus.

The low amplitude electrical signals from the photomultiplier in the stopped flow study for the  $[\text{Cu}(\text{Me}_6\text{Tren})\text{X}]^+/\text{OH}^-$  system, precluded investigation

at very low ligand concentrations. However, at comparable low ligand concentrations able to be investigated in the two systems,  $[\text{Cu}(\text{Me}_6\text{Tren})\text{OH}_2]^{2+}/\text{X}^-$  and  $[\text{Cu}(\text{Me}_6\text{Tren})\text{OH}]^+/\text{X}^-$ , the  $k_{\text{obs}}$  values are similar. This is consistent with the assumption that the rate constant,  $k_{32}$ , is the same for these two ligand substitution systems.

From purely spectroscopic considerations there would be a greater change in ligand field strength in the  $[\text{Cu}(\text{Me}_6\text{Tren})\text{OH}_2]^{2+}/\text{X}^-$  system.

Spectral studies show smaller absorbance changes for the  $\text{Cu}(\text{Me}_6\text{Tren})\text{OH}]^+/\text{X}^-$  system, compared to that in the  $[\text{Cu}(\text{Me}_6\text{Tren})\text{OH}_2]^{2+}/\text{X}^-$  system, at the same ligand concentration, (see FIGS. (3.17) to (3.21)).

*Temperature jump analysis of the system,  $[\text{Cu}(\text{Me}_6\text{Tren})\text{OH}]^+/\text{X}^-$  system was unsuccessful owing to the unmeasurably small amplitude signals.*

FIG. (3.15)

The variation of the observed first order rate constant  $k_{\text{obs}}$  for the approach to equilibrium of the  $[\text{Cu}(\text{Me}_6\text{Tren})\text{OH}]^+/\text{N}_3^-$  and  $[\text{Cu}(\text{Me}_6\text{Tren})\text{OH}]^+/\text{OCN}^-$  systems, plotted against  $[\text{N}_3^-]$  and  $[\text{OCN}^-]$  respectively at 298 K. The above systems are shown by  $\blacksquare$  and  $\blacktriangle$  symbols for  $X^- = \text{N}_3^-$  and  $\text{OCN}^-$  respectively. Kinetic data in the plot of  $k_{\text{obs}}$  versus  $[X^-]$  was obtained using the stopped flow spectrophotometric technique.

*The formation of  $[\text{Cu}(\text{Me}_6\text{Tren})\text{X}]^+$ : (where  $X^- = \text{N}_3^-, \text{OCN}^-$ )*

This was investigated at  $\lambda = 386$  and  $360$  nm respectively and at  $\text{pH} = 10.9 \pm (0.05)$ . The  $[\text{Cu}(\text{Me}_6\text{Tren})\text{OH}]^+$  was constant at  $4.0 \times 10^{-4}$  mol dm $^{-3}$ .  
total

The ligand ( $X^-$ ) concentration was varied from

$5.0 \times 10^{-3}$  mol dm $^{-3}$  to  $5.0 \times 10^{-1}$  mol dm $^{-3}$  for  $X^- = \text{N}_3^-$  at 298 K

and from

$1.0 \times 10^{-2}$  mol dm $^{-3}$  to  $5.0 \times 10^{-1}$  mol dm $^{-3}$  for  $X^- = \text{OCN}^-$  at 298 K

The relevant spectra for the above systems appear in FIGS. (3.17), (3.18) and (3.19).

The individual spectrophotometric data points in the plot of  $k_{\text{obs}}$  over the entire ligand concentration range, for the systems above, appear in Appendix (3.6).

$k_{obs} s^{-1}$

FIG 3.15

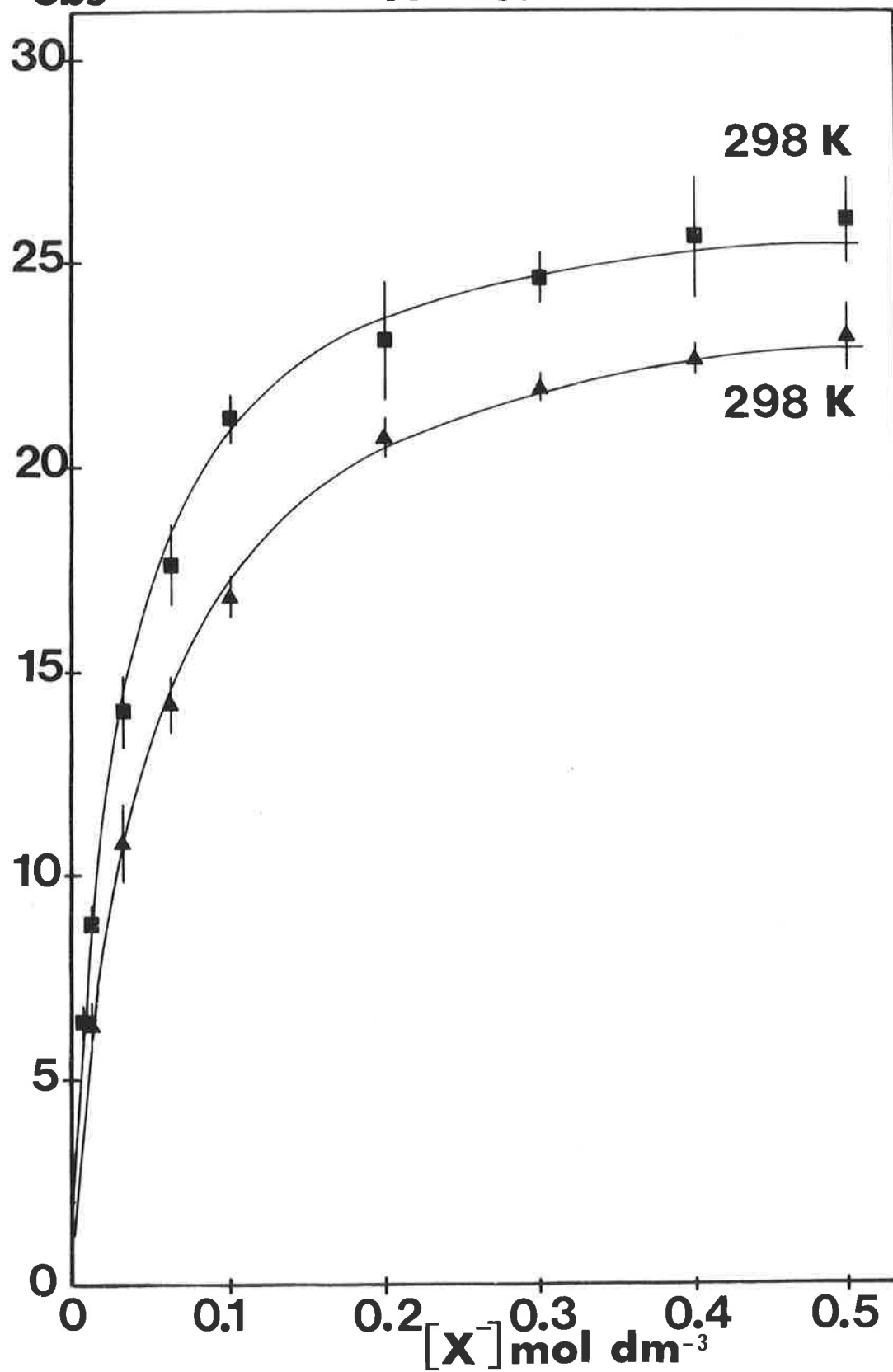


FIG. (3.16)

The variation of the observed first order rate constant  $k_{\text{obs}}$  for the approach to equilibrium of the  $[\text{Cu}(\text{Me}_6\text{Tren})\text{OH}]^+/\text{NCS}^-$  system, plotted against  $[\text{NCS}^-]$ , at 298 K. The above system is shown by the  $\odot$  symbol. Kinetic data in the plot of  $k_{\text{obs}}$  versus  $[\text{X}^-]$  was obtained using the stopped flow spectrophotometric technique.

*The formation of  $[\text{Cu}(\text{Me}_6\text{Tren})\text{X}]^+$ : (where  $\text{X}^- = \text{NCS}^-$ )*

This was investigated at  $\lambda = 370 \text{ nm}$  at  $\text{pH} = 10.9 \pm (0.05)$ . The  $[\text{Cu}(\text{Me}_6\text{Tren})\text{OH}^+]_{\text{total}}$  was constant at  $4.0 \times 10^{-4} \text{ mol dm}^{-3}$ .

The ligand ( $\text{X}^-$ ) concentration was varied from

$5.0 \times 10^{-3} \text{ mol dm}^{-3}$  to  $5.0 \times 10^{-1} \text{ mol dm}^{-3}$  for  $\text{X}^- = \text{NCS}^-$  at 298 K

The relevant spectra for the above system appear in FIGS. (3.20) and (3.21).

The individual spectrophotometric data points in the plot of  $k_{\text{obs}}$  over the entire ligand concentration range for the system above, appear in Appendix (3.6).

$k_{obs} s^{-1}$

FIG 3.16

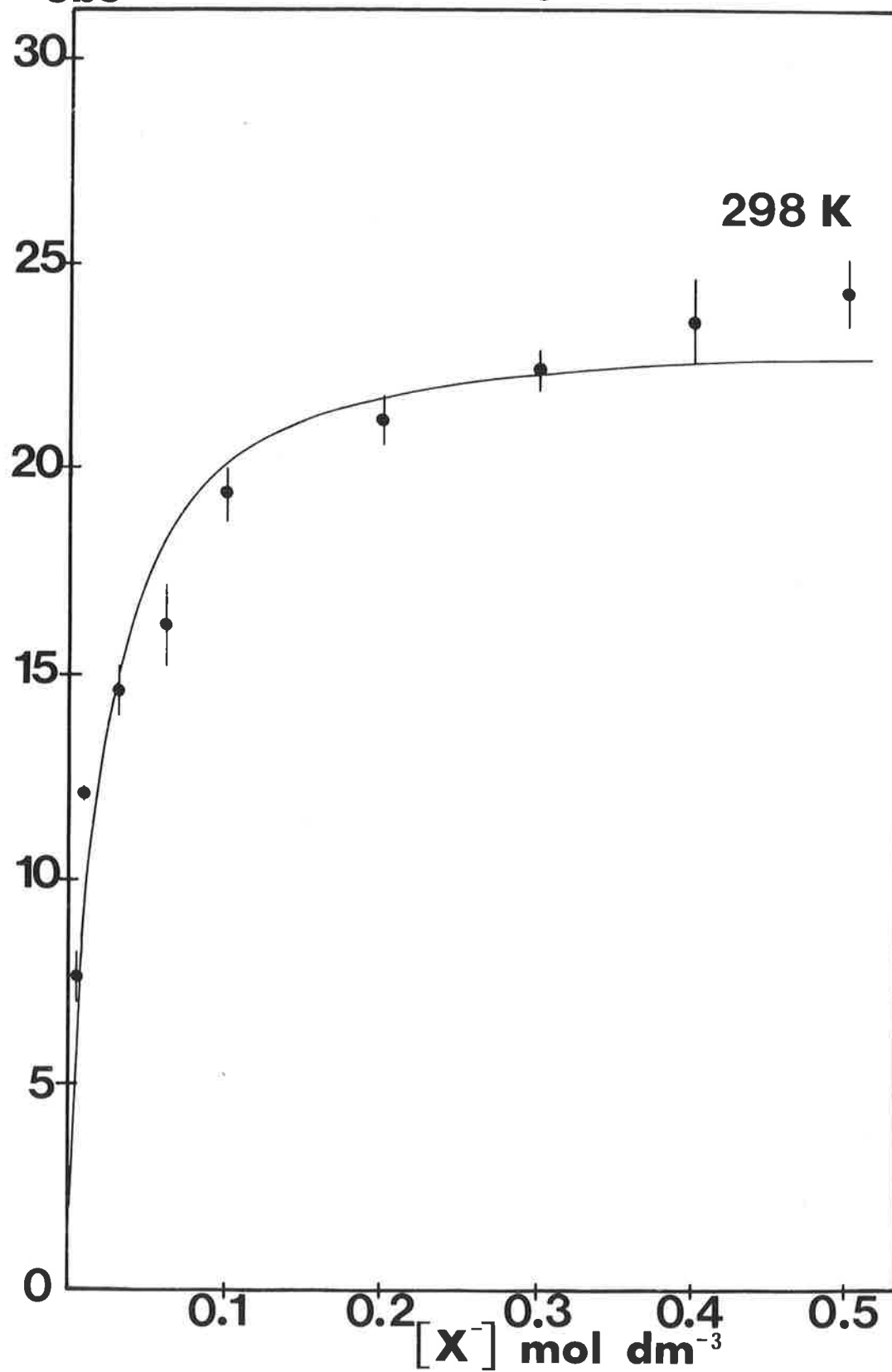




FIG. (3.17)

THE SPECTRAL VARIATION ACCOMPANYING THE FORMATION OF  $[\text{Cu}(\text{Me}_6\text{Tren})\text{N}_3]^+$  IN THE LIGAND SUBSTITUTION SYSTEMS,  $[\text{Cu}(\text{Me}_6\text{Tren})\text{OH}_2]^{2+}/\text{N}_3^-$  and  $[\text{Cu}(\text{Me}_6\text{Tren})\text{OH}]^+/\text{N}_3^-$ .

(the ionic strength =  $1.0 \text{ mol dm}^{-3}$  (sodium perchlorate))

The initial individual metal ion and ligand concentrations in the reaction solutions are:

	$[\text{Cu}(\text{Me}_6\text{Tren})\text{OH}^+]$ $\text{mol dm}^{-3} (\times 10^4)$	$[\text{N}_3^-]$ $\text{mol dm}^{-3}$	pH
A	2.80	0.0	10.90
B	2.80	0.52	10.90
	$[\text{Cu}(\text{Me}_6\text{Tren})\text{OH}_2^{2+}]$ $\text{mol dm}^{-3} (\times 10^4)$	$[\text{N}_3^-]$ $\text{mol dm}^{-3}$	pH
C	2.80	0.0	6.80
D	2.80	0.52	6.80
	$[\text{Cu}(\text{Me}_6\text{Tren})\text{OH}^+] + [\text{Cu}(\text{Me}_6\text{Tren})\text{OH}_2^{2+}]$ $\text{mol dm}^{-3} (\times 10^4)$	$[\text{N}_3^-]$ $\text{mol dm}^{-3}$	pH
E	2.80	0.52	8.50
F	2.80	0.52	10.00

FIG. (3.17) illustrates the smaller absorbance change in the near UV-visible region between (A and B) and (C and D) at the same wavelength.

*Note:* The kinetic measurements for the two systems discussed above were obtained at  $\lambda = 386 \text{ nm}$  where this phenomenon occurs.

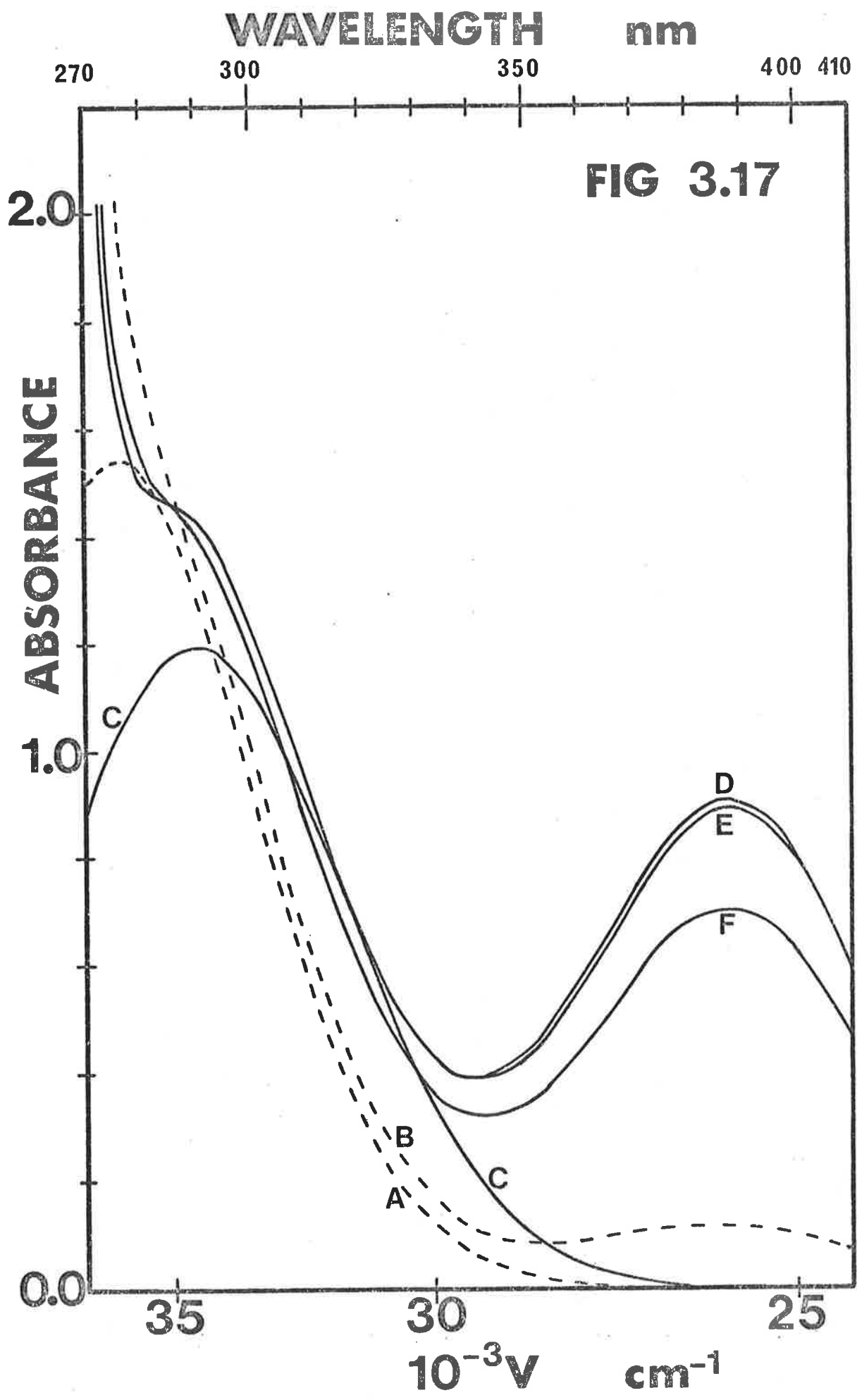


FIG. (3.18)

THE SPECTRAL VARIATION ACCOMPANYING THE FORMATION OF  $[\text{Cu}(\text{Me}_6\text{Tren})\text{N}_3]^+$  IN THE LIGAND SUBSTITUTION SYSTEMS,  $[\text{Cu}(\text{Me}_6\text{Tren})\text{OH}_2]^{2+}/\text{N}_3^-$  and  $[\text{Cu}(\text{Me}_6\text{Tren})\text{OH}]^+/\text{N}_3^-$ .

(the ionic strength =  $1.0 \text{ mol dm}^{-3}$  (sodium perchlorate))

The initial individual metal ion and ligand concentrations in the reaction solutions are:

	$[\text{Cu}(\text{Me}_6\text{Tren})\text{OH}^+]$ $\text{mol dm}^{-3} (\times 10^4)$	$[\text{N}_3^-]$ $\text{mol dm}^{-3}$	pH
A	8.0	0.0	10.90
B	8.0	0.52	10.90
	$[\text{Cu}(\text{Me}_6\text{Tren})\text{OH}_2^{2+}]$ $\text{mol dm}^{-3} (\times 10^4)$	$[\text{N}_3^-]$ $\text{mol dm}^{-3}$	pH
C	8.0	0.0	6.80
D	8.0	0.52	6.80
	$[\text{Cu}(\text{Me}_6\text{Tren})\text{OH}^+] + [\text{Cu}(\text{Me}_6\text{Tren})\text{OH}_2^{2+}]$ $\text{mol dm}^{-3} (\times 10^4)$	$[\text{N}_3^-]$ $\text{mol dm}^{-3}$	pH
E	8.0	0.52	8.50

FIG. (3.18) illustrates the smaller absorbance change in the high wavelength visible region between (A and B) and (C and D) at the same wavelength.

WAVELENGTH nm

650

700

750

800

850

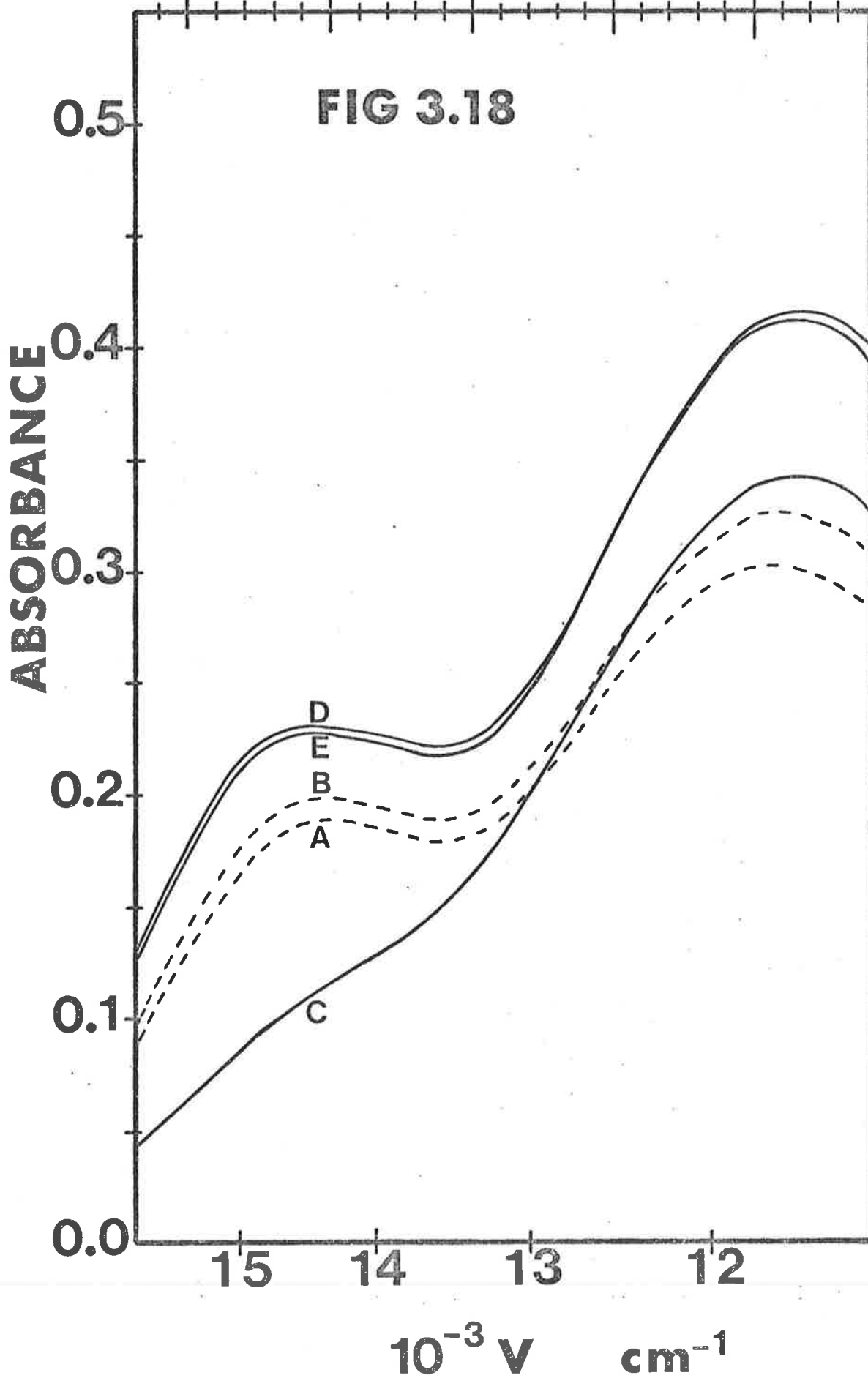


FIG. (3.19)

THE SPECTRAL VARIATION ACCOMPANYING THE FORMATION OF  $[\text{Cu}(\text{Me}_6\text{Tren})\text{OCN}]^+$  IN THE LIGAND SUBSTITUTION SYSTEMS,  $[\text{Cu}(\text{Me}_6\text{Tren})\text{OH}_2]^{2+}/\text{OCN}^-$  and  $[\text{Cu}(\text{Me}_6\text{Tren})\text{OH}]^+/\text{OCN}^-$ .

(the ionic strength =  $1.0 \text{ mol dm}^{-3}$  (sodium perchlorate))

The initial individual metal ion and ligand concentrations in the reaction solutions are:

	$[\text{Cu}(\text{Me}_6\text{Tren})\text{OH}^+]$ $\text{mol dm}^{-3} (\times 10^4)$	$[\text{OCN}^-]$ $\text{mol dm}^{-3}$	pH
A	8.0	0.0	10.90
B	8.0	0.52	10.90
	$[\text{Cu}(\text{Me}_6\text{Tren})\text{OH}_2^{2+}]$ $\text{mol dm}^{-3} (\times 10^4)$	$[\text{OCN}^-]$ $\text{mol dm}^{-3}$	pH
C	8.0	0.0	6.82
D	8.0	0.52	6.82
	$[\text{Cu}(\text{Me}_6\text{Tren})\text{OH}^+] + [\text{Cu}(\text{Me}_6\text{Tren})\text{OH}_2^{2+}]$ $\text{mol dm}^{-3} (\times 10^4)$	$[\text{OCN}^-]$ $\text{mol dm}^{-3}$	pH
E	8.0	0.52	10.00

FIG. (3.19) illustrates the smaller absorbance change in the high wavelength visible region, (650 to 750 nm) between (A and B) and (C and D) at the same wavelength.

*Note:* The kinetic measurements for the two systems discussed above were obtained at  $\lambda = 710 \text{ nm}$  where this phenomenon occurs.

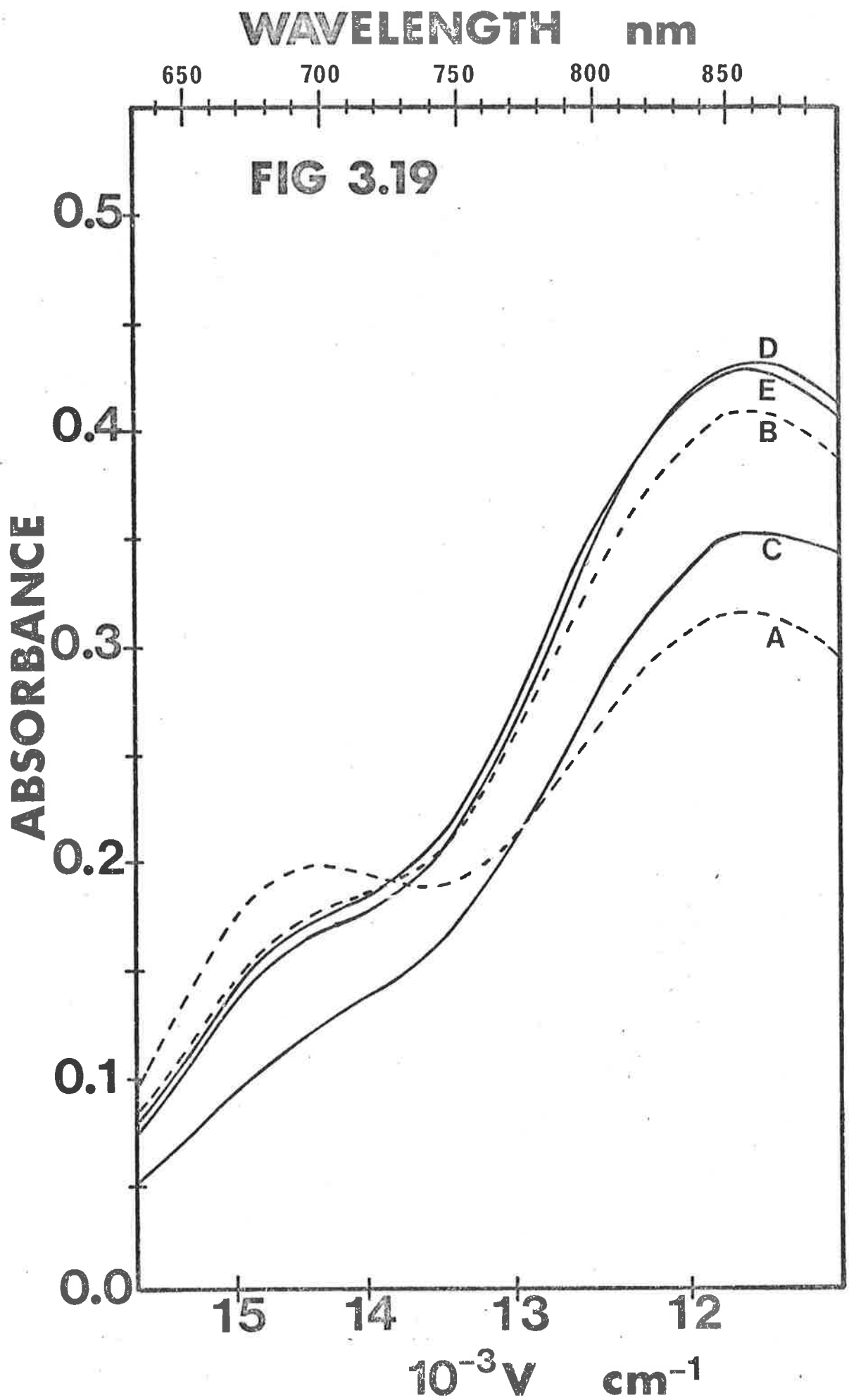


FIG. (3.20)

THE SPECTRAL VARIATION ACCOMPANYING THE FORMATION OF  $[\text{Cu}(\text{Me}_6\text{Tren})\text{NCS}]^+$  IN THE LIGAND SUBSTITUTION SYSTEMS,  $[\text{Cu}(\text{Me}_6\text{Tren})\text{OH}_2]^{2+}/\text{NCS}^-$  and  $[\text{Cu}(\text{Me}_6\text{Tren})\text{OH}]^+/\text{NCS}^-$ .

(the ionic strength =  $1.0 \text{ mol dm}^{-3}$  (sodium perchlorate))

The initial individual metal ion and ligand concentrations in the reaction solutions are:

	$[\text{Cu}(\text{Me}_6\text{Tren})\text{OH}^+]$ $\text{mol dm}^{-3} (\times 10^4)$	$[\text{NCS}^-]$ $\text{mol dm}^{-3}$	pH
A	2.80	0.0	10.90
B	2.80	0.52	10.90
	$[\text{Cu}(\text{Me}_6\text{Tren})\text{OH}_2^{2+}]$ $\text{mol dm}^{-3} (\times 10^4)$	$[\text{NCS}^-]$ $\text{mol dm}^{-3}$	pH
C	2.80	0.0	6.80
D	2.80	0.52	6.80
	$[\text{Cu}(\text{Me}_6\text{Tren})\text{OH}^+] + [\text{Cu}(\text{Me}_6\text{Tren})\text{OH}_2^{2+}]$ $\text{mol dm}^{-3} (\times 10^4)$	$[\text{NCS}^-]$ $\text{mol dm}^{-3}$	pH
E	2.80	0.52	8.50

FIG. (3.20) illustrates the smaller absorbance change in the UV-visible region between (A and B) and (C and D) at the same wavelength.

*Note:* The kinetic measurements for the two systems discussed above were obtained at  $\lambda = 370 \text{ nm}$  where this phenomenon occurs.

WAVELENGTH nm

320 350 400 440

FIG 3.20

ABSORBANCE

0.5  
0.4  
0.3  
0.2  
0.1  
0.0

31 30 29 28 27 26 25 24 23

$10^{-3} \nu$   $\text{cm}^{-1}$

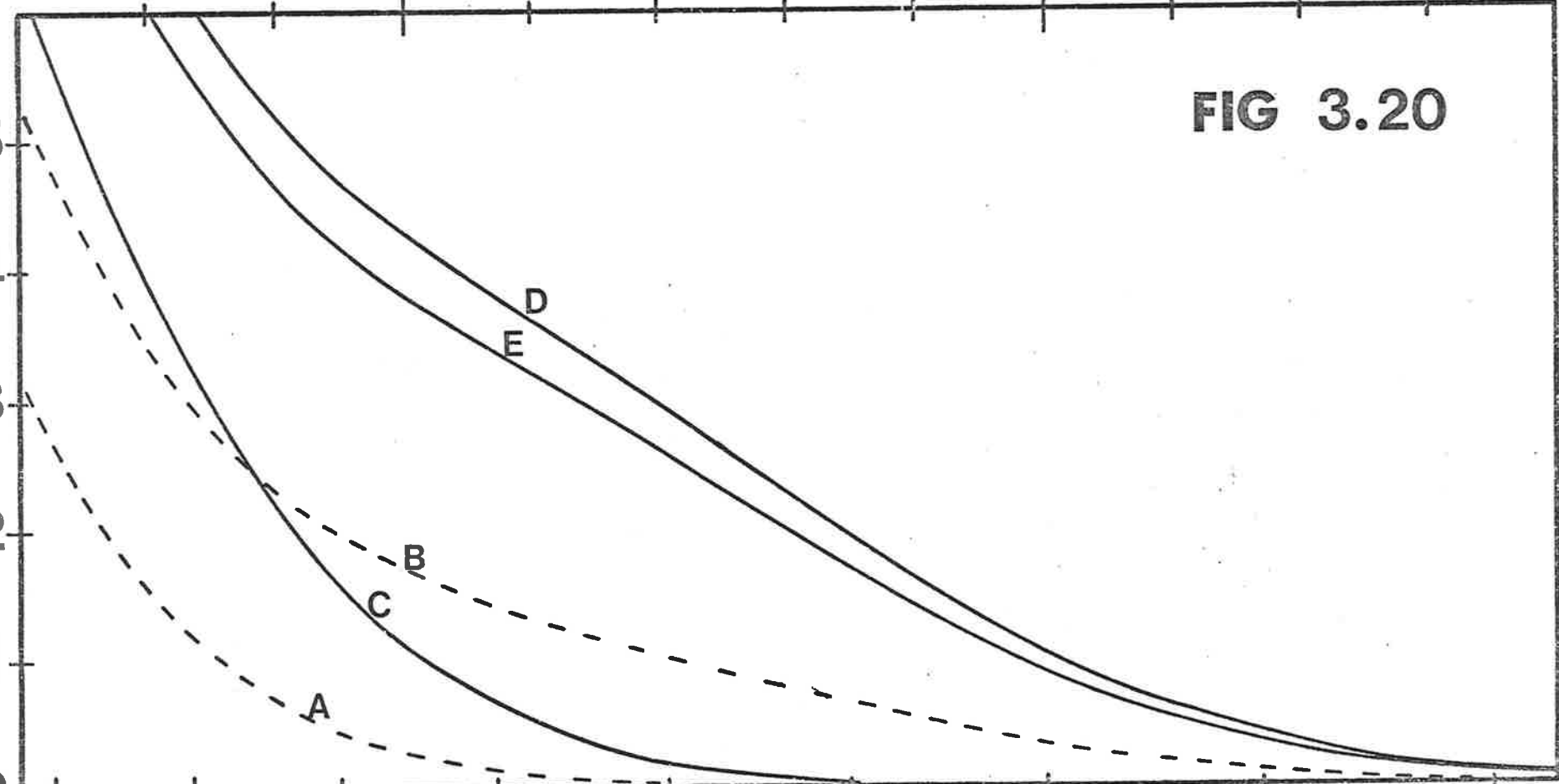




FIG. (3.21)

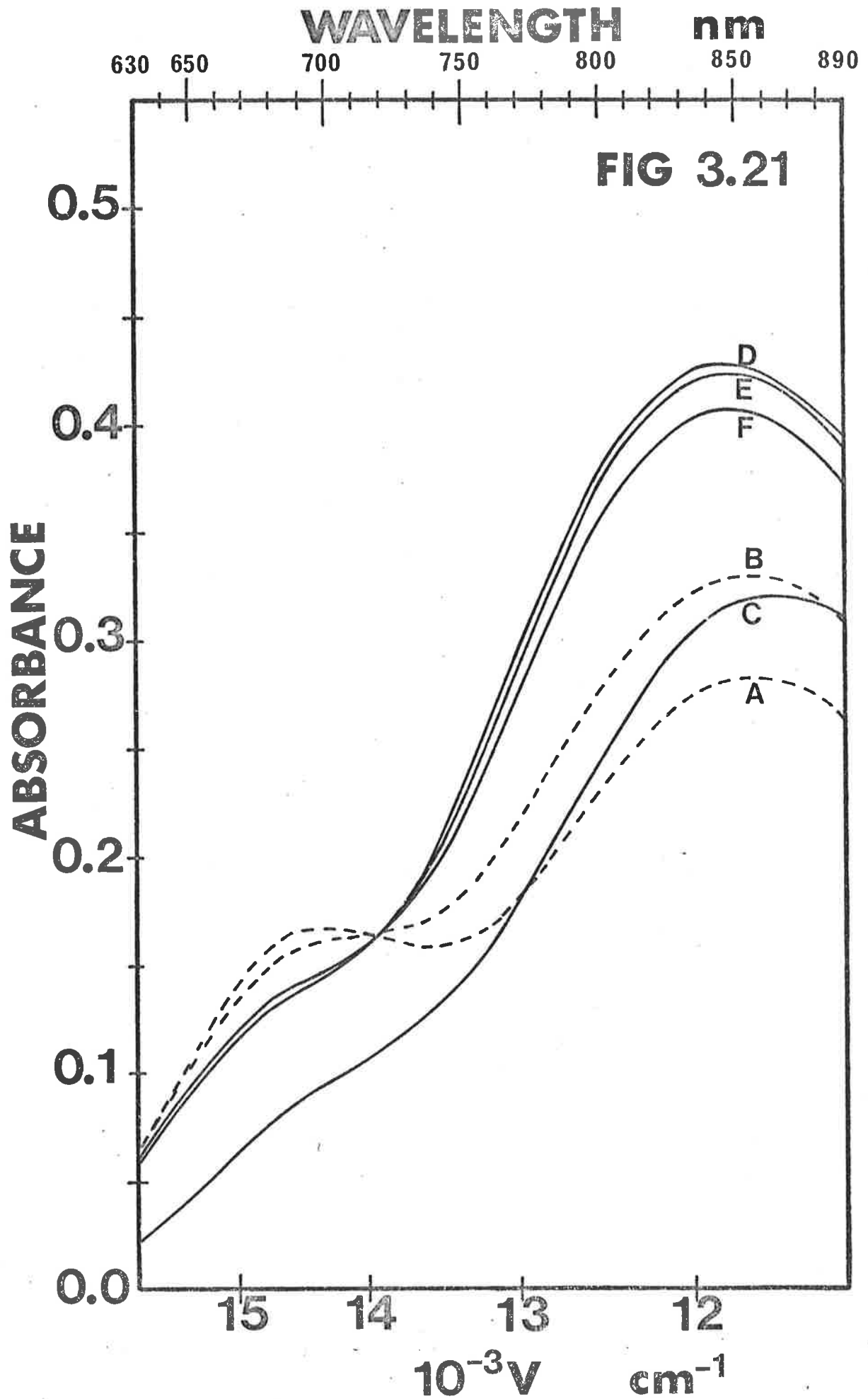
THE SPECTRAL VARIATION ACCOMPANYING THE FORMATION OF  $[\text{Cu}(\text{Me}_6\text{Tren})\text{NCS}]^+$  IN THE LIGAND SUBSTITUTION SYSTEMS,  $[\text{Cu}(\text{Me}_6\text{Tren})\text{OH}_2]^{2+}/\text{NCS}^-$  and  $[\text{Cu}(\text{Me}_6\text{Tren})\text{OH}]^+/\text{NCS}^-$ .

(the ionic strength =  $1.0 \text{ mol dm}^{-3}$  (sodium perchlorate))

The initial individual metal ion and ligand concentrations in the reaction solutions are:

	$[\text{Cu}(\text{Me}_6\text{Tren})\text{OH}^+]$ $\text{mol dm}^{-3} (\times 10^4)$	$[\text{NCS}^-]$ $\text{mol dm}^{-3}$	pH
A	7.5	0.0	10.90
B	7.5	0.52	10.90
	$[\text{Cu}(\text{Me}_6\text{Tren})\text{OH}_2^{2+}]$ $\text{mol dm}^{-3} (\times 10^4)$	$[\text{NCS}^-]$ $\text{mol dm}^{-3}$	pH
C	7.5	0.0	6.80
D	7.5	0.52	6.80
	$[\text{Cu}(\text{Me}_6\text{Tren})\text{OH}^+] + [\text{Cu}(\text{Me}_6\text{Tren})\text{OH}_2^{2+}]$ $\text{mol dm}^{-3} (\times 10^4)$	$[\text{NCS}^-]$ $\text{mol dm}^{-3}$	pH
E	7.5	0.52	8.50

FIG. (3.21) illustrates the smaller absorbance change in the high wavelength visible region between (A and B) and (C and D) at the same wavelength.



II A comparative discussion of kinetic data in the two anation systems,  $[\text{Cu}(\text{Me}_6\text{Tren})\text{OH}]^+/\text{X}^-$  and  $[\text{Cu}(\text{Me}_6\text{Tren})\text{OH}_2]^{2+}/\text{X}^-$  at 298 K.

*Comparative kinetic data for anation in the systems  $[\text{Cu}(\text{Me}_6\text{Tren})\text{OH}_2]^{2+}/\text{X}^-$  and  $[\text{Cu}(\text{Me}_6\text{Tren})\text{OH}]^+/\text{X}^-$  are shown in the following tables,*

TABLE (3.25)

*Kinetic data for the anation of  $[\text{Cu}(\text{Me}_6\text{Tren})\text{OH}]^+$  ....(1)*

*Kinetic data for the anation of  $[\text{Cu}(\text{Me}_6\text{Tren})\text{OH}_2]^{2+}$ ....(2)*

	$\text{X}^- = \text{N}_3^-$ $k_{23} \text{ (s}^{-1}\text{)}$	$\text{X}^- = \text{NCS}^-$ $k_{23} \text{ (s}^{-1}\text{)}$	$\text{X}^- = \text{OCN}^-$ $k_{23} \text{ (s}^{-1}\text{)}$
(1)	$25.1 \pm (0.4)$	$21.5 \pm (0.9)$	$23.8 \pm (0.3)$
(2)	$34.6 \pm (1.3)$	$34.4 \pm (0.4)$	$46.1 \pm (0.8)$

TABLE (3.26)

*$K_{\text{IP}}$  data at 298 K for the system,  $[\text{Cu}(\text{Me}_6\text{Tren})\text{OH}]^+/\text{X}^-$  ....(3)*

*$K_{\text{IP}}$  data at 298 K for the system,  $[\text{Cu}(\text{Me}_6\text{Tren})\text{OH}_2]^{2+}/\text{X}^-$ ....(4)*

	$\text{X}^- = \text{N}_3^-$ $K_{\text{IP}} \text{ (mol}^{-1} \text{ dm}^3\text{)}$	$\text{X}^- = \text{NCS}^-$ $K_{\text{IP}} \text{ (mol}^{-1} \text{ dm}^3\text{)}$	$\text{X}^- = \text{OCN}^-$ $K_{\text{IP}} \text{ (mol}^{-1} \text{ dm}^3\text{)}$
(3)	$31.9 \pm (1.7)$	$55.7 \pm (8.9)$	$21.6 \pm (1.1)$
(4)	$24.4 \pm (2.8)$	$38.3 \pm (1.9)$	$14.2 \pm (0.7)$

The kinetic data at 298 K was obtained from analysis using programme NONLIN, using the same  $k_{32}$  value at 298 K for both systems, see eqns. (3.1) and (3.30) on pages 66 and 120 respectively

The kinetic data for the anation reaction in the systems,  $[\text{Cu}(\text{Me}_6\text{Tren})\text{OH}]^+/\text{X}^-$  and  $[\text{Cu}(\text{Me}_6\text{Tren})\text{OH}_2]^{2+}/\text{X}^-$  are compared in Table (3.25). The experimentally obtained  $k_{23}$  values at 298 K are slower in the  $[\text{Cu}(\text{Me}_6\text{Tren})\text{OH}]^+/\text{X}^-$  system. This was expected since  $k_{23}$  in both systems represents the rate determining loss of  $\text{OH}^-$  and  $\text{H}_2\text{O}$  from their respective complexes. The  $\text{OH}^-$  has a higher surface charge density than does  $\text{H}_2\text{O}$  which on electrostatic arguments should result in a stronger Cu-OH bond by comparison with that for Cu-OH<sub>2</sub>. As a consequence of this, the primary hydroxide exchange rate in  $[\text{Cu}(\text{Me}_6\text{Tren})\text{OH}]^+$  should be slower than the primary water exchange rate in  $[\text{Cu}(\text{Me}_6\text{Tren})\text{OH}_2]^{2+}$ , paralleling the situation with the experimentally obtained  $k_{23}$  data.

The different bond strengths of Cu-OH and Cu-OH<sub>2</sub> would result in different  $\Delta H^\ddagger$  values in the transition state energy determination, for the two anation systems,  $[\text{Cu}(\text{Me}_6\text{Tren})\text{OH}]^+/\text{X}^-$  and  $[\text{Cu}(\text{Me}_6\text{Tren})\text{OH}_2]^{2+}/\text{X}^-$ . This was not tested quantitatively as one temperature only was employed for the  $[\text{Cu}(\text{Me}_6\text{Tren})\text{OH}]^+/\text{X}^-$  system.

The ion pair equilibrium association constant ( $K_{\text{IP}}$ ) data is shown in Table (3.26), for the two systems referred to above. In the case of  $\text{X}^- = \text{N}_3^-$ , for the  $[\text{Cu}(\text{Me}_6\text{Tren})\text{OH}_2]^{2+}/\text{X}^-$  system, the  $K_{\text{IP}}$  value of 28.9 is quoted. This value was determined by averaging the three temperature  $K_{\text{IP}}$  data for  $\text{X}^- = \text{N}_3^-$  (shown in Table (3.5)) because no trend is discernible from this data. The  $K_{\text{IP}}$  values at 298 K for the two systems,  $[\text{Cu}(\text{Me}_6\text{Tren})\text{OH}_2]^{2+}/\text{X}^-$  and  $[\text{Cu}(\text{Me}_6\text{Tren})\text{OH}]^+/\text{X}^-$  are similar being 28.9 and 31.9 mol<sup>-1</sup> dm<sup>3</sup> respectively. However, for the  $\text{NCS}^-$  and  $\text{OCN}^-$  ions the  $K_{\text{IP}}$  values are not similar for these two systems shown above.

The fact that the  $[\text{Cu}(\text{Me}_6\text{Tren})\text{OH}]^+/\text{X}^-$  system has at best similar  $K_{\text{IP}}$  values to that for the  $[\text{Cu}(\text{Me}_6\text{Tren})\text{OH}_2]^{2+}/\text{X}^-$  system is unusual considering the individual charges of the associating ions. Lower  $K_{\text{IP}}$  values for the  $[\text{Cu}(\text{Me}_6\text{Tren})\text{OH}]^+/\text{X}^-$  system were expected. It is considered that this phenomenon suggests the environment of the entering group may be important as well as the charges on reactant species.

CHAPTER THREE: RESULTS AND DISCUSSION

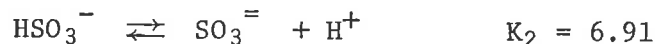
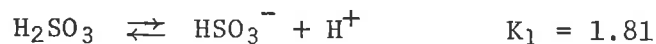
Section F: A preliminary study of the Cu(II) Me<sub>6</sub>Tren sulphito system (at 298 K)

- I A kinetic study (at 298 K) of the Cu(II) Me<sub>6</sub>Tren sulphito system at pH = 7.00 ± (.01)
- II A kinetic study (at 298 K) at various pH values for the Cu(II) Me<sub>6</sub>Tren sulphito system

Section F: A preliminary study of the Cu(II) Me<sub>6</sub>Tren sulphito system  
(at 298 K)

A preliminary study of ligand substitution in the sulphito system  
(at 298 K), [Cu(Me<sub>6</sub>Tren)OH<sub>2</sub>]<sup>2+</sup>/(SO<sub>3</sub><sup>=</sup>/HSO<sub>3</sub><sup>-</sup>) is presented.

Sulphurous acid has two dissociation equilibrium constants as follows,



(in an aqueous environment at 291 K)

and this afforded an opportunity to study the effect of protonation on the kinetics of substitution in the system, [Cu(Me<sub>6</sub>Tren)OH<sub>2</sub>]<sup>2+</sup>/(SO<sub>3</sub><sup>=</sup>/HSO<sub>3</sub><sup>-</sup>). Experimental limitations occurred at both ends of the pH range of investigation.

The low pH analysis was conducted to a lower limit of 5.83. Below this pH the electrical signals from the photomultiplier in the temperature jump apparatus were very small, resulting in substantial uncertainty in any  $\frac{1}{\tau}$  data evaluated. Together with this, in a highly acidic medium the [Cu(Me<sub>6</sub>Tren)OH<sub>2</sub>]<sup>2+</sup> complex is susceptible to complete dissociation. This phenomenon has been investigated<sup>24</sup> using the stopped flow spectrophotometric method, for the dissociation of five coordinate [Cu(Me<sub>6</sub>Tren)OH<sub>2</sub>]<sup>2+</sup> and the nickel(II) and cobalt(II) analogues in perchloric acid solution. It was concluded that a single process observed for all three metal complexes is attributed to the dissociation of the first amine group. The kinetic and activation data obtained, is shown in Table (3.27).

TABLE (3.27)

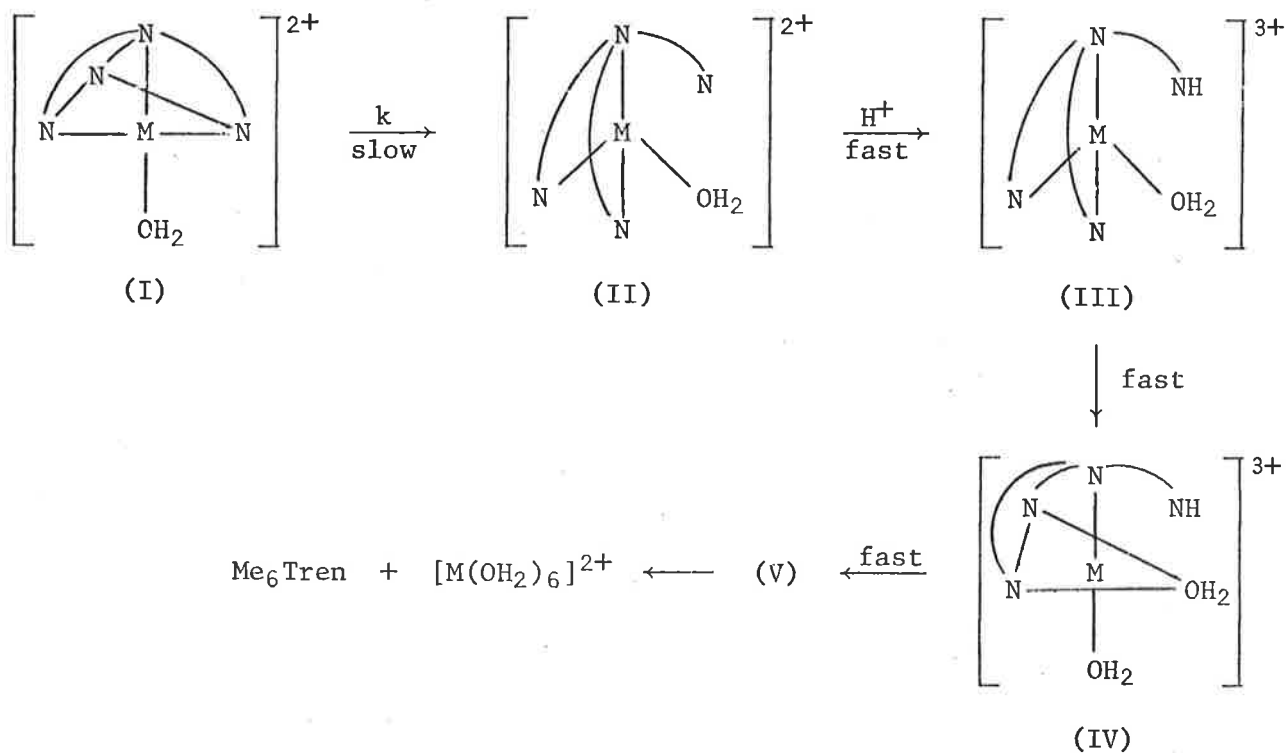
Activation parameters for the dissociation of  $[M(\text{Me}_6\text{Tren})\text{OH}_2]^{2+}$  in  
 $1.0 \text{ mol dm}^{-3}$  perchloric acid at  $2.0 \text{ mol dm}^{-3}$  ionic strength  
 adjusted with sodium perchlorate

Complex	$k(293 \text{ K})$ $\text{s}^{-1}$	$\Delta H^\ddagger$ $(\text{kJ mol}^{-1})$	$\Delta S^\ddagger$ $(\text{J K}^{-1} \text{ mol}^{-1})$
$[\text{Cu}(\text{Me}_6\text{Tren})\text{OH}_2]^{2+}$	$28.0 \pm (0.8)$	$+81.1 \pm (2.5)$	$+59.9 \pm (8.4)$
$[\text{Co}(\text{Me}_6\text{Tren})\text{OH}_2]^{2+}$	$0.97 \pm (0.01)$	$+61.9 \pm (2.9)$	$-33.5 \pm (9.8)$
$[\text{Ni}(\text{Me}_6\text{Tren})\text{OH}_2]^{2+}$	$7.87 \pm (0.04)$	$+58.9 \pm (1.3)$	$-26.4 \pm (4.6)$

data abstracted from ref. 24

The variation of  $\Delta H^\ddagger$  was suggested to occur in part from variation in the ring strain in the  $\text{Me}_6\text{Tren}$  ligand with different central metal ions. Increases in ring strain decrease  $\Delta H^\ddagger$ .<sup>25,26</sup> The variation of  $\Delta S^\ddagger$  data<sup>24</sup> suggests the involvement of water in the transition state and the geometry of that state may vary with the metal ion in the general complex  $[M(\text{Me}_6\text{Tren})\text{OH}_2]^{2+}$ .

It was postulated<sup>24</sup> that the rate determining step is the dissociation of the first of three equivalent amine groups of  $\text{Me}_6\text{Tren}$  in a reaction scheme shown below,



A detailed explanation of the above sequence is shown in ref. 24. The above discussions highlight the necessity of working at pH values which prevent the dissociation of the  $[M(\text{Me}_6\text{Tren})\text{OH}_2]^{2+}$  complex.

Experimental limitations also occurred at high pH. The amplitude of the photomultiplier electrical signal decreases significantly once the pH at which the kinetic investigation is undertaken exceeds the  $\text{pK}_a$  of  $[\text{Cu}(\text{Me}_6\text{Tren})\text{OH}_2]^{2+}$ . The following table shows the  $\text{pK}_a$  of  $[\text{Cu}(\text{Tren})\text{OH}_2]^{2+}$  and  $[\text{Cu}(\text{Me}_6\text{Tren})\text{OH}_2]^{2+}$  at various temperatures,<sup>27</sup>

TABLE (3.28)

$\text{pK}_a$  values for the complexes: (Ionic strength =  $1.0 \text{ mol dm}^{-3}$   
(sodium perchlorate))

	$\text{pK}_a$ (288 K)	$\text{pK}_a$ (298 K)	$\text{pK}_a$ (308 K)
$[\text{Cu}(\text{Me}_6\text{Tren})\text{OH}_2]^{2+}$	$8.71 \pm (0.02)$	$8.52 \pm (0.01)$	$8.37 \pm (0.01)$
$[\text{Cu}(\text{Tren})\text{OH}_2]^{2+}$	$9.29 \pm (0.02)$	$9.37 \pm (0.01)$	$9.45 \pm (0.01)$

Table abstracted from ref. 27

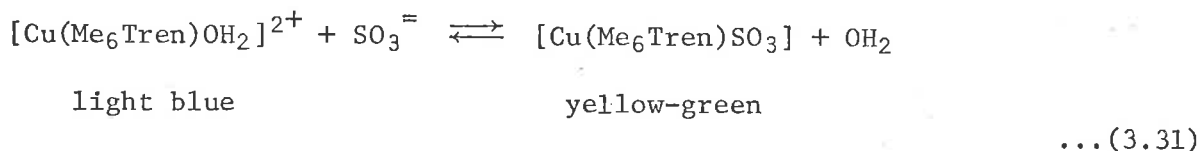
Experimentally, the amplitude of the electrical signal begins to diminish for the ligand substitution in the  $[\text{Cu}(\text{Me}_6\text{Tren})\text{OH}_2]^{2+}/(\text{SO}_3^{=} / \text{HSO}_3^-)$  system at a pH comparable with the  $\text{pK}_a$  (298 K) of 8.52. This phenomenon of decreasing amplitudes with increasing pH was found in the kinetic study of the  $[\text{Cu}(\text{Me}_6\text{Tren})\text{OH}]^+/\text{X}^-$  system, (where  $\text{X}^- = \text{N}_3^-$ ,  $\text{NCS}^-$  or  $\text{OCN}^-$ ) as discussed in Section E.

In the kinetic study at various pH values (to be mentioned later), colour changes were observed which relate to the equilibrium variation with pH for the following,  $\text{HSO}_3^- \rightleftharpoons \text{SO}_3^{=} + \text{H}^+$   
At low pH where the substituting ligand is most probably  $\text{HSO}_3^-$ , the reaction mixture is light yellow in colour, gradually increasing to a dark green in the pH range (6.4 to 7.0).

In the kinetic study at a single pH ( $7.00 \pm (.01)$ ) over a range of



$[\text{SO}_3^=]$ , colour changes were observed for the different reaction mixtures. This is attributed to the change in the equilibrium position in the following reaction sequence,



The spectral variation (at pH = 6.91) accompanying the formation of both the Cu(II)Tren and Cu(II)Me<sub>6</sub>Tren sulphito complexes is shown in FIGS. (3.24) and (3.25) respectively.

I A kinetic study (at 298 K) of the Cu(II)Me<sub>6</sub>Tren sulphito system at pH = 7.00 ± (.01)

The stopped flow study of ligand substitution in the system,  $[\text{Cu}(\text{Me}_6\text{Tren})\text{OH}_2]^{2+}/(\text{SO}_3^=/\text{HSO}_3^-)$  at 298 K, is shown in FIG. (3.22) as a plot of  $k_{\text{obs}}$  versus  $[\text{SO}_3^=]$ . The  $\text{pK}_a$  for the following equilibrium,  $\text{HSO}_3^- \rightleftharpoons \text{SO}_3^= + \text{H}^+$  in an aqueous environment at 291 K is 6.91. However, in the present studies, from the plot of  $\frac{1}{\tau}$  against pH (see FIG. (3.23)) a  $\text{pK}_a$  value of 6.48 was determined in a 1.0 mol dm<sup>-3</sup> ionic strength (sodium perchlorate medium), at 298 K. These two different  $\text{pK}_a$  values are consistent with the fact that different mediums and temperatures were used in their determination. In the plot of  $k_{\text{obs}}$  against  $[\text{SO}_3^=]$  shown in FIG. (3.22) the  $\text{pK}_a$  value of 6.48 was used to calculate  $[\text{SO}_3^=]$  because the conditions of kinetic investigation were the same as in the  $\text{pK}_a$  determination. The plot of  $k_{\text{obs}}$  against  $[\text{SO}_3^=]$  was found to be a straight line of positive slope for the  $[\text{SO}_3^=]$  range investigated. Mixing effects (Schleiren phenomenon) and the "dead time" of the stopped flow apparatus (see chapter two) prevented quantitative investigation of this substitution system at higher  $[\text{SO}_3^=]$  than shown in FIG. (3.22). However, a qualitative investigation at these higher  $[\text{SO}_3^=]$  indicated a further significant increase in the observed rate suggesting a continuation of the straight line of positive slope.

FIG. (3.22)

The variation of the observed first order rate constant  $k_{\text{obs}}$  for the approach to equilibrium of the  $[\text{Cu}(\text{Me}_6\text{Tren})\text{OH}_2]^{2+}/(\text{HSO}_3^-, \text{SO}_3^=)$  system, plotted against  $[\text{SO}_3^=]$ .

*Stopped flow spectrophotometric measurements:* ( $\lambda = 425 \text{ nm}$  and  
pH =  $7.00 \pm 0.01$ )

The metal ion concentration,  $[\text{Cu}(\text{Me}_6\text{Tren})\text{OH}_2^{2+}]$  was constant at  $6.0 \times 10^{-4} \text{ mol dm}^{-3}$ .

The ligand concentration was varied from

$6.76 \times 10^{-3} \text{ mol dm}^{-3}$  to  $1.91 \times 10^{-1} \text{ mol dm}^{-3}$  at 298 K

The spectral variation (at pH = 6.91) for the formation of the Cu(II)Tren and Cu(II)Me<sub>6</sub>Tren sulphito complexes appears in FIGS. (3.24) and (3.25) respectively.

The individual spectrophotometric data points in the kinetic plot of  $k_{\text{obs}}$  against  $[\text{SO}_3^=]$  appear in Appendix (3.7).

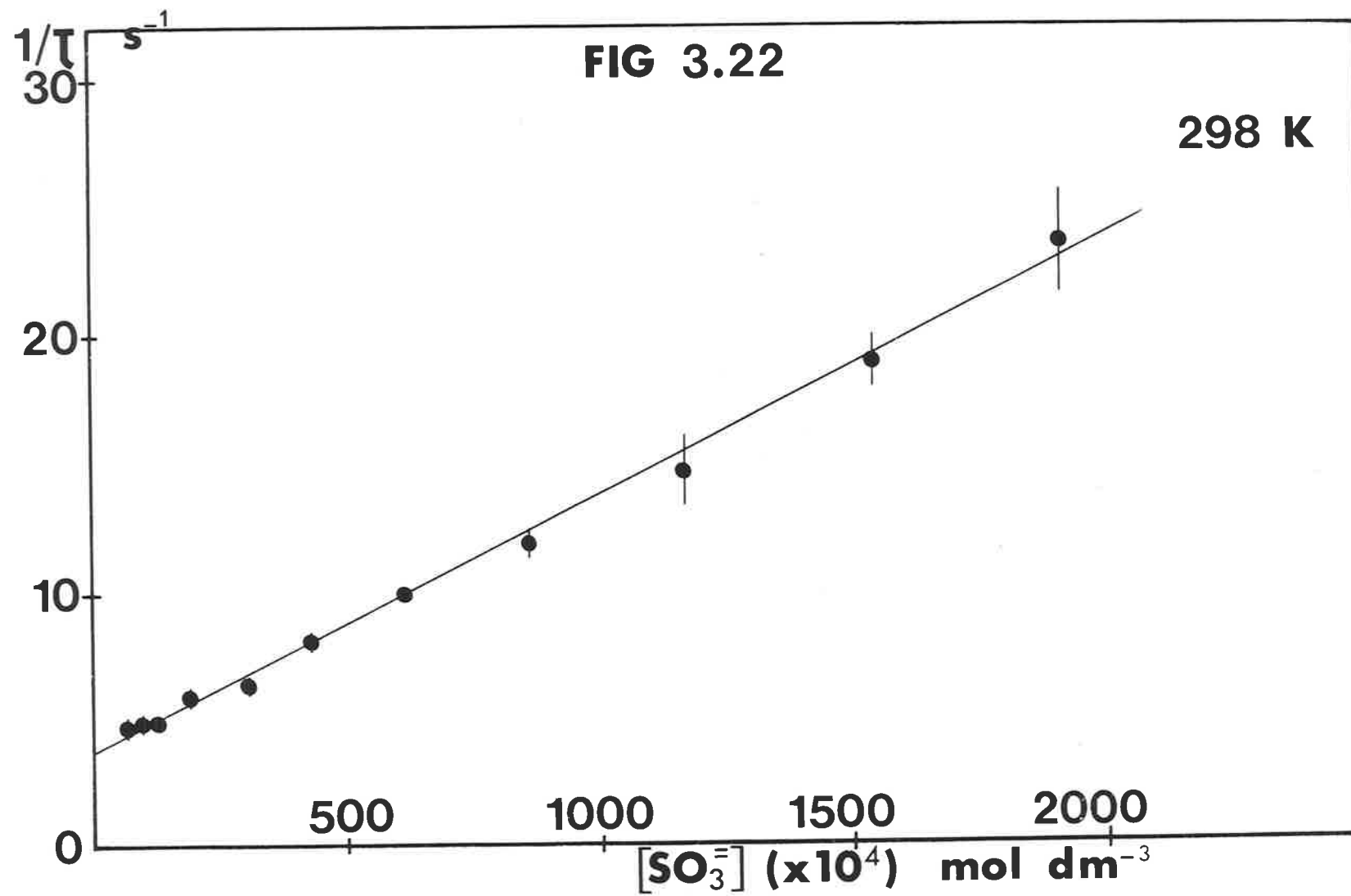


FIG. (3.23)

The variation of the  $k_{\text{obs}} \left( \frac{1}{\tau} \right)$  with pH, at 298 K was investigated for the  $\text{SO}_3^{=}/\text{HSO}_3^-$  substitution in  $[\text{Cu}(\text{Me}_6\text{Tren})\text{OH}_2]^{2+}$ . The metal ion and  $[\text{Na}_2\text{SO}_3]$  were constant for the pH investigation.

$$[\text{Cu}(\text{Me}_6\text{Tren})\text{OH}_2^{2+}]_{\text{initial}} = 6.0 \times 10^{-4} \text{ mol dm}^{-3}$$

$$[\text{Na}_2\text{SO}_3]_{\text{initial}} = 1.52 \times 10^{-1} \text{ mol dm}^{-3}$$

The temperature jump apparatus (as described in chapter two) was used for the pH investigation at  $\lambda = 425 \text{ nm}$ .

The individual spectrophotometric data points in the plot of  $\frac{1}{\tau}$  versus pH appear in Appendix (3.8).

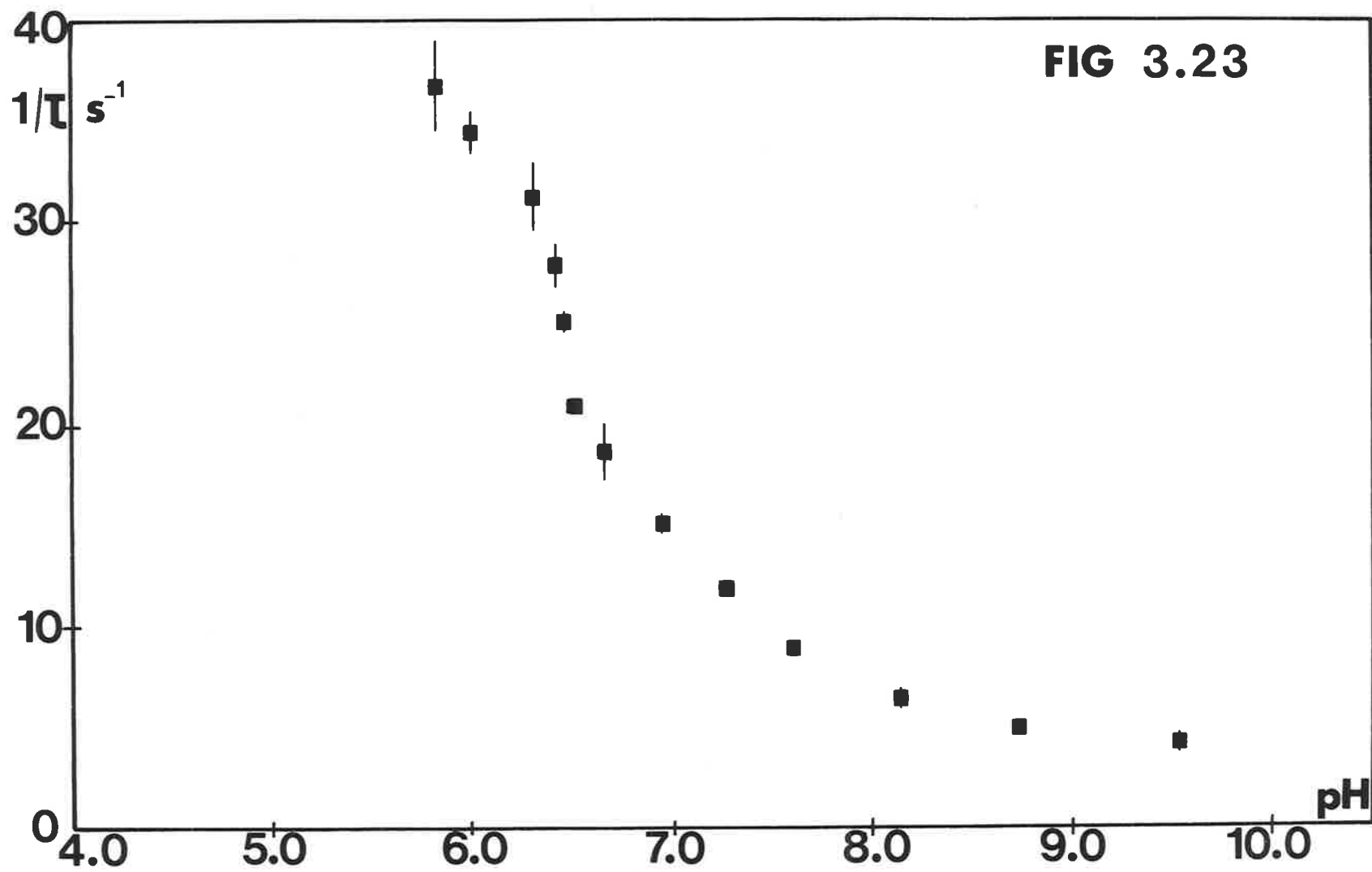


FIG. (3.24)

THE SPECTRAL VARIATION ACCOMPANYING THE FORMATION OF THE COPPER Tren SULPHITO COMPLEX IN THE SYSTEM,  $[\text{Cu}(\text{Tren})\text{OH}_2]^{2+}/(\text{SO}_3^{=}, \text{HSO}_3^{-})$

(the pH =  $6.91 \pm (.03)$  and the ionic strength =  $1.0 \text{ mol dm}^{-3}$

(sodium perchlorate))

The initial individual metal ion and sulphite concentrations in the reaction solutions are:

	$[\text{Cu}(\text{Tren})\text{OH}_2]^{2+}$ $\text{mol dm}^{-3} (\times 10^4)$	$[\text{Na}_2\text{SO}_3]$ $\text{mol dm}^{-3} (\times 10^3)$
A	1.93	0.0
B	1.93	4.99
C	1.93	9.98
D	1.93	15.0
E	1.93	20.0

The  $\lambda_{\text{max}}$  = 260 nm for  $[\text{Cu}(\text{Tren})\text{OH}_2]^{2+}$

The  $\lambda_{\text{max}}$  = 378 nm for the copper tren sulphito complex

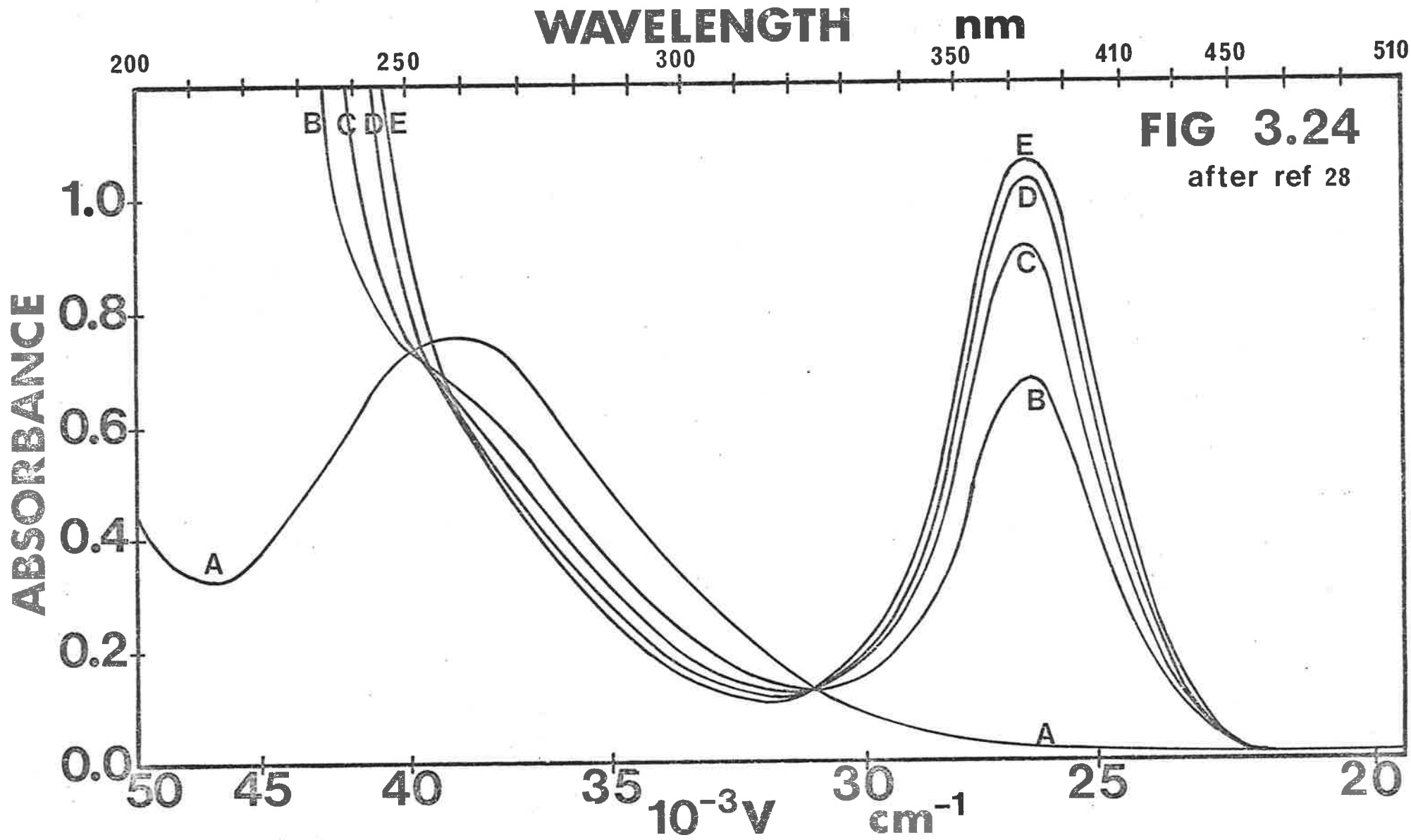


**FIG 3.24**  
after ref 28

FIG. (3.25)

THE SPECTRAL VARIATION ACCOMPANYING THE FORMATION OF THE COPPER Me<sub>6</sub>Tren  
SULPHITO COMPLEX IN THE SYSTEM, [Cu(Me<sub>6</sub>Tren)OH<sub>2</sub>]<sup>2+</sup>/(SO<sub>3</sub><sup>=</sup>, HSO<sub>3</sub><sup>-</sup>)

The pH = 6.91 ± (.03) and the ionic strength = 1.0 mol dm<sup>-3</sup>  
(sodium perchlorate))

The initial individual metal ion and sulphite concentrations in the  
reaction solutions are:

	[Cu(Me <sub>6</sub> Tren)OH <sub>2</sub> ] <sup>2+</sup> mol dm <sup>-3</sup> (× 10 <sup>4</sup> )	[Na <sub>2</sub> SO <sub>3</sub> ] mol dm <sup>-3</sup> (× 10 <sup>3</sup> )
A	1.95	5.02
B	1.95	10.0
C	1.95	30.1
D	1.95	50.1
E	1.95	90.2

The λ<sub>max</sub> = 291 nm for [Cu(Me<sub>6</sub>Tren)OH<sub>2</sub>]<sup>2+</sup>

The λ<sub>max</sub> = 425 nm for the copper Me<sub>6</sub>Tren sulphito complex.



WAVELENGTH nm

250

300

350

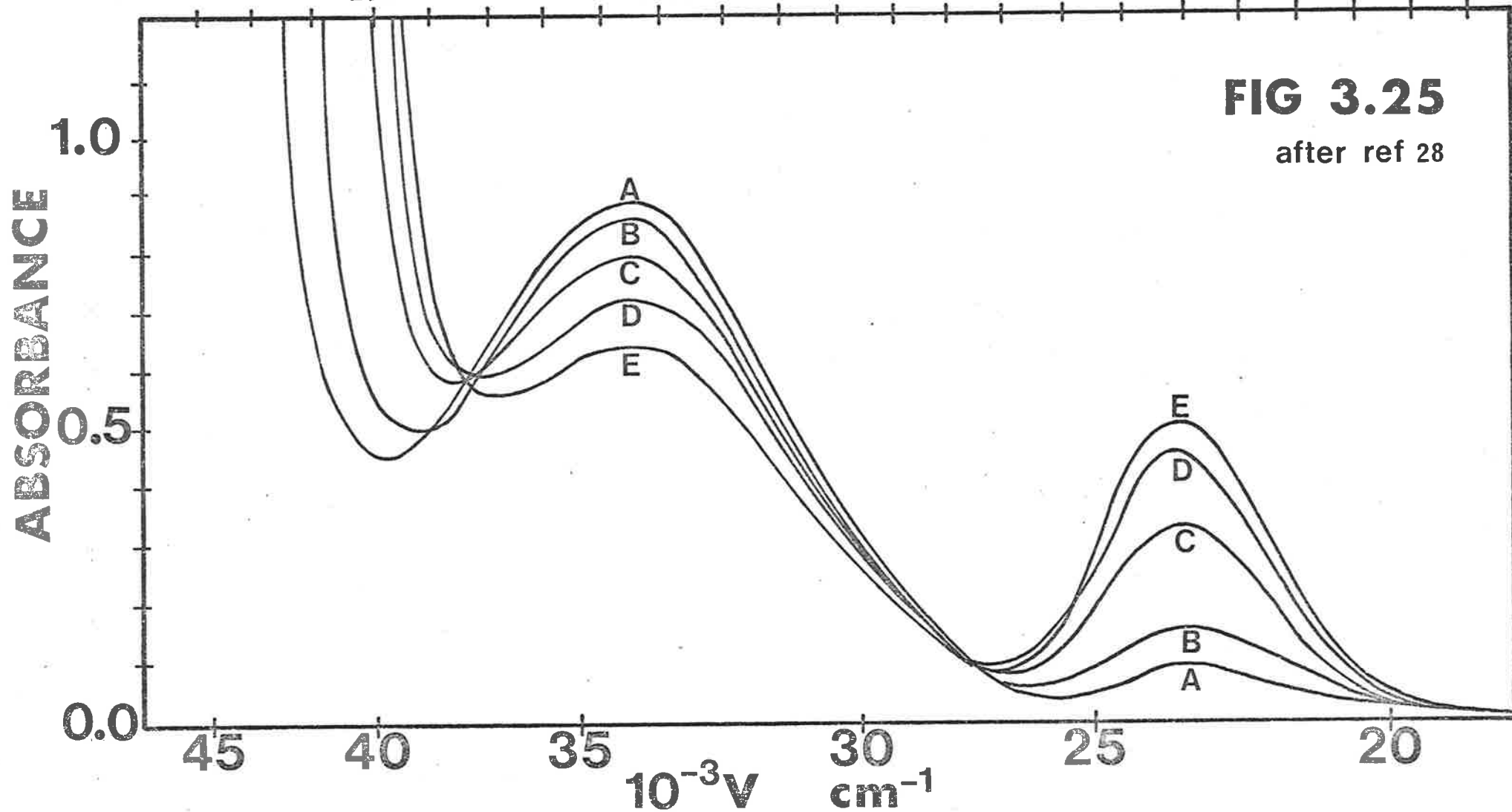
410

450

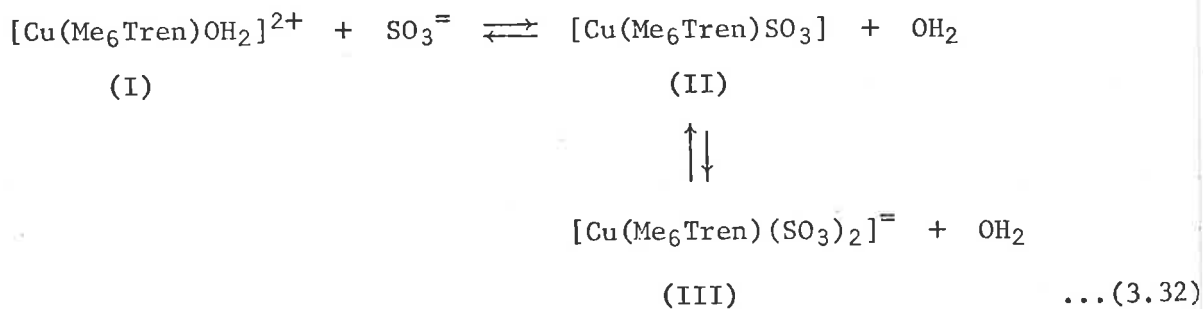
530

FIG 3.25

after ref 28

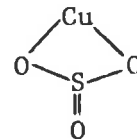


The suggestion is that ligand substitution may take place as shown in the following mechanism,



Step I  $\rightarrow$  II would incorporate the ion pair intermediate in an  $I_d$  mechanism because of the charges on the associating metal ion complex and the ligand species.

Step II  $\rightarrow$  III would be an associative mechanism with the  $\text{SO}_3^{\ominus}$  ligand substituting to form a pseudo octahedral structure in comparison with the trigonal bipyramidal configuration of species II. This postulate although inferring considerable strain at the already sterically crowded labile site is preferred to an intra-molecular rearrangement of  $\text{SO}_3^{\ominus}$  to form in which the observed rate would be independent of  $[\text{SO}_3^{\ominus}]$ .



Plots of absorbance versus  $\log [\text{SO}_3^-]$  for the  $\text{Cu(II)Me}_6\text{Tren}$  and  $\text{Cu(II)Tren}$  sulphito substitution systems were obtained from previous investigations<sup>28</sup> in an aqueous environment at  $\text{pH} = 6.91$ . In each case, the absorbance increased with increasing  $[\text{SO}_3^-]$  until a plateau region was reached, corresponding to conversion of all of the available  $[\text{Cu(Me}_6\text{Tren)OH}_2]^{2+}$  into the sulphito complex. On reaching this plateau region, further increases in  $[\text{SO}_3^-]$  resulted in a reduction of the measured absorbance. This phenomenon occurred for both  $[\text{Cu(Tren)OH}_2]^{2+}$  and  $[\text{Cu(Me}_6\text{Tren)OH}_2]^{2+}$  reactions with  $\text{HSO}_3^-/\text{SO}_3^-$ .

This correlates with the reaction sequence shown in equation (3.32) in which the conversion of species II to species III represents a configurational change (trigonal bipyramidal to octahedral, respectively). The octahedral structure is more symmetrical and has a lower extinction coefficient, which was shown experimentally in the plots of absorbance versus  $[\text{SO}_3^-]$ .

The following  $k_{32}$  data was obtained from the kinetic plots of  $k_{\text{obs}}$  versus  $[\text{SO}_3^-]$  by a rectilinear analysis.

$$\text{For the aquation of } [\text{Cu(Me}_6\text{Tren)SO}_3] \quad k_{32} = 3.67 \pm (0.17) \text{ (s}^{-1}\text{)}$$

$$\text{For the aquation}^{28} \text{ of } [\text{Cu(Tren)SO}_3] \quad k_{32} = 5.64 \pm (0.36) \times 10^3 \text{ (s}^{-1}\text{)}$$

The ratio of aquation for,  $k_{32}(\text{Cu(Tren)SO}_3)/k_{32}(\text{Cu(Me}_6\text{Tren)SO}_3)$ , is  $0.15 \times 10^4$  which parallels similar ratios obtained for  $\text{N}_3^-$ ,  $\text{NCS}^-$  substitution in  $[\text{Cu(Tren)OH}_2]^{2+}$  and  $[\text{Cu(Me}_6\text{Tren)OH}_2]^{2+}$  (see discussion in Section C).

It is suggested that the major contribution to the large differences in observed rates for the two systems studied, is from the steric constraints of the methyl groups in the complex  $[\text{Cu(Me}_6\text{Tren)SO}_3]$  compared with the more open site afforded the  $\text{SO}_3^-$  leaving group in  $[\text{Cu(Tren)SO}_3]$ .

It should be noted that although the substitution system is complicated by the presence of two possible substituting species, the considerably greater aquation rate in the  $[\text{Cu(Tren)X}]^+$  compared to  $[\text{Cu(Me}_6\text{Tren)X}]^+$  complexes

found from studies with  $\text{N}_3^-$  and  $\text{NCS}^-$  is also applicable to the sulphito systems.

II A kinetic study (at 298 K) at various pH values for the  $\text{Cu(II)Me}_6\text{Tren}$  sulphito system

The results of a kinetic study at various pH values is shown in FIG. (3.23). A sigmoidal shape for the plot of  $\frac{1}{\tau}$  versus pH was obtained in a medium of  $1.0 \text{ mol dm}^{-3}$  ionic strength (sodium perchlorate). The experimental aspects of this study have been discussed. A detailed mechanistic interpretation although attempted, proved impracticable owing to the complicated nature of the system under investigation.

## REFERENCES

1. H. Strehlow and W. Knoche, *Ber. Bunsenges physik Chem.*, 72, 2357 (1968).
2. H. Strehlow, in "XXIIIrd International Congress of Pure and Applied Chemistry", Volume 4., Special Plenary lectures, Boston. U.S.A., Butterworths, London, (1971), p 525.
3. N. Bjerrum, *Kgl. Danske Videnskab Selskab.*, 7, 9 (1926).
4. R.M. Fuoss, *J. Amer. Chem. Soc.*, 80, 5059 (1958).
5. "Electrolyte Solutions", R.A. Robinson and R.H. Stokes, Butterworths, 2nd Edn, London., (1959), p 139.
6. "Mechanisms of Inorganic Reactions", F. Basolo and R.G. Pearson, Wiley, 2nd Edn, New York., (1967), p 37.
7. M. Eigen and R.G. Wilkins, *Advan. Chem. Ser.*, 49, 55 (1965).
8. D.P. Rablen, H.W. Dodgen and J.P. Hunt, *J. Amer. Chem. Soc.*, 94, 1771 (1972).
9. R.J. West and S.F. Lincoln, *J. Chem. Soc, Dalton.*, 281 (1974).
10. R.J. West and S.F. Lincoln, *Inorg. Chem.*, 12, 494 (1973).
11. P.C. Jain and E.C. Lingafelter, *J. Amer. Chem. Soc.*, 89, 724 (1967).
12. M. Di Vaira and P.L. Orioli, *Acta Cryst, B.*, 24, 595 (1968).
13. "Theoretical Inorganic Chemistry", M.C. Day and J. Selbin, Reinhold, New York., (1962), p 454.
14. R.E. Connick and R.S. Marianelli, *Abst. Amer. Chem. Soc. Div. Phys. Chem. Summer Symposium.*, Buffalo, June, (1965).
15. R.G. Pearson, *Journal of Chem. Educ.*, 45, 581, 643 (1968).
16. S.F. Pavkovic and D.W. Meek, *Inorg. Chem.*, 4, 20 (1965).
17. "The Chemistry of Coordination Compounds", J.C. Bailar, Jr., and D.H. Busch, J.C. Bailar, Jr., Ed., Reinhold, New York., (1956), p 62.

18. F. Basolo and R.K. Murmann, *J. Amer. Chem. Soc.*, 74, 2373 (1952).
19. H.D. Kaesz and F.G.A. Stone, *J. Amer. Chem. Soc.*, 82, 6213 (1960).
20. H.C. Brown and M.D. Taylor, *J. Amer. Chem. Soc.*, 69, 1332 (1947).
21. J.H. Coates, G.J. Gentle and S.F. Lincoln, *Nature.*, 249, 773 (1974).
22. M. Ciampolini and P. Paoletti, *Inorg. Chem.*, 6, 1261 (1967).
23. A Haim, *Inorg. Chem.*, 9, 426 (1970).
24. S.F. Lincoln and C.D. Hubbard, *J. Chem. Soc., Dalton*, 2513 (1974).
25. R.G. Wilkins, *Accounts Chem. Res.*, 3, 408 (1970).
26. S.J. Ranney and C.S. Garner, *Inorg. Chem.*, 10, 2437 (1971).
27. G.J. Gentle, Honours Thesis, University of Adelaide (1973).
28. P.R. Collins, Honours Thesis, University of Adelaide (1974).

## GENERAL CONCLUSIONS

In the most completely characterised systems,  $[\text{Cu}(\text{Me}_6\text{Tren})\text{OH}_2]^{2+}/\text{X}^-$ , (where  $\text{X}^- = \text{N}_3^-$ ,  $\text{NCS}^-$  or  $\text{OCN}^-$ ) and  $[\text{Cu}(\text{Tren})\text{OH}_2]^{2+}/\text{X}^-$ , (where  $\text{X}^- = \text{N}_3^-$ ,  $\text{NCS}^-$ ), the divalent copper tren complexes were  $\sim 10^4$  times more labile than their corresponding divalent copper N-methylated analogue. Both of the above polyamine complexes show a reduced lability when compared with the complex,  $[\text{Cu}(\text{OH}_2)_6]^{2+}$ . This probably arises from removal of the Jahn Teller effect by chelation as in the divalent copper Tren and  $\text{Me}_6\text{Tren}$  complexes.

Factors that contribute to the greater lability of the divalent copper tren complexes compared with its N-methylated analogue, are as follows,

1. Steric hindrance effects of the methyl groups attached to the secondary nitrogens in  $[\text{Cu}(\text{Me}_6\text{Tren})\text{OH}_2]^{2+}$ , resulting in constraints on the labile site and the entire complex structure.
2. The local environment of the labile site, whether hydrophobic or hydrophilic.
3. Electron donating facilities of the secondary nitrogens in the multi-dentate polyamine ligand, towards the central metal ion.

The Eigen ( $I_d$ ) mechanism is considered to be operative for the systems mentioned above.

The substitution systems,  $[\text{Cu}(\text{Me}_6\text{Tren})\text{OH}_2]^{2+}/\text{X}^-$ , (where  $\text{X}^- = \text{Br}^-$ ,  $\text{Cl}^-$ ) are also considered to be consistent with an Eigen ( $I_d$ ) mechanism, in which  $k_{32} \gg k_{23}$ . It appears that the outer coordination sphere is important in determining the magnitude of the rate constants,  $k_{32}$  and  $k_{23}$ .

The substitution systems,  $[\text{Cu}(\text{Me}_6\text{Tren})\text{OH}]^+/\text{X}^-$ , (where  $\text{X}^- = \text{N}_3^-$ ,  $\text{NCS}^-$  or  $\text{OCN}^-$ ), exhibit the usual Eigen curve for the plot of  $k_{\text{obs}}$  over the entire accessible ligand concentration range. The reduced lability ( $k_{23}$ ) of the system,  $[\text{Cu}(\text{Me}_6\text{Tren})\text{OH}]^+/\text{X}^-$  compared with that for  $[\text{Cu}(\text{Me}_6\text{Tren})\text{OH}_2]^{2+}/\text{X}^-$ , is attributed to the fact that the Cu-OH bond is stronger than the Cu-OH<sub>2</sub> bond.

ADDENDUM: Implications of the kinetic studies in the metallo-enzyme  
zinc carbonic anhydrase

In the most completely categorised substitution systems presented in this thesis, the divalent copper Tren complexes were found to be  $\sim 10^4$  times more labile than their N-methylated analogues. Differences in labile site environment are considered to contribute in part to this increased lability. Steric constraints on the labile site are of major importance in explaining these large differences in observed rates.

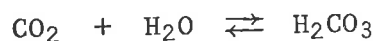
Comparison of the model system,  $[\text{Cu}(\text{Me}_6\text{Tren})\text{OH}_2]^{2+}$  and carbonic anhydrase.

(a) The model system,  $[\text{Cu}(\text{Me}_6\text{Tren})\text{OH}_2]^{2+}$ :

- (i) the labile site is an aqua ligand bound to the central metal ion in a hydrophobic environment
- (ii) the  $[\text{Cu}(\text{Me}_6\text{Tren})\text{OH}_2]^{2+}$  complex is five coordinate (trigonal bipyramidal)

(b) Carbonic anhydrase:<sup>1,2</sup>

- (i) the labile site is an aqua ligand bound to a metal ion usually zinc (but it can be Co(II) or Cu(II)), within a hydrophobic environment
- (ii) the zinc carbonic anhydrase has a distorted four coordinate tetrahedral structure. The zinc is coordinated to three imidazole groups and one water molecule in the active site. The divalent zinc ion necessary for enzyme activity is situated at the bottom of a cleft, lined with hydrophobic groups in the protein molecule
- (iii) zinc carbonic anhydrase is a catalytic metallo-enzyme<sup>2</sup> which greatly enhances the rate of the following reaction,



The active site in carbonic anhydrase appears to exhibit great specificity toward incoming substrates and this is attributed to the geometrical



configuration of the zinc carbonic anhydrase enzyme.<sup>3,4</sup>

Among the elements of the first transition series, divalent cobalt and zinc ions readily assume distorted geometries in model complexes. They are most effective in enzymes catalyzing substitution reactions as for instance in carbonic anhydrase and carboxy peptidase. The divalent nickel and copper<sup>5</sup> both have more regular geometries in model complexes and are less active or inactive when substituted in these proteins. In model systems by contrast, nickel and especially copper is more active catalytically than either cobalt or zinc.<sup>5</sup>

The central metal ion coordination geometries and constraints must be important factors for both the action of metallo-enzymes and as shown in these studies, for the substitution system  $[\text{Cu}(\text{Me}_6\text{Tren})\text{OH}_2]^{2+}/\text{X}^-$ .

The inordinately greater lability of the hydrophilic labile site in  $[\text{Cu}(\text{Tren})\text{OH}_2]^{2+}$  complex compared to that for  $[\text{Cu}(\text{Me}_6\text{Tren})\text{OH}_2]^{2+}$ , ( $\sim 10^4$  times) may eventually lead to an understanding of the reason why zinc in carbonic anhydrase is,

- (i) in a coordination of restricted geometry imposed by the multi-dentate ligands of the protein structure

and

- (ii) the significance of the active site being in a hydrophobic rather than hydrophilic environment

It should be noted that the metal complexes studied in this thesis have only a tenuous resemblance to the metallo-enzyme but general conclusions from the kinetics of substitution reactions in these metal complexes studied, may be useful.

## REFERENCES

1. R.H. Prince and P.R. Woolley, *Angew. Chem. Internat. Edn, Engl.*, 11, 408 (1972).
2. A.E. Dennard and R.J.P. Williams, in "Transition Metal Chemistry: Volume 2", R.L. Carlin, Ed., M. Dekker, Inc., New York, (1966), p 116.
3. Y. Pocker, L. Bjorkquist and D.W. Bjorkquist, *Biochem.*, 16, 3967 (1977).
4. M.L. Ludwig and W.N. Lipscomb, in "Inorganic Biochemistry: Volume 1", G.L. Eichhorn, Ed., Elsevier, Amsterdam., (1973), p 448.
5. L. Bertini, G. Canti, C. Luchinat and A. Scozzafava, *Inorg. Chim. Acta.*, 22, L23 (1977).

Appendices of the kinetic data

Appendix (3.1)

The  $k_{\text{obs}}$  data over the entire azide ( $\text{N}_3^-$ ) concentration range in the three temperature study of the formation of  $[\text{Cu}(\text{Me}_6\text{Tren})\text{N}_3]^+$  is shown. The  $[\bar{a} + \bar{b}]$  was calculated using programme NONLIN (see Section A).

$[\bar{a} + \bar{b}] \times 10^4$ mol dm <sup>-3</sup>	$\frac{1}{\tau}$ (s <sup>-1</sup> )	$[\bar{a} + \bar{b}] \times 10^4$ mol dm <sup>-3</sup>	$\frac{1}{\tau}$ (s <sup>-1</sup> )
6.79	1.41 ± (0.16)	4.79	2.63 ± (0.10)
9.93	1.68 ± (0.02)	5.38	2.70 ± (0.08)
13.2	1.94 ± (0.07)	6.90	2.83 ± (0.06)
16.7	2.17 ± (0.06)	10.1	3.28 ± (0.02)
20.2	2.52 ± (0.08)	13.5	3.65 ± (0.07)
23.9	2.61 ± (0.04)	16.9	4.11 ± (0.13)
31.3	3.04 ± (0.17)	20.5	4.63 ± (0.04)
38.9	3.39 ± (0.08)	24.1	5.09 ± (0.14)
46.5	3.64 ± (0.12)	31.5	5.94 ± (0.20)
58.2	4.06 ± (0.06)	39.1	6.77 ± (0.03)
67.9	4.26 ± (0.15)	46.8	7.47 ± (0.08)
.....	.....	58.4	8.72 ± (0.37)
.....	.....	68.1	9.22 ± (0.20)
$[\text{N}_3^-] \times 10^4$ mol dm <sup>-3</sup>	$k_{\text{obs}}$ (s <sup>-1</sup> )	77.9	10.0 ± (0.5)
70	4.37 ± (0.13)	$[\text{N}_3^-] \times 10^4$ mol dm <sup>-3</sup>	$k_{\text{obs}}$ (s <sup>-1</sup> )
100	5.04 ± (0.13)	70	8.08 ± (0.29)
140	5.66 ± (0.11)	100	9.93 ± (0.29)
180	6.35 ± (0.41)	140	11.5 ± (0.4)
220	6.89 ± (0.24)	180	13.0 ± (0.5)
260	7.25 ± (0.20)	260	14.3 ± (0.5)
340	7.77 ± (0.15)	340	15.3 ± (0.5)
600	9.34 ± (0.16)	440	17.2 ± (0.3)
780	10.2 ± (0.1)	780	21.7 ± (0.1)
1020	11.9 ± (0.3)	1020	24.6 ± (0.8)
1320	13.3 ± (0.2)	1620	29.9 ± (1.7)
1620	14.0 ± (0.3)	1920	31.7 ± (1.6)
1920	14.5 ± (0.2)	2460	33.3 ± (1.5)
2460	15.1 ± (0.3)	3000	33.9 ± (0.8)
3000	15.2 ± (0.1)		

Temperature Jump Spectrophotometric measurements, before,.....  $[\text{Cu}(\text{Me}_6\text{Tren})\text{OH}_2^{2+}]_{\text{initial}}$   
=  $3.92 \times 10^{-4}$  mol dm<sup>-3</sup>

Stopped Flow Spectrophotometric measurements, after,.....  $[\text{Cu}(\text{Me}_6\text{Tren})\text{OH}_2^{2+}]_{\text{initial}}$   
=  $3.92 \times 10^{-4}$  mol dm<sup>-3</sup>

The ionic strength was maintained at 1.0 mol dm<sup>-3</sup> (sodium perchlorate)

## Appendix (3.1) Contd...

308 K

$[\bar{a} + \bar{b}] \times 10^4$ mol dm <sup>-3</sup>	$\frac{1}{\tau}$ (s <sup>-1</sup> )
4.71	5.13 ± (0.13)
5.27	5.27 ± (0.19)
6.70	5.68 ± (0.18)
9.78	5.95 ± (0.19)
13.1	6.83 ± (0.28)
16.5	7.30 ± (0.16)
20.0	8.31 ± (0.21)
23.7	8.86 ± (0.23)
31.1	10.6 ± (0.2)
38.7	12.0 ± (0.2)
46.4	13.8 ± (0.2)
58.0	15.9 ± (0.4)
67.8	17.7 ± (0.5)
77.6	19.8 ± (0.2)

.....

.....

$[\text{N}_3^-] \times 10^4$ mol dm <sup>-3</sup>	$k_{\text{obs}}$ (s <sup>-1</sup> )
70	18.4 ± (0.5)
100	24.0 ± (1.4)
140	31.4 ± (2.1)
180	32.6 ± (1.5)
220	34.6 ± (0.5)
260	35.9 ± (0.7)
300	38.2 ± (0.3)
440	43.3 ± (1.4)
600	47.0 ± (1.7)
780	50.5 ± (2.0)
1020	56.0 ± (1.1)
1620	64.6 ± (1.0)
1920	66.9 ± (3.3)
2460	70.9 ± (2.2)
3000	72.1 ± (2.2)

Temperature Jump Spectrophotometric measurements, before,.....  $[\text{Cu}(\text{Me}_6\text{Tren})\text{OH}_2^{2+}]_{\text{initial}}$   
 $= 3.92 \times 10^{-4}$  mol dm<sup>-3</sup>

Stopped Flow Spectrophotometric measurements, after,.....  $[\text{Cu}(\text{Me}_6\text{Tren})\text{OH}_2^{2+}]_{\text{initial}}$   
 $= 6.00 \times 10^{-4}$  mol dm<sup>-3</sup>

The ionic strength was maintained at 1.0 mol dm<sup>-3</sup> (sodium perchlorate)

Appendix (3.2)

The  $k_{\text{obs}}$  data over the entire thiocyanate ( $\text{NCS}^-$ ) concentration range in the three temperature study of the formation of  $[\text{Cu}(\text{Me}_6\text{Tren})\text{NCS}]^+$ . The  $[\bar{a} + \bar{b}]$  was calculated using programme NONLIN (see Section A).

288 K		298 K	
$[\bar{a} + \bar{b}] \times 10^4$ mol dm <sup>-3</sup>	$\frac{1}{\tau}$ (s <sup>-1</sup> )	$[\bar{a} + \bar{b}] \times 10^4$ mol dm <sup>-3</sup>	$\frac{1}{\tau}$ (s <sup>-1</sup> )
8.42	1.64 ± (0.09)	8.19	2.83 ± (0.17)
9.76	1.76 ± (0.16)	9.44	3.16 ± (0.18)
12.6	1.76 ± (0.08)	12.2	3.47 ± (0.13)
15.7	2.04 ± (0.13)	15.2	3.70 ± (0.22)
19.8	2.09 ± (0.05)	19.2	4.06 ± (0.20)
24.0	2.22 ± (0.18)	23.5	4.68 ± (0.43)
45.9	3.58 ± (0.09)	45.5	6.71 ± (0.58)
.....		.....	
$[\text{NCS}^-] \times 10^4$ mol dm <sup>-3</sup>	$k_{\text{obs}}$ (s <sup>-1</sup> )	$[\text{NCS}^-] \times 10^4$ mol dm <sup>-3</sup>	$k_{\text{obs}}$ (s <sup>-1</sup> )
60	5.15 ± (0.35)	60	9.39 ± (0.57)
100	6.56 ± (0.40)	100	11.9 ± (0.6)
140	7.65 ± (0.53)	140	13.4 ± (0.6)
220	8.90 ± (0.55)	220	16.0 ± (0.9)
300	10.0 ± (0.7)	300	18.0 ± (1.2)
400	11.1 ± (0.8)	400	18.7 ± (0.1)
500	11.8 ± (0.7)	500	21.1 ± (0.8)
760	13.1 ± (0.5)	640	23.2 ± (0.7)
1000	13.8 ± (0.2)	840	24.1 ± (1.2)
1480	15.1 ± (0.2)	1000	25.8 ± (2.1)
2000	16.2 ± (0.2)	1480	28.9 ± (2.0)
3000	16.6 ± (0.8)	2000	29.7 ± (0.9)
4000	16.5 ± (0.6)	2400	30.6 ± (2.0)
5000	16.9 ± (0.2)	4000	30.8 ± (1.4)
		5000	30.4 ± (1.8)

Temperature Jump spectrophotometric measurements, before.....,  $[\text{Cu}(\text{Me}_6\text{Tren})\text{OH}_2^{2+}]$   
 $= 6.00 \times 10^{-4}$  mol dm<sup>-3</sup> initial

Stopped Flow spectrophotometric measurements, after.....,  $[\text{Cu}(\text{Me}_6\text{Tren})\text{OH}_2^{2+}]$   
 $= 6.00 \times 10^{-4}$  mol dm<sup>-3</sup> initial

The ionic strength was maintained at 1.0 mol dm<sup>-3</sup> (sodium perchlorate).

Appendix (3.2) cont..

308 K

$[\bar{a} + \bar{b}] \times 10^4$ mol dm <sup>-3</sup>	$\frac{1}{\tau}$ (s <sup>-1</sup> )
8.01	5.59 ± (0.24)
9.20	5.49 ± (0.20)
11.9	6.45 ± (0.52)
14.8	7.13 ± (0.39)
18.8	8.02 ± (0.36)
23.1	8.39 ± (0.27)
45.1	11.0 ± (0.4)
.....	.....
$[\text{NCS}^-] \times 10^4$ mol dm <sup>-3</sup>	$k_{\text{obs}}$ (s <sup>-1</sup> )
60	17.2 ± (0.4)
100	23.3 ± (1.5)
140	25.9 ± (0.9)
220	30.5 ± (1.1)
300	36.0 ± (1.3)
400	41.8 ± (3.5)
500	47.7 ± (0.9)
760	53.2 ± (6.4)
1000	55.2 ± (2.2)
2000	58.4 ± (2.9)
4000	60.1 ± (4.2)
5000	59.8 ± (3.6)
6000	60.5 ± (2.7)

Temperature Jump spectrophotometric measurements, before.....,  $[\text{Cu}(\text{Me}_6\text{Tren})\text{OH}_2^{2+}]$   
 =  $6.00 \times 10^{-4}$  mol dm<sup>-3</sup> initial

Stopped Flow spectrophotometric measurements, after.....,  $[\text{Cu}(\text{Me}_6\text{Tren})\text{OH}_2^{2+}]$   
 =  $6.00 \times 10^{-4}$  mol dm<sup>-3</sup> initial

The ionic strength was maintained at 1.0 mol dm<sup>-3</sup> (sodium perchlorate)

Appendix (3.3)

The experimentally obtained spectrophotometric stopped flow data in the plot of  $k_{\text{obs}}$  versus  $[\text{OCN}^-]$ , over a three temperature range.

288 K		298 K	
$[\text{OCN}^-] \times 10^4$ $\text{mol dm}^{-3}$	$k_{\text{obs}}$ $(\text{s}^{-1})$	$[\text{OCN}^-] \times 10^4$ $\text{mol dm}^{-3}$	$k_{\text{obs}}$ $(\text{s}^{-1})$
5.00	$0.50 \pm (.04)$	5.00	$1.56 \pm (0.15)$
20.0	$1.03 \pm (.06)$	20.0	$2.03 \pm (0.09)$
30.0	$1.01 \pm (.02)$	30.0	$2.35 \pm (0.20)$
40.0	$1.50 \pm (.08)$	40.0	$2.79 \pm (0.13)$
50.0	$1.71 \pm (.04)$	50.0	$3.21 \pm (0.05)$
60.0	$2.00 \pm (0.14)$	60.0	$3.45 \pm (0.24)$
100	$3.00 \pm (0.16)$	100	$5.48 \pm (0.29)$
200	$4.44 \pm (0.31)$	140	$7.47 \pm (0.35)$
300	$5.82 \pm (0.40)$	220	$11.5 \pm (0.2)$
400	$8.68 \pm (0.24)$	300	$14.5 \pm (0.4)$
540	$9.59 \pm (0.24)$	400	$17.3 \pm (0.2)$
760	$13.7 \pm (1.1)$	500	$19.2 \pm (1.0)$
1000	$15.0 \pm (0.5)$	640	$23.3 \pm (0.8)$
1480	$17.4 \pm (0.5)$	840	$27.1 \pm (1.1)$
2000	$19.2 \pm (0.5)$	1000	$30.0 \pm (0.3)$
3000	$20.3 \pm (1.1)$	1480	$34.3 \pm (0.5)$
4000	$22.0 \pm (0.2)$	2000	$35.5 \pm (0.2)$
5000	$22.0 \pm (1.2)$	3000	$36.1 \pm (1.8)$
		5000	$38.1 \pm (1.3)$
		6000	$40.4 \pm (2.0)$
			$41.1 \pm (2.2)$

This system was investigated at a  $[\text{Cu}(\text{Me}_6\text{Tren})\text{OH}_2^{2+}]_{\text{initial}} = 5.0 \times 10^{-5} \text{ mol dm}^{-3}$

The ionic strength was maintained at  $1.0 \text{ mol dm}^{-3}$  (sodium perchlorate)

## Appendix (3.3) contd...

[OCN <sup>-</sup> ] × 10 <sup>4</sup> mol dm <sup>-3</sup>	308 K k <sub>obs</sub> (s <sup>-1</sup> )
5.00	3.80 ± (0.27)
10.0	3.71 ± (0.33)
20.0	4.30 ± (0.26)
30.0	4.74 ± (0.21)
40.0	5.18 ± (0.09)
50.0	5.61 ± (0.28)
60.0	6.11 ± (0.48)
100	8.21 ± (0.19)
140	11.9 ± (0.3)
220	17.4 ± (0.3)
300	19.5 ± (0.8)
400	24.3 ± (0.6)
500	29.5 ± (0.3)
640	35.9 ± (1.1)
840	38.4 ± (0.7)
1000	45.7 ± (2.1)
1480	54.1 ± (4.3)
2000	61.1 ± (3.7)
3000	63.9 ± (0.4)
4000	67.5 ± (3.8)
5000	68.1 ± (4.0)

This system was investigated at a [Cu(Me<sub>6</sub>Tren)OH<sub>2</sub><sup>2+</sup>]<sub>initial</sub> = 5.0 × 10<sup>-5</sup> mol dm<sup>-3</sup>

The ionic strength was maintained at 1.0 mol dm<sup>-3</sup> (sodium perchlorate)



Appendix (3.4)

The individual temperature jump spectrophotometric data points in the three temperature and one temperature studies, for the formation of  $[\text{Cu}(\text{Tren})\text{N}_3]^+$  and  $[\text{Cu}(\text{Tren})\text{NCS}]^+$  respectively. The  $[\text{Cu}(\text{Tren})\text{OH}_2^{2+}]_{\text{initial}}$  is  $1.52 \times 10^{-3} \text{ mol dm}^{-3}$  in the  $\text{N}_3^-$  kinetic analysis.

TEMP: 278 K (the formation of  $[\text{Cu}(\text{Tren})\text{N}_3]^+$ )

$\frac{1}{\tau} \times 10^{-4}$ (s <sup>-1</sup> )	a $[a_0 + b_0] \times 10^3$ mol dm <sup>-3</sup>	b $[\bar{a} + \bar{b}] \times 10^3$ mol dm <sup>-3</sup>	c $[\bar{a} + \bar{b}] \times 10^3$ mol dm <sup>-3</sup>
5.51 ± (0.17)	2.32	1.72	1.48
5.82 ± (0.21)	2.72	1.87	1.56
6.04 ± (0.32)	3.12	2.06	1.69
6.23 ± (0.12)	3.52	2.28	1.88
6.77 ± (0.32)	7.52	5.36	5.01
7.75 ± (0.41)	9.52	7.17	7.87
8.45 ± (0.34)	13.5	11.0	10.7
9.73 ± (0.52)	17.5	14.8	14.7
11.2 ± (0.5)	21.5	18.8	18.6
12.3 ± (1.0)	25.5	22.7	22.6

TEMP: 288 K (the formation of  $[\text{Cu}(\text{Tren})\text{N}_3]^+$ )

$\frac{1}{\tau} \times 10^{-4}$ (s <sup>-1</sup> )	a $[a_0 + b_0] \times 10^3$ mol dm <sup>-3</sup>	b $[\bar{a} + \bar{b}] \times 10^3$ mol dm <sup>-3</sup>	c $[\bar{a} + \bar{b}] \times 10^3$ mol dm <sup>-3</sup>
10.1 ± (0.3)	2.32	1.72	1.48
10.3 ± (0.3)	2.72	1.87	1.56
10.2 ± (0.1)	3.12	2.06	1.69
10.3 ± (0.3)	3.52	2.28	1.88
11.4 ± (0.3)	5.52	3.68	3.26
12.6 ± (0.1)	7.52	5.36	5.01
12.2 ± (0.5)	9.52	7.17	6.87
13.9 ± (0.4)	13.5	11.0	10.7
15.2 ± (1.1)	17.5	14.8	14.7
16.4 ± (0.5)	21.5	18.8	18.6
17.4 ± (0.4)	25.5	22.7	22.6

a:  $[a_0 + b_0]$  is the sum of the initial concentrations of metal ion and ligand respectively

b:  $[\bar{a} + \bar{b}]$  is the sum of the equilibrium concentrations using  $K_{\text{eq}}(\text{overall}) = 500$   
mol<sup>-1</sup> dm<sup>3</sup>

c:  $[\bar{a} + \bar{b}]$  is the sum of the equilibrium concentrations using  $K_{\text{eq}}(\text{overall}) = 1000$   
mol<sup>-1</sup> dm<sup>3</sup>

The ionic strength was maintained at  $1.0 \text{ mol dm}^{-3}$  (sodium perchlorate).

Appendix (3.4) contd.

TEMP: 298 K (the formation of  $[\text{Cu}(\text{Tren})\text{N}_3]^+$ )

$\frac{1}{\tau} \times 10^{-4}$ (s <sup>-1</sup> )	a [a <sub>0</sub> + b <sub>0</sub> ] × 10 <sup>3</sup> mol dm <sup>-3</sup>	b [ $\bar{a}$ + $\bar{b}$ ] × 10 <sup>3</sup> mol dm <sup>-3</sup>	c [ $\bar{a}$ + $\bar{b}$ ] × 10 <sup>3</sup> mol dm <sup>-3</sup>
15.0 ± (0.2)	1.92	1.60	1.47
15.1 ± (0.7)	2.32	1.72	1.48
15.2 ± (0.5)	2.72	1.87	1.56
15.5 ± (0.3)	3.12	2.06	1.69
15.7 ± (0.3)	3.52	2.28	1.88
16.7 ± (0.4)	5.52	3.68	3.26
17.3 ± (0.4)	7.52	5.36	5.01
17.7 ± (0.4)	9.52	7.17	6.87
19.2 ± (0.1)	13.5	11.0	10.7
20.7 ± (0.5)	17.5	14.8	14.7
22.2 ± (0.4)	21.5	18.8	18.6
23.2 ± (0.4)	25.5	22.7	22.6

Temperature jump data at 288 K for the formation of  $[\text{Cu}(\text{Tren})\text{NCS}]^+$ , using a  $[\text{Cu}(\text{Tren})\text{OH}_2^{2+}]_{\text{initial}}$  of  $5.03 \times 10^{-3}$  mol dm<sup>-3</sup>

$\frac{1}{\tau} \times 10^{-4}$ (s <sup>-1</sup> )	a [a <sub>0</sub> + b <sub>0</sub> ] × 10 <sup>3</sup> mol dm <sup>-3</sup>	b [ $\bar{a}$ + $\bar{b}$ ] × 10 <sup>3</sup> mol dm <sup>-3</sup>	c [ $\bar{a}$ + $\bar{b}$ ] × 10 <sup>3</sup> mol dm <sup>-3</sup>
23.3 ± (0.5)	9.03	4.42	3.47
23.6 ± (0.6)	11.0	5.01	3.88
24.4 ± (0.8)	13.0	6.06	4.97
25.2 ± (0.7)	15.0	7.42	6.45
25.2 ± (0.8)	17.0	8.99	8.14
25.6 ± (0.5)	19.0	10.7	9.93
26.6 ± (0.5)	21.0	12.4	11.8
27.6 ± (0.6)	23.0	14.3	13.7
28.6 ± (0.6)	27.0	18.0	17.5
29.4 ± (0.5)	31.0	21.8	21.4

The ionic strength was maintained at 1.0 mol dm<sup>-3</sup> (sodium perchlorate)

a: [a<sub>0</sub> + b<sub>0</sub>] is the sum of the initial concentration of metal ion and ligand respectively

b: [ $\bar{a}$  +  $\bar{b}$ ] is the sum of the equilibrium concentrations, using K<sub>eq</sub> (overall) = 500 mol<sup>-1</sup> dm<sup>3</sup>

c: [ $\bar{a}$  +  $\bar{b}$ ] is the sum of the equilibrium concentrations, using K<sub>eq</sub> (overall) = 1000 mol<sup>-1</sup> dm<sup>3</sup>

Appendix (3.5)

Spectrophotometric data points of the three temperature stopped flow study in the two systems,  $[\text{Cu}(\text{Me}_6\text{Tren})\text{OH}_2]^{2+}/\text{Br}^-$  and  $[\text{Cu}(\text{Me}_6\text{Tren})\text{OH}_2]^{2+}/\text{Cl}^-$

278 K		288 K		298 K	
$[\text{Br}^-] \times 10^4$ mol dm <sup>-3</sup>	$k_{\text{obs}}$ (s <sup>-1</sup> )	$[\text{Br}^-] \times 10^4$ mol dm <sup>-3</sup>	$k_{\text{obs}}$ (s <sup>-1</sup> )	$[\text{Br}^-] \times 10^4$ mol dm <sup>-3</sup>	$k_{\text{obs}}$ (s <sup>-1</sup> )
240	31.4 ± (2.8)	320	61.7 ± (2.2)	240	42.7 ± (1.7)
720	31.2 ± (1.2)	520	61.4 ± (1.4)	720	42.9 ± (0.9)
1520	30.7 ± (1.3)	720	60.6 ± (1.0)	1520	42.1 ± (1.2)
3040	31.1 ± (2.4)	960	61.8 ± (1.1)	3040	41.5 ± (2.1)
4000	32.8 ± (1.0)	1200	61.6 ± (0.9)	4000	42.4 ± (2.7)
4960	30.6 ± (0.7)	1520	60.7 ± (0.9)	4960	42.2 ± (2.9)
		2000	59.9 ± (0.4)		
		3040	61.3 ± (1.9)		
		4000	60.8 ± (1.1)		
		4960	61.9 ± (2.7)		

278 K		288 K		298 K	
$[\text{Cl}^-] \times 10^4$ mol dm <sup>-3</sup>	$k_{\text{obs}}$ (s <sup>-1</sup> )	$[\text{Cl}^-] \times 10^4$ mol dm <sup>-3</sup>	$k_{\text{obs}}$ (s <sup>-1</sup> )	$[\text{Cl}^-] \times 10^4$ mol dm <sup>-3</sup>	$k_{\text{obs}}$ (s <sup>-1</sup> )
240	12.5 ± (1.0)	240	27.8 ± (0.0)	240	52.3 ± (2.1)
720	13.1 ± (0.8)	400	27.8 ± (0.4)	720	52.9 ± (1.8)
1520	12.7 ± (0.6)	560	28.2 ± (0.4)	1520	51.4 ± (1.2)
3040	11.8 ± (0.1)	720	27.3 ± (0.6)	3040	51.1 ± (3.3)
4000	11.9 ± (0.2)	960	27.1 ± (0.7)	4000	52.5 ± (3.8)
4960	12.3 ± (0.9)	1200	27.5 ± (0.4)	4960	52.4 ± (4.0)
		1520	26.9 ± (0.2)		
		2000	26.2 ± (0.2)		
		3040	26.1 ± (0.7)		
		4000	25.9 ± (1.3)		
		4960	26.0 ± (1.6)		

The ionic strength was maintained at 1.0 mol dm<sup>-3</sup> (sodium perchlorate)

Appendix (3.6)

Spectrophotometric data points for the one temperature (298 K) stopped flow study in the systems,  $[\text{Cu}(\text{Me}_6\text{Tren})\text{OH}]^+/\text{N}_3^-$ ,  $[\text{Cu}(\text{Me}_6\text{Tren})\text{OH}]^+/\text{NCS}^-$  and  $[\text{Cu}(\text{Me}_6\text{Tren})\text{OH}]^+/\text{OCN}^-$

$\text{N}_3^-$ ( $\lambda = 386$ nm)		$\text{NCS}^-$ ( $\lambda = 370$ nm)		$\text{OCN}^-$ ( $\lambda = 360$ nm)	
$[\text{N}_3^-] \times 10^4$ mol dm <sup>-3</sup>	$k_{\text{obs}}$ (s <sup>-1</sup> )	$[\text{NCS}^-] \times 10^4$ mol dm <sup>-3</sup>	$k_{\text{obs}}$ (s <sup>-1</sup> )	$[\text{OCN}^-] \times 10^4$ mol dm <sup>-3</sup>	$k_{\text{obs}}$ (s <sup>-1</sup> )
50	6.41 ± (0.32)	50	7.63 ± (0.69)	-	-
100	8.79 ± (0.42)	100	12.1 ± (0.1)	100	6.30 ± (0.60)
300	14.0 ± (0.9)	300	14.6 ± (0.6)	300	10.8 ± (0.9)
600	17.6 ± (1.0)	600	16.2 ± (1.0)	600	14.2 ± (0.7)
1000	21.2 ± (0.6)	1000	19.4 ± (0.6)	1000	16.8 ± (0.5)
2000	23.1 ± (1.5)	2000	21.2 ± (0.6)	2000	20.7 ± (0.5)
3000	24.6 ± (0.7)	3000	22.4 ± (0.5)	3000	21.9 ± (0.3)
4000	25.6 ± (1.6)	4000	23.6 ± (1.1)	4000	22.6 ± (0.4)
5000	26.1 ± (1.1)	5000	24.3 ± (0.8)	5000	23.2 ± (0.8)

The  $[\text{Cu}(\text{Me}_6\text{Tren})\text{OH}]^+_{\text{initial}} = 4.0 \pm 10^{-4}$  mol dm<sup>-3</sup>

and the pH = 10.9 ± (.05) at an ionic strength of 1.0 mol dm<sup>-3</sup> (sodium perchlorate)

Appendix (3.7)

Spectrophotometric data points for the ligand concentration dependence of  $\frac{1}{\tau}$  ( $s^{-1}$ ) at pH  $7.00 \pm 0.01$  and  $\lambda = 425$  nm.

$[\text{Na}_2\text{SO}_3] \times 10^4$ mol dm <sup>-3</sup>	$[\text{SO}_3^=] \times 10^4$ mol dm <sup>-3</sup>	$k_{\text{obs}}$ ( $s^{-1}$ )
88.0	67.6	$4.69 \pm (0.28)$
128	98.3	$4.90 \pm (0.27)$
168	129	$4.85 \pm (0.14)$
248	191	$5.83 \pm (0.26)$
400	307	$6.29 \pm (0.23)$
560	430	$8.05 \pm (0.34)$
800	615	$9.89 \pm (0.18)$
1120	860	$11.9 \pm (0.5)$
1520	1167	$14.7 \pm (1.3)$
2000	1536	$18.9 \pm (1.0)$
2480	1905	$23.5 \pm (2.0)$

In the stopped flow study, the  $[\text{Cu}(\text{Me}_6\text{Tren})\text{OH}_2]^{2+}$  initial was constant at  $6.0 \times 10^{-4}$  mol dm<sup>-3</sup>.

In Appendix (3.7) the  $[\text{SO}_3^=]$  was calculated using a  $\text{pK}_a$  of 6.48 for the equilibrium  $\text{HSO}_3^- \rightleftharpoons \text{SO}_3^= + \text{H}^+$  at 298 K in a medium of 1.0 mol dm<sup>-3</sup> ionic strength (sodium perchlorate). This value was determined from the pH study shown in FIG. (3.23).

Appendix (3.8)

Spectrophotometric data points for the one temperature (298 K) temperature jump study of  $\frac{1}{\tau}$  versus pH at an ionic strength of 1.0 mol dm<sup>-3</sup> (sodium perchlorate)

$\frac{1}{\tau}$ (s <sup>-1</sup> )	pH ± (.01)	[H <sup>+</sup> ] × 10 <sup>7</sup> mol dm <sup>-3</sup>
36.7 ± (2.2)	5.83	15.0
34.4 ± (1.0)	6.00	10.0
31.2 ± (1.7)	6.30	5.00
27.8 ± (0.9)	6.42	3.80
25.0 ± (0.3)	6.46	3.47
20.9 ± (0.1)	6.52	3.02
18.7 ± (1.4)	6.66	2.21
15.1 ± (0.2)	6.95	1.12
11.8 ± (0.2)	7.26	0.55
8.89 ± (0.10)	7.60	0.25
6.38 ± (0.19)	8.13	0.074
4.86 ± (0.04)	8.73	0.019
4.07 ± (0.22)	9.53	0.003

The above data was obtained at  $\lambda = 425$  nm, for the substitution system, [Cu(Me<sub>6</sub>Tren)OH<sub>2</sub>]<sup>2+</sup>/(HSO<sub>3</sub><sup>-</sup>, SO<sub>3</sub><sup>=</sup>)